Université d'Ottawa | University of Ottawa

Department of Chemistry and Biomolecular Sciences | Département de chimie et sciences biomoléculaires

Faculty of Science | Faculté des sciences

Activity-Based Protein Profiling Reveals Changes to the Regulation of Enzymatic Activity by the Hepatitis C Virus

Geneviève Ferraro Desrochers

Thesis submitted in partial fulfillment of the requirements

for the degree of doctorate in philosophy in chemistry

Abstract

Biological systems, their physical structure and their functions, are built, maintained, and controlled by the activity of enzymes. Understanding how enzymes contribute to the regulation of various pathways and processes allows us to gain a deeper understanding of the entirety of the biological system. As changes in enzyme activity are often essential for the pathogenesis of multiple and varied diseases, identifying these changes represents a crucial step to both understanding the disease and preventing its progression within the individual. Enzymes' functional output can be controlled by numerous different mechanisms, including control of transcription and translation, subcellular localisation, co-factor interactions, or chemical modification to specific amino acids. Activity-based protein profiling allows the potential for activity of target enzymes to be measured, thereby gaining a more accurate representation of the functional state of the biological system. In this work, profiling differential enzyme activity allows the discovery of previously unknown links between metabolic regulatory enzymes and infection by the hepatitis C virus (HCV). The novel probe wortmannin-yne is described and is shown to be able to report on the activity multiple kinases, including MAPK1, whose activity is dysregulated during HCV replication. Novel probes designed to target a smaller selection of kinases, phosphatidylinositol kinases, are reported and are shown to be capable of measuring HCV-induced changes to not only kinase activity but also regulatory protein-protein interactions with the phosphoinositide kinases. Lastly, the role of microRNA-27b in the HCV-induced dysregulation of lipid metabolic enzymes is examined. Three novel targets of microRNA-27b are identified, and their dysregulation is shown to have an effect on the life cycle of HCV. Altogether, this work has developed new tools for the study of metabolic enzymes and identified new avenues of investigation into the dysregulation of lipid metabolism.

Acknowledgements

I would like to thank my supervisor Dr. John Pezacki for his mentorship and support over the course of my graduate studies. John has guided me in my journey to becoming a scientist, providing invaluable feedback on my research and my writing.

To my former colleagues Dr. Ragunath Singaravelu, Dr. Allison Sherratt, Dr. Dana Foss, Shifawn O'Hara, Dr. Megan Powdrill and Dr. Miroslava Strmiskova, thank you for being great role models, and for being all your help in leaning how to design experiments and manage projects.

I would to thank my co-workers who have helped me with my projects, either performing experiments or giving second opinions on experimental results, presentations, scholarship application, and written papers. Thanks for everything you've helped me with over the years, Roxana Filip, Tyler Shaw, Nadine and Noreen Ahmed, Rhea Alonzi, Tiffany Stern, and Dr. David Prescott.

Lastly, thanks to my mom, Margaret Ellen Ferraro, my dad, Yvan Paul Desrochers, and my sister, Solange Ferraro Desrochers, for their endless support and encouragement.

Table of Contents

List of Tables

List of Figures

List of Abbreviations

Abbreviation	Full name
2-BP	2-bromopalmitate
AADAC	Aryl-acetamide deacetylase
ABC	Ammonium bicarbonate
ABHD10	α/β hydrolase domain containing protein 10
ABHD11	α/β hydrolase domain containing protein 11
ABHD12	α/β hydrolase domain containing protein 12
ABHD4	α/β hydrolase domain containing protein 4
ABHD5	α/β hydrolase domain containing protein 5
ABHD6	α/β hydrolase domain containing protein 6
ABP	Activity-based probe
ABPP	Activity-based protein profiling
ACBD3	Acyl-Coenzyme A binding domain containing 3
ACOT	Acyl-Coenzyme A thioesterase
ACOT1	Acyl-Coenzyme A thioesterase 1
ACOT2	Acyl-Coenzyme A thioesterase 2
AfBP	Affinity-based probe
Ago-HITS-CLIP	Argonaut-linked high-throughput sequencing of RNA isolated by crosslinking immunoprecipitation
AKT	RAC-alpha serine/threonine-protein kinase
AKT2	RAC-alpha serine/threonine-protein kinase 2
APEH	Acylamino acid releasing enzyme

ARF1	ADP ribosylation factor 1
ARP1	Apolipoprotein A-I regulatory protein 1/Nuclear receptor subfamily 2 group F member 2/COUP transcription factor 2
ATM	Ataxia telangiectasia mutated
BPLF1	Epstein-Barr virus large tegument protein deneddylase
Br2	Bromoethylamine
Br3	Bromopropylamine
BSA	Bovine serum albumin
CALM1	Calmodulin-1
CAMK1	Calcium/calmodulin-dependent protein kinase type 1
CAMK2D	Calcium/calmodulin-dependent protein kinase type II subunit delta
CD8	Cluster of differentiation 8
CDK1	Cyclin dependent kinase 1
CDK18	Cyclin dependent kinase 18
CDK2	Cyclin dependant kinase 2
CEPBP	CCAAT/enhancer-binding protein β
CES1	Carboxylesterase 1
CID	Collision-induced dissociation
CMPK1	Cytosine monophosphate kinase 1
COPI	Coat protein complex 1
COPII	Coat protein complex 2
CPVL	Carboxypeptidase vitellogenic like
CSK	C terminal Src kinase
CSNK2	Casein kinase II

CSNK2A1	Casein kinase II subunit α 1
CSNK2A2	Casein kinase II subunit α 2
CTSA	Cathepsin A
DAA	Direct-acting antiviral
DAK	Dihydroxyacetone kinase
DC assay	Detergent compatible assay
DFSA	alkyne-hinged 3-fluorosialyl fluoride
Di-Ub	Di-ubiquitin
diUb-VME	Di-ubiquitin-vinyl methyl ester
DMEM	Dulbecco's modified eagle medium
DMSO	Dimethyl sulfoxide
DNA-PK	DNA pyruvate kinase
DPP4	Dipeptidyl peptidase 4
DPP7	Dipeptidyl peptidase 7
DPP8	Dipeptidyl peptidase 8
DPP9	Dipeptidyl peptidase 9
DTT	Dithiothreitol
DUB	Deubiquitinating enzyme
EBV	Epstein-Barr virus
EGFR	Epidermal growth factor receptor
EI	Electron ionisation
ERK	Extracellular signal-regulated kinase
ESD	Early in short days
ETFA	Electron transfer flavoprotein subunit α, mitochondrial

FA	Formic acid
FAAH	Fatty acid amide hydrolase
FASN	Fatty acid synthase
FBS	Fetal bovine serum
FDR	False discovery rate
fMLP	N-Formylmethionyl-leucyl-phenylalanine
FP	Fluorophosphonate
FTMS	Fourier transform mass spectrometry
GAK	Cyclin G associated kinase
GAPDH	Glyceraldehyde-3-phosphate dehydrogenase
GP1	Ebola glycoprotein 1
GRB2	Growth factor receptor-bound protein 2
GSK3β	Glycogen synthase kinase 3 β
HA (IAV)	Haemagglutinin
HAUb	Haemagglutinin-Ubiquitin
HAUb-MVE	Haemagglutinin-Ubiquitin-Methylvinyl ester
HCC	Hepatocellular carcinoma
HCMV	Human cytomegalovirus
HCV	Hepatitis C virus
HDAC	Histone deacetylaces
HDL	High density lipoprotein
HHV-1	Herpes simplex virus 1
HIV	Human immunodeficiency virus

HMC-1	Human mast cell line 1
HMGCS1	Hydroxymethylglutaryl-Coenzyme A synthase 1
HNF1A/HNF1α	Hepatocyte nuclear factor 1α
HNF4A/HNF4α	Hepatocyte nuclear factor 4α
HPLC	High performance liquid chromatography
HRMS	High resolution mass spectrometry
Huh7.5-FGR	Huh7.5-full genomic replicon
HyCoSuL	Hybrid Combinatorial Substrate Library
IAV	Influenza A virus
IFN-γ	Interferon γ
IKK	Inhibitor of nuclear factor κB kinase
IL-7	Interleukin 7
IκB	Inhibitor of nuclear factor κB
IκBα	Inhibitor of nuclear factor κB subunit α
JUN	Transcription factor activator protein 1
KD	Knock-down
LC-MS/MS	Liquid chromatography tandem mass spectrometry
LDL	Low density lipoprotein
LIPC	Lipase C
LIS1	Lissencephaly-1 protein
LMP2	Low molecular mass protein 2
LMP7	Low molecular mass protein 7
LPCAT1	Lysophosphatidylcholine acyltransferase 1

LTQ-Orbitrap	Linear trap quadropole Orbitrap
LYPLA1	Lysophospholipase 1
LYPLA2	Lysophospholipase 2
LYPLAL1	Lysophospholipase-like protein 1
M48	Murine herpesvirus 1 large tegument protein deneddylase
MAP2K1	Dual specificity mitogen-activated protein kinase kinase 1
MAPK	Mitogen-activated protein kinase
MAPK1	Mitogen-activated protein kinase 1
MCMV	Murine cytomegalovirus
MDV	Marek's disease virus
MEM	Minimum essential media
MGLL	Monoglyceride lipase
MHC	Major histocompatibility complex
MHV-68	Murine gamme herpesvirus 68
miR-27b	microRNA-27b (hsa-miR-27b-3p)
miRNA	microRNA
Mono-Ub	Mono-ubiquitin
MS/MS	Tandem mass spectrometry
NA	Neuraminidase
NCEH1	Neutral cholesterol ester hydrolase 1
NFAT	Nuclear factor of activated T cell
NFκB	Nuclear factor κ-light-chain-enhancer of activated B cells
NME1	Nucleoside diphosphate kinase A

NR1H4	Nuclear receptor subfamily 1 group H member 4/Bile acid receptor
NR2F2	Nuclear receptor subfamily 2 group F member 2/Apolipoprotein A-I regulatory protein 1/COUP transcription factor 2
NS2B	Viral non-structural protein 2B
NS3	Viral non-structural protein 3
NS5A	Viral non-structural protein 5A
PACSIN 1	Protein kinase C and casein kinase substrate in neurons protein 1
PAF	Platelet activating factor
PAFAH1B1	Platelet activating factor 1B subunit 1
PAFAH1B2	Platelet activating factor 1b subunit 2
PAFAH1B3	Platelet activating factor 1b subunit 3
PAFAH2	Platelet activating factor 2
PAK2	p21-activated kinase 2
PAL	Photo-affinity labelling
PCK2	Phosphoenolpyruvate carboxykinase 2
PDFSA	Protected alkyne-hinged 3-fluorosialyl fluoride
PFKL	Phosphofructokinase, Liver
PFKM	Phosphofructokinase, Muscle
PI	Phosphoinositide
PI3K	Phosphoinositide 3-kinase
PI4KA	Phosphoinositide 4-kinase α
PI4KB	Phosphoinositide 4-kinase β
PI4P	Phosphoinositide 4-phosphate

PIK	Phosphoinositide kinase
PIKBPyne	Phosphoinositide kinase benzophenone alkyne
PIKK	Phosphoinositide 3-kinase related kinase
PIP	Phosphorylated phosphoinositide
PIP4K2A	Phosphatidylinositol 5-phosphate 4-kinase type-2 alpha
PLPro	Papain-like protease
PNPLA6	Patatin-like phospholipase domain-containing protein 6
PPAR	Peroxisome proliferator activated receptor
PPARG/PPARγ	Peroxisome proliferator activated receptor γ
PPARGC1A	Peroxisome proliferator activated receptor γ cofactor 1 α
PPARA/PPARα	Peroxisome proliferator activated receptor α
PPME1	Pectinesterase PPME1
PPT2	Palmitoyl-protein thioesterase 2
PREP	Prolyl endopeptidase
PREPL	Prolyl endopeptidase-like
PRKAR1A	Protein kinase cAMP-dependent type I regulatory subunit α
PS	Phenyl sulfonate ester
PSMA2	proteasome 20S subunit α 2
PSMA3	proteasome 20S subunit α 3
PSMA6	proteasome 20S subunit α 6
PSMB3	proteasome 20S subunit β 3
PSMB5	proteasome 20S subunit β 5
PSMC6	proteasome 26S subunit, ATPase 6

PSME1	proteasome activator subunit 1
PSME2	proteasome activator subunit 2
PTM	Post-translational modification
PTP1D	Protein-tyrosine phosphatase 1D
pUL48	Human cytomegalovirus high molecular weight protein
PVDF	Polyvinylidene difluoride
qRT-PCR	Quantitative reverse transcription polymerase chain reaction
RAC-β	RAC-β serine/threonine-protein kinase
RBBP9	retinoblastoma-binding protein 9
RIN	GTP-binding protein Rit2
RISC	RNA-induced silencing complex
RIT	GTP-binding protein Rit1
RNAi	RNA interference
RO	Replication organelle
RT (HIV virus)	Reverse transcriptase
RT (incubation)	Room temperature
RTA	Ready to assemble
s.e.m.	Standard error of the mean
SARS	Severe acute respiratory syndrome
SARS-CoV	Severe acute respiratory syndrome coronavirus
SARS-CoV-2	Severe acute respiratory syndrome coronavirus 2
SDS	Sodium dodecyl sulfate
SDS-PAGE	Sodium dodecyl sulfate polyacrylamide gel electrophoresis

SHC/SHC1	Src homology 2 domain-containing-transforming protein C1
SIAE	Sialate O-acetylesterase
siRNA	short interfering RNA
SOS	Son of sevenless
STAT5	**Signal transducer and activator of transcription 5**
TAK1	ransforming growth factor-β-activated kinase 1
TAMRA	tetramethylrhodamine
TBRG4	Transforming growth factor beta regulator 4
TBS	Tris-buffered saline
TBST	Tris-buffered saling with Tween-20
TBTA	Tris(benzyltriazolylmethyl)amine
TCEP-HCl	Tris(2-carboxyethyl)phosphine *hydrochloride*
TEAB	Tetraethylammonium bicarbonate
TGX	Tris-Glycine eXtended
TLC	Thin layer chromatography
TLR	Toll-like receptor
TMPRSS13	Transmembrane protease serine 13
TPP2	Tripeptidyl-peptidase 2
TRAF6	Tumor necrosis factor receptor-associated factor 6
TUBB	Tubulin β-chain
UCH37	Ubiquitin carboxyl-terminal hydrolase isozyme L5
UCH-L3	Ubiquitin carboxyl-terminal hydrolase isozyme L3
UCH-L1	Ubiquitin carboxyl-terminal hydrolase isozyme L1

UL36	Large tegument protein deneddylase
USP15	Ubiquitin-specific-processing protease 15
USP7	Ubiquitin-specific-processing protease 7
USP9X	Ubiquitin-specific protease 9, X chromosome
UTR	Untranslated region
UV	Ultraviolet
VCN	Vinylcyanide
VLDL	Very low density lipoprotein
VME	Vinylmethyl ester
VS	Vinylmethylsulfone
VSPh	Vinyl phenylsulfone
WM	Wortmannin
WM-yne	Wortmannin-alkyne

Chapter 1: The History of Activity-Based Protein Profiling and Host-Virus Interactions

Updated from version initially published: Geneviève F. Desrochers, John Paul Pezacki (2019) *ABPP and Host–Virus Interactions*. Curr Top Microbiol Immunol. 420:131-154

1.1 General overview of host-virus interactions during infection

Successful viral infection, as well as any resultant antiviral response, relies on numerous sequential interactions between host and viral factors. These interactions can take the form of affinity-based interactions between viral and host macromolecules or active, enzyme-based interactions, consisting both of direct enzyme activity performed by viral enzymes and indirect modulation of the activity of the host cell's enzymes via viral interference. This activity has the potential to transform the local microenvironment to the benefit or detriment of both the virus and the host, favouring either the continuation of the viral life cycle or the host's anti-viral response. Comprehensive characterisation of enzymatic activity during viral infection is therefore necessary for the understanding of virally-induced diseases. Activity-based protein profiling techniques have been established as effective and practicable tools with which to interrogate the regulation of enzymes' catalytic activity and the roles the played by these enzymes in various cell processes. This chapter will review the contributions of these techniques in characterising the roles of both host and viral enzymes during viral infection in humans.

Viruses, as infectious biological agents which lack the ability to replicate independently, lack translational and metabolic machinery, and are therefore obligate intracellular parasites. Viral particles consist of either an RNA or DNA genome surrounded by a protein capsid which protects the genetic material. Certain viruses are additionally enveloped by a lipid bilayer derived from host membranes. In order to propagate, viruses must use host cell systems to assemble new RNA, DNA, proteins, and lipid envelopes. Though details of viral life cycles vary from virus to virus, there are five general stages:

attachment and cell entry, translation of viral proteins, replication of the genome, assembly of the viral particle, and egress from the cell. (Fig 1.1) Activity-based profiling has been used broadly to characterise host-virus interactions of these five stages. The approaches used and the discoveries these techniques accorded will be highlighted herein.

The molecular processes involved in virus propagation require the diversion of energy, molecular building blocks, and other essential resources away from the host cell's systems and into pathways and processes needed by the virus. It is important to note that metabolic energy is consumed not only by the synthesis of new viral particles, but also by the remodelling of the cellular environment to meet the demands of the virus. Viruses require specific and often tightly regulated conditions to propagate efficiently. A good example lies in the replication of positive-strand RNA viruses, which occurs within specialised regions called replication organelles (RO).[1] These organelles create an optimal environment for replication, allowing the concentration of the required host and viral factors and shielding viral RNA from the innate immune response.[1] The morphology of these organelles differs from virus to virus: they can be spherical or tubular, originate from the ER, Golgi body, endosome or lysosome, and be composed of single, double, or multi-membrane vesicles.[1,2] These membranes furthermore possess specific lipid profiles unique to each virus. The Rubella virus RO requires elevated saturated fatty acid levels, while West Nile virus, hepatitis C virus, and enteroviruses require high cholesterol.[3,4] The hepatitis C RO also requires elevated levels of sphingolipids and phosphorylated phosphoinosides (PIPs).[3–5] The large amount of metabolic energy required to change the lipid profile of a cell in this manner necessitates significant perturbation of normal lipid homeostasis.

The diversion of metabolic energy and the remodelling of host cell architecture is initiated by viral enzymes; however, direct modification of cellular architecture by viral enzymes is not always feasible due to the small range of functionalities encoded by viruses. Viral genomes can be extremely small: the

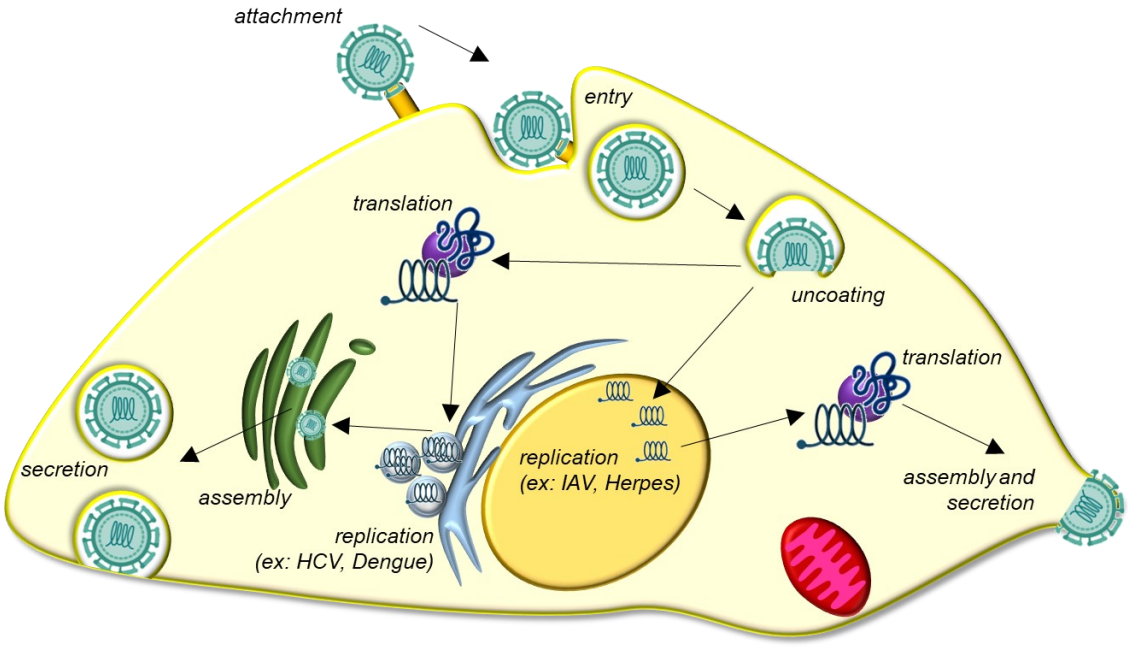

Figure 1.1: Viruses utilise multiple host systems throughout their life cycle. Life cycles differ between viruses. Positive-strand RNA viruses (ex: HCV) follow the path illustrated on the left: receptor binding, internalisation, protein translation, replication within membranous structures in the cytosol, assembly and secretion. Viruses such as influenza A and herpesviruses follow the path on the right: replication within the nucleus, export to the cytoplasm, protein translation, assembly, and budding from the cell.

hepatitis B virus, for example, has a genome 3.2 kb long.[6] As a result, viruses utilise the machinery of the cells they infect to replicate their own genome and assemble new viral particles for release and subsequent reinfection of new host cells.

Changes in host cell function can be induced either directly by the virus itself, as homeostatic responses to virus-induced changes, or as immunological responses to infection. Functional changes are induced either directly or indirectly as the result of changes to the catalytic activity of both viral and host-derived enzymes. Interrogating changes to enzymatic activity during viral infection is therefore essential to form a complete understanding of the mechanisms of virus infection. Activity-based protein profiling (ABPP) techniques[7,8] are ideally suited to answering questions on the perturbation of enzyme function by host-virus interactions. These techniques use small molecule probes to covalently label active enzymes, while inactive enzymes remain unmodified. By including reporter tags in these probes, it is possible to quantitatively report differences in levels of active enzyme within complex proteomic samples.

This chapter will describe the contributions made by ABPP to the understanding of host-virus interactions. ABPP has supplied a diverse toolbox of activity-based probes which have been applied to study both viral and host enzymes: identifying host enzymes dysregulated during different stages of viral infection, determining how the virus effects these changes, and characterizing viral enzymes' functionalities, structure, and catalytic and inhibitory mechanisms (Fig 1.2).

1.2 Viral entry

For most viruses, the entry process consists of recognition of their target cell, attachment to the cells' membrane, internalisation of the virus into the cell, usually by an endocytic pathway, and the release of viral genetic material into the cytosol of the cell. In the case of enveloped viruses, this requires the fusion of the viral envelope with the endosomal membrane to form a pore through which the genetic material

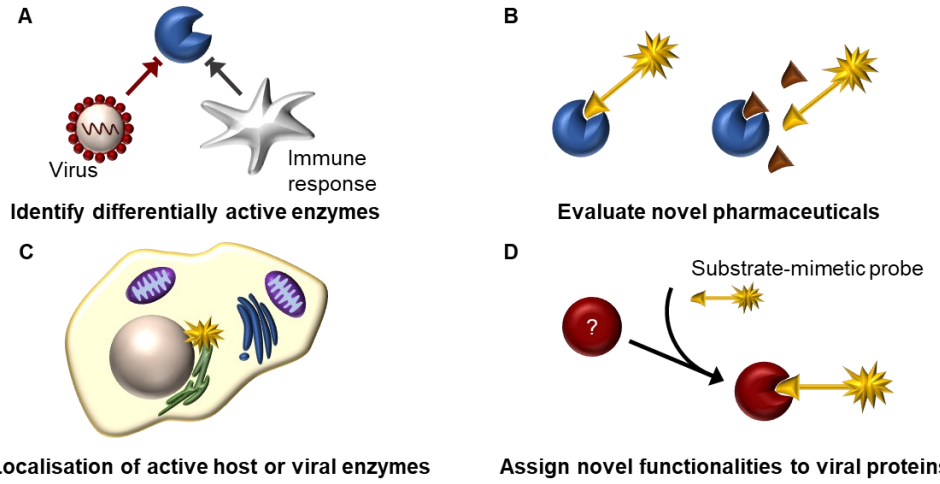

Figure 1.2: Contributions of ABPP to the understanding of host-virus interactions. A) Activity-based profiling identifies and quantifies changes to enzymatic activity caused by the virus or by the host's anti-viral defense mechanisms. B) Competitive activity-based labelling evaluates the effectiveness of novel anti-viral compounds. C) Fluorophore conjugated activity-based probes allow imaging of active enzyme localisation. D) Activity-based labelling with substrate-mimetic activity-based probes identifies new targets for viral enzymes.

passes. The mechanism of formation of this pore varies between viruses, many of which require significantly different host cell conditions or factors to induce fusion.

A major focus in efforts to design novel pharmaceuticals has been the development of cell entry inhibitors. Targeting cell entry prevents the spread of infection as well as the irreversible damage to tissues caused by infection. Furthermore, as host factors and not viral factors are usually targeted, it can impede the emergence of drug-resistant strains. Anti-viral pharmaceuticals targeting cell entry have been developed against hepatitis B virus, human immunodeficiency virus (HIV) and herpesviruses,[9–11] and entry inhibitors against other viruses such as HCV are currently being developed.[12,13]

Viruses such as the SARS coronavirus have been shown to require the activity of lysosomal cathepsins, such as cathepsin L, in order to enter the cytosol.[14] Cathepsin L cleaves the SARS-CoV spike protein, found on the viral envelope, thereby activating it and allowing membrane fusion to proceed.[14] It has furthermore been demonstrated to play an accessory role in Ebola infection, cleaving the GP1 protein in conjunction with cathepsin B and triggering membrane fusion.[15] The epoxide-based peptide-mimetic probe DCG-04 was developed to label cysteine proteases, a class which includes cathepsins.[16] Shah *et al* applied this probe to study novel entry inhibitors of the SARS and Ebola viruses by competitive ABPP, wherein the inhibition of ABP-labelling of enzymes by inhibitors is measured.[17] Cells treated with their novel inhibitors demonstrated significantly reduced labelling by DCG-04, indicating that they were able to target cathepsin L in live cells, and suggesting that they inhibited viral entry by targeting cathepsin L.[17] This study demonstrates how an ABP can be applied in the development of novel pharmaceuticals targeting cell entry.

1.3 Viral replication

Members of the *flaviviridae* family significantly remodel their host cell architecture to form an environment favourable for replication. The hepatitis C virus, one of the most studied viruses from this family, induces the formation of double membrane vesicles inside a membranous web derived from the endoplasmic reticulum.[1] The formation of the membranous web during HCV infection necessitates significant alterations to the local lipid profile, which result from viral hijacking of lipid metabolic enzymes.[1] Activity-based protein profiling has been used to identify which enzymes are targeted by the virus, and to determine how their regulation is modulated.

1.3.1 Role of triglycerides

One of the most pronounced HCV-induced changes to cell architecture is the appearance of larger and more numerous lipid droplets near sites of viral replication.[1] This is the result of both increases in fatty acid synthesis and decreases in fatty acid oxidation and secretion.[18]

Fatty acid synthase (FASN), the enzyme responsible for *de novo* synthesis of fatty acids, was associated with HCV replication as early as 2002; however the nature of the interactions between HCV and FASN were not completely characterised.[19] A probe based on the β-lactone inhibitor orlistat, orlistat-alkyne, shown to strongly and selectively label active FASN,[20] was used to investigate how HCV altered FASN activity. By comparing changes in protein expression and probe labelling, Nasheri *et al* determined that FASN activity was significantly enhanced during HCV replication by increases both in protein expression as well as post-translational activation.[21] Imaging of active FASN using the orlistat-alkyne probe demonstrated that HCV does not alter the localisation of active FASN, indicating that the post-translational regulation of FASN occurs by another mechanism.[21] Increased activity of FASN during HCV replication was further confirmed using probes containing a β-lactam warhead.[22]

HCV-mediated upregulation of intracellular lipids has been shown to be regulated via numerous mechanisms: in addition to increases in lipid synthesis, decreases in lipolysis and lipid secretion have also been demonstrated to play a significant role.[18] Singaravelu *et al* used a novel activity-based probe with a phenyl sulfonate ester warhear (PS) to identify enzymes displaying differential activity during HCV replication.[23] The PS probe was shown to label an enzyme involved in the β-oxidation of fatty acids, the electron transfer flavoprotein subunit alpha (ETFA). Comparison of labelling in HCV-replicating and naïve cells shows a decrease in ETFA activity during HCV replication, suggesting that targeting of ETFA may be a mechanism by which HCV reduces lipid oxidation and increases intracellular lipid levels.[23]

In a more recent study, Nourbakhsh *et al* used a fluorescently labelled fluorophosphonate probe (Fig 1.3a shows a desthiobiotin-labelled variant) to profile serine hydrolase activity in infected versus naïve hepatoma cells. They identified one enzyme, arylacetamide deacetylase (AADAC), which was significantly down-regulated during HCV infection.[24] It was subsequently demonstrated that AADAC induces lipolysis and VLDL secretion of lipids, thereby decreasing the levels of intracellular triglycerides.[24] Altogether, this study demonstrated that HCV decreases the activity of the serine hydrolase AADAC in order to increase intracellular lipid levels via the inhibition of lipolysis and lipid secretion.

1.3.2 Role of phosphatidylinositides

Phosphatidylinositides (PIs) are minor components of intracellular membranes which play important roles in establishing organelle identity and in propagating cell signalling, and certain species have additionally been shown to be able to induce high membrane curvature.[25] A phosphorylated species of PI, PI4P, has been shown to be upregulated in the membranous web induced by HCV and other closely related viruses; it has been hypothesised that this plays a role in establishing the morphology of the

membranous web.[5,26] PI4P is synthesised from PI by four PI-kinases (PIKs) which are differentially localised within the cell.[26] The identity of the kinases which contribute to HCV-mediated up-regulation of PI4P levels within the replication complex has been a subject of significant interest.[26,27] While PIKs such as PI4KA are well-established as HCV host factors, the role of other PIKs, such as PI4KB, during infection remained ambiguous.[27]

In order to investigate the activity of PI4Ks during HCV infection, Sherratt *et al* synthesised a novel activity-based probe, PIKBPyne, derived from the well-known reversible PIK active-site inhibitor PIK93.[28] (Fig 1.3b) The warhead of this probe contained a PIK93 group to enable selective interaction with active PIKs, and a UV-inducible benzophenone crosslinker to form a covalent bond between the probe and its protein target. Using this probe, it was shown that PI4KB activity, but not expression, is upregulated by HCV infection.[28] This finding illustrates the important role ABPP can play in characterising the dysregulation of host factors by viruses.

1.3.3 Role of cholesterol

The double-membrane vesicles of the HCV replication sites have been shown to contain elevated levels of cholesterol.[1] Activity-based probes have been applied to characterise the processes by which cholesterol metabolism is hijacked during HCV replication.

Fluorophosphonate-based probes were used to profile serine hydrolase activity during HCV replication, in order to identify enzymes differentially regulated by the virus.[29,30] Carboxylesterase 1 (CES1), a liver-abundant serine hydrolase which displays cholesteryl ester hydrolase activity, was identified as a target of activity-based labelling by both fluorophosphonate-based and peptide-based probes containing either a serine or a threonine moiety.[29–31] CES1 activity plays a role in decreasing the levels of intracellular cholesteryl ester, as well as the secretion of intracellular triglycerides by the VLDL pathway.[31,32] CES1

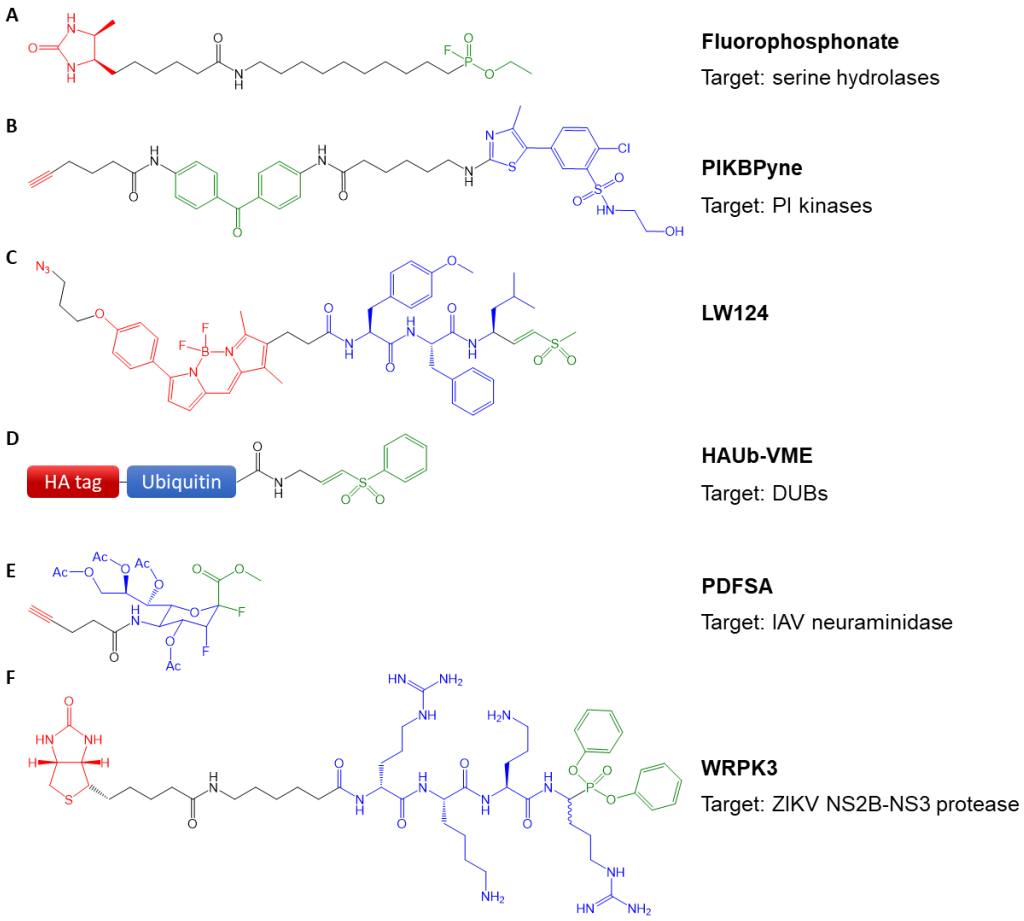

Figure 1.3: Examples of types of activity-based probes used to interrogate host-virus interactions. Targeting groups shown in blue, reactive groups shown in green, and reporter tags or handles for attachment of reporter tags shown in red. A) Inhibitor-based fluorophosphonate conjugated to desthiobiotin possesses a broad specificity towards host cell serine hydrolases. B) Inhibitor-based PIKBPyne labels specific host cell lipid kinases, phosphatidylinositol kinases type III. C) Peptide-mimetic LW124 selectively labels proteasomal subunit β5 and immunoproteasomal subunit β5i. The BODIPY group allows LW124 to be used as a fluorescent probe, while the azide handle allows the attachment of affinity tags for purification of labelled targets. D) Substrate-mimetic HAUb-MVE targets deubiquitinating enzymes from both viruses and host cells. The HA tag allows detection of labelling and purification of labelled enzymes. E) Substrate-derived PDFSA targets neuraminidases on the envelope of the influenza A virus. F) Peptide-based WRPK3 contains unnatural amino acids and specifically labels Zika virus NS2B-NS3 protease.

activity is not always correlated to its expression, suggesting that the regulation of CES1 function relies on post-translational modifications and interactions.[31] Activity-based labelling is therefore ideally suited for interrogating the function of CES1. Both flurophosphonate and the peptide-based probes demonstrated significantly increased activity during HCV replication, suggesting that CES1 is activated as part of the host cell's anti-viral strategy to counteract the virally-induced increases in cholesterol and triglycerides.[29,30]

β-lactam warhead probes, described above, have also been used to investigate cholesterol metabolic enzymes. These probes have been shown to label hydroxymethylglutaryl-CoA synthase 1 (HMGCS1), an enzyme which catalyses an early step in cholesterol synthesis.[22,33] Labelling with the β-lactam probe showed an increases HMGCS1 activity during HCV replication, suggesting that differential activation of this enzyme is a mechanism by which HCV induces the formation of a favourable replication environment.[22] This finding provided further confirmation of the suggested role of HMGCS1 in HCV infection.[34]

This section has described ABPs which target lipid metabolic enzymes and how they have been used to profile changes to the regulation of lipids during viral infection. Hijacking of lipid homeostasis is a major contributor to the diversion of metabolic energy during infection. However, other metabolic pathways are also perturbed during infection: glycolysis in particular is targeted by multiple diverse viruses, including HCV, influenza A virus, and several herpesviruses, though the mechanisms by which glycolysis is mis-regulated are not fully understood.[35] The development of novel probes targeting glucose metabolic enzymes represents an opportunity to increase our understanding of metabolic flux during viral infection.

1.4 Programmed cell death

A fundamental aspect of the innate immune response to infection lies in the activation of apoptotic and cell death pathways upon viral invasion of the cell in order to restrict the spread of infection throughout the host.[36] Commercial peptide-based probes, FLICA™, have been established as chemical-based tools to study apoptosis.[37] These probes are designed to report on the activity of caspaces, enzymes essential to the progression of apoptosis.[37] Using these probes, Furman *et al* determined that norovirus infection induces apoptosis, as demonstrated by the significant increase in caspace activity. Mass spectrometry analysis of enzymes labelled by these probes revealed that they are equally capable of reporting on the activity of the cysteine protease cathepsin B. It was shown that cathepsin B is activated during norovirus infection, and acts as an upstream activator of the apoptotic pathway.[37]

Cathepsin D is a lysosomal aspartic peptidase which has also been shown to induce apoptosis.[38] Using a peptide-based probe containing a phenylalanine targeting group, Blais *et al* demonstrated that HCV significantly down-regulates the activity of cathepsin D, suggesting that HCV decreases cathepsin D activity in order to avoid apoptosis of infected cells.[30] Activation of anti-apoptotic genes was also demonstrated during infection of Dengue virus, a close relative of HCV. Novel ATP-based probes containing acyl phosphate warheads were used to profile the activity of kinases during Dengue infection.[39] The activity of DNA-dependant protein kinase (DNA-PK), an anti-apoptotic enzyme which recognises and repairs DNA double-stranded breaks, was shown to be significantly upregulated by Dengue infection.[39] Altogether, ABPP has shown that both HCV and Dengue virus act to counteract the activation of the apoptotic pathway.

1.5 Viral evasion of the immune response

In addition to their role in apoptosis, cathepsins are also involved in the regulation of inflammation and the recruitment of the adaptive immune response during infection. Cathepsin G, for example, participates

in the degradation of proteins for presentation by the major histocompatibility complex,[40] and has also been shown to negatively regulate STAT5 transcriptional activation,[41] as well the inflammatory response.[40] A novel peptide-based probe, Mars116, developed to label cathepsin G, was used to investigate the immune response during Epstein-Barr virus (EBV) infection. Labelling with Mars116 showed a significant decrease in cathepsin G activity 12 days after infection. The activity of four other cathepsins, cathepsins X, B, and S, by DAP22c, another peptide-based ABP, were similarly down-regulated. This decrease in the activities of immune-linked cathepsins is suggestive of an immune escape strategy by EBV.[42]

1.5.1 Viral alterations to proteasome activity

The proteasome is a multi-subunit structure responsible for the degradation of damaged or excess proteins within the cell, and plays an essential role in protein quality control, cell signalling, immune responses, and apoptosis.[43] A specialised form of the proteasome, the immunoproteasome, consists of many of the same regulatory subunits in addition to three variant catalytic subunits found only in the immunoproteasome.[44] This specialised form of the proteasome plays a role in directing the activity of the adaptive immune system. It is induced during infection and generates peptides with a hydrophobic C terminus for cell-surface display in MHC class I molecules. CD8 T cells survey these peptides and propagate an immune response upon recognition of foreign material.[44] The existence of mixed proteasomes, containing both the constitutively expressed and immunoproteasome subunits, has also been demonstrated, indicating that both categories of catalytic subunits could be implicated in immune response.[43]

The catalytically active proteasomal subunits, though they are threonine and not serine hydrolases,[45,46] have been shown to be labelled by the activity-based probe fluorophosphonate.[47] (Fig 1.3a) Using a fluorophosphonate-based probe, Shahiduzzaman *et al* have shown that the activity of several proteasomal

subunits, PSMA2, PSMA3, PSMA6, PSMB3, increased during influenza A infection, most likely due to increases in immunoproteasome activation as part of the anti-viral response.[47] Monitoring the activity of the immunoproteasome in this manner has the potential to provide valuable information of the extent of the immune response to various pathogens. However, a complete understanding of the activity of this complex cannot be achieved through flurophosphonate alone, as, although it was able to interrogate the activity of a few proteasomal subunits, several other subunits were not detected.

Probes able to specifically and quantitatively assess the activities of all the possible catalytic subunits of the proteasome have been developed by various groups over the past decade. The first to be developed, MV151, is a peptide-mimetic probe conjugated to a BODIPY fluorophore, and labels all catalytically active proteasome subunits.[48] Other more specific probes were later developed: LW124, a probe specific for the β1 subunit and LMP2, its immunoproteasome analogue, and MVB127, a probe specific for β5 and its analogue LMP7.[49,50] (Fig 3c)

These probes were applied by Keller *et al* to investigate perturbation to the proteasome system during viral infection. Proteasome activity was shown to be increased during murine gamma-herpes virus infection using the general-use MV151 probe. LW124 and MVB127 were used to assess the changes to catalytic activity of the proteasomal subunits versus the activity of their immunoproteasomal analogues during infection. The identity of the labelled subunits was determined based on their reactivity and their molecular weight, as determined by in-gel fluorescent imaging. It was demonstrated that while the activity of the proteasomal subunits remained relatively unchanged, the activity of the immunoproteasome subunits increased significantly during the early stages of infection, before decreasing as the infection progressed.[50] While these probes had been previously demonstrated to be specific proteasome probes,[48,49] Keller *et al* were the first to demonstrate how they can be used to

specifically assess regulatory changes to the activity of the immunoproteasome in the context of viral infection.[50]

These increases in proteasome activity represent part of the host's response to viral infection, wherein proteasomal degradation of proteins is increased in order to generate antigenic peptides for the recruitment of the adaptive immune response. Viral targeting of proteasomal activity could therefore be a potential immune evasion strategy. Recently, Nasheri *et al* used a β-lactone based activity-based probe, orlistat-alkyne, to label active proteasome subunits and thereby interrogate proteasome activity during hepatitis C virus infection.[46] It was shown that the activity of multiple members of the proteasome system displayed decreased activity in HCV infected cells. PSMB5, which displays broad specificity and chymotrypsin-like hydrolase activity,[45] PSMC6, an ATPase which regulates proteasome activity,[51] and two immunoproteasomal subunits, PSME1, and PSME2 [52] were down-regulated between 40% to 80%.[46] Interestingly, changes to protein expression did not match the observed changes in enzymatic activity.[46] Altogether, this suggests that HCV targets proteasomal degradation by altering both protein expression and post-translational regulation as part of its efforts to evade the immune response. Altogether, these studies describe multiple activity-based protein profiling tools which, in addition to traditional proteomics, can be used to gain a better understanding of the virally induced perturbation of host cell systems.

1.5.2 NFκB signalling during herpesvirus infection

Nuclear factor κB (NFκB) is a transcription factor, activated during viral infection, which induces the expression of genes involved in the innate immune response.[53] The signalling cascade which is responsible for the activation of NFκB during infection relies in great part on the ubiquitination of key signal transducers.[54] The auto-ubiquitination of the ubiquitin ligase TRAF6 promotes the activity of the TAK1 kinase.[54] The IκB kinase (IKK) complex is then activated via TAK1-mediated phosphorylation

and TRAF6-mediated ubiquitination.[54,55] Phosphorylation of IκB results in its ubiquitination and subsequent degradation.[53] NFκB is sequestered in the cytoplasm by IκB; upon its degradation, NFκB translocates to the nucleus and induces the expression of anti-viral, pro-inflammatory, and pro-apoptotic genes.[53]

The activity of enzymes responsible for the regulation of ubiquitination is therefore of interest when investigating host-virus interactions due to the importance of ubiquitination to the immune response to infection. Deubiquitinating enzymes (DUBs) are enzymes responsible for removing ubiquitin from ubiquitinated proteins. As they are cysteine proteases, they are excellent candidates for activity-based probes.[56]

HAUb probes are based on modified ubiquitin proteins, and mimic the natural substrate of DUBs, allowing them to specifically target DUBs. Ubiquitin is recombinantly expressed with the haemagglutinin tag HA, which functions as a reporter of enzyme labelling. A thiol-reactive group functioning as the warhead is subsequently added to the C-terminus via intein-based chemical ligation. Several variants were produced, containing a several different warheads: chloroethylamine (Cl), bromoethylamine (Br2), bromopropylamine (Br3), glycine vinylmethylsulfone (VS), glycine vinyl methylester (VME), glycine vinyl phenylsulfone (VSPh), and glycine vinylcyanide (VCN).[56] Immunoblotting and MS/MS profiling of labelled DUBs demonstrated a slight but significant difference in the labelling patterns of the HAUb probes [56,57]. The probe containing vinyl methylester warhead (HAUb-VME, Fig 1.3d) displayed the broadest labelling capacity and was used in most subsequent studies.[56,57]

After developing these probes, Ovaa *et al* applied them to interrogate the activity of host cell deubiquitinating proteins during infection by EBV.[57] Herpesviruses, such as EBV, are large double-

stranded DNA viruses and have been shown to modulate the immune response via multiple different mechanisms.[58] Using the HAUb-VME probe, Ovaa *et al.* labelled active host cell deubiquitinating enzymes, and identified multiple DUBs whose activity was increased during infection: UCH-L3, USP15, UCH-L1, UCH37, USP7, and USP9X. Several of these enzymes have been shown to regulate the NFκB pathway. USP15 negatively regulates NFκB activation by deubiquitinating IκB,[59] while USP7 decreases NFkB signalling by deubiquitinating TRAF6 and IKK.[60] USP37, on the other hand, has been shown to be required for IκB-α degradation and therefore NFkB activity.[61] Altogether, Ovaa *et al* demonstrated that the herpesvirus EBV differentially regulates DUBs implicated in the regulation of the innate immune response, suggesting a pro-viral immune evasion mechanism.

1.5.3 Virally-encoded deubiquitinases

Kattenhorn *et al* applied the HAUb-VME probes designed by Borodovsky *et al* to study the perturbation of ubiquitination-regulating enzymes during infection of Herpes simplex virus 1 (HHV-1), a herpesvirus related to EBV. MS/MS analysis of labelled proteins identified an enzyme which did not correspond to any known DUB, and whose sequence was found to correspond to a viral protein with unknown function, the large tegument protein deneddylase (UL36).[62]

Perturbation of the host cell by viruses is usually indirect, as the limited size of viral genomes means the virus cannot itself encode the functionalities it requires. Herpesviruses, however, are large, double-stranded DNA viruses, and possess larger and more complex genomes than the simpler RNA viruses discussed elsewhere in this chapter. HHV-1, for example, encodes approximately 80 proteins.[63]

As UL36 does not share significant sequence homology with any other DUB known at the time,[62] tradition bioinformatics could therefore not have predicted its function. This discovery highlights one of the unique advantages of activity-based protein profiling: it reports directly on the functional output of

an enzymes and allows the identification of novel targets. UL36 has recently been shown to deubiquitinate IκBα, preventing its degradation and promoting the sequestration of NFκB outside of the nucleus, and thereby interfering with the activation of the innate immune response.[64]

Following this discovery, several research groups postulated the existence of homologous deubiquitinating enzymes in closely related viruses whose function had remained undiscovered due to their lack of homology to previously characterised DUBs. Having been established as an effective probe of herpesvirus deubiquitinating enzymes, HAUb-VME was used to interrogate the activity of viral proteins from several different viruses.

Schlieker *et al*. identified an Epstein-Barr virus protein, BPLF1, and a murine cytomegalovirus protein (MCMV), M48, which possessed significant sequence homology to the HHV-1 UL36.[65] They subsequently demonstrated that both BPLF1 and M48 were labelled by the HAUb-VME probe, indicating that these proteins were enzymes which targeted and hydrolysed ubiquitinated proteins.[65] It was later shown that BPFL1 acts similarly to HHV-1's UL36, inhibiting the activation of NFκB by catalysing the removal of ubiquitin from the sequestering protein IκBα.[55] It has furthermore been demonstrated that BPLF1 exerts additional control over the NFκB pathway, deubiquitinates both TRAF6 and subunits of IKK, thereby inhibiting the propagation of toll-like receptor (TLR) signalling and the resultant activation of NFκB.[55,66] Taken together, this demonstrates that EBV uses the virally encoded DUB functions to inhibit the activation of the anti-viral innate immune response.

Another herpesvirus, human cytomegalovirus (HCMV), has also been shown to encode a deubiquitinating enzyme.[67] HAUb-VME labelled a high molecular weight enzyme, pUL48, whose role in infection had previously been unknown. In the absence of pUL48 deubiquitinating activity, virion production was significantly inhibited, though not entirely blocked, indicating that pUL48

deubiquitinating activity contributes to, but is not required for, virion production. HAUb-VME has also been used to identify similar deubiquitinating proteins in murine gamma herpesvirus 68 (MHV-68) and Marek's disease virus (MDV).[68,69] Competitive ABPP was later used to characterise the catalytic mechanism of deubiquitinating enzymes: UL36, the deubiquitinating enzyme of Marek's disease virus, was shown to be a cysteine protease,[70] which suggests the other closely-related enzymes identified by HAUb-VME may possess this mechanism as well.

Assigning novel functionalities is one of the more well-known uses of ABPP, and an essential primary step in characterising poorly understood enzymes which opens up further avenues of investigation. Identifying the reactivity of an enzyme allows the determination of its specific targets and therefore its biological role. The ubiquitin chains targeted by the DUBs discussed in this section are linked to each other by one of seven different linkage sub-types, corresponding to the location of the lysine residue to which the next ubiquitin is bound: Lys^{6}, Lys^{11}, Lys^{27}, Lys^{29}, Lys^{33}, Lys^{48}, and Lys^{63}. New diUb-VME probes were developed containing two ubiquitin moieties conjugated by one of the seven possible linkage types, thereby allowing the determination of DUB's linkage specificity.[71] These probes were used to interrogate the substrate specificity of the SARS coronavirus papain-like protease (PLPro), a dubiquitinating enzyme, thought to play a role in innate immune evasion.[72] The structural basis of PLPro's specificity was determined by co-crystallising it in conjunction with a diUb-VME probe. Co-crystallisation of enzymes with their substrates is often challenging, as the enzyme will catalyse the substrate and release the products. Using a substrate-mimetic ABP ensures that it is retained within the active site, preserving the interactions which give rise to specificity as well as the active conformation of the enzyme. This showed that PLpro interacts with the two ubiquitin moieties, but has few interactions with the interface between the two,[72] suggesting that specificity originates from the orientation of the ubiquitin proteins in the S1 and S2 pockets, and not from recognition of the linkage itself. Screening with a panel of Ub-VME probes containing mono-Ub or di-Ub and possessing different linkage types

demonstrated that PLpro possessed a similarly low labelling efficiency for mono-Ub and most di-Ub probes.[72] This lends further support to the idea that interactions with a properly-oriented S2 ubiquitin stabilise the enzyme-substrate complex and contribute to the specificity of SARS PLPro.

In this section, a number of probes against deubiquitinating enzymes – both host and virally derived – have been described. Future work using these probes to characterise the selectivity of these deubiquitinating proteins has the potential to provide both a clearer understanding of the nature of their targets and the pathways they control.

1.6 Viral assembly and egress

The last stage of the viral life cycle consists of the assembly of the viral particle and its release into the extracellular space. The majority of the contributions made by ABPP towards the understanding of virus infection have focused on viral entry and replication. In some cases, this has been due to limitations in cell culture models of infection: these models could replicate the genome but were unable to efficiently assemble infectious particles.[73] As viral assembly and egress do rely on host factors to translocate to the plasma membrane and exit the cell, profiling enzymatic activity during these processes is of significant interest.

Hijacking of cellular trafficking plays a significant role in the packaging and secretion of viruses. The COPI system is essential for correct localisation of influenza A virus (IAV) particles, while HCV utilises the COPII system to travel from the ER to the Golgi, at which point they can be trafficked through the VLDL secretory pathway.[74,75] These systems are regulated in part by Rab GTPases, host cell enzymes which play an important role in trafficking throughout the cell,[76] and which have been implicated in the egress of multiple viruses.[74,77,78] Rab11 has been shown to be essential for the trafficking of IAV RNA from the perinuclear region to the plasma membrane.[74] Another Rab protein, Rab1, has been proposed

to mediate transport of nascent HCV virions from the ER to the Golgi.[77] Rab proteins have also been shown to play a role in DNA virus egress in the case of herpesviruses.[78] Altogether, this suggests that Rab GTPase activity could be an interesting target for activity-based profiling during viral infection.

IAV budding been shown to involve the activity of a class of ATPases, the mitochondrial F1FO-ATPases. These enzymes localise to the plasma membrane and are necessary for efficient budding of new virions, though the precise nature of their contribution has yet to be fully understood.[74] ATP-based probes have previously been used to profile host enzyme activity during Dengue infection,[39] and applying them to profile the changes in activity of various ATPases during IAV infection could yield new information with regards to how enzymes are recruited and utilised during viral egress.

Lipid regulatory systems, which play an important role in earlier stages of viral life cycles, continue to play an important role in viral egress. HCV once again provides a good example of this dependence on host lipids, as its egress relies on the very-low-density-lipoparticle (VLDL) secretory pathway to release the mature virus particle into the bloodstream.[1] Certain VLDL-associated enzymes, such as the triglyceride-recruiting enzyme ABHD5 or the phospholipid synthesis enzyme LPCAT1, have been identified as pro- or anti-viral HCV host factors. However, the interactions between these enzymes and HCV is not fully understood.[79,80] Interrogating enzymes which regulate the VLDL pathway could therefore reveal novel information clarifying how it is hijacked by HCV. Even viruses such as influenza, which do not rely on a lipid secretory pathway, still alter the cell's lipid profile in order to exit into the bloodstream.[74] Influenza virus egress occurs by budding from the plasma membrane, a process requiring an altered membrane lipid composition.[74] Profiling changes to lipid regulatory networks during the assembly and egress of virions could therefore yield new information and improve our understanding of host-virus interactions during the late stages of infection of a diverse set of viruses.

In general, activity-based profiling on these later stages of viral infection has the potential to uncover novel host factors requirements for productive infections. Targeting the secretion of new virions could play an important role within combinatorial anti-viral strategies to limit the spread of viral infections.

1.7 Selective labelling of individual viral enzymes

Selective labelling of viral enzymes enables the measurement of their activity within a complex proteome. While viral enzymes can be labelled by broadly-reactive probes such as fluorophosphonate or HAUb-VME, as discussed in the preceding sections, it can be difficult to detect them amongst the more numerous host cell enzymes which are labelled simultaneously.[30] For this reason, specific and selective probes have been developed against multiple viral enzymes.

The infectious particle of IAV, the most common cause of the flu, incorporates two viral enzymes on its surface, haemagglutinin (HA) and neuraminidase (NA).[81] NA is known to play many roles; the most well-established being its sialidase activity which cleaves sialic acid from the nascent virions following virion secretion [81]. NA enzymatic activity has also been suggested to play a role in viral entry, though the mechanism by which this could occur has not been well established.[81,82] The NA active site is highly conserved between strains of IAV strains, making NA an attractive target for chemical probes as well as therapeutic drugs.[81]

In 2005, Lu *et al* reported the synthesis of a mechanism-based neuramidinase probe, consisting of a sialic acid targeting moiety and an *ortho*-difluoromethylphenyl warhead attached to a biotin reporter tag.[83] They demonstrated that this probe was able to specifically label neuraminidases, and could be used to detect neuraminidase activity. Of particular interest in this study was a demonstration of a more uncommon application of activity-based probes for isolation of viral particles. Immobilised probe bound to NA enzymes present on the particle surface, thereby enabling the isolation of the entire virion.[83] While

this probe was able to form a covalently label IAV NA, there were several limitations. Its large size and multiple rings necessitated millimolar concentrations to label even purified protein. The probe was also unable to penetrate cell membranes, which precluded the application of this probe in complex systems. Lastly, though the sialic acid did convey some selectivity, the difluoromethylphenyl warhead nevertheless reacted non-specifically with multiple targets in a complex environment.[84]

A more streamlined probe was reported by Tsai *et al.* Instead of the inclusion of a separate warhead group in addition to the sialic acid moiety, the sialic acid sugar was modified to include fluorine at C2 and C3, displacing a hydroxyl group and a hydrogen, respectively. The electron-withdrawing property of the fluorines transforms the probe into an irreversible mechanism-based inhibitor. Two probes were made: DFSA and an ester-protected probe, PDFSA, both containing the sialic acid warhead and an alkyne handle.[84] (Fig 1.3e) PDFSA is able to label NA *in situ* at micromolar concentrations, allowing imaging of sub-cellular localisation of the viral enzyme during infection.[84] PDFSA was able to label wild-type NA as well as mutant NA resistant to active-site anti-virals, indicating that this probe could be applied to screen for the presence of drug-resistant strains by competitive ABPP.[84]

The Zika virus has recently been the subject of international attention following the South American outbreak which caused a dramatic increase in the rates of microencephaly in newborn infants.[85] The Zika virus, like most positive-strand RNA viruses, encodes a serine protease, NS3, which cleaves the precursor polyprotein into the mature viral proteins. As activity of the NS3 protease is essential to the establishment of a productive infection, the development of tools capable of characterising its activity and regulation is of great interest.

Proteases are capable of displaying high selectivity for the specific amino acid sequences they cleave. While it is possible to design activity-based probes based on these sequences, these probes risk lacking

specificity to individual proteases due to the overlapping substrate specificity of closely related enzymes. Recently, this problem was addressed by using unnatural amino acids to expand the chemical space of their peptides' building blocks. The Hybrid Combinatorial Substrate Library (HyCoSuL) uses 102 unnatural amino acids in addition to the twenty canonical ones to build optimal substrates containing a variable 4-amino acid sequence targeting the S1-S4 pockets of the protease active site.[86] To allow specific activity-based labelling, a fluorogenic coumarin and a diphenyl phosphate warhead are added.[86] This library has previously been used to design probes targeting human proteases.[87–89] Recently, the HyCoSuL methodology was applied to design a probe, WRPK3, which rapidly labels Zika's NS3 protease at low nanomolar concentrations.[90] (Fig 1.3f) This same methodology was subsequently used in the study of the proteases from the closely related Dengue and West Nile viruses. A small library of probes were developed, including probes capable of selectively labelling proteases from a single virus, as well as less-specific pan-viral probes which targeted proteases from Dengue, West Nile, and Zika viruses.[91] These probes have the potential to be applied to interrogate NS3 activity during flavivirus infection, and demonstrate a useful application of unnatural amino acids which has the potential to be used to design activity-based probes against other viral proteases.

ABPs against proteases from Enterovirus 71 and Middle Eastern Respiratory Syndrome viruses have recently been reported.[92] Contrary to the above example, the design of these probes was based on previously established inhibitors possessing a loosely peptido-mimetic structure. Labelling of the viral protease by these probes in the context of an infection of a host cell revealed the existence of host proteins capable of targeting similar substrates. Further investigation revealed that the activity of host proteases contributed to the cleavage of the viral polyprotein, and could compensate for the absence of the viral protease.[92] The development of novel anti-virals often focuses on discovering selective inhibitors against the viral protease;[93–98] this study implies that this strategy may not be sufficient to prevent polyprotein cleavage and the propagation of the virus.

The above examples of virus-targeting probes were designed by mimicking the natural substrate of the enzyme: either carbohydrates or peptides. However, viral polymerases and transcriptases play essential roles in the viral life cycle, and therefore represent important targets both for the study of viral function and for the development of novel drugs.[99–104] One of the most-targeted viral enzyme in HIV drug therapies is the reverse transcriptase (RT).[105] A nucleic acid-mimetic probe was recently developed which labels the active form of this enzyme favourable compared to the inactive form. Furthermore, by conjugating this probe with a known RT inhibitor to form a bifunctional molecule, a significant increase to the inhibition of the RT potential was achieved.[106]

1.8 Conclusions

Over the past decades, activity-based protein profiling has proven to be a useful chemical proteomics tool for the interrogation of the role enzymes play in viral infection, providing information not otherwise accessible by traditional genomic and proteomic methods. ABPP has been used to quantify enzymatic activity, detect changes in the localisation of active enzymes, identify protein-protein interactions regulating activity, and assign novel functionalities to proteins playing important roles in viral infection. When considered as a part of a larger body of research, they have greatly contributed to our understanding of viral infection and host response.

1.9 Thesis objectives

The hepatitis C virus, as of 2015, is thought to currently infect over 70 million people world-wide. Approximately 20% of chronically infected individuals will develop severe complications, the most common of which are decompensated cirrhosis of the liver and hepatocellular carcinoma.[107] These are the result of HCV-induced dysregulation of intracellular systems, which occurs as the virus attempts to alter the cellular environment to favour the production of novel virions and to avoid the immune response mounted by the host. Infected cells display an increase in the unfolded protein response as well as

autophagy, while the mitochondrial network is fragmented in order to mitochondrially-mediated immune activation.[1] As discussed earlier in this chapter, the lipid profile and metabolism of the cell undergo a significant alteration, which results in the establishment of a pro-viral and pro-oncogenic environment.[108] In addition to the hepatic pathologies mentioned above, the compromised function of the liver results in myriad extrahepatic morbidities, including diabetes, renal disease, and cardiovascular disease, among others.[107]

To gain a better understanding of how these dysregulations of cell systems occur, activity-based protein profiling has been applied to identify modulations of enzyme activity resulting from host-pathogen interactions during infection by the hepatitis C virus. In the second chapter, a kinase-directed probe is used to profile broadly profile changes to the activity of kinases from a range of cellular pathways during viral replication. In the third, the functions of a targeted activity-based probe are expanded to interrogate protein-protein interactions of active enzymes during viral replication, as well as report on their catalytic activity. In the fourth chapter, an activity-based probe is used to identify functional effectors of a virally-modulated microRNA, miR-27b. The nature of the links between these effectors, miR-27b, and the propagation of the hepatitis C virus is investigated. In the fifth chapter, future research to characterise the mechanisms of virus and miRNA mediated alteration of enzyme activity as well as the results of these alterations are discussed.

1.10 References

(1) Neufeldt, C. J.; Cortese, M.; Acosta, E. G.; Bartenschlager, R. Rewiring Cellular Networks by Members of the Flaviviridae Family. *Nat. Rev. Microbiol.* **2018**, *16* (3), 125–142.

(2) Novoa, R. R.; Calderita, G.; Arranz, R.; Fontana, J.; Granzow, H.; Risco, C. Virus Factories: Associations of Cell Organelles for Viral Replication and Morphogenesis. *Biol. Cell* **2005**, *97* (2), 147–172.

(3) Harak, C.; Lohmann, V. Ultrastructure of the Replication Sites of Positive-Strand RNA Viruses. *Virology* **2015**, *479–480*, 418–433.

(4) Paul, D.; Bartenschlager, R. Flaviviridae Replication Organelles: Oh, What a Tangled Web We Weave. *Annu. Rev. Virol.* **2015**, *2* (1), 289–310.

(5) Hsu, N.-Y.; Ilnytska, O.; Belov, G.; Santiana, M.; Chen, Y.-H.; Takvorian, P. M.; Pau, C.; van der Schaar, H.; Kaushik-Basu, N.; Balla, T.; et al. Viral Reorganization of the Secretory Pathway Generates Distinct Organelles for RNA Replication. *Cell* **2010**, *141* (5), 799–811.

(6) Liang, T. J. Hepatitis B: The Virus and Disease. *Hepatology* **2009**, *49* (S5), S13–S21.

(7) Barglow, K. T.; Cravatt, B. F. Activity-Based Protein Profiling for the Functional Annotation of Enzymes. *Nat. Methods* **2007**, *4* (10), 822–827.

(8) Cravatt, B. F.; Wright, A. T.; Kozarich, J. W. Activity-Based Protein Profiling: From Enzyme Chemistry to Proteomic Chemistry. *Annu. Rev. Biochem.* **2008**, *77* (1), 383–414.

(9) Sun, D.; Zhu, L.; Yao, D.; Chen, L.; Fu, L.; Ouyang, L. Recent Progress in Potential Anti-Hepatitis B Virus Agents: Structural and Pharmacological Perspectives. *Eur. J. Med. Chem.* **2018**, *147*, 205–217.

(10) de Castro, S.; Camarasa, M.-J. Polypharmacology in HIV Inhibition: Can a Drug with Simultaneous Action against Two Relevant Targets Be an Alternative to Combination Therapy? *Eur. J. Med. Chem.* **2018**, *150*, 206–227.

(11) De Clercq, E.; Li, G. Approved Antiviral Drugs over the Past 50 Years. *Clin. Microbiol. Rev.* **2016**, *29* (3), 695–747.

(12) Qian, X.-J.; Zhu, Y.-Z.; Zhao, P.; Qi, Z.-T. Entry Inhibitors: New Advances in HCV Treatment. *Emerg. Microbes Infect.* **2016**, *5* (1), e3.

(13) Xiao, F.; Fofana, I.; Thumann, C.; Mailly, L.; Alles, R.; Robinet, E.; Meyer, N.; Schaeffer, M.; Habersetzer, F.; Doffoël, M.; et al. Synergy of Entry Inhibitors with Direct-Acting Antivirals Uncovers Novel Combinations for Prevention and Treatment of Hepatitis C. *Gut* **2015**, *64* (3),

483–494.

(14) Bosch, B. J.; Bartelink, W.; Rottier, P. J. M. Cathepsin L Functionally Cleaves the Severe Acute Respiratory Syndrome Coronavirus Class I Fusion Protein Upstream of Rather than Adjacent to the Fusion Peptide. *J. Virol.* **2008**, *82* (17), 8887–8890.

(15) Chandran, K.; Sullivan, N. J.; Felbor, U.; Whelan, S. P.; Cunningham, J. M. Endosomal Proteolysis of the Ebola Virus Glycoprotein Is Necessary for Infection. *Science* **2005**, *308* (5728), 1643–1645.

(16) Greenbaum, D.; Medzihradszky, K. F.; Burlingame, A.; Bogyo, M. Epoxide Electrophiles as Activity-Dependent Cysteine Protease Profiling and Discovery Tools. *Chem. Biol.* **2000**, *7* (8), 569–581.

(17) Shah, P. P.; Wang, T.; Kaletsky, R. L.; Myers, M. C.; Purvis, J. E.; Jing, H.; Huryn, D. M.; Greenbaum, D. C.; Smith, A. B.; Bates, P.; et al. A Small-Molecule Oxocarbazate Inhibitor of Human Cathepsin L Blocks Severe Acute Respiratory Syndrome and Ebola Pseudotype Virus Infection into Human Embryonic Kidney 293T Cells. *Mol. Pharmacol.* **2010**, *78* (2), 319–324.

(18) Syed, G. H.; Amako, Y.; Siddiqui, A. Hepatitis C Virus Hijacks Host Lipid Metabolism. *Trends Endocrinol. Metab.* **2010**, *21* (1), 33–40.

(19) Su, A. I.; Pezacki, J. P.; Wodicka, L.; Brideau, A. D.; Supekova, L.; Thimme, R.; Wieland, S.; Bukh, J.; Purcell, R. H.; Schultz, P. G.; et al. Nonlinear Partial Differential Equations and Applications: Genomic Analysis of the Host Response to Hepatitis C Virus Infection. *Proc. Natl. Acad. Sci.* **2002**, *99* (24), 15669–15674.

(20) Yang, P.-Y.; Liu, K.; Ngai, M. H.; Lear, M. J.; Wenk, M. R.; Yao, S. Q. Activity-Based Proteome Profiling of Potential Cellular Targets of Orlistat--an FDA-Approved Drug with Anti-Tumor Activities. *J. Am. Chem. Soc.* **2010**, *132* (2), 656–666.

(21) Nasheri, N.; Joyce, M.; Rouleau, Y.; Yang, P.; Yao, S.; Tyrrell, D. L.; Pezacki, J. P. Modulation of Fatty Acid Synthase Enzyme Activity and Expression during Hepatitis C Virus Replication.

Chem. Biol. **2013**, *20* (4), 570–582.

(22) Nasheri, N.; McKay, C. S.; Fulton, K.; Twine, S.; Powdrill, M. H.; Sherratt, A. R.; Pezacki, J. P. Hydrophobic Triaryl-Substituted β-Lactams as Activity-Based Probes for Profiling Eukaryotic Enzymes and Host-Pathogen Interactions. *ChemBioChem* **2014**, *15* (15), 2195–2200.

(23) Singaravelu, R.; Blais, D. R.; McKay, C. S.; Pezacki, J. Activity-Based Protein Profiling of the Hepatitis C Virus Replication in Huh-7 Hepatoma Cells Using a Non-Directed Active Site Probe. *Proteome Sci.* **2010**, *8* (1), 5.

(24) Nourbakhsh, M.; Douglas, D. N.; Pu, C. H.; Lewis, J. T.; Kawahara, T.; Lisboa, L. F.; Wei, E.; Asthana, S.; Quiroga, A. D.; Law, L. M. J.; et al. Arylacetamide Deacetylase: A Novel Host Factor with Important Roles in the Lipolysis of Cellular Triacylglycerol Stores, VLDL Assembly and HCV Production. *J. Hepatol.* **2013**, *59* (2), 336–343.

(25) McMahon, H. T.; Gallop, J. L. Membrane Curvature and Mechanisms of Dynamic Cell Membrane Remodelling. *Nature* **2005**, *438* (7068), 590–596.

(26) Bishé, B.; Syed, G.; Siddiqui, A. Phosphoinositides in the Hepatitis C Virus Life Cycle. *Viruses* **2012**, *4* (12), 2340–2358.

(27) Delang, L.; Paeshuyse, J.; Neyts, J. The Role of Phosphatidylinositol 4-Kinases and Phosphatidylinositol 4-Phosphate during Viral Replication. *Biochem. Pharmacol.* **2012**, *84* (11), 1400–1408.

(28) Sherratt, A. R.; Nasheri, N.; McKay, C. S.; O'Hara, S.; Hunt, A.; Ning, Z.; Figeys, D.; Goto, N. K.; Pezacki, J. P. A New Chemical Probe for Phosphatidylinositol Kinase Activity. *ChemBioChem* **2014**, *15* (9), 1253–1256.

(29) Blais, D. R.; Lyn, R. K.; Joyce, M. A.; Rouleau, Y.; Steenbergen, R.; Barsby, N.; Zhu, L.-F.; Pegoraro, A. F.; Stolow, A.; Tyrrell, D. L.; et al. Activity-Based Protein Profiling Identifies a Host Enzyme, Carboxylesterase 1, Which Is Differentially Active during Hepatitis C Virus Replication. *J. Biol. Chem.* **2010**, *285* (33), 25602–25612.

(30) Blais, D. R.; Brûlotte, M.; Qian, Y.; Bélanger, S.; Yao, S. Q.; Pezacki, J. P. Activity-Based Proteome Profiling of Hepatoma Cells during Hepatitis C Virus Replication Using Protease Substrate Probes. *J. Proteome Res.* **2010**, *9* (2), 912–923.

(31) Ross, M. K.; Streit, T. M.; Herring, K. L. Carboxylesterases: Dual Roles in Lipid and Pesticide Metabolism. *J. Pestic. Sci.* **2010**, *35* (3), 257–264.

(32) Zhao, B.; Song, J.; St. Clair, R. W.; Ghosh, S. Stable Overexpression of Human Macrophage Cholesteryl Ester Hydrolase Results in Enhanced Free Cholesterol Efflux from Human THP1 Macrophages. *Am. J. Physiol. Physiol.* **2007**, *292* (1), C405–C412.

(33) Mazein, A.; Watterson, S.; Hsieh, W.-Y.; Griffiths, W. J.; Ghazal, P. A Comprehensive Machine-Readable View of the Mammalian Cholesterol Biosynthesis Pathway. *Biochem. Pharmacol.* **2013**, *86* (1), 56–66.

(34) Kapadia, S. B.; Chisari, F. V. Hepatitis C Virus RNA Replication Is Regulated by Host Geranylgeranylation and Fatty Acids. *Proc. Natl. Acad. Sci. U. S. A.* **2005**, *102* (7), 2561–2566.

(35) Goodwin, C. M.; Xu, S.; Munger, J. Stealing the Keys to the Kitchen: Viral Manipulation of the Host Cell Metabolic Network. *Trends Microbiol.* **2015**, *23* (12), 789–798.

(36) Barber, G. N. Host Defense, Viruses and Apoptosis. *Cell Death Differ.* **2001**, *8* (2), 113–126.

(37) Furman, L. M.; Maaty, W. S.; Petersen, L. K.; Ettayebi, K.; Hardy, M. E.; Bothner, B. Cysteine Protease Activation and Apoptosis in Murine Norovirus Infection. *Virol. J.* **2009**, *6* (1), 139.

(38) Benes, P.; Vetvicka, V.; Fusek, M. Cathepsin D—Many Functions of One Aspartic Protease. *Crit. Rev. Oncol. Hematol.* **2008**, *68* (1), 12–28.

(39) Vetter, M. L.; Rodgers, M. A.; Patricelli, M. P.; Yang, P. L. Chemoproteomic Profiling Identifies Changes in DNA-PK as Markers of Early Dengue Virus Infection. *ACS Chem. Biol.* **2012**, *7* (12), 2019–2026.

(40) Burster, T.; Macmillan, H.; Hou, T.; Boehm, B. O.; Mellins, E. D. Cathepsin G: Roles in Antigen Presentation and Beyond. *Mol. Immunol.* **2010**, *47* (4), 658–665.

(41) Schuster, B.; Hendry, L.; Byers, H.; Lynham, S. F.; Ward, M. A.; John, S. Purification and Identification of the STAT5 Protease in Myeloid Cells. *Biochem. J.* **2007**, *404* (1), 81–87.

(42) Zou, F.; Schmon, M.; Sienczyk, M.; Grzywa, R.; Palesch, D.; Boehm, B. O.; Sun, Z. L.; Watts, C.; Schirmbeck, R.; Burster, T. Application of a Novel Highly Sensitive Activity-Based Probe for Detection of Cathepsin G. *Anal. Biochem.* **2012**, *421* (2), 667–672.

(43) Kammerl, I. E.; Meiners, S. Proteasome Function Shapes Innate and Adaptive Immune Responses. *Am. J. Physiol. Lung Cell. Mol. Physiol.* **2016**, *311* (2), L328-36.

(44) Ferrington, D. A.; Gregerson, D. S. Immunoproteasomes. In *Progress in molecular biology and translational science*; 2012; Vol. 109, pp 75–112.

(45) Marques, A. J.; Palanimurugan, R.; Matias, A. C.; Ramos, P. C.; Dohmen, R. J. Catalytic Mechanism and Assembly of the Proteasome. *Chem. Rev.* **2009**, *109* (4), 1509–1536.

(46) Nasheri, N.; Ning, Z.; Figeys, D.; Yao, S.; Goto, N. K.; Pezacki, J. P. Activity-Based Profiling of the Proteasome Pathway during Hepatitis C Virus Infection. *Proteomics* **2015**, *15* (22), 3815–3825.

(47) Shahiduzzaman, M.; Ezatti, P.; Xin, G.; Coombs, K. M. Proteasomal Serine Hydrolases Are Up-Regulated by and Required for Influenza Virus Infection. *J. Proteome Res.* **2014**, *13* (5), 2223–2238.

(48) Verdoes, M.; Florea, B. I.; Menendez-Benito, V.; Maynard, C. J.; Witte, M. D.; van der Linden, W. A.; van den Nieuwendijk, A. M. C. H.; Hofmann, T.; Berkers, C. R.; van Leeuwen, F. W. B.; et al. A Fluorescent Broad-Spectrum Proteasome Inhibitor for Labeling Proteasomes In Vitro and In Vivo. *Chem. Biol.* **2006**, *13* (11), 1217–1226.

(49) Li, N.; Kuo, C.-L.; Paniagua, G.; van den Elst, H.; Verdoes, M.; Willems, L. I.; van der Linden, W. A.; Ruben, M.; van Genderen, E.; Gubbens, J.; et al. Relative Quantification of Proteasome Activity by Activity-Based Protein Profiling and LC-MS/MS. *Nat. Protoc.* **2013**, *8* (6), 1155–1168.

(50) Keller, I. E.; Vosyka, O.; Takenaka, S.; Kloß, A.; Dahlmann, B.; Willems, L. I.; Verdoes, M.; Overkleeft, H. S.; Marcos, E.; Adnot, S.; et al. Regulation of Immunoproteasome Function in the Lung. *Sci. Rep.* **2015**, *5* (1), 10230.

(51) Coux, O.; Tanaka, K.; Goldberg, A. L. Structure and Functions of the 20S and 26S Proteasomes. *Annu. Rev. Biochem.* **1996**, *65* (1), 801–847.

(52) de Graaf, N.; van Helden, M. J. G.; Textoris-Taube, K.; Chiba, T.; Topham, D. J.; Kloetzel, P.-M.; Zaiss, D. M. W.; Sijts, A. J. A. M. PA28 and the Proteasome Immunosubunits Play a Central and Independent Role in the Production of MHC Class I-Binding Peptides in Vivo. *Eur. J. Immunol.* **2011**, *41* (4), 926–935.

(53) Oeckinghaus, A.; Ghosh, S. The NF- B Family of Transcription Factors and Its Regulation. *Cold Spring Harb. Perspect. Biol.* **2009**, *1* (4), a000034–a000034.

(54) Wertz, I. E.; Dixit, V. M. Signaling to NF- B: Regulation by Ubiquitination. *Cold Spring Harb. Perspect. Biol.* **2010**, *2* (3), a003350–a003350.

(55) van Gent, M.; Braem, S. G. E.; de Jong, A.; Delagic, N.; Peeters, J. G. C.; Boer, I. G. J.; Moynagh, P. N.; Kremmer, E.; Wiertz, E. J.; Ovaa, H.; et al. Epstein-Barr Virus Large Tegument Protein BPLF1 Contributes to Innate Immune Evasion through Interference with Toll-like Receptor Signaling. *PLoS Pathog.* **2014**, *10* (2), e1003960.

(56) Borodovsky, A.; Ovaa, H.; Kolli, N.; Gan-Erdene, T.; Wilkinson, K. D.; Ploegh, H. L.; Kessler, B. M. Chemistry-Based Functional Proteomics Reveals Novel Members of the Deubiquitinating Enzyme Family. *Chem. Biol.* **2002**, *9* (10), 1149–1159.

(57) Ovaa, H.; Kessler, B. M.; Rolen, U.; Galardy, P. J.; Ploegh, H. L.; Masucci, M. G. Activity-Based Ubiquitin-Specific Protease (USP) Profiling of Virus-Infected and Malignant Human Cells. *Proc. Natl. Acad. Sci.* **2004**, *101* (8), 2253–2258.

(58) Cruz-Muñoz, M. E.; Fuentes-Pananá, E. M. Beta and Gamma Human Herpesviruses: Agonistic and Antagonistic Interactions with the Host Immune System. *Front. Microbiol.* **2017**, *8*, 2521.

(59) Harhaj, E. W.; Dixit, V. M. Deubiquitinases in the Regulation of NF-KB Signaling. *Cell Res.* **2011**, *21* (1), 22–39.

(60) Nanduri, B.; Suvarnapunya, A. E.; Venkatesan, M.; Edelmann, M. J. Deubiquitinating Enzymes as Promising Drug Targets for Infectious Diseases. *Curr. Pharm. Des.* **2013**, *19* (18), 3234–3247.

(61) Mazumdar, T.; Gorgun, F. M.; Sha, Y.; Tyryshkin, A.; Zeng, S.; Hartmann-Petersen, R.; Jørgensen, J. P.; Hendil, K. B.; Eissa, N. T. Regulation of NF-KappaB Activity and Inducible Nitric Oxide Synthase by Regulatory Particle Non-ATPase Subunit 13 (Rpn13). *Proc. Natl. Acad. Sci. U. S. A.* **2010**, *107* (31), 13854–13859.

(62) Kattenhorn, L. M.; Korbel, G. A.; Kessler, B. M.; Spooner, E.; Ploegh, H. L. A Deubiquitinating Enzyme Encoded by HSV-1 Belongs to a Family of Cysteine Proteases That Is Conserved across the Family Herpesviridae. *Mol. Cell* **2005**, *19* (4), 547–557.

(63) Macdonald, S. J.; Mostafa, H. H.; Morrison, L. A.; Davido, D. J. Genome Sequence of Herpes Simplex Virus 1 Strain KOS. *J. Virol.* **2012**, *86* (11), 6371–6372.

(64) Ye, R.; Su, C.; Xu, H.; Zheng, C. Herpes Simplex Virus 1 Ubiquitin-Specific Protease UL36 Abrogates NF-KB Activation in DNA Sensing Signal Pathway. *J. Virol.* **2017**, *91* (5), e02417-16.

(65) Schlieker, C.; Korbel, G. A.; Kattenhorn, L. M.; Ploegh, H. L. A Deubiquitinating Activity Is Conserved in the Large Tegument Protein of the Herpesviridae. *J. Virol.* **2005**, *79* (24), 15582–15585.

(66) Saito, S.; Murata, T.; Kanda, T.; Isomura, H.; Narita, Y.; Sugimoto, A.; Kawashima, D.; Tsurumi, T. Epstein-Barr Virus Deubiquitinase Downregulates TRAF6-Mediated NF-KB Signaling during Productive Replication. *J. Virol.* **2013**, *87* (7), 4060–4070.

(67) Wang, J.; Loveland, A. N.; Kattenhorn, L. M.; Ploegh, H. L.; Gibson, W. High-Molecular-Weight Protein (PUL48) of Human Cytomegalovirus Is a Competent Deubiquitinating Protease: Mutant Viruses Altered in Its Active-Site Cysteine or Histidine Are Viable. *J. Virol.* **2006**, *80* (12), 6003–6012.

(68) Gredmark, S.; Schlieker, C.; Quesada, V.; Spooner, E.; Ploegh, H. L. A Functional Ubiquitin-Specific Protease Embedded in the Large Tegument Protein (ORF64) of Murine Gammaherpesvirus 68 Is Active during the Course of Infection. *J. Virol.* **2007**, *81* (19), 10300–10309.

(69) Jarosinski, K.; Kattenhorn, L.; Kaufer, B.; Ploegh, H.; Osterrieder, N. A Herpesvirus Ubiquitin-Specific Protease Is Critical for Efficient T Cell Lymphoma Formation. *Proc. Natl. Acad. Sci.* **2007**, *104* (50), 20025–20030.

(70) Lin, J.; Ai, Y.; Zhou, H.; Lv, Y.; Wang, M.; Xu, J.; Yu, C.; Zhang, H.; Wang, M. UL36 Encoded by Marek's Disease Virus Exhibits Linkage-Specific Deubiquitinase Activity. *Int. J. Mol. Sci.* **2020**, *21* (5).

(71) Mulder, M. P. C.; El Oualid, F.; ter Beek, J.; Ovaa, H. A Native Chemical Ligation Handle That Enables the Synthesis of Advanced Activity-Based Probes: Diubiquitin as a Case Study. *ChemBioChem* **2014**, *15* (7), 946–949.

(72) Békés, M.; van der Heden van Noort, G. J.; Ekkebus, R.; Ovaa, H.; Huang, T. T.; Lima, C. D. Recognition of Lys48-Linked Di-Ubiquitin and Deubiquitinating Activities of the SARS Coronavirus Papain-like Protease. *Mol. Cell* **2016**, *62* (4), 572–585.

(73) Lohmann, V.; Bartenschlager, R. On the History of Hepatitis C Virus Cell Culture Systems. *J. Med. Chem.* **2014**, *57* (5), 1627–1642.

(74) Pohl, M. O.; Lanz, C.; Stertz, S. Late Stages of the Influenza A Virus Replication Cycle—a Tight Interplay between Virus and Host. *J. Gen. Virol.* **2016**, *97* (9), 2058–2072.

(75) Syed, G. H.; Khan, M.; Yang, S.; Siddiqui, A. Hepatitis C Virus Lipoviroparticles Assemble in the Endoplasmic Reticulum (ER) and Bud off from the ER to the Golgi Compartment in COPII Vesicles. *J. Virol.* **2017**, *91* (15), e00499-17.

(76) Hutagalung, A. H.; Novick, P. J. Role of Rab GTPases in Membrane Traffic and Cell Physiology. *Physiol. Rev.* **2011**, *91* (1), 119–149.

(77) Takacs, C. N.; Andreo, U.; Dao Thi, V. L.; Wu, X.; Gleason, C. E.; Itano, M. S.; Spitz-Becker, G. S.; Belote, R. L.; Hedin, B. R.; Scull, M. A.; et al. Differential Regulation of Lipoprotein and Hepatitis C Virus Secretion by Rab1b. *Cell Rep.* **2017**, *21* (2), 431–441.

(78) Hogue, I. B.; Bosse, J. B.; Hu, J.-R.; Thiberge, S. Y.; Enquist, L. W. Cellular Mechanisms of Alpha Herpesvirus Egress: Live Cell Fluorescence Microscopy of Pseudorabies Virus Exocytosis. *PLoS Pathog.* **2014**, *10* (12), e1004535.

(79) Vieyres, G.; Welsch, K.; Gerold, G.; Gentzsch, J.; Kahl, S.; Vondran, F. W. R.; Kaderali, L.; Pietschmann, T. ABHD5/CGI-58, the Chanarin-Dorfman Syndrome Protein, Mobilises Lipid Stores for Hepatitis C Virus Production. *PLOS Pathog.* **2016**, *12* (4), e1005568.

(80) Beilstein, F.; Lemasson, M.; Pène, V.; Rainteau, D.; Demignot, S.; Rosenberg, A. R. Lysophosphatidylcholine Acyltransferase 1 Is Downregulated by Hepatitis C Virus: Impact on Production of Lipo-Viro-Particles. *Gut* **2017**, *66* (12), 2160–2169.

(81) Wohlbold, T.; Krammer, F. In the Shadow of Hemagglutinin: A Growing Interest in Influenza Viral Neuraminidase and Its Role as a Vaccine Antigen. *Viruses* **2014**, *6* (6), 2465–2494.

(82) Su, B.; Wurtzer, S.; Rameix-Welti, M.-A.; Dwyer, D.; van der Werf, S.; Naffakh, N.; Clavel, F.; Labrosse, B. Enhancement of the Influenza A Hemagglutinin (HA)-Mediated Cell-Cell Fusion and Virus Entry by the Viral Neuraminidase (NA). *PLoS One* **2009**, *4* (12), e8495.

(83) Lu, C.-P.; Ren, C.-T.; Lai, Y.-N.; Wu, S.-H.; Wang, W.-M.; Chen, J.-Y.; Lo, L.-C. Design of a Mechanism-Based Probe for Neuraminidase To Capture Influenza Viruses. *Angew. Chemie Int. Ed.* **2005**, *44* (42), 6888–6892.

(84) Tsai, C.-S.; Yen, H.-Y.; Lin, M.-I.; Tsai, T.-I.; Wang, S.-Y.; Huang, W.-I.; Hsu, T.-L.; Cheng, Y.-S. E.; Fang, J.-M.; Wong, C.-H. Cell-Permeable Probe for Identification and Imaging of Sialidases. *Proc. Natl. Acad. Sci. U. S. A.* **2013**, *110* (7), 2466–2471.

(85) Lei, J.; Hansen, G.; Nitsche, C.; Klein, C. D.; Zhang, L.; Hilgenfeld, R. Crystal Structure of Zika Virus NS2B-NS3 Protease in Complex with a Boronate Inhibitor. *Science (80-.).* **2016**, *353*

(6298), 503–505.

(86) Kasperkiewicz, P.; Poreba, M.; Snipas, S. J.; Parker, H.; Winterbourn, C. C.; Salvesen, G. S.; Drag, M. Design of Ultrasensitive Probes for Human Neutrophil Elastase through Hybrid Combinatorial Substrate Library Profiling. *Proc. Natl. Acad. Sci.* **2014**, *111* (7), 2518–2523.

(87) Kasperkiewicz, P.; Poreba, M.; Snipas, S. J.; Lin, S. J.; Kirchhofer, D.; Salvesen, G. S.; Drag, M. Design of a Selective Substrate and Activity Based Probe for Human Neutrophil Serine Protease 4. *PLoS One* **2015**, *10* (7), e0132818.

(88) Poreba, M.; Solberg, R.; Rut, W.; Lunde, N. N.; Kasperkiewicz, P.; Snipas, S. J.; Mihelic, M.; Turk, D.; Turk, B.; Salvesen, G. S.; et al. Counter Selection Substrate Library Strategy for Developing Specific Protease Substrates and Probes. *Cell Chem. Biol.* **2016**, *23* (8), 1023–1035.

(89) Poreba, M.; Rut, W.; Vizovisek, M.; Groborz, K.; Kasperkiewicz, P.; Finlay, D.; Vuori, K.; Turk, D.; Turk, B.; Salvesen, G. S.; et al. Selective Imaging of Cathepsin L in Breast Cancer by Fluorescent Activity-Based Probes. *Chem. Sci.* **2018**, *9* (8), 2113–2129.

(90) Rut, W.; Zhang, L.; Kasperkiewicz, P.; Poreba, M.; Hilgenfeld, R.; Drąg, M. Extended Substrate Specificity and First Potent Irreversible Inhibitor/Activity-Based Probe Design for Zika Virus NS2B-NS3 Protease. *Antiviral Res.* **2017**, *139*, 88–94.

(91) Rut, W.; Groborz, K.; Zhang, L.; Modrzycka, S.; Poreba, M.; Hilgenfeld, R.; Drag, M. Profiling of Flaviviral NS2B-NS3 Protease Specificity Provides a Structural Basis for the Development of Selective Chemical Tools That Differentiate Dengue from Zika and West Nile Viruses. *Antiviral Res.* **2020**, *175*.

(92) Sun, Y.; Zheng, Q.; Wang, Y.; Pang, Z.; Liu, J.; Yin, Z.; Lou, Z. Activity-Based Protein Profiling Identifies ATG4B as a Key Host Factor for Enterovirus 71 Proliferation. *J. Virol.* **2019**, *93* (24).

(93) Bissoyi, A.; Pattanayak, S. K.; Bit, A.; Patel, A.; Singh, A. K.; Behera, S. S.; Satpathy, D. Chapter 4 - Alphavirus Nonstructural Proteases and Their Inhibitors; Gupta, S. P. B. T.-V. P. and T. I., Ed.; Academic Press, 2017; pp 77–104.

(94) Norder, H.; De Palma, A. M.; Selisko, B.; Costenaro, L.; Papageorgiou, N.; Arnan, C.; Coutard, B.; Lantez, V.; De Lamballerie, X.; Baronti, C.; et al. Picornavirus Non-Structural Proteins as Targets for New Anti-Virals with Broad Activity. *Antiviral Res.* **2011**, *89* (3), 204–218.

(95) Banerjee, D.; Reddy, K. R. Review Article: Safety and Tolerability of Direct-Acting Anti-Viral Agents in the New Era of Hepatitis C Therapy. *Aliment. Pharmacol. Ther.* **2016**, *43* (6), 674–696.

(96) Kang, C.; Keller, T. H.; Luo, D. Zika Virus Protease: An Antiviral Drug Target. *Trends Microbiol.* **2017**, *25* (10), 797–808.

(97) Patick, A. K.; Potts, K. E. Protease Inhibitors as Antiviral Agents. *Clin. Microbiol. Rev.* **1998**, *11* (4), 614 LP – 627.

(98) Dai, W.; Zhang, B.; Jiang, X.-M.; Su, H.; Li, J.; Zhao, Y.; Xie, X.; Jin, Z.; Peng, J.; Liu, F.; et al. Structure-Based Design of Antiviral Drug Candidates Targeting the SARS-CoV-2 Main Protease. *Science (80-.).* **2020**, *368* (6497), 1331 LP – 1335.

(99) Furuta, Y.; Komeno, T.; Nakamura, T. Favipiravir (T-705), a Broad Spectrum Inhibitor of Viral RNA Polymerase. *Proc. Japan Acad. Ser. B Phys. Biol. Sci.* **2017**, *93* (7), 449–463.

(100) Gordon, C. J.; Tchesnokov, E. P.; Feng, J. Y.; Porter, D. P.; Gotte, M. The Antiviral Compound Remdesivir Potently Inhibits RNA-Dependent RNA Polymerase from Middle East Respiratory Syndrome Coronavirus. *J. Biol. Chem.* **2020**.

(101) Lin, C.-L.; Kao, J.-H. Review Article: Novel Therapies for Hepatitis B Virus Cure – Advances and Perspectives. *Aliment. Pharmacol. Ther.* **2016**, *44* (3), 213–222.

(102) Martínez, M. J.; Salim, A. M.; Hurtado, J. C.; Kilgore, P. E. Ebola Virus Infection: Overview and Update on Prevention and Treatment. *Infect. Dis. Ther.* **2015**, *4* (4), 365–390.

(103) Herrero, L. J.; Zakhary, A.; Gahan, M. E.; Nelson, M. A.; Herring, B. L.; Hapel, A. J.; Keller, P. A.; Obeysekera, M.; Chen, W.; Sheng, K.-C.; et al. Dengue Virus Therapeutic Intervention Strategies Based on Viral, Vector and Host Factors Involved in Disease Pathogenesis. *Pharmacol. Ther.* **2013**, *137* (2), 266–282.

(104) Bunchorntavakul, C.; Reddy, K. R. Review Article: The Efficacy and Safety of Daclatasvir in the Treatment of Chronic Hepatitis C Virus Infection. *Aliment. Pharmacol. Ther.* **2015**, *42* (3), 258–272.

(105) Engelman, A.; Cherepanov, P. The Structural Biology of HIV-1: Mechanistic and Therapeutic Insights. *Nat. Rev. Microbiol.* **2012**, *10* (4), 279–290.

(106) Shaw, T. A.; Ablenas, C. J.; Desrochers, G. F.; Powdrill, M. H.; Bilodeau, D. A.; Vincent-Rocan, J.-F.; Niu, M.; Monette, A.; Mouland, A. J.; Beauchemin, A. M.; et al. A Bifunctional Nucleoside Probe for the Inhibition of the Human Immunodeficiency Virus-Type 1 Reverse Transcriptase. *Bioconjug. Chem.* **2020**, *31* (5), 1537–1544.

(107) Spearman, C. W.; Dusheiko, G. M.; Hellard, M.; Sonderup, M. Hepatitis C. *Lancet* **2019**, *394* (10207), 1451–1466.

(108) Paul, D.; Madan, V.; Bartenschlager, R. Hepatitis C Virus RNA Replication and Assembly: Living on the Fat of the Land. *Cell Host Microbe* **2014**, *16* (5), 569–579.

Chapter 2: Profiling Kinase Activity during Hepatitis C Virus Replication Using a Wortmannin Probe

Initially published as Geneviève F. Desrochers, Allison R. Sherratt, David R. Blais, Neda Nasheri, Zhibin Ning, Daniel Figeys, Natalie K. Goto, and John Paul Pezacki. (2015) Profiling Kinase Activity During Hepatitis C Replication Using a Wortmannin Probe. ACS Infec. Dis. 1 (9) 443–452

2.1 Statement of contribution

Geneviève F. Desrochers performed biological profiling experiments. Allison R. Sherratt, David R. Blais, and Neda Nasheri performed the initial biological characterisation of the wortmannin probe. Zhibin Ning and Daniel Figeys performed all mass spectrometry. John Paul Pezacki was responsible for the original project design. The manuscript was written by Geneviève F. Desrochers and John Paul Pezacki.

2.1.1 Acknowledgments

We thank Dr. C. S. McKay and M. Chigrinova for help with the preparation of the wortmannin-yne probe.

2.2 Summary

To complete its life cycle, the hepatitis C virus (HCV) induces changes to numerous aspects of its host cell. As kinases act as regulators of many pathways utilized by HCV, they are likely enzyme targets for virally induced inhibition or activation. Herein, we used activity-based protein profiling (ABPP), which allows for the identification of active enzymes in complex protein samples and the quantification of their activity, to identify kinases that displayed differential activity in HCV-expressing cells. We utilized an ABPP probe, wortmannin-yne, based on the kinase inhibitor wortmannin, which contains a pendant alkyne group for bioconjugation using bio-orthogonal chemistry. We observed changes in the activity of kinases involved in the mitogen-activated protein kinase pathway, apoptosis pathways, and cell cycle

control. These results establish changes to the active kinome, as reported by wortmannin-yne, in the proteome of human hepatoma cells actively replicating HCV. The observed changes include kinase activity that affects viral entry, replication, assembly, and secretion, implying that HCV is regulating the pathways that it uses for its life cycle through modulation of the active kinome.

2.3 Introduction

The hepatitis C virus (HCV) is a small, positive-sense RNA virus consisting of a 3′ and 5′ untranslated region (UTR) flanking a coding region for a polyprotein, later cleaved into three structural and seven non-structural proteins.[1] It currently infects between 2 and 3% of the global population and presents a global health threat in both developed and undeveloped countries.[1] No vaccine is currently available.[2] Although recent direct-acting antivirals (DAAs) currently show promise, with a cure rate between 70 and 95%,[3] their long-term therapeutic potential is limited by the virus's high heterogeneity, which leads to a low barrier to drug resistance and the development of escape mutants. Furthermore, DAAs display different degrees of success in producing a significant reduction in viremia across the various HCV genotypes.[2] The development of host-targeting antivirals addresses this issue, targeting aspects of the host cell required for viral propagation and thereby reducing the possibility of escape mutants when used in conjunction with DAAs. To propagate efficiently, HCV must alter the host cell machinery it uses to enter, replicate, assemble, and secrete from the cell.[1,4] Investigating host factors required for replication and infection allows for a better understanding of how HCV and related RNA viruses utilize host cells and can serve as targets for the development of host-targeting antivirals. Many of the biochemical pathways HCV needs to manipulate to create a pro-viral environment are controlled by kinases, which are therefore attractive targets both for the virus and for drug therapies.

HCV has been shown to depend on the activity of a wide variety of kinases. These kinases include C-Src kinase (CSK),[5] cell cycle regulatory kinases,[6] choline kinases,[7] and phosphatidylinositol

4-kinases.[8–14] Kinases involved in the AKT-PI3K pathway,[15,16] mitogen-activated protein kinase pathway,[7,15] and apoptotic pathway,[15] as well as kinases that act as growth factors and initiation factors,[7] have also been implicated. Alternatively, certain kinases have been shown to act as HCV suppressors, such as protein kinase C and casein substrate in neurons 1 (PACSIN 1), cyclin-dependent kinase regulatory subunit, and a kinase in the MAPK pathway, mitogen-activated protein kinase kinase 5.[17]

It has been shown that, as a result of this dependence, HCV modifies the activity of numerous kinases to promote the production of new virions. The activities of pro-viral kinases, such as phosphoinositide kinases PI3K,[18–20] PI4KA, and, potentially, PI4KB,[13,21–24] are up-regulated by HCV to create an environment more favourable for the various stages of the viral life cycle. To the same end, HCV is also known to suppress kinase activity to inhibit the NF-κB pathway, the insulin signalling pathway, and immune response, where affected proteins include protein kinase R and inducible IκB kinase.[7,25–27] However, the effect of viral infection on the activity of many kinases shown to play a role in HCV infection has yet to be determined. The identification of kinases that display differential activity in response to HCV infection allows us to elucidate the mechanisms by which HCV propagates and to identify novel drug targets not previously associated with HCV.

As the activities of kinases are regulated by a number of post-translational regulatory mechanisms, it is necessary to use methods that go beyond traditional abundance-based proteomics to obtain an accurate portrait of changes in the state of the cell. Activity-based protein profiling (ABPP) uses probes with active-site directed reactive groups, typically based on previously identified inhibitors, to assess the catalytic ability of target enzymes.[28,29] The development of rapid, bio-orthogonal "click" chemistry has made it possible to attach the bulky reporter tag to the probe after labelling to increase the permeability of the activity-based probe. ABPP can be combined with stable isotope dimethyl labelling followed by LC-MS/MS, a high-throughput method by which proteins can be identified and their relative quantities

across two samples compared, to identify enzymes that display differential activity between two samples.[30,31] ABPP has previously been used in the labelling and identification of kinases[24,32–35] and in the context of viral infections[24,36–41] to label and quantify the activity of enzymes and kinases specifically.[24,37]

Wortmannin (Fig 2.1a) is a small fungal-derived molecule that acts as an irreversible inhibitor against a range of kinases in the phosphoinositide kinase family of enzymes, as well as members of the protein-phosphorylating phosphoinositide 3-kinase related kinase (PIKK) family.[42] It has also been shown to have antiviral properties against HCV[8,13] and should therefore be capable of targeting kinases relevant to the life cycle of HCV. Wortmannin inactivates its target enzymes through the formation of a covalent bond with a catalytic lysine residue.[43] The formation of this covalent bond between wortmannin and an active enzyme allows a modified wortmannin molecule to act as a selective label of specific active kinases. It has previously been modified to act as an activity-based probe and has been shown to report on the activity PI3K, polo-like kinase of 1, and DNA-dependent protein kinases.[44,45] In this paper, we used a wortmannin-based probe, wortmannin-yne, (Fig 2.1b) to investigate the activity of kinases in response to HCV infection. The activity dependent labelling of a range of kinases is demonstrated, and we show that HCV induces a change in the activity of several kinases implicated in viral infection, metabolism, hepatic disorders, and cell stress response.

2.4 Methods

Wortmannin-yne was synthesized as previously reported.[24] The inclusion of the tethered alkyne was shown to not adversely affect targeting of wortmannin. Wortmannin-yne continues to covalently bind to the active sites of phosphatidylinositide and other kinases.[24]

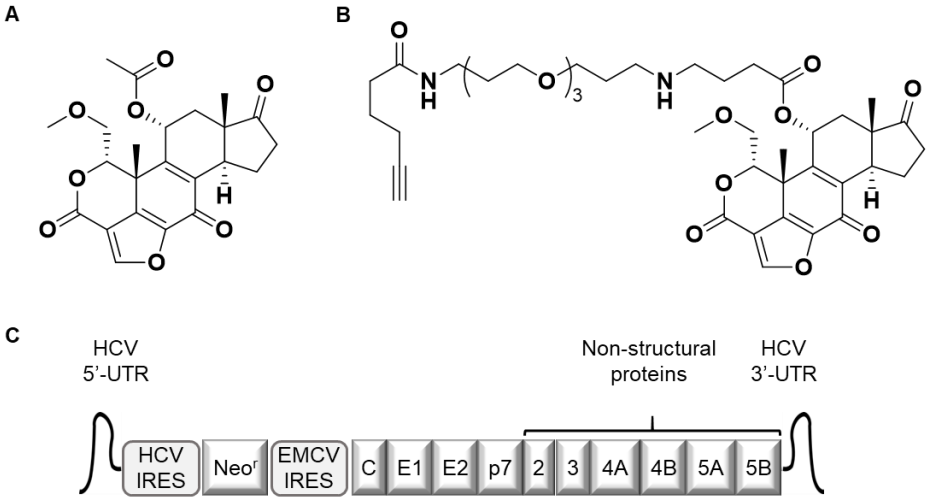

Figure 2.1: Probes used to target active kinases and schematic of the HCV replicon used. A) Wortmannin; B) wortmannin-derived clickable ABPP probe, wortmannin-yne, containing a bio-orthogonal alkyne moiety. C) Schematic representation of the HCV model, bicistronic full-genomic replicon with an S2204I adaptive mutation in NS5A (Huh7.5-FGR)

2.4.1 Cell Culture and Reagents

The human hepatoma cell line Huh-7.5 was grown in DMEM supplemented with 100 nM nonessential amino acids, 50 U/mL penicillin, 50 µg/mL streptomycin, and 10% FBS (CANSERA, Rexdale, ON, Canada). The Huh-7.5 cells stably expressing the full genomic replicons (genotype 1B, con1), a kind gift from Dr. Charles Rice (Rockefeller University, New York, NY, USA), were maintained in the same culture medium supplemented with 250 µg/mL G418 Geneticin (GIBCO-BRL, Burlington, ON, Canada).

2.4.2 Proteome Extraction and Labelling

Confluent cells (90−100%) were washed and pooled in ice-cold cell culture lysis buffer (1% Triton-X, 10 mM sodium phosphate buffer (PBS), pH 7.4). Cells were then lysed by sonication (30% duty cycle, 15 pulses, Sonifier 250, Branson Ultrasonic). The proteome extract was cleared by centrifugation at 20000g and 4 °C for 5 min, quantified with the DC protein assay (Bio-Rad), and diluted to 1 mg/mL for the fluorescent gels or to 2 mg/mL for the activity pulldowns. Proteome samples were treated with 10 µM wortmannin-yne for 1 h at room temperature. Competitive inhibition samples were incubated with 200 µM wortmannin for 30 min at 37 °C prior to labelling. Copper-catalysed azide-alkyne click chemistry and streptavidin enrichment of labelled samples were performed as previously described,[46] with the addition of an acetone precipitation step after the click reaction.

2.4.3 Preparation for Mass Spectrometry

On-bead samples were washed with 50 mM ammonium bicarbonate (ABC) and reduced with 10 mM DTT in 50 mM ABC for 15 min at 65 °C. Samples were rotated with 25 mM iodoacetamide in the dark at room temperature for 30 min. The samples were pelleted, the supernatant was discarded, and the beads were washed with ABC. Samples were digested for 16 h in 10 ng/µL trypsin in ABC and analysed by mass spectrometric analysis.

2.4.4 Dimethyl Labelling

"Light"-labelled peptides were mixed with formaldehyde (0.16%) and sodium cyanoborohydride (0.025 M). "Heavy"-labelled peptides were mixed with ^{13}C deuterated formaldehyde (0.16%) and sodium cyanoborodeuteride (0.025M). The samples were rotated for 1 h at room temperature, and the reaction was quenched by the sequential addition of ammonia solution (0.13%) and formic acid (0.32%). Samples were mixed and cleaned in a reverse-phase tC18 Sep-Pak column (Waters, Milford, MA, USA).

2.4.5 Reversed-Phase Liquid Chromatography (RP-LC)

An Agilent 1100 capillary-HPLC system (Agilent Technologies, Santa Clara, CA, USA) was hooked up with an LTQ-Orbitrap mass spectrometer (Thermo Electron, Waltham, MA, USA). The solvent system consists of buffer A (0.1% formic acid (FA) in water) and buffer B (0.1% FA in acetonitrile). Dried-down protein digest was acidified with 0.5% (V/V) FA and loaded on a 75 μm i.d. × 100 mm fused silica analytical column packed inhouse with 3 μm ReproSil-Pur C18 beads (100 Å; Dr. Maisch GmbH, Ammerbuch, Germany) at a flow rate of 2 μL/min for 15 min. A flow of 20 μL/min from HPLC was split into 200 nL/min to perform the peptide separation. Gradient elution was set as 5−35% buffer B over 2 h for the on-bead digestion and over 1 h for the in-solution digestion, followed by 2 min at 100% buffer B and 10 min at 2% buffer B to re-equilibrate for the next run.

2.4.6 MS Analysis

An LTQ-Orbitrap mass spectrometer (ThermoFisher Scientific, San Jose, CA, USA), equipped with a nanoelectrospray interface, was operated in positive ion mode. The spray voltage was set to 2.0 kV and the temperature of the heated capillary was 200 °C. The instrument method consisted of one full MS scan from m/z 300 to 1700, followed by data-dependent MS/MS scan of the five most intense ions, a dynamic exclusion repeat count of 1 in 30 s, and an exclusion duration of 90 s. The full mass was scanned in Orbitrap analyser with R = 60000 (defined at m/z 400), and the subsequent MS/MS analyses were

performed in the LTQ analyser. All of the measurements in the Orbitrap mass analyser were performed with a real-time internal calibration by the lock mass of background ion 445.120025 in order to improve mass accuracy. The charge state rejection function was enabled, and charge states with unknown and single charge state were excluded for subsequent MS/MS analysis. All data were recorded with Xcalibur software (ThermoFisher Scientific, San Jose, CA, USA).

2.4.7 Data Analysis, Mascot

All raw files were converted into .mgf files by Proteomics Tools7 and searched using Mascot. Cysteine carbamidomethylation was selected as a fixed modification and the methionine oxidation and protein N-terminal acetylation were selected as variable modifications. Enzyme specificity was set to trypsin, allowing for up to two missing trypsin cleavages not allowing for cleavage of N-terminal to proline. The precursor ion mass tolerances were 7 ppm, and fragment ion mass tolerance was 0.8 Da. The .dat files generated by Mascot were parsed and filtered by BuildSummary4 using a peptide FDR of 1% and a minimum length of six amino acids for peptide identification. All of the identifications from reversed database were removed.

2.4.8 Western Blotting

Labelled proteins were removed from beads by boiling at 95°C in gel loading buffer (0.1 M Tris, pH 6.8, 10% glycerol, 4% SDS, 0.02% bromophenol blue, 30 mM DTT) for 10 min. Samples were resolved by SDS-PAGE under reducing conditions (10% gel) and transferred to a Hybond-P PVDF membrane (Amersham Biosciences). The membranes were blocked using 2.5% bovine serum albumin (BSA) in Tris-buffered saline (TBS) with 0.05% Tween-20. Membranes were incubated with MAPK1 (1:500) (Santa Cruz), Akt (1:500) (Cell Signalling), or PTP1D (1:4000) (BD Biosciences) in 3% milk in TBST at 4°C overnight. Membranes were subsequently incubated for 1 h with donkey or mouse monoclonal

antibodies (Jackson ImmunoResearch Laboratories) diluted in 3% milk in TBST. Signal was generated using the ECL Plus Western Blotting System (GE Healthcare) as recommended by the manufacturer.

2.4.9 In Vitro 1D Fluorescent Gel Analysis

Cell lysates were treated with 10 μM wortmannin-yne in DMSO for 1 h at room temperature. The copper-catalysed azide−alkyne click reaction was performed by incubation with click buffer (200 μM rhodamine azide, 2 mM TCEP-HCl, 200 μM TBTA, 2 mM CuSO4) at 25 °C for 1 h with mixing. Following the incubation, the reaction was quenched by acetone precipitation, and the sample was dried and resolved by SDS-PAGE using a 10% acrylamide gel. Gels were scanned with FM BIOIII Mutiview scanner (Hitachi) and stained with Coomassie.

2.5 Results and Discussion

To understand the dependence of HCV on host factors and to develop new monitoring and treatment strategies, it is necessary to identify novel host−virus interactions. To this end, we have searched for host factors that are required for viral propagation. The perturbation of individual enzymes or pathways provides useful clues as to the identity of targetable host factors that are required by the virus. By measuring catalytic activity, the functional end-point of all enzymes, and also the effector of the methods by which enzymatic activity can be regulated, ABPP methods provide a more accurate portrait of the proteome alterations made by HCV.

2.5.1 Proteome Labelling Using Wortmannin-yne

To test the efficacy of wortmannin-yne as a probe in a complex mixture of proteins, Huh7.5 cell lysates were labelled in vitro with various concentrations of wortmannin-yne and tagged with a fluorescent marker. Wortmannin-yne labelled numerous targets and showed most effective labelling at 10 μM.

Competitive inhibition with wortmannin and heat denaturation both resulted in a decrease in wortmannin-yne labelling (Fig 2.2).

The inhibition of wortmannin-yne labelling by protein denaturation indicates that wortmannin-yne acts as an activity-based probe, whereas the inhibition of numerous bands by the competitive inhibitor wortmannin indicates that the target range of the probe retains significant similarity to the parent molecule. The presence of uninhibitable bands is due to structural differences between the inhibitor wortmannin and the probe-wortmannin-yne, which results in a slight difference in the range of enzymes targeted, consistent with previous results.[44,45] The Coomassie stain showed similar band intensities in every lane, indicating identical amounts and composition of protein in each sample (Fig 2.2c).

2.5.2 Wortmannin-yne Target Identification by Comparative ABPP

To assess changes in kinase activity caused by HCV, naïve Huh7.5 and Huh7.5 cells expressing the full genomic replicon, Huh7.5-FGR (Fig 2.1c), were lysed and the proteomes labelled *in vitro* with wortmannin-yne. The lysates were subsequently tagged with biotin-azide via copper-catalysed click chemistry. The labelled proteome was separated from the unlabelled proteome by affinity pull-down and analysed by LC-MS/MS. The relative kinase activities of the HCV replicon-containing and naïve samples were determined by calculating the ratio of the spectral counts from the two samples. Due to the low number of spectral counts per hit, this method yielded only semi-quantitative results (Tables 2.1 and 2.2).[47]

To confirm our results, we used a method that combines ABPP with dimethyl labelling followed by mass spectrometry.[31] As shown in Fig 2.3, the tryptic digests of the wortmannin-yne labelled proteomes were dimethylated with either “heavy” or “light” formaldehyde, then combined and analysed by LC-MS/MS. To eliminate bias caused by the nature of the stable isotope label, the dimethyl labelling was performed

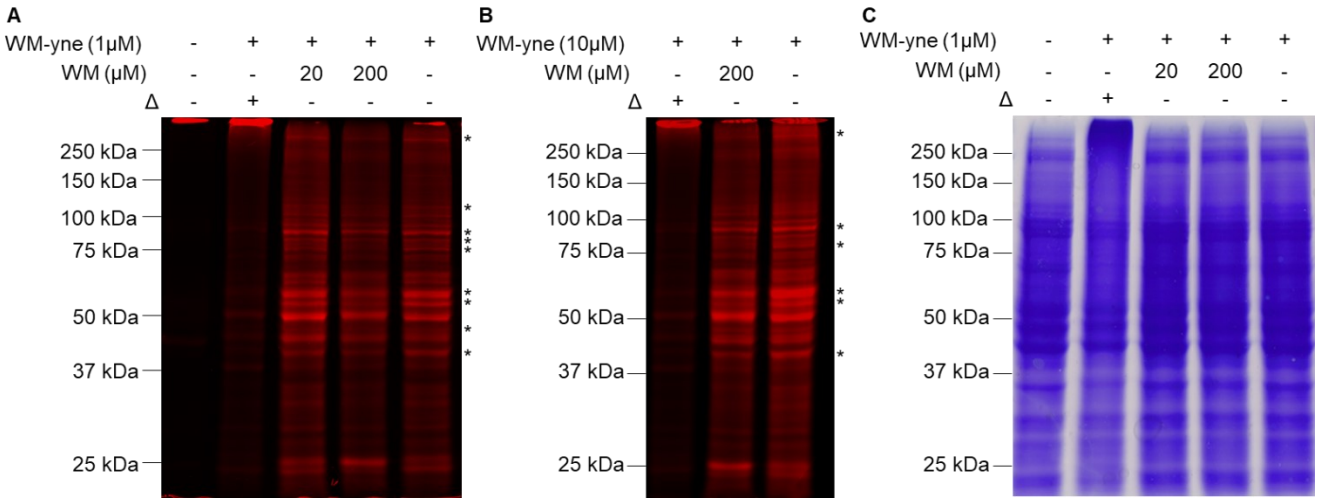

Figure 2.2: Wortmannin-yne labelling of Huh7.5 proteome. Huh7.5 cell lysates were pre-incubated with the competitive inhibitor wortmannin (WM) at 37 °C for 30 min or heat denatured for 10 min (symbolized by Δ) before incubation with increasing concentrations of wortmannin-yne (WM-yne) and subsequent attachment of a fluorescent rhodamine tag via click chemistry. Labelled proteomes were visualized by fluorescent scanning at 65% sensitivity for samples labelled with 1 μM wortmannin-yne and at 50% sensitivity for samples labelled by 10 μM wortmannin-yne. Proteins exhibiting decreased labelling in the presence of inhibitor are marked by an asterisk.

in reciprocal pairs: one sample contained "light"-labelled peptides from Huh7.5 cells and "heavy"-labelled peptides from Huh7.5-FGR cells, and the other pair contained "heavy"-labelled peptides from Huh7.5 cells and "light"-labelled peptides from Huh7.5-FGR cells. The peak intensities for the identified proteins were used to calculate the ratio of the enzymes' activities between Huh7.5 and HCV-containing cells. Wortmannin-yne labelling demonstrated differential activity in a large number of enzymes, enabling the assessment of HCV-induced changes in activity of numerous enzymes using a single probe.

TOPPGENE enrichment analysis was conducted on protein hits. Analysis of kinases displaying differential activity showed that HCV activates kinases involved in the mitogen-activated protein kinase (MAPK) pathway, cell cycle regulation, and tumour suppression (Table 2.3). Other individual kinases that had previously been associated with HCV entry, replication, and assembly were also identified and demonstrated differential activity in the presence of HCV (Tables 2.1 and 2.2).

2.5.3 Kinases Involved in Insulin Signalling

The protein kinase Akt acts as a central hub between extracellular signals and the regulation of several cellular pathways, the most significant of which is insulin signaling.[48] Comparative ABPP by MS shows an HCV-mediated decrease in the activity of protein kinase Akt. (Table 2.1) Glycogen synthase kinase 3 beta (GSK3β), a downstream target of insulin signalling that inhibits insulin-mediated glycogen synthesis,[49] displayed increased activity in HCV-expressing cells. (Table 2.2) These results are consistent with hypothesized mechanisms for hepatitis C associated insulin resistance[49,50] and agree with previous research, which showed that HCV proteins decrease Akt activity while increasing GSK3β activity.[18,51–56] Contrary to these findings, other researchers have shown that HCV increases the activity of Akt[15,57] and that GSK3β is inactivated in cells expressing either the HCV core protein[58] or the sub-genomic HCV replicon.[59]

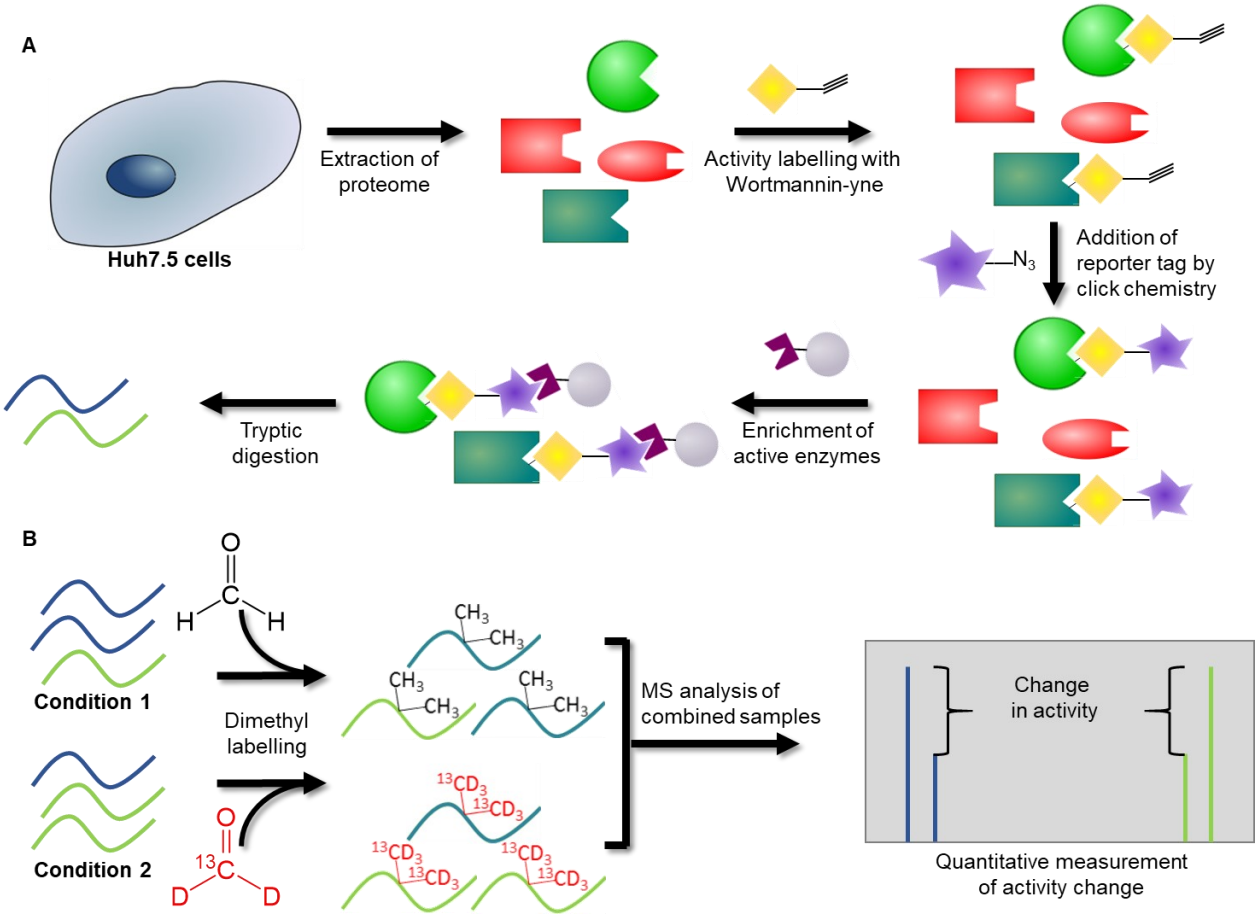

Figure 2.3. Scheme of the activity-based protein profiling methods used to identify differentially active kinases. (A) The active proteome isolated from naïve hepatoma cells or hepatoma cells stably expressing an HCV replicon is labelled by wortmannin-yne and subsequently attached to an affinity tag. The tagged proteome was isolated by affinity pull-down digested by trypsin. Peptides could be analysed by LC-MS/MS or undergo further manipulation. (B) Additional steps were used in ABPP-dimethyl labelling. Digested peptides are labelled with either "light" or "heavy" formaldehyde. The samples are mixed and the targets identified and quantified by LC-MS/MS.

Table 2.1: Kinases Displayed Down-Regulated Activities in Hepatoma Cells Expressing the HCV Full-Genomic Replicon

Protein Names	Gene Names	Accession #	Spectral counts[a]	Dimethyl labelling		
				Trial 1[b]	Trial 2[b]	Mean
Dual specificity mitogen-activated protein kinase	MAP2K1	Q02750	0/1			
RAC-beta serine/threonine-protein kinase	AKT2	P31751	0/1			
Serine/threonine-protein kinase PAK 2	PAK2	Q13177	0/1			
Cyclin-dependent kinase 2	CDK2	P24941	0/1			
Casein kinase II subunit alpha	CSNK2A1	Q5U5J2	6/12	0.45	0.77	0.61
Cyclin-dependent kinase 18	CDK18	Q07002		0.60	0.75	0.65
Phosphatidylinositol 5-phosphate 4-kinase type-2	PIP4K2A	P48426		0.39	0.92	0.66
Casein kinase II subunit alpha	CSNK2A2	P19784	3/5	0.61	0.83	0.72
Cyclin-dependent kinase 1	CDK1	P06493		0.58	0.75	0.66
Mitogen-activated protein kinase 1	MAPK1	P28482	3/7	0.81	1.03	0.92
UMP-CMP kinase	CMPK1	P30085	4/6	0.72	0.74	0.73
Bifunctional ATP-dependent	DAK	Q3LXA3	2/1	0.54	0.67	0.63

[a]Kinase activity is reported as the fraction of the spectral count from Huh7.5-FGR cells over the spectral count of Huh7.5 cells.

[b]The reported ratio for one trial is the mean of a reciprocal pair of samples. One sample contained “light”-labelled peptides from Huh7.5 cells and “heavy”-labelled peptides from Huh7.5-FGR cells, and the other contained “heavy”-labelled peptides from Huh7.5 cells and “light”-labelled peptides from Huh7.5-FGR cells

Table 2.2: Kinases That Displayed Up-Regulated Activities in Hepatoma Cells Expressing the HCV Full-Genomic Replicon

Protein Names	Gene Names	Accession	Spectral counts[a]	Dimethyl labelling		
				T 1[b]	T 2[b]	Mean
6-phosphofructokinase, muscle type	PFKM	P08237	3/1	0.97	1.22	1.10
Calcium/calmodulin-dependent protein kinase type II subunit delta	CAMK2D	Q13557	2/2	1.71	1.85	1.78
Phosphoenolpyruvate carboxykinase [GTP], mitochondrial	PCK2	Q16822	1/1	1.32	2.62	1.97
6-phosphofructokinase, liver type	PFKL	P17858		1.58	1.74	1.66
Cyclin-G-associated kinase	GAK	O14976		1.70	2.35	2.02
Nucleoside diphosphate kinase A	NME1	P15531	1/0	2.19	2.78	2.38
RAC-beta serine/threonine-protein kinase	AKT2	P31751	1/0			
Calcium/calmodulin-dependent protein kinase type 1	CAMK1	Q14012	1/0			
Calmodulin	CALM1	H0Y7A7	1/0			
cAMP-dependent protein kinase type I-alpha regulatory subunit	PRKAR1A	P10644	1/0			
Serine-protein kinase ATM	ATM	Q13315	1/0			
Cell cycle progression restoration protein 2	TBRG4	Q969Z0	1/0			
Glycogen synthase kinase-3 beta	GSK3B	P49841	2/0			

[a]Kinase activity is reported as the fraction of the spectral count from Huh7.5-FGR cells over the spectral count of Huh7.5 cells.

[b]The reported ratio for one trial is the mean of a reciprocal pair of samples. One sample contained “light”-labelled peptides from Huh7.5 cells and “heavy”-labelled peptides from Huh7.5-FGR cells, and the other contained “heavy”-labelled peptides from Huh7.5 cells and “light”-labelled peptides from Huh7.5-FGR cells

Table 2.3. Pathways Identified by TOPPGENE Gene Enrichment Analysis

Pathway Name	pValue	$n_{genes\ input}$	$n_{genes\ annotation}$	Ratio labelled to pathway genes
ERK activation	7.81E-08	3	5	0.60
RAF/MAP kinase cascade	9.31E-07	3	10	0.30
Condensation of Prometaphase Chromosomes	1.70E-06	3	12	0.25
RB Tumor Suppressor/Checkpoint Signaling in response to DNA damage	2.21E-06	3	13	0.23
Ca++/ Calmodulin-dependent Protein Kinase Activation	2.81E-06	3	14	0.21
GRB2 events in EGFR signalling	2.81E-06	3	14	0.21
SOS-mediated signalling	2.81E-06	3	14	0.21
Signalling to p38 via RIT and RIN	3.51E-06	3	15	0.20
SHC-mediated signalling	3.51E-06	3	15	0.20
SHC1 events in EGFR signalling	3.51E-06	3	15	0.20
Cell Cycle: G1/S Check Point	2.79E-07	4	28	0.14
Signal transduction by L1	7.07E-07	4	35	0.11
NFAT and Hypertrophy of the heart (Transcription in the broken heart)	9.38E-10	6	54	0.11
fMLP induced chemokine gene expression in HMC-1 cells	8.90E-07	4	37	0.11
Fc Epsilon Receptor I Signalling in Mast Cells	1.11E-06	4	39	0.10
IFN-gamma pathway	1.23E-06	4	40	0.10
Bioactive Peptide Induced Signalling Pathway	1.65E-06	4	43	0.09
IL-7 Signalling Pathway	1.81E-06	4	44	0.09
Glioma	1.83E-07	5	65	0.08
EGFR signalling pathway	1.88E-08	6	88	0.07

Prior studies assessed the activities of Akt and GSK3β by measuring the activating phosphorylations of Akt Thr308 and Ser473 and the inactivating phosphorylation of GSK Ser9 by Akt. However, recent research has shown that this is not an accurate measurement of the activity of these kinases, as additional post-translational modifications can modulate Akt or GSK3β independently of phosphorylation.[48,49,60,61] The use of comparative ABPP avoids these potential sources of inaccuracy, as the activities of the enzymes themselves are necessary for labelling.

2.5.4 Kinases Essential to Host Cell Metabolism

Key metabolic regulatory kinases displayed differential activity in the presence of HCV. Phosphoenolpyruvate carboxykinase (PCK2), a key rate-limiting enzyme in hepatic gluconeogenesis,[57] showed increased activity in HCV-infected cells. This agrees with previous research, which showed that PCK2 has higher transcription and protein levels in HCV-expressing cells.[57,62] Additionally, two isoforms of ATP-dependent 6-phosphofructokinase (PFKM and PFKL), an enzyme whose activity positively regulates the rate of glycolysis,[63] were also labelled by the wortmannin probe. Quantification by spectral counting showed a three-fold increase in PFKM activity in HCV-replicon cells. This result was not supported by the intensity comparison method used in the dimethyl labelling, which showed only a modest increase in activity. The dimethyl labelling experiments did, however, show an average 66% increase in the activity of PFKL, the more abundantly expressed liver isoform. Increases in phosphofructokinase activity have previously been shown in biopsy samples from patients suffering from acute hepatitis.[64]

2.5.5 Kinases Involved in the MAPK Pathway

Both spectral counting and dimethyl-labelling quantification revealed altered activity in MAPK pathways kinases. As shown in Table 2.1, the activities of mitogen-activated protein kinase 1 (MAPK1) and dual specificity mitogen-activated protein kinase kinase 1 (MAP2K1), the kinase that activates

MAPK1,[65] were downregulated in HCV-containing cells compared to naïve cells. (Table 2.1) Pathway enrichment analysis of differentially active kinases indicates that the MAPK pathway is strongly inhibited by HCV. (Table 2.3)

To confirm that MAPK1 activity is decreased in HCV replicon samples, active kinases of Huh7.5 and Huh7.5-FGR cells labelled with wortmannin-yne were isolated by affinity enrichment and detected by western immunoblotting to confirm both the wortmannin-yne labelling of MAPK pathway kinases and the dimethyl-labelling-based quantification of activity. MAPK1 showed a decrease in activity in Huh7.5-FGR cells, which agrees with the mass spectrometry quantification (Fig 2.4). A decrease in MAPK1 abundance was also observed, suggesting that the decrease in MAPK1 activity is due to lower transcription levels and not solely due to post-translational regulation.

These results are in agreement with previous studies, which have shown that expression of the HCV replicon inhibits the activation of the MAPK pathway via interaction between non-structural protein 5A (NS5A) and upstream regulators, and that the chemical inhibition of MAP2K1 increases HCV replication.[15,65–68] In addition to confirming that the MAPK pathway is inhibited by HCV replication, these results show that the wortmannin-yne probe is a valuable tool, which can be used to assess the activation of the MAPK pathway in Huh7.5 cells.[69,70]

2.5.6 Kinases Implicated in Cell Cycle Regulation

HCV has previously been shown to decrease the proliferation of hepatocytes by inhibiting cell cycle progression.[71–74] Comparative ABPP with wortmannin-yne revealed multiple perturbations in the activity of cell cycle regulatory proteins. Cyclin-dependent kinase 1 (CDK1), which facilitates the onset of mitosis,[75] and cyclin-dependent kinase 2 (CDK2), which promotes passage through the G1/S barrier,[76] both displayed decreased activity in the presence of HCV (Table 2.1). This is in agreement with previous

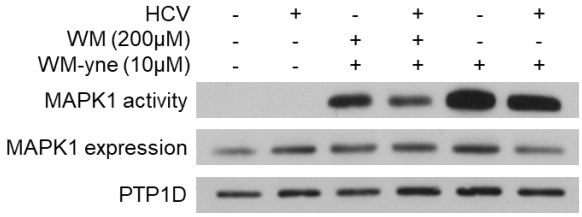

Figure 2.4: Western blot analysis of wortmannin-yne pulldown in HCV expressing cell lines. Cell lysate proteins probed with wortmannin-yne were affinity enriched, separated using SDS-PAGE, and probed with antibodies against MAPK1 and PTP1D.

research, which showed that chemical inhibition of CDK2 increases viral replication.[66] Cell cycle restoration protein 2 (TBRG4), a kinase that has been shown to block cell cycle arrest at the G1/S barrier,[77] was activated in the presence of HCV (Table 2.2). Altogether, this suggests that in the presence of HCV, normal cell cycle progression is perturbed via the inhibition of CDK1 and CDK2 and that cell cycle progression is rescued by the activation of the cell cycle progression restoration protein 2.

Kinases regulating apoptosis also displayed differential activation. Serine protein kinase ATM (ATM) demonstrated higher activity in HCV-expressing cells (Table 2.2). ATM is a regulator of multiple pathways leading to cell cycle arrest and apoptosis. It has previously been shown to be activated and to promote cell cycle arrest and apoptosis in response to high lipid levels and oxidative stress, both conditions caused by HCV.[1,78,79] The activities of two subunits of casein kinase II, (CSNK2) another kinase that has been shown to play a role in cell cycle arrest and promotion of apoptosis,[80] were decreased in the presence of HCV (Table 2.1). Our data suggest that the high lipid levels and oxidative stress caused by HCV activate ATM, promoting cell cycle arrest and apoptosis. The activation of the pro-apoptotic pathways may be countered in part by the inhibition of CSNK2, as the depletion of CSNK2 has previously been shown to bypass cell cycle arrest.[80]

2.5.7 Kinases Associated with the Assembly of HCV Infectious Particles

Two kinases identified by wortmannin-yne labelling, CSNK2 and cyclin-G associated kinase (GAK), have previously been associated with HCV assembly. GAK is a kinase that has been shown to promote both viral entry and viral assembly, but does not affect replication.[81,82] Table 2.2 shows that it displayed increased activity in Huh7.5-FGR cells, suggesting that GAK activity is up-regulated by HCV to promote efficient assembly of viral particles and to help enable viral entry during the cycle of infection.

Assembly of HCV infectious particles is regulated by the viral protein NS5A, which acts as a switch between HCV replication and assembly, promoting virion assembly when hyperphosphorylated.[83] CNSK2 has been shown to phosphorylate NS5A and promote the switch from viral replication to viral assembly.[83] Our results indicate that CSNK2 displayed reduced activity in Huh7.5-FGR cells (Table 2.1), which replicate the HCV genome but do not assemble or secrete infectious particles.[84] Previous research has shown that a decrease in casein kinase activity can increase the production of infectious viral particles.[85] Taken together, this suggests that in cells in which HCV replication occurs, CSNK2 activity is downregulated to promote the continued replication of the virus. This is consistent with the notion that CNSK2 acts as a master regulator of replication of HCV.

In this paper, we have shown that wortmannin-yne is capable of acting as a probe for high-throughput identification of individual kinases that have altered enzyme activity during HCV replication. As numerous kinases can be labelled by wortmannin-yne, this probe is a valuable tool that can be used to assess differences in both the activity of individual kinases and activation of signalling pathways, for instance, the insulin signalling pathway and the MAPK pathway. Using wortmannin-yne to perform activity-based profiling of HCV genomic replicon expressing cells, we have shown that HCV replication inhibits MAPK signalling and misregulates other enzymes, such as kinases involved in cell cycle control and in tumour suppression, as summarized in Fig 2.5. These kinases represent not only biomarkers for HCV infection but also potential targets for the development of new drug therapies. The misregulation of kinase signalling appears to be important both for the remodelling of the cell by HCV and for the host cell's response to these alterations. These changes occur in the host cell as a result of the expression of the complete viral proteome and of viral replication and, as such, can be assumed to be representative of the effects of HCV infection. The replicon system used herein expresses all of the HCV genome and forms active replication complexes; however, it does not assemble or secrete virions. Thus, there may be some additional changes within the active kinome during a real infection in the human liver in the context

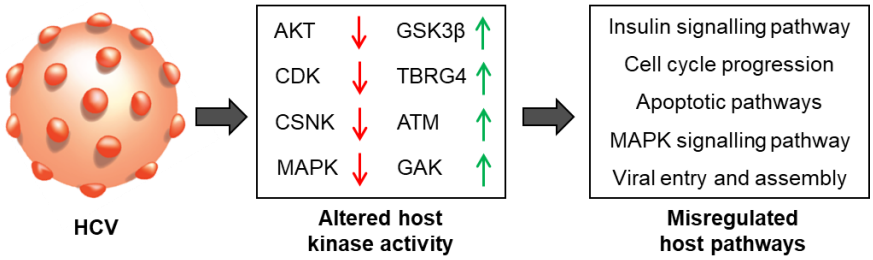

Figure 2.5: HCV-induced change in kinase activity affects host and host−virus interactions. RAC-β serine/threonine-protein kinase (AKT), glycogen synthase kinase 3-β (GSK3β), cyclin-dependent kinases (CDK), cyclin-G associated kinase (GAK), cell cycle progression restoration protein (TBRG4), casein kinase (CSNK), serine protein kinase ATM (ATM), and mitogen-activated pathway kinases (MAPK) displayed altered activity in HCV-replicon containing cells when probed with activity-based probe wortmannin-yne, leading to the misregulation of host pathways.

of the changes in enzyme activity measured herein. We are currently exploring the mechanistic aspects of these changes in activity.

2.6 References

(1) Alvisi, G.; Madan, V.; Bartenschlager, R. Hepatitis c Virus and Host Cell Lipids: An Intimate Connection. *RNA Biol.* **2011**, *8* (2), 258–269.

(2) Conteduca, V.; Sansonno, D.; Russi, S.; Pavone, F.; Dammacco, F. Therapy of Chronic Hepatitis C Virus Infection in the Era of Direct-Acting and Host-Targeting Antiviral Agents. *J. Infect.* **2014**, *68* (1), 1–20.

(3) Ashraf, M. U.; Iman, K.; Khalid, M. F.; Salman, H. M.; Shafi, T.; Rafi, M.; Javaid, N.; Hussain, R.; Ahmad, F.; Shahzad-Ul-Hussan, S.; et al. Evolution of Efficacious Pangenotypic Hepatitis C Virus Therapies. *Med. Res. Rev.* **2019**, *39* (3), 1091–1136.

(4) Herker, E.; Ott, M. Unique Ties between Hepatitis C Virus Replication and Intracellular Lipids. *Trends Endocrinol. Metab.* **2011**, *22* (6), 241–248.

(5) Supekova, L.; Supek, F.; Lee, J.; Chen, S.; Gray, N.; Pezacki, J.; Schlapbach, A.; Schultz, P. Identification of Human Kinases Involved in Hepatitis C Virus Replication by Small Interference RNA Library Screening. *J. Biol. Chem.* **2008**, *283* (1), 29–36.

(6) Munakata, T.; Inada, M.; Tokunaga, Y.; Wakita, T.; Kohara, M.; Nomoto, A. Suppression of Hepatitis C Virus Replication by Cyclin-Dependent Kinase Inhibitors. *Antiviral Res.* **2014**, *108*, 79–87.

(7) Li, Q.; Zhang, Y.-Y.; Chiu, S.; Hu, Z.; Lan, K.-H.; Cha, H.; Sodroski, C.; Zhang, F.; Hsu, C.-S.; Thomas, E.; et al. Integrative Functional Genomics of Hepatitis C Virus Infection Identifies Host Dependencies in Complete Viral Replication Cycle. *PLoS Pathog.* **2014**, *10* (5), e1004163–e1004163.

(8) Tai, A. W.; Benita, Y.; Peng, L. F.; Kim, S.-S.; Sakamoto, N.; Xavier, R. J.; Chung, R. T. A

Functional Genomic Screen Identifies Cellular Cofactors of Hepatitis C Virus Replication. *Cell host & microbe* **2009**, *5* (3), 298—307.

(9) Vaillancourt, F. H.; Pilote, L.; Cartier, M.; Lippens, J.; Liuzzi, M.; Bethell, R. C.; Cordingley, M. G.; Kukolj, G. Identification of a Lipid Kinase as a Host Factor Involved in Hepatitis C Virus RNA Replication. *Virology* **2009**, *387* (1), 5–10.

(10) Borawski, J.; Troke, P.; Puyang, X.; Gibaja, V.; Zhao, S.; Mickanin, C.; Leighton-Davies, J.; Wilson, C. J.; Myer, V.; Cornellataracido, I.; et al. Class III Phosphatidylinositol 4-Kinase Alpha and Beta Are Novel Host Factor Regulators of Hepatitis C Virus Replication. *J. Virol.* **2009**, *83* (19), 10058–10074.

(11) Bishé, B.; Syed, G. H.; Field, S. J.; Siddiqui, A. Role of Phosphatidylinositol 4-Phosphate (PI4P) and Its Binding Protein GOLPH3 in Hepatitis C Virus Secretion. *J. Biol. Chem.* **2012**, *287* (33), 27637–27647.

(12) Trotard, M.; Lepère-Douard, C.; Régeard, M.; Piquet-Pellorce, C.; Lavillette, D.; Cosset, F.-L.; Gripon, P.; Le Seyec, J. Kinases Required in Hepatitis C Virus Entry and Replication Highlighted by Small Interference RNA Screening. *FASEB J.* **2009**, *23* (11), 3780–3789.

(13) Berger, K. L.; Kelly, S. M.; Jordan, T. X.; Tartell, M. A.; Randall, G. Hepatitis C Virus Stimulates the Phosphatidylinositol 4-Kinase III Alpha-Dependent Phosphatidylinositol 4-Phosphate Production That Is Essential for Its Replication. *J. Virol.* **2011**, *85* (17), 8870–8883.

(14) Lim, Y.-S.; Hwang, S. B. Hepatitis C Virus NS5A Protein Interacts with Phosphatidylinositol 4-Kinase Type IIIalpha and Regulates Viral Propagation. *J. Biol. Chem.* **2011**, *286* (13), 11290–11298.

(15) He, Y.; Nakao, H.; Tan, S.-L.; Polyak, S. J.; Neddermann, P.; Vijaysri, S.; Jacobs, B. L.; Katze, M. G. Subversion of Cell Signaling Pathways by Hepatitis C Virus Nonstructural 5A Protein via Interaction with Grb2 and P85 Phosphatidylinositol 3-Kinase. *J. Virol.* **2002**, *76* (18), 9207–9217.

(16) Liu, Z.; Tian, Y.; Machida, K.; Lai, M. M. C.; Luo, G.; Foung, S. K. H.; Ou, J. J. Transient Activation of the PI3K-AKT Pathway by Hepatitis C Virus to Enhance Viral Entry. *J. Biol. Chem.* **2012**, *287* (50), 41922–41930.

(17) Lee, A.; Liu, S.; Wang, T. Identification of Novel Human Kinases That Suppress Hepatitis C Virus Infection. *J. Viral Hepat.* **2014**, *21* (10), 716–726.

(18) Aytug, S.; Reich, D.; Sapiro, L. E.; Bernstein, D.; Begum, N. Impaired IRS-1/PI3-Kinase Signaling in Patients with HCV: A Mechanism for Increased Prevalence of Type 2 Diabetes. *Hepatology* **2003**, *38* (6), 1384–1392.

(19) Mannová, P.; Beretta, L. Activation of the N-Ras-PI3K-Akt-MTOR Pathway by Hepatitis C Virus: Control of Cell Survival and Viral Replication. *J. Virol.* **2005**, *79* (14), 8742–8749.

(20) Street, A.; Macdonald, A.; Crowder, K.; Harris, M. The Hepatitis C Virus NS5A Protein Activates a Phosphoinositide 3-Kinase-Dependent Survival Signaling Cascade. *J. Biol. Chem.* **2004**, *279* (13), 12232–12241.

(21) Reiss, S.; Rebhan, I.; Backes, P.; Romero-Brey, I.; Erfle, H.; Matula, P.; Kaderali, L.; Poenisch, M.; Blankenburg, H.; Hiet, M.-S.; et al. Recruitment and Activation of a Lipid Kinase by Hepatitis C Virus NS5A Is Essential for Integrity of the Membranous Replication Compartment. *Cell Host Microbe* **2011**, *9* (1), 32–45.

(22) Hsu, N.-Y.; Ilnytska, O.; Belov, G.; Santiana, M.; Chen, Y.-H.; Takvorian, P. M.; Pau, C.; van der Schaar, H.; Kaushik-Basu, N.; Balla, T.; et al. Viral Reorganization of the Secretory Pathway Generates Distinct Organelles for RNA Replication. *Cell* **2010**, *141* (5), 799–811.

(23) Bianco, A.; Reghellin, V.; Donnici, L.; Fenu, S.; Alvarez, R.; Baruffa, C.; Peri, F.; Pagani, M.; Abrignani, S.; Neddermann, P.; et al. Metabolism of Phosphatidylinositol 4-Kinase IIIα-Dependent PI4P Is Subverted by HCV and Is Targeted by a 4-Anilino Quinazoline with Antiviral Activity. *PLOS Pathog.* **2012**, *8* (3), e1002576.

(24) Sherratt, A. R.; Nasheri, N.; McKay, C. S.; O'Hara, S.; Hunt, A.; Ning, Z.; Figeys, D.; Goto, N.

K.; Pezacki, J. P. A New Chemical Probe for Phosphatidylinositol Kinase Activity. *ChemBioChem* **2014**, *15* (9), 1253–1256.

(25) Karamichali, E.; Foka, P.; Tsitoura, E.; Kalliampakou, K.; Kazazi, D.; Karayiannis, P.; Georgopoulou, U.; Mavromara, P. HCV NS5A Co-Operates with PKR in Modulating HCV IRES-Dependent Translation. *Infect. Genet. Evol.* **2014**, *26*, 113–122.

(26) Serfaty, L.; Capeau, J. Hepatitis C, Insulin Resistance and Diabetes: Clinical and Pathogenic Data. *Liver Int.* **2009**, *29* (s2), 13–25.

(27) Del Campo, J. A.; Romero-Gómez, M. Steatosis and Insulin Resistance in Hepatitis C: A Way out for the Virus? *World J. Gastroenterol.* **2009**, *15* (40), 5014–5019.

(28) Cravatt, B. F.; Wright, A. T.; Kozarich, J. W. Activity-Based Protein Profiling: From Enzyme Chemistry to Proteomic Chemistry. *Annu. Rev. Biochem.* **2008**, *77* (1), 383–414.

(29) Fonović, M.; Bogyo, M. Activity-Based Probes as a Tool for Functional Proteomic Analysis of Proteases. *Expert Rev. Proteomics* **2008**, *5* (5), 721–730.

(30) Boersema, P. J.; Raijmakers, R.; Lemeer, S.; Mohammed, S.; Heck, A. J. R. Multiplex Peptide Stable Isotope Dimethyl Labeling for Quantitative Proteomics. *Nat. Protoc.* **2009**, *4* (4), 484–494.

(31) Li, N.; Kuo, C.-L.; Paniagua, G.; van den Elst, H.; Verdoes, M.; Willems, L. I.; van der Linden, W. A.; Ruben, M.; van Genderen, E.; Gubbens, J.; et al. Relative Quantification of Proteasome Activity by Activity-Based Protein Profiling and LC-MS/MS. *Nat. Protoc.* **2013**, *8* (6), 1155–1168.

(32) Kalesh, K. A.; Sim, D. S. B.; Wang, J.; Liu, K.; Lin, Q.; Yao, S. Q. Small Molecule Probes That Target Abl Kinase. *Chem. Commun.* **2010**, *46* (7), 1118–1120.

(33) Patricelli, M. P.; Nomanbhoy, T. K.; Wu, J.; Brown, H.; Zhou, D.; Zhang, J.; Jagannathan, S.; Aban, A.; Okerberg, E.; Herring, C.; et al. In Situ Kinase Profiling Reveals Functionally Relevant Properties of Native Kinases. *Chem. Biol.* **2011**, *18* (6), 699–710.

(34) Patricelli, M. P.; Szardenings, A. K.; Liyanage, M.; Nomanbhoy, T. K.; Wu, M.; Weissig, H.; Aban, A.; Chun, D.; Tanner, S.; Kozarich, J. W. Functional Interrogation of the Kinome Using Nucleotide Acyl Phosphates. *Biochemistry* **2007**, *46* (2), 350–358.

(35) Ortega, C.; Liao, R.; Anderson, L. N.; Rustad, T.; Ollodart, A. R.; Wright, A. T.; Sherman, D. R.; Grundner, C. Mycobacterium Tuberculosis Ser/Thr Protein Kinase B Mediates an Oxygen-Dependent Replication Switch. *PLOS Biol.* **2014**, *12* (1), e1001746.

(36) Nourbakhsh, M.; Douglas, D. N.; Pu, C. H.; Lewis, J. T.; Kawahara, T.; Lisboa, L. F.; Wei, E.; Asthana, S.; Quiroga, A. D.; Law, L. M. J.; et al. Arylacetamide Deacetylase: A Novel Host Factor with Important Roles in the Lipolysis of Cellular Triacylglycerol Stores, VLDL Assembly and HCV Production. *J. Hepatol.* **2013**, *59* (2), 336–343.

(37) Nasheri, N.; McKay, C. S.; Fulton, K.; Twine, S.; Powdrill, M. H.; Sherratt, A. R.; Pezacki, J. P. Hydrophobic Triaryl-Substituted β-Lactams as Activity-Based Probes for Profiling Eukaryotic Enzymes and Host-Pathogen Interactions. *ChemBioChem* **2014**, *15* (15), 2195–2200.

(38) Desrochers, G. F.; Sherratt, A. R.; Blais, D. R.; Nasheri, N.; Ning, Z.; Figeys, D.; Goto, N. K.; Pezacki, J. P. Profiling Kinase Activity during Hepatitis C Virus Replication Using a Wortmannin Probe. *ACS Infect. Dis.* **2015**, *1* (9), 443–452.

(39) Blais, D. R.; Brûlotte, M.; Qian, Y.; Bélanger, S.; Yao, S. Q.; Pezacki, J. P. Activity-Based Proteome Profiling of Hepatoma Cells during Hepatitis C Virus Replication Using Protease Substrate Probes. *J. Proteome Res.* **2010**, *9* (2), 912–923.

(40) Blais, D. R.; Lyn, R. K.; Joyce, M. A.; Rouleau, Y.; Steenbergen, R.; Barsby, N.; Zhu, L.-F.; Pegoraro, A. F.; Stolow, A.; Tyrrell, D. L.; et al. Activity-Based Protein Profiling Identifies a Host Enzyme, Carboxylesterase 1, Which Is Differentially Active during Hepatitis C Virus Replication. *J. Biol. Chem.* **2010**, *285* (33), 25602–25612.

(41) Singaravelu, R.; Blais, D. R.; McKay, C. S.; Pezacki, J. Activity-Based Protein Profiling of the Hepatitis C Virus Replication in Huh-7 Hepatoma Cells Using a Non-Directed Active Site

Probe. *Proteome Sci.* **2010**, *8* (1), 5.

(42) Liu, J.; Hu, Y.; Waller, D. L.; Wang, J.; Liu, Q. Natural Products as Kinase Inhibitors. *Nat. Prod. Rep.* **2012**, *29* (3), 392–403.

(43) Wymann, M. P.; Bulgarelli-Leva, G.; Zvelebil, M. J.; Pirola, L.; Vanhaesebroeck, B.; Waterfield, M. D.; Panayotou, G. Wortmannin Inactivates Phosphoinositide 3-Kinase by Covalent Modification of Lys-802, a Residue Involved in the Phosphate Transfer Reaction. *Mol. Cell. Biol.* **1996**, *16* (4), 1722 LP – 1733.

(44) Yee, M.; Fas, S. C.; Stohlmeyer, M. M.; Wandless, T. J.; Cimprich, K. A. A Cell-Permeable, Activity-Based Probe for Protein and Lipid Kinases. *J. Biol. Chem.* **2005**, *280* (32), 29053–29059.

(45) Liu, Y.; Shreder, K. R.; Gai, W.; Corral, S.; Ferris, D. K.; Rosenblum, J. S. Wortmannin, a Widely Used Phosphoinositide 3-Kinase Inhibitor, Also Potently Inhibits Mammalian Polo-like Kinase. *Chem. Biol.* **2005**, *12* (1), 99–107.

(46) Lavanchy, D.; Blais, D. R.; McKay, C. S.; Pezacki, J. P.; Lavanchy, D.; Lindenbach, B.; Rice, C.; Ploss, A.; Evans, M.; Gaysinskaya, V.; et al. The Global Burden of Hepatitis C. *Liver Int.* **2009**, *29* (1), 74–81.

(47) Zhang, G.; Annan, R. S.; Carr, S. A.; Neubert, T. A. Overview of Peptide and Protein Analysis by Mass Spectrometry. *Curr. Protoc. Protein Sci.* **2010**, *62* (1), 16.1.1-16.1.30.

(48) Chan, C.-H.; Jo, U.; Kohrman, A.; Rezaeian, A. H.; Chou, P.-C.; Logothetis, C.; Lin, H.-K. Posttranslational Regulation of Akt in Human Cancer. *Cell Biosci.* **2014**, *4* (1), 59.

(49) Rayasam, G. V.; Tulasi, V. K.; Sodhi, R.; Davis, J. A.; Ray, A. Glycogen Synthase Kinase 3: More than a Namesake. *Br. J. Pharmacol.* **2009**, *156* (6), 885–898.

(50) Bose, S. K.; Ray, R. Hepatitis C Virus Infection and Insulin Resistance. *World J. Diabetes* **2014**, *5* (1), 52–58.

(51) Pazienza, V.; Clément, S.; Pugnale, P.; Conzelman, S.; Foti, M.; Mangia, A.; Negro, F. The

Hepatitis C Virus Core Protein of Genotypes 3a and 1b Downregulates Insulin Receptor Substrate 1 through Genotype-Specific Mechanisms. *Hepatology* **2007**, *45* (5), 1164–1171.

(52) Hsieh, M.-J.; Lan, K.-P.; Liu, H.-Y.; Zhang, X.-Z.; Lin, Y.-F.; Chen, T.-Y.; Chiou, H.-L. Hepatitis C Virus E2 Protein Involve in Insulin Resistance through an Impairment of Akt/PKB and GSK3β Signaling in Hepatocytes. *BMC Gastroenterol.* **2012**, *12* (1), 74.

(53) Bernsmeier, C.; Duong, F.; Christen, V.; Pugnale, P.; Negro, F.; Terracciano, L.; Heim, M. Virus-Induced over-Expression of Protein Phosphatase 2A Inhibits Insulin Signalling in Chronic Hepatitis C. *J. Hepatol.* **2008**, *49*, 429–440.

(54) Alberstein, M.; Zornitzki, T.; Zick, Y.; Knobler, H. Hepatitis C Core Protein Impairs Insulin Downstream Signalling and Regulatory Role of IGFBP-1 Expression. *J. Viral Hepat.* **2012**, *19* (1), 65–71.

(55) Kawaguchi, T.; Yoshida, T.; Harada, M.; Hisamoto, T.; Nagao, Y.; Ide, T.; Taniguchi, E.; Kumemura, H.; Hanada, S.; Maeyama, M.; et al. Hepatitis C Virus Down-Regulates Insulin Receptor Substrates 1 and 2 through Up-Regulation of Suppressor of Cytokine Signaling 3. *Am. J. Pathol.* **2004**, *165* (5), 1499–1508.

(56) Gao, T.; Qin, Z.; Ren, H.; Zhao, P.; Qi, Z. Inhibition of IRS-1 by Hepatitis C Virus Infection Leads to Insulin Resistance in a PTEN-Dependent Manner. *Virol. J.* **2015**, *12* (1), 12.

(57) Deng, L.; Shoji, I.; Ogawa, W.; Kaneda, S.; Soga, T.; Jiang, D.; Ide, Y.-H.; Hotta, H. Hepatitis C Virus Infection Promotes Hepatic Gluconeogenesis through an NS5A-Mediated, FoxO1-Dependent Pathway. *J. Virol.* **2011**, *85* (17), 8556 LP – 8568.

(58) Liu, J.; Ding, X.; Tang, J.; Cao, Y.; Hu, P.; Zhou, F.; Shan, X.; Cai, X.; Chen, Q.; Ling, N.; et al. Enhancement of Canonical Wnt/β-Catenin Signaling Activity by HCV Core Protein Promotes Cell Growth of Hepatocellular Carcinoma Cells. *PLoS One* **2011**, *6* (11), e27496–e27496.

(59) Park, C.-Y.; Choi, S.-H.; Kang, S.-M.; Kang, J.-I.; Ahn, B.-Y.; Kim, H.; Jung, G.; Choi, K.-Y.; Hwang, S. B. Nonstructural 5A Protein Activates β-Catenin Signaling Cascades:

Implication of Hepatitis C Virus-Induced Liver Pathogenesis. *J. Hepatol.* **2009**, *51* (5), 853–864.

(60) Li, R.; Wei, J.; Jiang, C.; Liu, D.; Deng, L.; Zhang, K.; Wang, P. Akt SUMOylation Regulates Cell Proliferation and Tumorigenesis. *Cancer Res.* **2013**, *73* (18), 5742 LP – 5753.

(61) Ali, A.; Hoeflich, K. P.; Woodgett, J. R. Glycogen Synthase Kinase-3: Properties, Functions, and Regulation. *Chem. Rev.* **2001**, *101* (8), 2527–2540.

(62) Bose, S. K.; Shrivastava, S.; Meyer, K.; Ray, R. B.; Ray, R. Hepatitis C Virus Activates the MTOR/S6K1 Signaling Pathway in Inhibiting IRS-1 Function for Insulin Resistance. *J. Virol.* **2012**, *86* (11), 6315 LP – 6322.

(63) Sola-Penna, M.; Da Silva, D.; Coelho, W. S.; Marinho-Carvalho, M. M.; Zancan, P. Regulation of Mammalian Muscle Type 6-Phosphofructo-1-Kinase and Its Implication for the Control of the Metabolism. *IUBMB Life* **2010**, *62* (11), 791–796.

(64) Taketa, K.; Shimamura, J.; Takesue, A.; Tanaka, A.; Kosaka, K. Undifferentiated Patterns of Key Carbohydrate-Metabolizing Enzymes in Injured Livers. II. Human Viral Hepatitis and Cirrhosis of the Liver. *Enzyme* **1976**, *21* (3), 200–210.

(65) Ndjomou, J.; Park, I.; Liu, Y.; Mayo, L. D.; He, J. J. Up-Regulation of Hepatitis C Virus Replication and Production by Inhibition of MEK/ERK Signaling. *PLoS One* **2009**, *4* (10), e7498–e7498.

(66) Pei, R.; Zhang, X.; Xu, S.; Meng, Z.; Roggendorf, M.; Lu, M.; Chen, X. Regulation of Hepatitis C Virus Replication and Gene Expression by the MAPK-ERK Pathway. *Virol. Sin.* **2012**, *27* (5), 278–285.

(67) Huang, Y.; Chen, X. C.; Konduri, M.; Fomina, N.; Lu, J.; Jin, L.; Kolykhalov, A.; Tan, S.-L. Mechanistic Link between the Anti-HCV Effect of Interferon Gamma and Control of Viral Replication by a Ras-MAPK Signaling Cascade. *Hepatology* **2006**, *43* (1), 81–90.

(68) Zhu, H.; Shang, X.; Terada, N.; Liu, C. STAT3 Induces Anti-Hepatitis C Viral Activity in Liver Cells. *Biochem. Biophys. Res. Commun.* **2004**, *324* (2), 518–528.

(69) Randall, G.; Panis, M.; Cooper, J. D.; Tellinghuisen, T. L.; Sukhodolets, K. E.; Pfeffer, S.; Landthaler, M.; Landgraf, P.; Kan, S.; Lindenbach, B. D.; et al. Cellular Cofactors Affecting Hepatitis C Virus Infection and Replication. *Proc. Natl. Acad. Sci.* **2007**, *104* (31), 12884 LP – 12889.

(70) Li, Q.; Brass, A. L.; Ng, A.; Hu, Z.; Xavier, R. J.; Liang, T. J.; Elledge, S. J. A Genome-Wide Genetic Screen for Host Factors Required for Hepatitis C Virus Propagation. *Proc. Natl. Acad. Sci.* **2009**, *106* (38), 16410 LP – 16415.

(71) Sarfraz, S.; Hamid, S.; Siddiqui, A.; Hussain, S.; Pervez, S.; Alexander, G. Altered Expression of Cell Cycle and Apoptotic Proteins in Chronic Hepatitis C Virus Infection. *BMC Microbiol.* **2008**, *8* (1), 133.

(72) Werling, K.; Szentirmay, Z.; Szepesi, A.; Schaff, Z.; Szalay, F.; Szabó, Z.; Telegdy, L.; David, K.; Stotz, G.; Tulassay, Z. Hepatocyte Proliferation and Cell Cycle Phase Fractions in Chronic Viral Hepatitis C by Image Analysis Method. *Eur. J. Gastroenterol. Hepatol.* **2001**, *13* (5), 489–493.

(73) Yang, X.-J.; Liu, J.; Ye, L.; Liao, Q.-J.; Wu, J.-G.; Gao, J.-R.; She, Y.-L.; Wu, Z.-H.; Ye, L.-B. HCV NS2 Protein Inhibits Cell Proliferation and Induces Cell Cycle Arrest in the S-Phase in Mammalian Cells through down-Regulation of Cyclin A Expression. *Virus Res.* **2006**, *121* (2), 134–143.

(74) Ohkawa, K.; Ishida, H.; Nakanishi, F.; Hosui, A.; Ueda, K.; Takehara, T.; Hori, M.; Hayashi, N. Hepatitis C Virus Core Functions as a Suppressor of Cyclin-Dependent Kinase-Activating Kinase and Impairs Cell Cycle Progression. *J. Biol. Chem.* **2004**, *279* (12), 11719–11726.

(75) Malumbres, M.; Barbacid, M. Cell Cycle, CDKs and Cancer: A Changing Paradigm. *Nat. Rev. Cancer* **2009**, *9* (3), 153–166.

(76) Neganova, I.; Vilella, F.; Atkinson, S. P.; Lloret, M.; Passos, J. F.; von Zglinicki, T.; O'Connor, J.-E.; Burks, D.; Jones, R.; Armstrong, L.; et al. An Important Role for CDK2 in G1 to S

Checkpoint Activation and DNA Damage Response in Human Embryonic Stem Cells. *Stem Cells* **2011**, *29* (4), 651–659.

(77) Edwards, M. C.; Liegeois, N.; Horecka, J.; DePinho, R. A.; Sprague, G. F.; Tyers, M.; Elledge, S. Human Cpr (Cell Cycle Progression Restoration) Genes Impart a Far(-) Phenotype on Yeast Cells. *Genetics* **1997**, *147* (3), 1063–1076.

(78) Daugherity, E. K.; Balmus, G.; Al Saei, A.; Moore, E. S.; Abi Abdallah, D.; Rogers, A. B.; Weiss, R. S.; Maurer, K. J. The DNA Damage Checkpoint Protein ATM Promotes Hepatocellular Apoptosis and Fibrosis in a Mouse Model of Non-Alcoholic Fatty Liver Disease. *Cell Cycle* **2012**, *11* (10), 1918–1928.

(79) Ivanov, A. V; Bartosch, B.; Smirnova, O. A.; Isaguliants, M. G.; Kochetkov, S. N. HCV and Oxidative Stress in the Liver. *Viruses* **2013**, *5* (2), 439–469.

(80) Sayed, M.; Pelech, S.; Wong, C.; Marotta, A.; Salh, B. Protein Kinase CK2 Is Involved in G2 Arrest and Apoptosis Following Spindle Damage in Epithelial Cells. *Oncogene* **2001**, *20* (48), 6994–7005.

(81) Neveu, G.; Barouch-Bentov, R.; Ziv-Av, A.; Gerber, D.; Jacob, Y.; Einav, S. Identification and Targeting of an Interaction between a Tyrosine Motif within Hepatitis C Virus Core Protein and AP2M1 Essential for Viral Assembly. *PLOS Pathog.* **2012**, *8* (8), e1002845.

(82) Neveu, G.; Ziv-Av, A.; Barouch-Bentov, R.; Berkerman, E.; Mulholland, J.; Einav, S. AP-2-Associated Protein Kinase 1 and Cyclin G-Associated Kinase Regulate Hepatitis C Virus Entry and Are Potential Drug Targets. *J. Virol.* **2015**, *89* (8), 4387 LP – 4404.

(83) Tellinghuisen, T. L.; Foss, K. L.; Treadaway, J. Regulation of Hepatitis C Virion Production via Phosphorylation of the NS5A Protein. *PLoS Pathog.* **2008**, *4* (3), e1000032–e1000032.

(84) Woerz, I.; Lohmann, V.; Bartenschlager, R. Hepatitis C Virus Replicons: Dinosaurs Still in Business? *J. Viral Hepat.* **2009**, *16* (1), 1–9.

(85) Kim, S.; Jin, B.; Choi, S. H.; Han, K.-H.; Ahn, S. H. Casein Kinase II Inhibitor Enhances

Production of Infectious Genotype 1a Hepatitis C Virus (H77S). *PLoS One* **2014**, *9* (12), e113938.

Chapter 3: Activity-Based PIK Probes Detect Changes to Protein-Protein Interactions During Hepatitis C Virus Replication

Initially published as Geneviève F. Desrochers, Craig McKay, Christina Cornacchia, John Paul Pezacki (2018) *Activity-Based PIK Probes Detect Changes to Protein-Protein Interactions.* ACS Infec. Dis. 4 (5), 752–757

3.1 Statement of contribution

Geneviève F. Desrochers performed all biochemical and biological cell work. Craig McKay and Christina Cornacchia performed the synthesis of the novel probes. John Paul Pezacki was responsible for the original project design. The manuscript was written by Geneviève F. Desrochers and John Paul Pezacki.

3.1.1 Acknowledgments

The authors acknowledge Dr. Allison Sherratt and Ashley Hunt for helpful discussion on this project.

3.2 Summary

Protein-protein interactions are integral to host-virus interactions and can contribute significantly to enzyme regulation by changing the localization of both host and viral enzymes within the cell, inducing conformational change relevant to enzyme activity, or recruiting other additional proteins to form functional complexes. Identifying the interactors of active enzymes using an activity-based protein profiling probe has allowed us to characterise both normal enzyme activation mechanisms, and the manner by which these are mechanisms are hijacked and altered by the hepatitis C virus (HCV). Here we report use of a novel activity-based probe, PIKBPyne, which labels PIKs in an activity-based manner, to investigate HCV-dependent changes in protein-protein interactions for PI4KB. Herein, we report the synthesis of new variations on PIKBPyne, compare their ability to label the interacting partners of PIKs, and demonstrate the utility of our approach in characterizing virus-mediated changes to host function.

3.3 Introduction

Protein-protein interactions play an important role host-virus interactions, including the hepatitis C virus (HCV), and are involved in the regulation of cellular growth and function, such as cell division and liver development and regeneration,[1,2] viral and cancer pathogenesis,[3,4] and the activation and evasion of the immune system.[3,5] Modulation of these interactions has become a focus for the development of novel therapeutics, and new drugs which disrupt key interactions are currently being developed.[5–7] The development of tools which enable the identification and characterization these interactions is therefore of great interest.

Photo-affinity labelling (PAL) is a technique which uses a photo-activatable crosslinking group to induce covalent bonds to target proteins.[8,9] Benzophenone, one of the most commonly used crosslinking groups, forms a radical upon irradiation with light at 365 nm which is able to react with amino acids or nucleotides.[10] It is widely used as a crosslinking group due to its selectivity, stability, compatibility with many synthetic strategies, and mild photoactivation conditions.[9,11] Incorporation of a benzophenone-containing unnatural amino acid into an engineered protein has previously been used to probe protein-protein interactions.[12–14] This strategy, while effective, relies on the expression of the protein of interest at higher than physiological levels. To avoid exogenous protein overexpression, recent research has focused on the development of small molecule probes. PAL probes have previously been used to label and characterise exchange factors, binding proteins, and enzymes in lysates and live cells.[8,15–22] Certain probes have additionally been shown to be able to detect protein-protein interactions between a protein of interest and its regulators, or specialized interactions dependent on the presence of post-translational modifications.[11,23] This ability to label enzymes either *in situ* or with minimal disruption enables the capture of transient or easily disrupted interactions, a clear advantage over other techniques such as co-immunoprecipitation.

Activity-based probes (ABPs) are small molecules typically based on covalent active-site enzyme inhibitors that either require enzyme activity to catalyse protein labelling or report on the active form using other molecular approaches including PAL.[24] These probes are typically then modified to contain a reporter group using bio-orthogonal chemistry.[24] In order to make probes out of non-covalent inhibitors, inhibitors have been combined with PAL to form new activity-based probes.[25–27] The first such example, from the Cravatt group, was a series of probes against histone deacetylaces (HDAC) used for photo-inducible enzyme labelling.[25,26] It was subsequently demonstrated that these probes, in addition to labelling the target enzyme, were also capable of labelling the target's associated proteins, and could therefore identify any proteins which interacted with and regulated the targeted enzyme.[26] We applied this strategy to design probes against phosphatidylinositol kinases (PIKs), and study one specific PIK, PI4KB. The phosphatidylinositol phosphates (PIPs) are key eukaryotic intracellular phospholipids, generated through the phosphorylation of the 3, 4, or 5 position of the inositol ring by PIKs.[28–30] Regulation of the various members of the PIK family of enzymes leads to the differences in the PI profile throughout the cell which regulate the membrane environment via the establishment of organelle identity, signal transduction, and the recruitment of proteins to membranes.[30] Disruption of normal PI distribution via hijacking of PIK regulation has been shown to play a role in virus-mediated cellular remodelling by positive-strand RNA viruses, including HCV, and Aichi virus, and other picornaviruses.[31–36]

The role of PI4KB in viral infection is of particular interest, as it has been shown that its increase in activity is due to post-translational activation.[37] Increased expression alone of PI4KB does not result in an increase to the level of its substrate, PI4P.[28] PI4KB must be activated by recruitment to the Golgi membrane, followed by phosphorylation and stabilization of its most active form via protein-protein interactions.[28,38,39] This makes the identification and quantification of protein-protein interactions of vital interest to investigating the methods by which viruses regulate enzyme activity. We have previously introduced an ABPP PAL probe, PIKBPyne (Fig 3.1, ABP1), based on the PIK inhibitor PIK93.[30] This

probe can report on the activities of several PIKs.[37] Although similar probes are sometimes referred to as affinity-based probes (AfBPs), we consider probe 1 and others herein to be ABPs because they only bind the active conformation of their target enzyme and distinguish active from inactive forms of their targets. Herein we report new probes based on PIKBPyne, with enhanced ability to capture and characterise the protein interactions, and demonstrate their utility in examining PI4KB activity and simultaneous alterations to protein-protein interactions during HCV replication.

3.4 Methods

3.4.1 Kinetic assay

Purified PI4KB (Sigma) was diluted in kinase buffer (12.5mM $MgCl_2$, 12.5mM $MnCl_2$, 75mM Tris-HCl, 25mM EGTA). IC_{50}s of probes 1-4 were measured using the ADP-Glo PI kinase kit (Progema) in reaction buffer (5mM $MgCl_2$, 5mM $MnCl_2$, 30mM Tris-HCl, 10mM EGTA, 5mM DTT, 2.5g/L BSA, 0.25g/L Triton-X) according to the manufacturer's protocol, using 100 μM ATP in a total reaction volume of 10μL.

3.4.2 Tissue culture

Huh7.5 human hepatoma cells were maintained in DMEM medium (Invitrogen) supplemented with 10% fetal bovine serum (CANSERA) and 100nM non-essential amino acids (GIBCO-BRL). The HCV full-genomic replicon cells (Huh7.5-FGR) were a kind gift from Charles Rice (Rockefeller University, USA) and Apath LLC (St. Louis, MO, USA). Cells stably expressing replicons were maintained in Huh7.5 culture medium supplemented with 250 μg/mL of G418 Geneticin (GIBCO-BRL).

3.4.3 siRNA transfection

Huh7.5 cells were seeded in 100 mm dishes and transfected with 10 nM siRNA against PI4KB and GAPDH (Dharmacon, Thermoscience). Cells were transfected again after 24 hours and lysed 48 hours

after the last transfection.

3.4.4 Proteome extraction

Proteins were lysed as previously described.[37] Proteins samples were quantified using the DC protein assay (Bio-Rad) according to the manufacturer's instructions.

3.4.5 Active proteome labelling and in-gel fluorescence

100µg of protein at 2mg/mL was labelled as previously described.[37] Labelled protein was fluorophore-tagged using click chemistry by the addition of 2 volumes of a stock solution containing 1mM CuSO4•5H2O, 100 µM TBTA (1:4 DMSO:t-butanol), 1 mM fresh TCEP, and 200 µM rhodamine azide in PBS. Samples were rotated for 45 minutes and the reaction was precipitated at -80°C in 4 volumes of acetone. The acetone was removed, and the proteins dissolved in SDS-PAGE loading buffer (0.1M Tris pH 6.8, 10% glycerol, 4% SDS, 0.02% bromophenol blue, 30mM DTT). Proteins were resolved on 10% TGX FastCast polyacrylamide gels (Bio-Rad), and fluorescence detected by the ChemiDoc MP system (Bio-Rad).

3.4.6 Active proteome labelling and western blotting

2 mg of protein at 2mg/mL was labelled and isolated as previously described,[37] using ABP3 (20µM) in place of probe 1 to label interacting proteins. Proteins were resolved on 12% TGX FastCast polyacrylamide gels (Bio-Rad) and transferred onto PVDF membrane using the Trans-Blot Turbo Transfer System (Bio-Rad). Immunoblotting was performed with mouse monoclonal antibodies anti-ACBD3 (Santa Cruz, 1:100 or 1:1000), anti-NS5A (Virogen, 1:4000), anti-β-tubulin (Santa Cruz, 1:1000) and anti-14-3-3 β (Santa Cruz, 1:250) and donkey monoclonal antibodies anti-PI4KB (Cell Signaling, 1:500) overnight at 4°C. Blots were subsequently probed with appropriate secondary

antibodies (Jackson Immunoresearch) and imaged using ECL clarity (Bio-Rad) in a ChemiDoc MP system (Bio-Rad).

3.5 Results and Discussion

Three new probes were synthesized, ABPs 2, 3 and 4, based on the original PIKBPyne probe.[37] (Fig 3.1) The probes all contain a PIK93 group to target the probe to PIK active sites, a benzophenone group to allow UV-mediated crosslinking to proteins, an alkyne handle to allow subsequent attachment of reporter tags, and a variable linker region between the targeting and crosslinking groups. This paper explores the effect of this linker region, either short (ABP 2), moderate (ABP 1), long (ABP 3), or rigid (ABP 4), on the labelling capabilities of the PIKBPyne group of probes. The details of the synthetic procedures are reported in the appendix.

PIK93 is a non-covalent competitive inhibitor of PI4KB, and interacts with the active site of its target enzymes, competing for the ATP-binding site.[40,41] These ABPs contain additional structures which may interfere with probe-active site interactions through steric hindrance or the gain and loss of hydrophobic or electrostatic interactions. It is therefore essential to assess the ability of these probes to interact with the active site of PI4KB. To this end, we determined the IC_{50} values of ABP 1-4 using the commercially available ADP-Glo and compared them to that of the original PIK93 inhibitor. The IC_{50} of PIK93 against PI4KB was determined to be 2.8nM, which agrees with literature values.[42] ABPs 1-3 demonstrated inhibition of PI4KB approximately 100-fold lower than PIK93, possessing IC_{50} values of 310, 480, and 360 nM, respectively (Table 3.1, Fig 3.3). The IC_{50} of ABP 4 was estimated to be approximately 7000 nM, 2000-fold higher than the IC_{50} of PIK93. We were unable to confidently determine the IC_{50} of ABP 4, as complete inhibition of enzyme activity was not achievable in this assay. The effective inhibition of enzymatic activity by ABPs 1-3 allows us to conclude that they are able to interact with the enzyme's active site as PIK93 does, albeit with lower affinity, and can be used to label PI4KB, while the higher

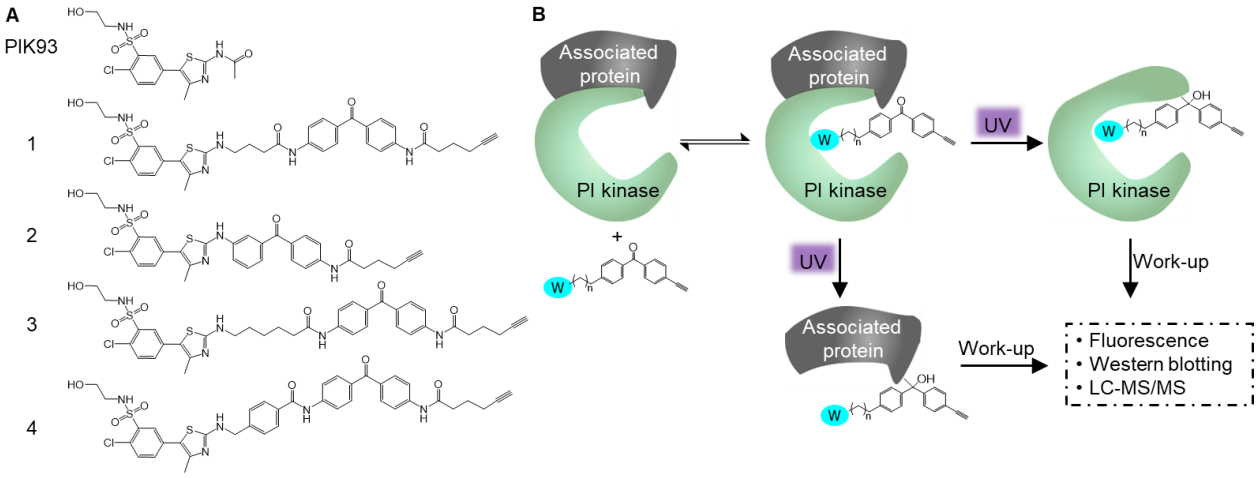

Figure 3.1: Activity-based protein profiling of PIKs. A) Structures of the PIK93 inhibitor and the PIKBPyne probes used to target PI kinases. B) Scheme of activity-based labelling of a target enzyme or an associated protein. W denotes the probe warhead.

IC_{50} of ABP 4 indicates that it could not effectively label PI4KB. We postulate that the structural rigidity of ABP 4 causes steric interactions that limit access of the probe to the enzyme active site, whereas ABPs 1-3 appear to bind to the PI4KB active site in a manner similar to PIK93.

We next compared the ability of the four probes to label proteins within a complex proteome. We found that ABPs 1, 2, and 3 demonstrated a similar pattern of labelled bands, with ABP3 displaying the strongest labelling, and ABP1 the weakest, while labelling by ABP4 was negligible. (Fig 3.2) This supports the conclusions drawn from the kinetic assay that ABPs 1-3 are able to interact with and label the enzyme active site, while the rigidity of ABP4 makes it unable to enter and label the active site. This is further supported by examination of the PI4KB crystal structure in complex with the PIK93 inhibitor, which shows an active site pocket too small to easily accommodate a rigid molecule.[41]

We have previously shown that ABP1 labels PI4KB.[37] It has previously been shown that ABPs containing benzophenone crosslinkers are capable of labelling interacting proteins which associate with the target enzyme, if the linker region extends the benzophenone photocrosslinking group outside of the active site pocket in the correct orientation.[26] Thus, we next investigated whether proteins interacting with PI4KB could be labelled by probes ABP 1-3.

Using mass spectrometry, we confirmed capture of known interactors of PI4KB using ABP 1-3. We used the IntAct Molecular Interaction Database[43] to identify potential interacting partners of PI4KB. LC-MS/MS on a PIBPyne-labelled proteome showed that several of these proteins were labelled by PIKBPyne (Table 3.2). Two such proteins, ACBD3 and a 14-3-3 protein, were of particular interest. Neither are known to have a nucleotide-binding site which could interact with PIKBPyne, and both have a well-characterized mechanism of interaction with PI4KB. The Golgi protein ACBD3, a membrane recruitment protein which plays essential roles in several cell signalling processes,[33,34,44–47] regulates the

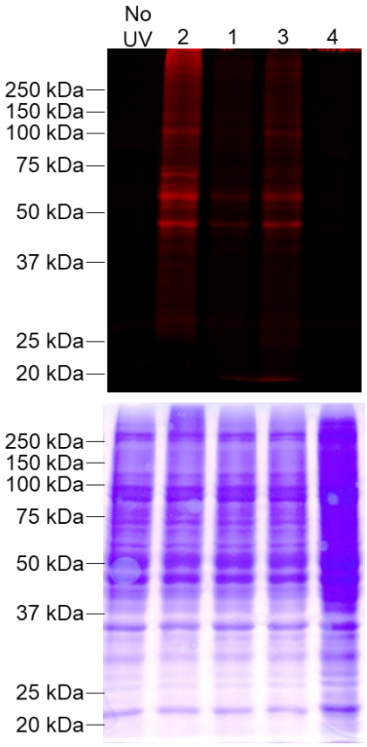

Figure 3.2: Fluorescent gel of active proteome labelling by ABPs 1-4. The proteome was labelled by PIKBPyne, and a fluorescent rhodamine reporter tag attached by copper-catalyzed click chemistry. Proteins were resolved by SDS-PAGE and visualized by fluorescent scanning. Coomassie stain is shown below.

Table 3.1: Inhibitory dose-response curve on PI4KB activity by PIK93 or PIKBPyne probes. Dose curves were generated using the ADP-Glo Lipid Kinase kit according to the manufacturer's protocol. Percent activity was calculated using a standard curve of ADP:ATP ratios, and dividing the concentration of ADP produced at each point by the ADP concentration in the absence of inhibitor (100% activity). IC_{50} values were determined using the sigmoidal dose-response model of the GraphPad Prism software.

Probe	IC_{50} (nM) ± SE	Relative K_I
PIK93	2.8 ± 0.7	1
1	310 ± 70	110 ± 40
2	480 ± 70	170 ± 50
3	360 ± 50	130 ± 40
4	7000 ± 5000	2000 ± 2000

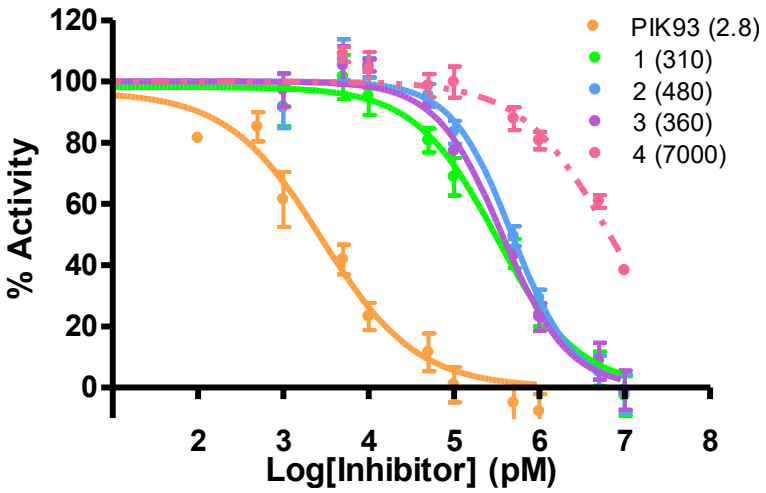

Figure 3.3: Inhibitory dose-response curve on PI4KB activity by PIK93 or PIKBPyne probes. Dose curves were generated using the ADP-Glo Lipid Kinase kit according to the manufacturer's protocol. Percent activity was calculated using a standard curve of ADP:ATP ratios, and dividing the concentration of ADP produced at each point by the ADP concentration in the absence of inhibitor (100% activity). The sigmoidal dose-response model of the GraphPad Prism software was used to determine the IC_{50} values (μM) indicated in parentheses.

activity of PI4KB by recruiting it to membranes containing its substrate.[48] Once recruited, PI4KB is activated by phosphorylation, and this active conformation is protected by interaction with 14-3-3 proteins.[38,39,49,50] Altogether, this suggests that our probe was able to label proteins interacting with its target, labelling the proteins interacting with active PI4KB.

We next asked whether labelling of these proteins could be blocked by incubation with the inhibitor PIK93. Competitive ABPP with PIK93 is able to eliminate labelling by ABP3 (Fig 3.4). Labelling of these proteins is therefore dependent on specific interactions with PIKBPyne. We subsequently verified that labelling of these proteins was dependent on the interaction of PIKBPyne with PI4KB. We used siRNA to knock-down PI4KB to 25% of its normal expression level (Fig 3.5). ABP3 was used to label the proteome, due to its longer linker length and stronger labelling (Fig 3.2). The labelled proteome was isolated and western blotting confirmed that both ACBD3 and 14-3-3β protein are labelled by PIKBPyne (Fig 3.6b, 3.6g, 3.6h). Although the expression levels of neither ACBD3 nor 14-3-3β change upon knock-down of PI4KB (Fig 3.6b, 3.6d, 3.6e), labelling of these regulatory proteins decreases by roughly 50% due to a decrease in the availability of PI4KB protein with which to interact (Fig 3.6g, 3.6h). We also examined the potential interaction of another protein, Golgi transport protein ADP-ribosylation factor 1 (ARF1), with PI4KB, however, in the cells and conditions studied we did not observe any discernible changes in PI4KB interactions. Overall, this data suggests that ABP3 labels these proteins due to their interaction with active PI4KB and provides further evidence that ABP3 is able to detect changes in protein-protein interactions by labelling target-associated proteins.

HCV relies on the activity of PIKs in order to change the cellular environment in its favour.[29,32,37,51–53] Having previously used a PIKBPyne probe to demonstrate that HCV effects an increase in the activity of PI4KB,[37] we next investigated the effect of HCV on the interaction between PI4KB and ACBD3. Naïve cells and cells expressing HCV-FGR, the HCV full-genomic replicon, (Fig 3.7a) were labelled

Table 3.2: PIKBPyne detects members of the PI4KB interactome. PI4KB interacting proteins were identified using the IntAct Molecular Interaction Database[43] and cross-referenced with proteins identified by LC-MS proteome labelling by PIK-BPyne.[37]

Gene ID	Peptide Count (Unique)
ACBD3	1 (1)
LAMP1	10 (3)
SFN; YWHAB; YWHAG; YWHAQ	5 (1)
XPO1	115 (26)

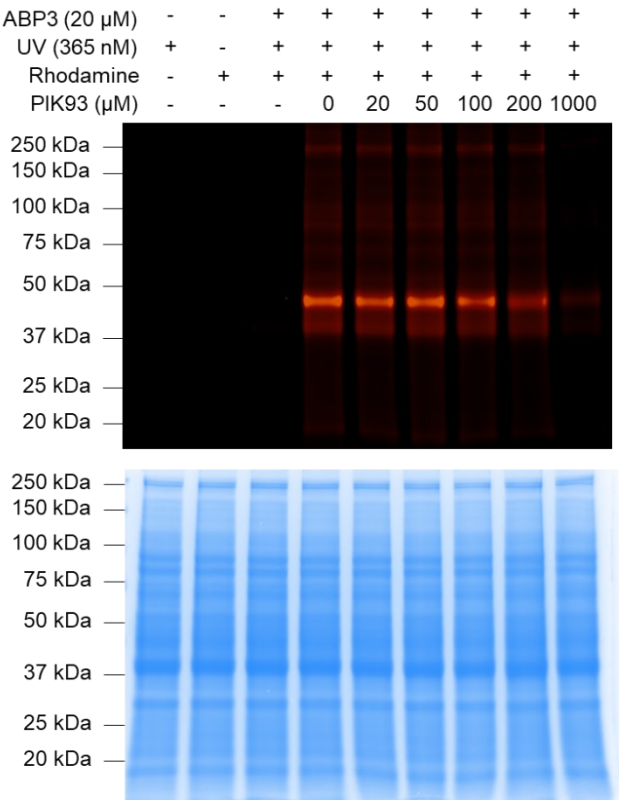

Figure 3.4: Competitive ABPP shows PIK93 inhibits labelling by ABP3. Huh7.5 proteome was incubated with increasing concentration of PIK93 inhibitor for 10 minutes, then labelled with ABP3 (20µM). Rhodamine was attached by copper-catalysed click chemistry and proteins were resolved by SDS-PAGE then visualized by fluorescent scanning. Coomassie stain is shown below.

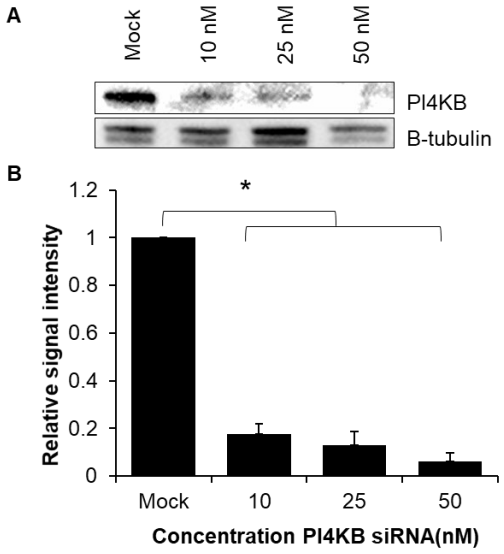

Figure 3.5: Knock-down of PI4KB by siRNA. Cells were transfected with PI4KB siRNA, transfected a second time after 24h, and lysed after 72h. Proteins were resolved by SDS-PAGE and analysed by western immunoblotting. n=2, * $p > 0.05$

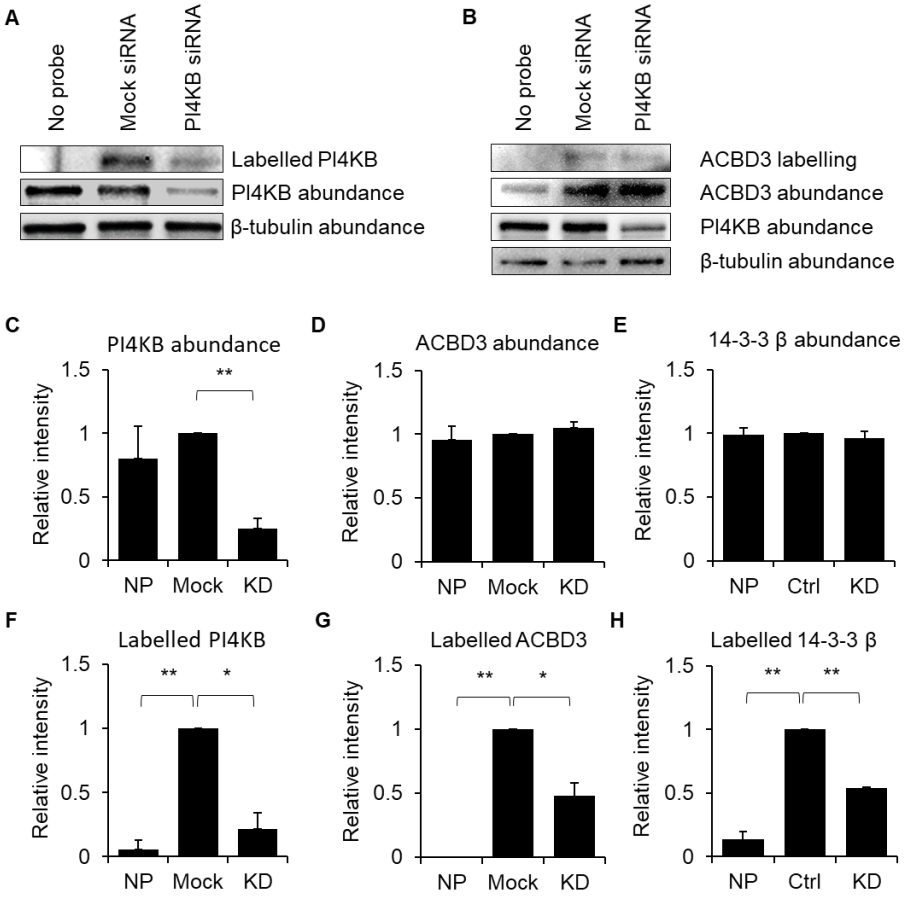

Figure 3.6: PIKBPyne labelling of interacting proteins. A-B) siRNA knock-down of PI4KB decreases A) abundance and labelling of PI4KB and B) labelling but not abundance of PIK-associated protein ACBD3. PI4KB was knocked down by transfection of 10nM siRNA, followed by a second transfection after 24h, and lysis and labelling with 20μM PIKBPyne after 72h. A biotin reporter tag was attached by copper-catalysed click chemistry, and the labelled proteins isolated by streptavidin enrichment, resolved by SDS-PAGE, and imaged by western blotting. C-H) Densitometric analysis of C) PI4KB abundance D) ACBD3 abundance E) 14-3-3 β abundance F) PIKBPyne labelling of PI4KB G) PIKBPyne labelling of ACBD3 H) PIKBPyne labelling of 14-3-3 β. n=3, * $p < 0.05$, ** $p < 0.01$

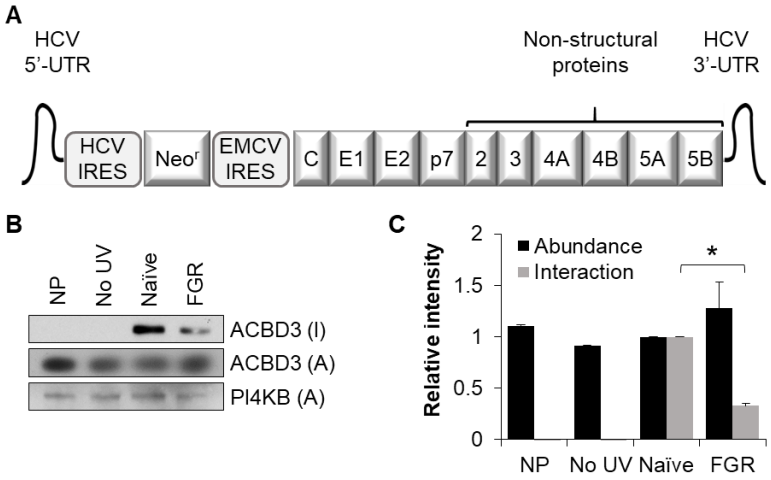

Figure 3.7: HCV interferes with interaction between ACBD3 and PI4KB. A) Schematic representation of the bicistronic full-genomic HCV replicon (FGR) used in this study. B) PIKBPyne-labelled proteins from naïve and HCV-FGR Huh7.5 cells were attached to a biotin reporter by copper-catalysed click chemistry and isolated by streptavidin enrichment. Isolated proteins were resolved by SDS-PAGE and analysed by western immunoblotting. C) Densitometric analysis of protein abundance and labelling. n=2, * $p < 0.05$

with ABP3 and the labelled proteome enriched and analysed by western blot. PI4KB expression remained constant in the presence of the replicon, which agrees with our previous research.[37] (Fig 3.7b, 3.7c) While abundance of ACBD3 does not significantly alter, labelling by ABP3 decreases by 67%. (Fig 3.7b, 3.7c) This confirms previous suggestions that the HCV protein NS5A disrupts the interaction between ACBD3 and PI4KB,[54] and suggests that this disruption is linked with active PI4KB. In contrast, we did not see a similar change for the interacting protein 14-3-3 or ARF1. The data from Fig 3.7 suggests that PI4KB is more active during HCV infection, but at a different location within the cell, with a different set of protein interactions driven at least in part by a change in interaction with ACBD3.

In summary, we have reported the design and synthesis of three new probes against PIKs and shown that probes with a flexible linker region interact with the active site of PI4KB and label a large number of proteins within a complex proteome. Most importantly, we have demonstrated that our probe design strategy allows our probes to quantitatively label protein-protein interactions. We have furthermore shown the utility of this methodology by demonstrating that the Golgi recruitment protein ACBD3 is labelled through its interactions with PI4KB, and that this interaction is interrupted by HCV.

3.6 References

(1) de Wit, J.; Ghosh, A. Specification of Synaptic Connectivity by Cell Surface Interactions. *Nat. Rev. Neurosci.* **2015**, *17* (1), 22–35.

(2) Sivakumar, S.; Gorbsky, G. J. Spatiotemporal Regulation of the Anaphase-Promoting Complex in Mitosis. *Nat. Rev. Mol. Cell Biol.* **2015**, *16* (2), 82–94.

(3) Messaoudi, I.; Amarasinghe, G. K.; Basler, C. F. Filovirus Pathogenesis and Immune Evasion: Insights from Ebola Virus and Marburg Virus. *Nat. Rev. Microbiol.* **2015**, *13* (11), 663–676.

(4) Aasen, T.; Mesnil, M.; Naus, C. C.; Lampe, P. D.; Laird, D. W. Gap Junctions and Cancer: Communicating for 50 Years. *Nat. Rev. Cancer* **2016**, *16* (12), 775–788.

(5) Morgan, B. P.; Harris, C. L. Complement, a Target for Therapy in Inflammatory and Degenerative Diseases. *Nat. Rev. Drug Discov.* **2015**, *14* (12), 857–877.

(6) Scott, D. E.; Bayly, A. R.; Abell, C.; Skidmore, J. Small Molecules, Big Targets: Drug Discovery Faces the Protein–Protein Interaction Challenge. *Nat. Rev. Drug Discov.* **2016**, *15* (8), 533–550.

(7) Cowen, L.; Ideker, T.; Raphael, B. J.; Sharan, R. Network Propagation: A Universal Amplifier of Genetic Associations. *Nat. Rev. Genet.* **2017**, *18* (9), 551–562.

(8) Teruya, K.; Rankin, G.; Chrysanthopoulos, P.; Tonissen, K.; Poulsen, S.-A. Characterisation of Photoaffinity-Based Chemical Probes Using Fluorescence Imaging and Native State Mass Spectrometry. *ChemBioChem* **2017**, *18* (8), 739–754.

(9) Sumranjit, J.; Chung, S. Recent Advances in Target Characterization and Identification by Photoaffinity Probes. *Molecules* **2013**, *18* (9), 10425–10451.

(10) Prestwich, G. D. Benzophenone Photoprobes for Phosphoinositides, Peptides and Drugs. *Photochem. Photobiol.* **1997**, *65* (2), 222–234.

(11) Murale, D. P.; Hong, S. C.; Haque, M. M.; Lee, J.-S. Photo-Affinity Labeling (PAL) in Chemical Proteomics: A Handy Tool to Investigate Protein-Protein Interactions (PPIs). *Proteome Sci.* **2016**, *15* (1), 14.

(12) Joiner, C. M.; Breen, M. E.; Clayton, J.; Mapp, A. K. A Bifunctional Amino Acid Enables Both Covalent Chemical Capture and Isolation of in Vivo Protein-Protein Interactions. *ChemBioChem* **2017**, *18* (2), 181–184.

(13) House, A. J.; Daye, L. R.; Tarpley, M.; Addo, K.; Lamson, D. S.; Parker, M. K.; Bealer, W. E.; Williams, K. P. Design and Characterization of a Photo-Activatable Hedgehog Probe That Mimics the Natural Lipidated Form. *Arch. Biochem. Biophys.* **2015**, *567*, 66–74.

(14) Shiota, T.; Nishikawa, S.; Endo, T. Analyses of Protein–Protein Interactions by In Vivo Photocrosslinking in Budding Yeast. In *Methods in molecular biology*; 2013; Vol. 1033, pp 207–217.

(15) Albertoni, B.; Hannam, J. S.; Ackermann, D.; Schmitz, A.; Famulok, M. A Trifluoromethylphenyl Diazirine-Based SecinH3 Photoaffinity Probe. *Chem. Commun.* **2012**, *48* (9), 1272–1274.

(16) Crump, C. J.; Murrey, H. E.; Ballard, T. E.; am Ende, C. W.; Wu, X.; Gertsik, N.; Johnson, D. S.; Li, Y.-M. Development of Sulfonamide Photoaffinity Inhibitors for Probing Cellular γ-Secretase. *ACS Chem. Neurosci.* **2016**, *7* (8), 1166–1173.

(17) Van Dyke, A. R.; Etemad, L. S.; Vessicchio, M. J.; Naclerio, G. A.; Jedson, V. Capture-Tag-Release: A Strategy for Small Molecule Labeling of Native Enzymes. *ChemBioChem* **2016**, *17* (17), 1602–1605.

(18) Sakurai, K.; Yamaguchi, T.; Mizuno, S. Design and Synthesis of Fluorescent Glycolipid Photoaffinity Probes and Their Photoreactivity. *Bioorg. Med. Chem. Lett.* **2016**, *26* (20), 5110–5115.

(19) Gregory, K. J.; Velagaleti, R.; Thal, D. M.; Brady, R. M.; Christopoulos, A.; Conn, P. J.; Lapinsky, D. J. Clickable Photoaffinity Ligands for Metabotropic Glutamate Receptor 5 Based on Select Acetylenic Negative Allosteric Modulators. *ACS Chem. Biol.* **2016**, *11* (7), 1870–1879.

(20) Marholz, L. J.; Chang, L.; Old, W. M.; Wang, X. Development of Substrate-Selective Probes for Affinity Pulldown of Histone Demethylases. *ACS Chem. Biol.* **2015**, *10* (1), 129–137.

(21) Anabuki, T.; Tsukahara, M.; Matsuura, H.; Takahashi, K. Tandem Photoaffinity Labeling of a Target Protein Using a Linker with Biotin, Alkyne and Benzophenone Groups and a Bioactive Small Molecule with an Azide Group. *Biosci. Biotechnol. Biochem.* **2016**, *80* (3), 432–439.

(22) Yestrepsky, B. D.; Kretz, C. A.; Xu, Y.; Holmes, A.; Sun, H.; Ginsburg, D.; Larsen, S. D. Development of Tag-Free Photoprobes for Studies Aimed at Identifying the Target of Novel Group A Streptococcus Antivirulence Agents. *Bioorg. Med. Chem. Lett.* **2014**, *24* (6), 1538–1544.

(23) Hatanaka, Y. Development and Leading-Edge Application of Innovative Photoaffinity Labeling. *Chem. Pharm. Bull.* **2015**, *63* (1), 1–12.

(24) Cravatt, B. F.; Wright, A. T.; Kozarich, J. W. Activity-Based Protein Profiling: From Enzyme

Chemistry to Proteomic Chemistry. *Annu. Rev. Biochem.* **2008**, *77* (1), 383–414.

(25) Salisbury, C. M.; Cravatt, B. F. Activity-Based Probes for Proteomic Profiling of Histone Deacetylase Complexes. *Proc. Natl. Acad. Sci. U. S. A.* **2007**, *104* (4), 1171–1176.

(26) Salisbury, C. M.; Cravatt, B. F. Optimization of Activity-Based Probes for Proteomic Profiling of Histone Deacetylase Complexes. *J. Am. Chem. Soc.* **2008**, *130* (7), 2184–2194.

(27) Andrews, S. S.; Hill, Z. B.; Perera, B. G. K.; Maly, D. J. Label Transfer Reagents to Probe P38 MAPK Binding Partners. *ChemBioChem* **2013**, *14* (2), 209–216.

(28) Balla, T. Phosphoinositides: Tiny Lipids With Giant Impact on Cell Regulation. *Physiol. Rev.* **2013**, *93* (3), 1019–1137.

(29) Bishé, B.; Syed, G.; Siddiqui, A. Phosphoinositides in the Hepatitis C Virus Life Cycle. *Viruses* **2012**, *4* (12), 2340–2358.

(30) Di Paolo, G.; De Camilli, P. Phosphoinositides in Cell Regulation and Membrane Dynamics. *Nature* **2006**, *443* (7112), 651–657.

(31) Zhang, L.; Hong, Z.; Lin, W.; Shao, R.-X.; Goto, K.; Hsu, V. W.; Chung, R. T. ARF1 and GBF1 Generate a PI4P-Enriched Environment Supportive of Hepatitis C Virus Replication. *PLoS One* **2012**, *7* (2), e32135.

(32) Tai, A. W.; Salloum, S. The Role of the Phosphatidylinositol 4-Kinase PI4KA in Hepatitis C Virus-Induced Host Membrane Rearrangement. *PLoS One* **2011**, *6* (10), e26300.

(33) Sasaki, J.; Ishikawa, K.; Arita, M.; Taniguchi, K. ACBD3-Mediated Recruitment of PI4KB to Picornavirus RNA Replication Sites. *EMBO J.* **2012**, *31* (3), 754–766.

(34) Greninger, A. L.; Knudsen, G. M.; Betegon, M.; Burlingame, A. L.; Derisi, J. L. The 3A Protein from Multiple Picornaviruses Utilizes the Golgi Adaptor Protein ACBD3 to Recruit PI4KIIIβ. *J. Virol.* **2012**, *86* (7), 3605–3616.

(35) Dorobantu, C. M.; Albulescu, L.; Harak, C.; Feng, Q.; van Kampen, M.; Strating, J. R. P. M.; Gorbalenya, A. E.; Lohmann, V.; van der Schaar, H. M.; van Kuppeveld, F. J. M. Modulation of

the Host Lipid Landscape to Promote RNA Virus Replication: The Picornavirus Encephalomyocarditis Virus Converges on the Pathway Used by Hepatitis C Virus. *PLOS Pathog.* **2015**, *11* (9), e1005185.

(36) McPhail, J. A.; Ottosen, E. H.; Jenkins, M. L.; Burke, J. E. The Molecular Basis of Aichi Virus 3A Protein Activation of Phosphatidylinositol 4 Kinase IIIβ, PI4KB, through ACBD3. *Structure* **2017**, *25* (1), 121–131.

(37) Sherratt, A. R.; Nasheri, N.; McKay, C. S.; O'Hara, S.; Hunt, A.; Ning, Z.; Figeys, D.; Goto, N. K.; Pezacki, J. P. A New Chemical Probe for Phosphatidylinositol Kinase Activity. *ChemBioChem* **2014**, *15* (9), 1253–1256.

(38) Hausser, A.; Storz, P.; Märtens, S.; Link, G.; Toker, A.; Pfizenmaier, K. Protein Kinase D Regulates Vesicular Transport by Phosphorylating and Activating Phosphatidylinositol-4 Kinase IIIβ at the Golgi Complex. *Nat. Cell Biol.* **2005**, *7* (9), 880–887.

(39) Hausser, A.; Link, G.; Hoene, M.; Russo, C.; Selchow, O.; Pfizenmaier, K. Phospho-Specific Binding of 14-3-3 Proteins to Phosphatidylinositol 4-Kinase III β Protects from Dephosphorylation and Stabilizes Lipid Kinase Activity. *J. Cell Sci.* **2006**, *119* (17), 3613–3621.

(40) Knight, Z. A.; Gonzalez, B.; Feldman, M. E.; Zunder, E. R.; Goldenberg, D. D.; Williams, O.; Loewith, R.; Stokoe, D.; Balla, A.; Toth, B.; et al. A Pharmacological Map of the PI3-K Family Defines a Role for P110α in Insulin Signaling. *Cell* **2006**, *125* (4), 733–747.

(41) Burke, J. E.; Inglis, A. J.; Perisic, O.; Masson, G. R.; McLaughlin, S. H.; Rutaganira, F.; Shokat, K. M.; Williams, R. L. Structures of PI4KIIIβ Complexes Show Simultaneous Recruitment of Rab11 and Its Effectors. *Science (80-.).* **2014**, *344* (6187), 1035–1038.

(42) Tai, A. W.; Bojjireddy, N.; Balla, T. A Homogeneous and Nonisotopic Assay for Phosphatidylinositol 4-Kinases. *Anal. Biochem.* **2011**, *417* (1), 97–102.

(43) Orchard, S.; Ammari, M.; Aranda, B.; Breuza, L.; Briganti, L.; Broackes-Carter, F.; Campbell, N. H.; Chavali, G.; Chen, C.; del-Toro, N.; et al. The MIntAct Project--IntAct as a Common Curation

Platform for 11 Molecular Interaction Databases. *Nucleic Acids Res.* **2014**, *42* (Database issue), D358-63.

(44) Sbodio, J. I.; Hicks, S. W.; Simon, D.; Machamer, C. E. GCP60 Preferentially Interacts with a Caspase-Generated Golgin-160 Fragment. *J. Biol. Chem.* **2006**, *281* (38), 27924–27931.

(45) Sbodio, J. I.; Paul, B. D.; Machamer, C. E.; Snyder, S. H. Golgi Protein ACBD3 Mediates Neurotoxicity Associated with Huntington's Disease. *Cell Rep.* **2013**, *4* (5), 890–897.

(46) Zhou, Y.; Atkins, J. B.; Rompani, S. B.; Bancescu, D. L.; Petersen, P. H.; Tang, H.; Zou, K.; Stewart, S. B.; Zhong, W. The Mammalian Golgi Regulates Numb Signaling in Asymmetric Cell Division by Releasing ACBD3 during Mitosis. *Cell* **2007**, *129* (1), 163–178.

(47) Cheah, J. H.; Kim, S. F.; Hester, L. D.; Clancy, K. W.; Patterson, S. E.; Papadopoulos, V.; Snyder, S. H. NMDA Receptor-Nitric Oxide Transmission Mediates Neuronal Iron Homeostasis via the GTPase Dexras1. *Neuron* **2006**, *51* (4), 431–440.

(48) Klima, M.; Tóth, D. J.; Hexnerova, R.; Baumlova, A.; Chalupska, D.; Tykvart, J.; Rezabkova, L.; Sengupta, N.; Man, P.; Dubankova, A.; et al. Structural Insights and in Vitro Reconstitution of Membrane Targeting and Activation of Human PI4KB by the ACBD3 Protein. *Sci. Rep.* **2016**, *6*, 23641.

(49) Couzens, A. L.; Knight, J. D. R.; Kean, M. J.; Teo, G.; Weiss, A.; Dunham, W. H.; Lin, Z.-Y.; Bagshaw, R. D.; Sicheri, F.; Pawson, T.; et al. Protein Interaction Network of the Mammalian Hippo Pathway Reveals Mechanisms of Kinase-Phosphatase Interactions. *Sci. Signal.* **2013**, *6* (302), rs15.

(50) Chalupska, D.; Eisenreichova, A.; Różyckib, B.; Rezabkova, L.; Humpolickova, J.; Klima, M.; Boura, E. Structural Analysis of Phosphatidylinositol 4-Kinase IIIβ (PI4KB) – 14-3-3 Protein Complex Reveals Internal Flexibility and Explains 14-3-3 Mediated Protection from Degradation in Vitro. *J. Struct. Biol.* **2017**, *In press*.

(51) Delang, L.; Paeshuyse, J.; Neyts, J. The Role of Phosphatidylinositol 4-Kinases and

Phosphatidylinositol 4-Phosphate during Viral Replication. *Biochem. Pharmacol.* **2012**, *84* (11), 1400–1408.

(52) Borawski, J.; Troke, P.; Puyang, X.; Gibaja, V.; Zhao, S.; Mickanin, C.; Leighton-Davies, J.; Wilson, C. J.; Myer, V.; Cornellataracido, I.; et al. Class III Phosphatidylinositol 4-Kinase Alpha and Beta Are Novel Host Factor Regulators of Hepatitis C Virus Replication. *J. Virol.* **2009**, *83* (19), 10058–10074.

(53) Keaney, E. P.; Connolly, M.; Dobler, M.; Karki, R.; Honda, A.; Sokup, S.; Karur, S.; Britt, S.; Patnaik, A.; Raman, P.; et al. 2-Alkyloxazoles as Potent and Selective PI4KIIIβ Inhibitors Demonstrating Inhibition of HCV Replication. *Bioorg. Med. Chem. Lett.* **2014**, *24* (16), 3714–3718.

(54) Hong, Z.; Yang, X.; Yang, G.; Zhang, L. Hepatitis C Virus NS5A Competes with PI4KB for Binding to ACBD3 in a Genotype-Dependent Manner. *Antiviral Res.* **2014**, *107*, 50–55.

Chapter 4: Activity-based protein profiling of metabolic microRNA-27b identifies new functional targets in the human liver

4.1 Statement of contribution

Geneviève F. Desrochers, Michele Bastienelli, and Tiffany Stern performed biochemical profiling experiments. Roxana Filip contributed to cell culture work. Geneviève Desrochers and John Paul Pezacki designed the project. The manuscript was written by Geneviève Desrochers and John Paul Pezacki.

4.2 Summary

MicroRNAs are short, non-coding RNAs which negatively and specifically regulate protein expression by either sequestering mRNA or targeting it for degradation. The cumulative effect of these subtle changes to protein expression allows microRNAs to broadly regulate cell systems and architecture. Hijacking of microRNAs is therefore an attractive strategy for viruses for whom host cell remodelling is essential for replication. The hepatitis C virus has been shown to upregulate expression of several microRNAs, one of which, miR-27b, has been shown to promote changes the cell's lipid profile, though the mechanisms by which this occurs have not been well established. To elucidate these mechanisms, it is important to identify both the direct and the indirect targets of microRNA regulation. While direct targets can be predicted based on their mRNA sequences, indirect targets, whose activities are affected via alterations in signalling pathway activity, are more difficult to identify. We have used a fluorophosphonate-containing activity-based probe, targeting serine hydrolases, to profile miR-27b induced changes to enzyme activity in the context of HCV infection. We identified several lipid metabolism enzymes whose activities are indirectly targeted by miR-27b via transcriptional or post-translational regulation. These enzymes represent potential downstream effectors of miR-27b used by HCV to alter lipid metabolism. Altogether, our results demonstrate new mechanisms by which miR-27b

mediates remodelling of cells' lipid profile. More generally, they highlight the usefulness of activity-based protein profiling for characterizing the role microRNAs play in cell function and disease pathogenesis.

4.3 Introduction

Cellular metabolism is composed of a complex set of interconnected systems controlled by myriad genes acting in concert. The functional output of these genes relies upon the interplay of multiple layers of regulatory mechanisms. RNA interference (RNAi) is one of these regulatory mechanisms capable of calibrating the function of protein-coding genes. This system uses a guide RNA which is loaded into the RNA interference silencing complex (RISC). The guide RNA selectively recognises sequences of interest, allowing this sequence to be targeted by RISC. Endogenous RNAi in mammals uses microRNA (miRNA): non-coding single strands of RNA with an average length of 22 nt.[1] Generally, miRNA targets the RISC complex to its target mRNAs, which it then either degrades or sequesters, thereby decreasing the abundance of the proteins they encode.[1]

The interaction between the 3' untranslated region of the mRNA and the 7-nucleotide-long "seed sequence" on the 5' end of the miRNA is typically essential for targeting, while any hydrogen bonds which form with the remainder of the miRNA act to fine-tune the interaction's stability and selectivity.[1] As the number of base-pairs formed is short and the complementarity imperfect, mRNAs are frequently targeted by multiple different miRNAs,[1,2] and a single miRNA will target numerous different mRNAs.[3,4] The set of genes targeted by a single miRNA tend to be functionally related, allowing a miRNA to exert a significant overall effect on a particular system or pathway by simultaneous synergistic targeting of multiple component parts.[4] (Fig 4.1)

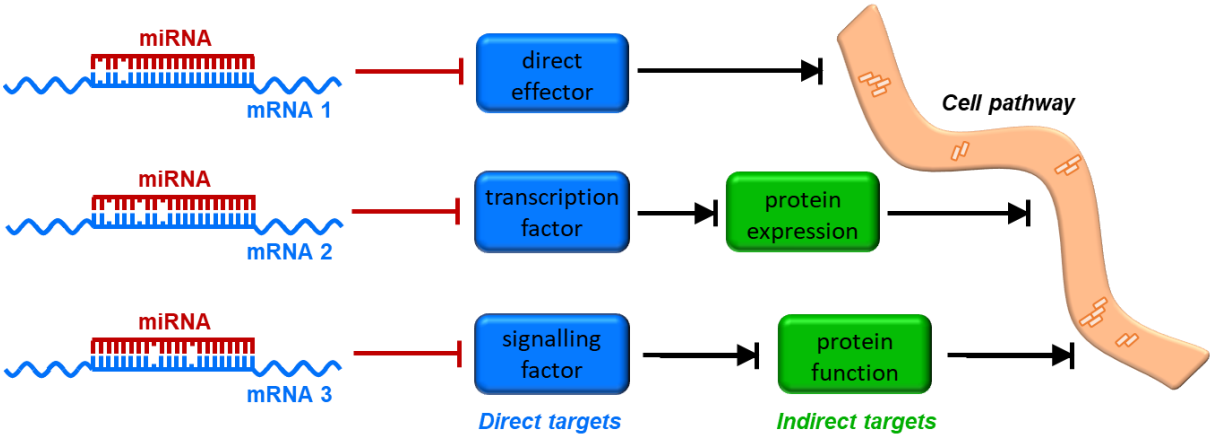

Figure 4.1: A single miRNA targets multiple mRNAs and regulates pathways using different mechanisms of action

This ability of miRNAs to broadly modulate cellular pathways and processes means that differential expression and dysregulation of miRNA function has the potential to either promote or inhibit diverse pathogeneses. The aberrant function of numerous different miRNAs plays a role in the development of chronic diseases such as cancers,[4–6] diabetes,[7] cardiovascular diseases,[8] liver cirrhosis,[9] and neurodegenerative disorders.[10] The progression of infectious diseases, either bacterial[11] or viral,[12–15] is also often associated with the dysregylation of the miRNA profile, either caused by the invading pathogen, or by the host in an effort to eliminate it. Conversely, recent work has demonstrated that the alterations to the miRNA profile caused by infection of viruses of the flavivirus family include upregulation of miRNAs which stimulate the host's antiviral response.[16–18]

The hepatitis C virus is one such flavivirus: a small, enveloped positive-strand RNA virus which preferentially infects the liver.[19] If the infection becomes chronic, the virus perturbs the normal function and architecture of host cells in order to evade the immune response and favour its own reproduction.[19] Remodelling of the host's lipid architecture is essential to the survival of the virus,[20] and contributes to the development of long-term complications such as liver fibrosis, steatosis, and hepatocellular carcinoma (HCC).[21–23]

miRNAs have been shown to play a significant role in liver diseases generally,[9] and in HCV[24,25] and the development of HCV-induced HCC in particular.[24,26] While normal levels of liver-expressed miRNAs have the potential to influence HCV, the infection itself is also capable of inducing a significant alteration to the miRNA population.[27–29]

The role of miRNAs in HCV infection was first demonstrated via the HCV-5'UTR and miR-122 interaction, which stabilises the viral RNA and sponges miR-122, altering the cell's transcriptome.[28,30] Several other direct interactions have been discovered;[25] however, a much larger number of miRNAs

indirectly affect HCV by altering diverse aspects of the cellular environment such as the interferon response, inflammation, cell growth and proliferation, Wnt and PI3K-Akt survival-related signalling, and lipid metabolism.[24,25] This last is of particular interest, as HCV infection is known to modulate metabolic regulation to achieve the specific lipid environment it requires.[19,20] Liver-abundant[31–33] lipid metabolism regulatory miRNAs 130b,[29] 185,[29] 124,[34] 27a,[35] and 27b[36] have been shown to play an essential role in the process.

miR-27b, one of the most abundant miRNAs in the liver,[31–33] is considered to be a central lynchpin in the maintenance of lipid homeostasis, targeting key factors in lipid metabolic pathways.[36–38] Expression of miR-27b increases extracellular[39] and intracellular lipids[36] and lipid deposits,[40] and regulates adipogenesis.[41–47] This is mainly driven by increased triglyceride content[36,46] while constant cholesterol levels are maintained by simultaneous targeting of influx, efflux, hydrolysis and synthesis.[48–50]

Metabolic regulation has been shown to have a significant impact on the immune response, and the study of the role of metabolism in regulating the function of immune cells has been dubbed "immunometabolism".[51] More recently, the role of metabolism in regulating the innate immune response in non-immune cells has been the subject on increasing interest.[14,29,52,53] miR-27b, in addition to acting as a central regulator of lipid metabolism, has been shown to modulate immune responses such as inflammation and cytokine production,[39,54] while miR-27b dysregulation is implicated in the progression of numerous chronic diseases. In addition to HCV,[36] miR-27b is implicated in the development of atherosclerosis[54] and multiple forms of cancer,[55–59] notably playing an oncogenic role in hepatocellular carcinoma,[60–63] which is induced by chronic HCV infection.[19] Characterising miR-27b regulation is therefore of interest in the study of how changes to lipid metabolism can play both a pro-viral and a immuno-modulatory role. Furthermore, a deeper understanding of the mechanisms by which miR-27b

modulates lipid metabolism will provide insight into novel strategies of combat not only HCV, but also conditions such as atherosclerosis and other obesity-related illnesses with which it is associated.[39,54]

As specific miRNA-mRNA interactions may alter key factors within larger pathways, they may result in significant changes downstream of the gene targeted. For this reason, to identify miRNA-induced changes to lipid metabolism, it is essential to profile functional targets: targets whose output is altered, and which are ultimately responsible for changes to cellular function and architecture.

Activity-based protein profiling (ABPP) uses small-molecule probes to quantify changes to enzyme activity.[64,65] Lipid metabolism is regulated in large part by the serine hydrolase class of enzymes,[66] whose activity can be detected using a fluorophosphonate-based probe. (Fig 4.2) This probe contains a fluorophosphate warhead, which forms a covalent bond to its enzyme targets upon nucleophilic attack by the active-site serine residue; critically, this the formation of this bond relies on the activity of the enzyme, and it will not form with inactive proteins.[67] A reporter tag conjugated to the warhead allows enzymes tagged with this probe to be identified and quantified.[64,67]

ABPP techniques have been broadly used to gain a deeper understanding of metabolic function[68] and to characterise enzyme dysregulation during infection.[69–71] In this work, ABPP is used to identify and characterise the functional effectors of miR-27b's regulation of lipid metabolism. The mechanisms by which miR-27b exerts this control, and the ultimate effects on cell function are investigated. A differential activity profile was established, from which the lipid metabolic enzymes LIPC, PAFAH1B3, and ACOT1/2 were confirmed as novel functional targets of miR-27b, expanding current understanding of the key role played by this miRNA in liver metabolism and HCV infection. More generally, this work

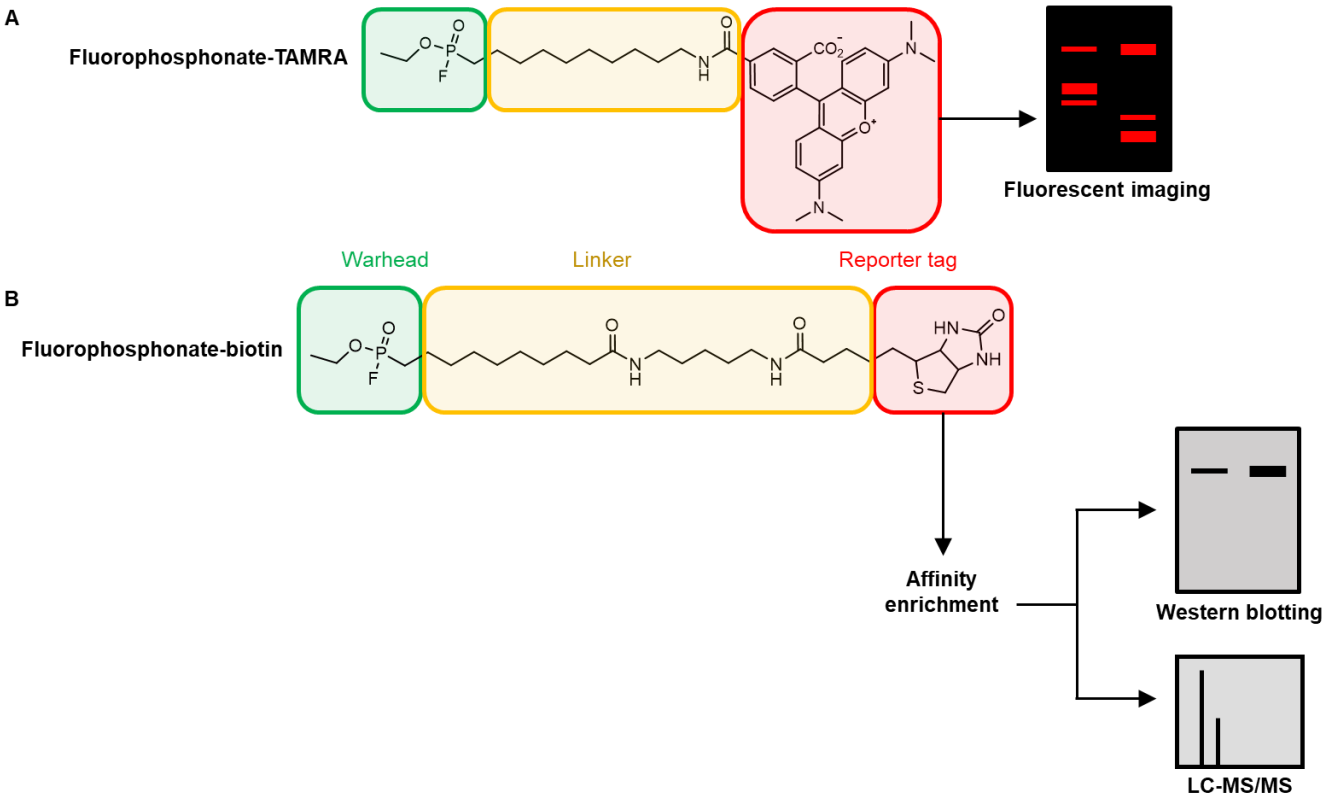

Figure 4.2: Chemical structures of fluorophosphonate probes and their applications. A) The fluorescent fluorophosphonate-TAMRA is used to label active enzymes for in-gel visualisation. B) Fluorophosphonate-biotin is used for affinity enrichment and detection by either western blotting or mass spectrometry.

highlights the need for the functional profiling of miRNA activity to fully understand their roles both in normal cell function and in disease.

4.4 Materials and Methods

4.4.1 Cell culture

HepG2 cells were maintained in MEM (Gibco), supplemented with 10% (V/V) fetal bovine serum. Huh7.5 cells were maintained in DMEM (Gibco) supplemented with 10% (V/V) fetal bovine serum (Wisent) and 10 mM non-essential amino acids (Millipore-Sigma). The $JFH1_T$ strain of the hepatitis C virus was a kind gift from the laboratory of Dr. Rodney Russel (Memorial University, Newfoundland, Canada). Huh7.5 cells were infected with $JFH1_T$ at a MOI of 0.1 for 5 hours in a one-quarter growth volume of unsupplemented DMEM, rocking plates every hour. Cells were transfected with 100 nM of hsa-miR-27b-3p *mir*Vana mimic, mimic negative control, hsa-miR-27b-3p *miR*Vana inhibitor, or inhibitor negative control (ThermoFisher Scientific) immediately following infection, using Lipofectamine RNAiMax Transfection Reagent (Invitrogen), according to the manufacturer's instructions, and lysed after 72 hours. Cells treated with benzamide (Calbiochem) or bezafibrate (Cedarlane) were incubated with 75 μM compound for 24h before lysis.

4.4.2 siRNA knockdowns

Expression knockdowns for ABPP were performed with Silencer™ Select Pre-Designed siRNAs ACOT1/2 (s54802, ThermoFisher), and Negative Control No. 1 (ThermoFisher), ON-TARGETplus PAFAH1B1 siRNA (5048, Horizon Dharmacon) and ON-TARGET GAPDH (Horizon Dharmacon) at 10 nM using RNAiMax according to the manufacturer's instruction, and cells were lysed after 48h. Expression knockdown for infectivity assays was performed using Silencer™ Select Pre-Designed siRNAs against ACOT1/2 (s54802, ThermoFisher) Negative Control No. 1 (ThermoFisher), PAFAH1B3 (s224162, ThermoFisher) and LIPC (s8202) at 10 nM using RNAiMax according to the manufacturer's

instructions. 48h after transfection cells were infected with $JFH1_T$ at an MOI of 0.1. RNA was harvested 48h after infection, and the growth media used to infect naïve cells. RNA from growth-media infected cells was harvested after 48h.

4.4.3 Lipidomic analysis

Huh7.5 cells transfected as above were trypsinised, spun down, and resuspended in 10 mM PBS, pH 7.4. Cells were washed by centrifugation and subsequent resuspension in PBS twice. Cells were diluted to a concentration of 3000 cells/µL. 300 µL of each sample were sent for analysis at Lipotype GmbH and the rest reserved for western blotting. Lipids were quantified in picomoles and normalised by the protein concentration of each sample.

4.4.4 Protein harvesting

Cells were washed twice in 10 mM PBS, pH 7.4. Cells were harvested in 10 mM PBS, pH 7.4 supplemented with 1% (v/v) Triton-X 100 (BioShop). Cells lysed by sonication with 15 1-second pulses and centrifuged at 20,000g at 4°C for 5 min. The supernatant was removed, and the protein content quantified by DC assay (Bio-Rad).

4.4.5 Fluorescent activity-based protein profiling

1 µM ActivX TAMRA-FP serine hydrolase probe (ThermoFisher Scientific) was rotated with 70 µg of protein, 1 µg/µL, at 37°C for 1 hour. Protein was precipitated with 14 volumes of acetone and chilled at -80°C for 20 min before centrifugation at 20,000g for 15 min at 4°C. Acetone was removed and the protein pellet was resuspended in SDS-PAGE gel loading buffer (3.5% (m/V) SDS, 0.018% (m/V) bromophenol blue, 9% (V/V) glycerol, 90mM Tris, 30mM DTT**)** by vortexing until the pellet was no longer visible, followed by heating at 95°C for 10 min. Proteins were resolved on a 10% TGX FastCast Acrylamide gel (Bio-Rad) and fluorescence visualised by Chemidoc MP imaging system.

4.4.6 Enrichment of proteins labelled by activity-based protein profiling

5 µM FP-Biotin (Santa Cruz Biotechnology) was incubated under rotation with 1-2 mg of protein at 1-2 mg/mL for 1 hour at 37°C. Protein was precipitated with 5 volumes of acetone and chilled at -80°C for 20 min. Protein was centrifuged at 4500g for 15 min at 4°C and acetone was removed. The protein pellet was resuspended in methanol by sonication with 5 1-second pulses, pelleted by centrifugation at 20,000g for 5 min at 4°C, and the methanol removed. Washing was repeated twice more. Protein was solubilised in 650 µL 2.5% (m/V) SDS in 10 mM PBS, pH 7.4 by sonication with 15 1-second pulses followed by heating at 65°C for 4 min. The solution was centrifuged at 6400g for 4 min at RT and an aliquot of 20 µL removed for use as an input control. The remainder of the solubilised protein was diluted in 9 mL of 10 mM PBS, pH 7.4 and incubated, rotating, with 100 µL of Pierce streptavidin-agarose beads, normal load (ThermoFisher Scientific) for 2 hours at RT. Beads were pelleted at 1400g for 2 min and transferred to micro Bio-Spin chromatography columns (Bio-Rad). Beads were washed thrice in 1% (m/v) SDS, thrice in 6M urea, and once in 10 mM PBS, pH 7.4.

4.4.7 Sample preparation for mass spectrometry analysis of activity-labelled proteins

Bead-bound activity-labelled proteins were washed thrice in 50 mM ammonium bicarbonate (ABC) and transferred to microcentrifuge tubes. Proteins were reduced by 10 mM DTT in ABC at 65°C for 15 min and alkylated by 24 mM iodoacetamide for 30 min at RT in the dark. Beads were centrifuged at 1400g for 2 min and the supernatant removed. Beads were washed thrice with 50 mM tetraethylammonium bicarbonate (TEAB) and suspended in 100 µL of 50 mM TEAB. Proteins were digested by 1 µg sequencing grade modified trypsin (Promega) overnight at 37°C. Beads were pelleted at 1400g for 2 min and the supernatant transferred to micro Bio-Spin chromatography columns. The solution was centrifuged at 1000g for 1 minute and the flow-through dried by vacuum centrifugation.

Peptides were reconstituted in 100 mM TEAB and labelled with 50 mM CH_3 (light), CD_3 (medium), or $^{13}CD_3$ (heavy) formaldehyde in the presence of 22 mM sodium cyanoborohydride (light and medium) or sodium cyanoborodeuteride (heavy) for 1 hour, rotating, at RT. The reaction was quenched with 0.13% (v/v) ammonium hydroxide and acidified with formic acid until the pH was under 5. Sample was desalted using Pierce C18 100-µL tips (ThermoFisher Scientific) according to the manufacturer's protocol and dried by vacuum centrifugation. Obtained peptide samples were re-suspended with 25 µL of 1% FA in water and 2 µL were injected into the LC/MS/MS.

4.4.8 LC-MS/MS

All experiments were performed on an Orbitrap Fusion (Thermo Scientific) coupled to an Ultimate3000 nanoRLSC (Dionex). Peptides were separated on an in-house packed column (Polymicro Technologies), 15 cm x 70 µm ID, Luna C18 (2), 3 µm, 100 Å (Phenomenex) employing a water/acetonitrile/0.1% formic acid gradient. Samples were loaded onto the column for 105 min at a flow rate of 0.30 µL/min. Peptides were separated using 2% acetonitrile in the first 7 min and then using a linear gradient from 2 to 38% of acetonitrile for 70 min, followed by gradient from 38 to 98% of acetonitrile for 9 min, then at 98% of acetonitrile for 10 min, followed by gradient from 98 to 2% of acetonitrile for 3 min and wash of 10 min at 2% of acetonitrile. Eluted peptides were directly sprayed into mass spectrometer using positive electrospray ionization (ESI) at an ion source temperature of 250°C and an ionspray voltage of 2.1 kV. The Orbitrap Fusion Tribrid was run in top speed mode. Full-scan MS spectra (m/z 350–2000) were acquired at a resolution of 60 000. Precursor ions were filtered according to monoisotopic precursor selection, charge state (+2 to + 7), and dynamic exclusion (30 s with a ± 10 ppm window). The automatic gain control settings were 4e5 for full FTMS scans and 1e4 for MS/MS scans. Fragmentation was performed with collision-induced dissociation (CID) in the linear ion trap. Precursors were isolated using a 2 m/z isolation window and fragmented with a normalized collision energy of 35%.

4.4.9 Peptide and protein identification

Proteome Discoverer 2.1 (ThermoFisher Scientific) was used for protein identification and quantification. The precursor mass tolerance was set at 10 ppm and 0.6 Da mass tolerance for fragment ions. Search engine: SEQUEST-HT implemented in Proteome Discovery was applied for all MS raw files. Search parameters were set to allow for dynamic modification of methionine oxidation, and static modification of cysteine carbamidomethylation as well as dimethyl modifications on lysine and N-terminus (light, medium, and heavy). The raw files were searched separately with "light", "medium", and "heavy" labels in the same workflow. The search database consisted of a nonredundant *Homo sapiens* protein sequences in FASTA file format from the UniProt/SwissProt database. The FDR was set to 0.05 for protein identifications. Quantification of peptides and proteins was performed using standard settings provided by Proteome Discoverer. The average fold change of the technical and biological replicates was calculated using differential abundance expressed in a $\log_{10}$ scale.

4.4.10 Sample preparation for western blotting of activity-labelled proteins

Bead-bound activity-labelled proteins were washed twice in 10 mM PBS, pH 7.4 and transferred to microcentrifuge tubes. Beads were centrifuged for 5 min at 1400g and the supernatant was removed. SDS-PAGE loading buffer was added and protein was released from beads by heating at 95°C for 15 min. The beads were cooled to RT and centrifuged for 5 min at 1400g. The supernatant was removed and proteins were analysed by western blotting

4.4.11 Western blotting

Proteins were resolved using a 10% TGX FastCast Acrylamide gel (Bio-Rad). Stain-free whole protein visualisation was activated by UV irradiation for 1 min using Chemidoc MP and whole protein was visualised at 302 nm by Chemidoc MP**.** Proteins were transferred using Trans-Blot Turbo RTA mini PVDF transfer kit (Bio-Rad) following the manufacturer's instructions, on the Trans-Blot Turbo Transfer

System (Bio-Rad) for 15 minutes at a constant 2.5 A. TGX-whole protein was imaged by Chemidoc MP. Blots were blocked for 30 min in 2.5% (m/V) bovine serum albumin (BSA) in tris-buffered saline with Tween-20 (TBST)(10 mM Tris, 0.15M NaCl, pH 8, 0.05% Tween-20). Blots were incubated with primary antibodies PAFAH1B3 1:200 (Santa Cruz, sc-393612), PAFAH1B1 1:500 (Abcam, ab2607**),** LIPC 1:500 (Santa Cruz, sc-21740), ACOT1/2 1:500 (Santa Cruz, sc-373917), GAPDH 1:10,000 (Ambion, AM4300), β-tubulin 1:4,000 (Abcam, ab6046), PPARG 1:500 (Abcam, ab178860) in 2.5% BSA in TBST overnight at 4°C. Blots were incubated for 1 hour at RT with the appropriate secondary antibody, peroxidase AffiniPure goat anti-mouse IgG (H+L) (Jackson ImmunoResearch Laboratories, 115-035-062) or Peroxidase AffiniPure Donkey Anti-Rabbit IgG (H+L) (Jackson ImmunoResearch Laboratories, 711-035-152), at 1:20,000 in 2.5% BSA in TBST. Chemiluminescence was detected using Clarity Western ECL Substrate (Bio-Rad) on Chemidoc MP running ImageLab 6.0 (Bio-Rad). Chemiluminescent signal quantification was performed using ImageLab 6.0 and the result normalised by TGX whole protein signal. Blots were stripped using ReBlot Plus Strong Antibody Stripping Solution (Millipore) according to the manufacturer's instruction before blotting was repeated.

4.4.12 Inhibition of palmitoylation

Cells at 90% confluency were treated for 6 hours with 20 μM 2-bromopalmitate (Sigma-Aldrich) then lysed and labelled with FP-biotin as above. Alternatively, untreated cells were lysed and the lysate rotated with 20 μM 2-bromopalmitate for 10 min at 37°C before labelling with FP-biotin as above.

4.4.13 RNA harvest, purification, and quantification

Cells were lysed and RNA purified using the RNeasy Plus Mini Kit (Qiagen), according to the manufacturer's instructions. Any sample containing live $JFH1_T$ virus was vortexed for 30 seconds after harvesting and incubated for five min at RT to destroy the virus before proceeding to gDNA elimination. Purified RNA was quantified by NanoDrop 1000 (ThermoFisher Scientific). cDNA was synthesised

using the iScript Reverse Transcription kit (Bio-Rad) according to the manufacturer's instructions. qPCR was performed using the SsoAdvanced Universal SYBR Green Supermix (BioRad), according to the manufacturer's instructions. Results were normalised using 18S RNA quantification.

4.4.14 3'-UTR assays

The LIPC 3'UTR dual luciferase construct and negative control was purchased from Genecopoeia. The miR-27b-3p seed site was mutated using KOD extreme polymerase (MilliporeSigma) using the following protocol: 120 s at 98°C, (30 s at 95°C, 60 s at 55°C, 440 s at 72°C eighteen times), 300 s at 72°C. DNA was digested with 0.6U/µL ANZA DpnI (Invitrogen) for 45 minutes, followed by heat inactivation for 15 minutes at 8 0°C. Mutagenesis was confirmed by sequencing at the McGill University and Génome Québec Innovation Centre. Cells were transfected with 1 µg of the UTR construct per mL of media, using Lipofectamine 2000 Transfection Reagent (Invitrogen) according to the manufacturer's instruction. After 24 hours, cells were transfected with 100 nM miR-27b-3p *mir*Vana mimic using Lipofectamine RNAiMax Transfection Reagent (Invitrogen) according to the manufacturer's instructions. Cells were lysed after 48 hours in Passive Lysis Buffer (Promega). Luciferase assays were performed as previously described[72] using a SpectraMax L (Molecular Devices). Luciferase signal was normalized over protein concentration quantified by DC assay (BioRad).

4.4.15 Wnt-reporter assays

Huh7.5 and HepG2 cells were seeded in a 12-well plate. The following day, cells were co-transfected with the 0.5 µg TOP/FOPflash constructs (Addgene) using Lipofectamine 2000 (Invitrogen) at half the recommended concentration, and 100 nM miR-27b mimic using Lipofectamine RNAiMax (Invitrogen) according to the manufacturer's instructions. After 24h, cells were treated with 5µM P11 in DMSO, 20 µM 2-bromopalmitate in EtOH, or vector alone. Cells were lysed 48h after transfection. Luciferase

activity was measured as previously described[72] and normalised over protein concentration quantified by DC assay (BioRad).

4.5 Results

Differential activation of serine hydrolases by miR-27b in naïve and HCV-infected cells was assessed by labelling proteome lysates from Huh7.5 hepatoma cells transfected with microRNA mimic, inhibitor, or their respective controls with the activity-based probe fluorophosphonate-TAMRA. Differential labelling, and therefore activity, of serine hydrolases was then visualised by fluorescent scanning of the proteins resolved on an SDS-PAGE gel. Multiple differential band intensities were observed in samples in which miR-27b had either been over-expressed or inhibited. (Fig 4.3)

Active serine hydrolases were identified using a biotinylated FP probe to selectively enrich labelled enzymes, followed by analysis of these enriched samples by LC-MS/MS. Thirty-six of the serine hydrolases detected were present in all four conditions, representing enzymes expressed with sufficiently high abundance in the Huh7.5 model. (Table 4.1, Fig 4.4) Pathway analysis using TOPPFUN was performed on enzymes exhibiting an abundance increase greater than 1.25-fold or decrease of less than 0.8-fold. This revealed that the pathways most significantly affected by miR-27b modulation of serine hydrolase activity were all involved in lipid metabolism, with an emphasis on phospholipids and glycerolipids. (Table 4.2)

To assess the functional consequences of this modulation of cells' lipid machinery, lipidomic analysis was performed to quantify miR-27b mediated changes to cellular lipids. Changes to the abundance of lipid species in cells over-expressing miR-27b were quantified by mass spectrometry (Table 4.1). A 70% increase in the overall quantity of triacylglycerides present was observed, (Fig 4.5a) with a trend towards desaturation. (Fig 4.5b) No significant changes were observed in any other lipid groups. (Fig 4.5a) To

link these changes in lipid composition to changes in enzymatic activity, the differential activity of the lipid hydrolases identified earlier by mass spectrometry was examined in greater detail. The activity of three enzymes of interest were confirmed to be modulated by miR-27b by activity-based labelling followed by western blotting: LIPC, PAFAH1B3, and ACOT1/ACOT2.

4.5.1 Hepatic Lipase (LIPC)

Hepatic lipase (LIPC) is a liver enzyme mainly localised to the cell surface of hepatocytes,[73] where it predominantly hydrolyses triglycerides, though it can also target other acyl-containing lipid species.[74] LIPC activity is primarily responsible for reducing the triglyceride abundance in both high- and low-density lipoproteins.[66,75]

The ABPP-MS screen demonstrated that LIPC was significantly less active in cells transfected with miR-27b mimic, while the presence of the miR-27b inhibitor increased enzyme activity. (Fig 4.6a) To determine whether this regulation of LIPC activity was pre- or post-translational, western blotting was performed on proteomes extracted from cells with and without exogenous expression of miR-27b or its inhibitor. These proteomes were labelled by FP-biotin and the active serine hydrolase fraction isolated by streptavidin enrichment before western blotting, to confirm the changes in activity seen by mass spectrometry. Fig 4.6c and Fig 4.6d shows a significant decrease in both LIPC activity and abundance in the presence of miR-27b, paralleled by an insignificant increase in LIPC activity and abundance when miR-27b was inhibited. qPCR showed a similar mimic-mediated decrease in mRNA, while the inhibitor left LIPC mRNA levels relatively unchanged. (Fig 4.6b) Overall, this indicates that the observed regulation of LIPC is based largely on changes to protein expression regulated at the mRNA level.

The seed site of miR-27b was found in the 3'-UTR of LIPC. (Fig 4.7a) A luciferase construct containing the 3'-UTR from LIPC was purchased and the seed site mutated. Cells were co-transfected with miR-

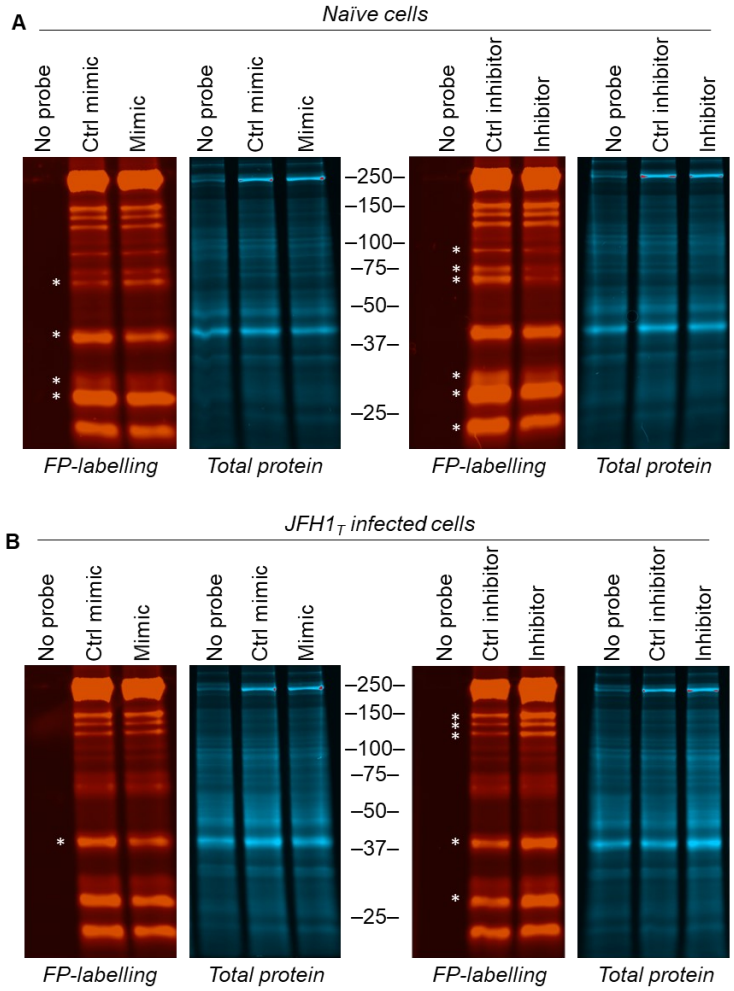

Figure 4.3: miR-27b alters the enzymatic activity of serine hydrolases. A) Naïve Huh7.5 cells and cells infected with the JFH1$_T$ strain of HCV were transfected with miR-27b mimic, inhibitor, or negative control. Cells were lysed after 72h, labelled with FP-rhodamine, resolved on a 10% SDS-PAGE gel and visualised by UV irradiation.

Table 4.1: Relative activity of serine hydrolases measured by ABPP-mass spectrometry. Naïve Huh7.5 cells and cells infected with the $JFH1_T$ strain of HCV were transfected with miR-27b mimic, inhibitor, or negative control. Cells were lysed after 72h and labelled with FP-biotin. The labelled proteome was isolated by streptavidin enrichment, isotopically labelled and differential labelling quantified by LC-MS/MS.

Gene	Mimic	Inhibitor	Mimic & HCV	Inhibitor & HCV
AADAC	1.22 ± 0.31	0.72 ± 0.12	0.85 ± 0.18	1.21 ± 0.17
ABHD10	1.04 ± 0.15	0.96 ± 0.19	1.04 ± 0.38	1.20 ± 0.31
ABHD11	0.94 ± 0.25	0.72 ± 0.28	1.76 ± 0.40	0.81 ± 0.08
ABHD12	1.11 ± 0.17	0.76 ± 0.27	1.11 ± 0.09	0.85 ± 0.11
ABHD4	0.99 ± 0.21	1.22 ± 0.55	1.37 ± 0.22	1.73± 1.02
ABHD6	1.16 ± 0.27	0.92 ± 0.20	1.11 ± 0.61	1.84 ± 0.3
ACOT1	0.12 ± 0.12	0.42 ± 0.36	0.79 ± 0.01	0.92 ± 0.1
ACOT2	1.68 ± 1.51	0.96 ± 0.35	0.76 ± 0.17	1.45 ± 0.25
APEH	1.09 ± 0.07	1.03 ± 0.22	1.25 ± 0.12	0.96 ± 0.04
CES1	0.64 ± 0.04	0.39 ± 0.13	0.69 ± 0.31	1.39 ± 0.16
CPVL	0.36 ± 0.17	0.34 ± 0.04	0.86 ± 0.07	1.23 ± 0.09
CTSA	0.92 ± 0.08	0.23 ± 0.18	0.98 ± 0.54	1.16 ± 0.35
DPP4	0.55 ± 0.14	0.59 ± 0.12	1.24 ± 0.34	1.40 ± 0.15
DPP7	2.09	0.19 ± 0.04	1.52 ± 0.62	0.97 ± 0.18
DPP8	1.47 ± 0.25	0.59 ± 0.50	1.46 ± 0.32	1.07 ± 0.13
DPP9	0.94 ± 0.12	0.75 ± 0.10	1.03 ± 0.27	1.11 ± 0.09
ESD	0.97 ± 0.22	0.94 ± 0.20	1.06 ± 0.66	0.75 ± 0.25
FAAH	0.6	0.79	8.15	9.91
FASN	1.10 ± 0.04	0.89± 0.08	1.06 ± 0.07	1.04 ± 0.04
LIPC	0.21 ± 0.14	1.28 ± 0.15	0.51 ± 0.09	1.50 ± 0.10
LYPLA1	0.25 ± 0.17	0.32 ± 0.05	1.20 ± 0.29	1.32 ± 0.17
LYPLA2	0.85 ± 0.12	0.60 ± 0.21	1.18 ± 0.31	0.96 ± 0.19
LYPLAL1	1.10 ± 0.14	0.37 ± 0.14	0.64 ± 0.24	0.76 ± 0.08
MGLL	0.74 ± 0.13	0.41 ± 0.17	1.69 ± 0.63	1.36 ± 0.28
NCEH1	1.27 ± 0.05	1.40 ± 0.17	1.13 ± 0.04	1.08 ± 0.08
PAFAH1B3	1.47 ± 0.16	0.94 ± 0.49	1.74 ± 0.46	1.11 ± 0.07
PAFAH2	0.91 ± 0.43	0.81 ± 0.17	1.05 ± 0.58	0.92 ± 0.09
PNPLA6	1.21 ± 0.25	0.78 ± 0.18	1.07 ± 0.16	0.74 ± 0.11
PPME1	0.44 ± 0.11	1.81 ± 0.78	1.28 ± 0.99	3.98
PPT2	0.89 ± 0.12	2.23 ± 1.27	0.95 ± 0.38	2.14 ± 0.40
PREP	0.76 ± 0.14	0.71 ± 0.16	1.67 ± 0.41	1.32 ± 0.11
PREPL	0.60 ± 0.16	0.77 ± 0.28	1.08 ± 0.18	0.96 ± 0.20
RBBP9	1.66 ± 1.18	3.36 ± 1.32	3.57	1.01
SIAE	1.23 ± 0.49	0.35 ± 0.22	1.20 ± 0.07	0.41 ± 0.17
TMPRSS13	0.89 ± 0.05	1.34 ± 0.02	1.302 ± 0.001	1.43 ± 0.09
TPP2	0.79 ± 0.12	0.64 ± 0.14	1.13 ± 0.05	1.09 ± 0.17

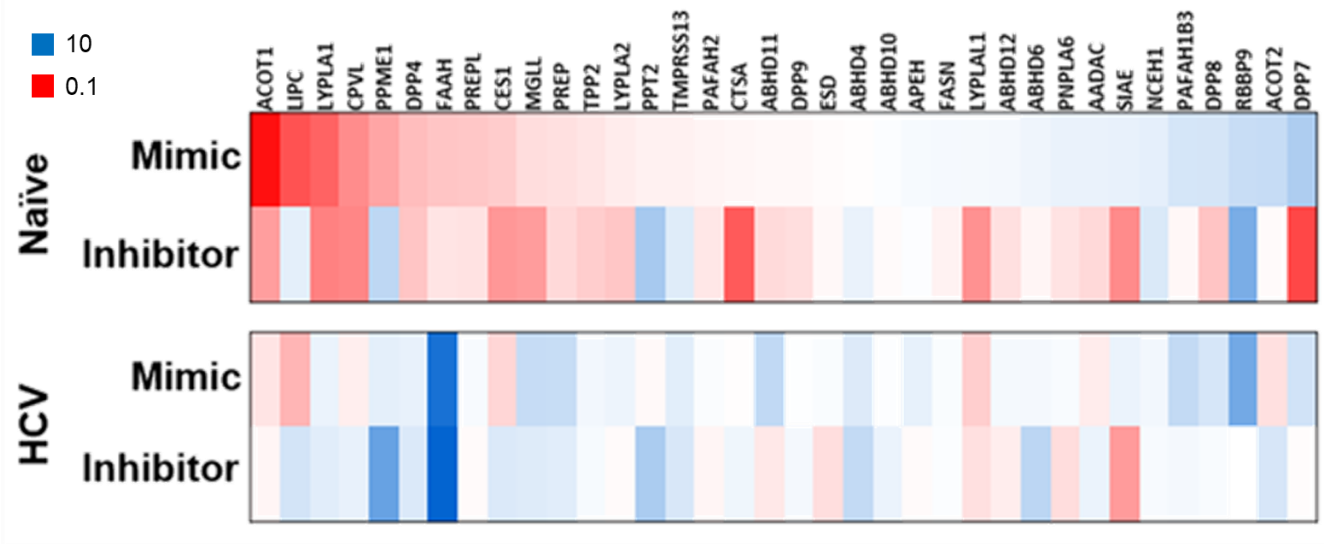

Figure 4.4: Heat map for the identification of differentially active serine hydrolases by ABPP-mass spectrometry. Naïve Huh7.5 cells and cells infected with the $JFH1_T$ strain of HCV were transfected with miR-27b mimic, inhibitor, or negative control. Cells were lysed after 72h and labelled with FP-biotin. The labelled proteome was isolated by streptavidin enrichment, isotopically labelled and differential labelling quantified by LC-MS/MS.

Table 4.2: Functional analysis of enzymes displaying miR-27b induced differential activity. Naïve Huh7.5 cells and cells infected with the JFH1$_T$ strain of HCV were transfected with miR-27b mimic, inhibitor, or negative control, lysed after 72h and labelled with FP-biotin. The labelled proteome was isolated by streptavidin enrichment, isotopically labelled and differential labelling was quantified by LC-MS/MS. Enzymes exhibiting an increase greater than 1.25-fold or a decrease of less than 0.8-fold were submitted for analysis but TOPFUNN.

Pathway	p-value of annotation	Hit in Query List
lipid catabolic process	2.45E-13	ABHD4, AADAC, MGLL, ACOT2, LIPC, PNPLA6, ABHD12, PLA2G15, FAAH, PAFAH1B3, PAFAH2, ABHD6
glycerolipid catabolic process	6.82E-12	AADAC, MGLL, LIPC, PNPLA6, ABHD12, PLA2G15, ABHD6
organic substance catabolic process	2.18E-11	ABHD4, AFMID, AADAC, MGLL, ACOT2, LIPC, PNPLA6, CTSA, CPVL, ABHD12, PLA2G15, LYPLAL1, ACHE, LYPLA2, ESD, ABHD10, FAAH, PAFAH1B3, PAFAH2, ABHD6
cellular lipid catabolic process	1.06E-10	AADAC, MGLL, ACOT2, LIPC, PNPLA6, ABHD12, PLA2G15, FAAH, ABHD6
lipid metabolic process	1.19E-10	ABHD4, AADAC, MGLL, ACOT1, FASN, ACOT2, LIPC, PNPLA6, CTSA, ABHD12, PLA2G15, ACHE, LYPLA2, FAAH, PAFAH1B3, PAFAH2, ABHD6
cellular lipid metabolic process	3.67E-10	ABHD4, AADAC, MGLL, ACOT1, FASN, ACOT2, LIPC, PNPLA6, CTSA, ABHD12, PLA2G15, ACHE, LYPLA2, FAAH, ABHD6
neutral lipid catabolic process	8.43E-09	AADAC, MGLL, LIPC, ABHD12, ABHD6
acylglycerol catabolic process	8.43E-09	AADAC, MGLL, LIPC, ABHD12, ABHD6
phospholipid catabolic process	1.63E-08	LIPC, PNPLA6, ABHD12, PLA2G15, ABHD6
glycerophospholipid catabolic process	2.75E-08	LIPC, PNPLA6, ABHD12, PLA2G15

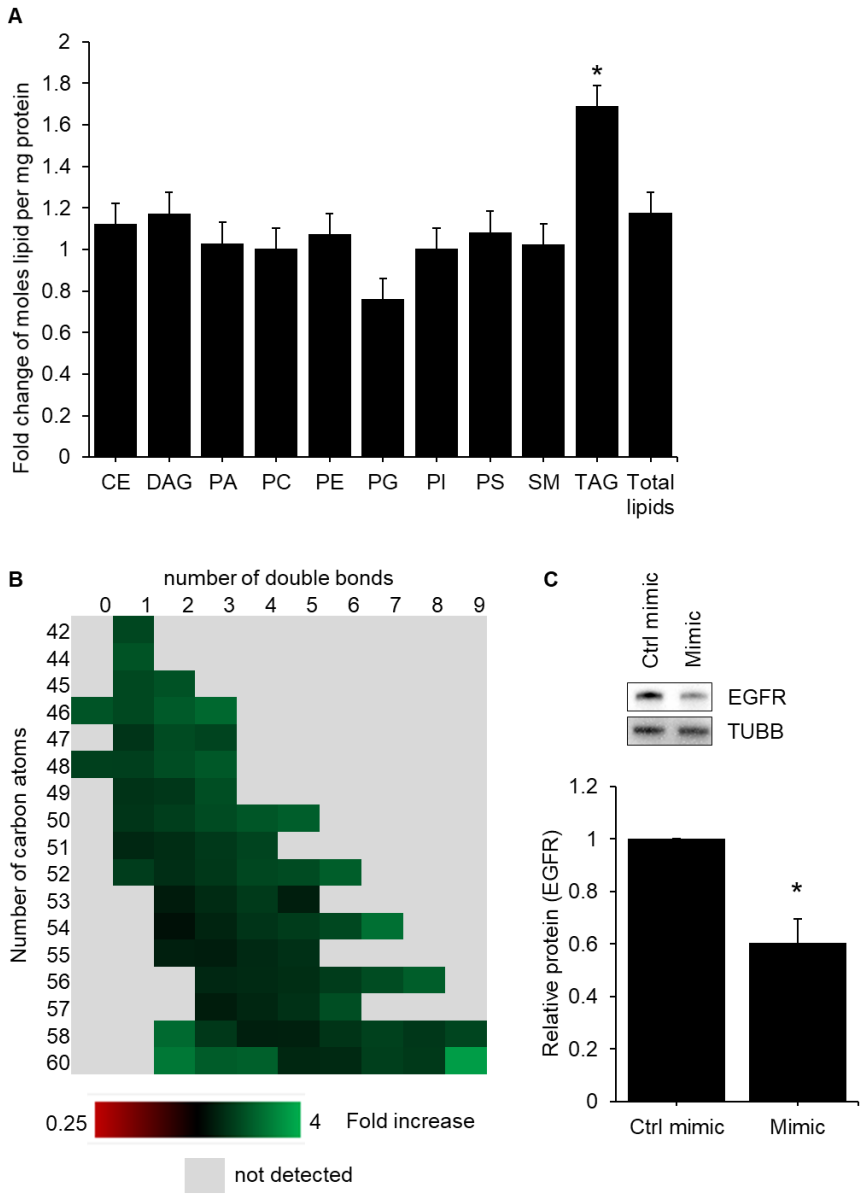

Figure 4.5: miR-27b selectively increases the abundance of triacylglycerols. Huh7.5 cells were transfected with miR-27b mimic or negative control. Cells were harvested after 72h and the lipid species quantified. A) Cumulative fold change of the lipid species in each class. B) Fold change of triglycerides of different lengths and desaturation. C) Western blotting on lysates of cells reserved from lipidomics samples against validated miR-27b targets. Values shown are normalised to the control-transfected sample. Data represents mean values ± s.e.m. n=3, *$p \leq 0.05$

27b mimic and either the purchased luciferase construct, the mutated construct, or an empty construct. No significant change in luciferase signal was observed in the presence of miR-27b, (Fig 4.7b) indicating that despite the presence of the canonical seed site, LIPC expression was not directly targeted by this microRNA.

Peroxisome proliferator-activated receptors (PPARs), are a group of transcription factors implicated in the regulation of lipid metabolism, and have more specifically been linked to the transcriptional regulation of LIPC.[76,77] Both PPARα and PPARγ were significantly decreased in the presence of miR-27b mimic (Fig 4.8), in agreement with previous findings.[36,38] To assess whether a reduction in PPAR activity was responsible for the decreased expression of LIPC, cells were treated with the pan-PPAR inhibitor benzamide[78] and LIPC activity quantified by using FP-biotin to label and enrich the active serine hydrolases. Western blotting showed a dramatic decrease in LIPC activity and expression, (Fig 4.8a,b) confirming that PPARs play a major role in the transcription of LIPC in the model system used. To investigate whether the miR-27b mediated decrease in LIPC expression was due to a decrease in PPAR signalling, cells transfected with miR-27b mimic were treated with the pan-PPAR activator bezafibrate.[79–81] While bezafibrate did increase LIPC expression and activity, the rescue represented only a small proportion of the decrease in activity induced by miR-27b. (Fig 4.8a,b) It was therefore apparent that other regulators were also utilized by miR-27b to decrease LIPC abundance.

To identify other factors implicated in miR-27b mediated regulation of LIPC expression, a literature search was performed to identify all known regulators of LIPC transcription. After eliminating LIPC regulatory genes which were not expressed in the Huh7 model, seven potential regulators were left: apolipoprotein A-I regulatory protein 1 (ARP1, also abbreviated NR2F2),[77] CCAAT/enhancer-binding protein β (CEPBP),[82] hepatic nuclear factor 1α (HNF1A),[77] hepatic nuclear factor 4α (HNF4A),[77] transcription factor AP-1 (JUN),[83] bile acid receptor (NR1H4),[84] and PPARγ coactivator 1α

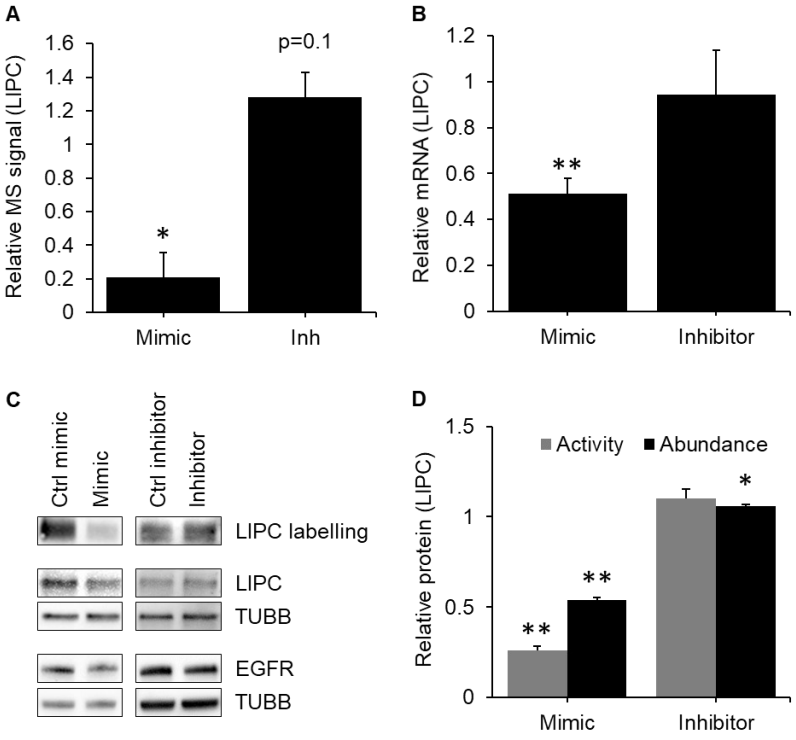

Figure 4.6: miR-27b decreases the activity and expression of LIPC. Huh7.5 cells were transfected with miR-27b mimic, inhibitor, or the respective negative control and lysed after 72h. Results represent signal from mimic or inhibitor-transfected samples normalised to their respective controls. A) LC-MS/MS relative quantification of FP-biotin labelled LIPC, n=3 B) qRT-PCR quantification of LIPC mRNA, n=4 C) Western blotting of LIPC labelling by FP-biotin compared to the total abundance of LIPC and known direct target EGFR. D) Densitometric analysis of western blotting against LIPC, n=3. Values shown are normalised to the control-transfected sample. Data represents mean values ± s.e.m. *$p \leq 0.05$, **$p \leq 0.01$

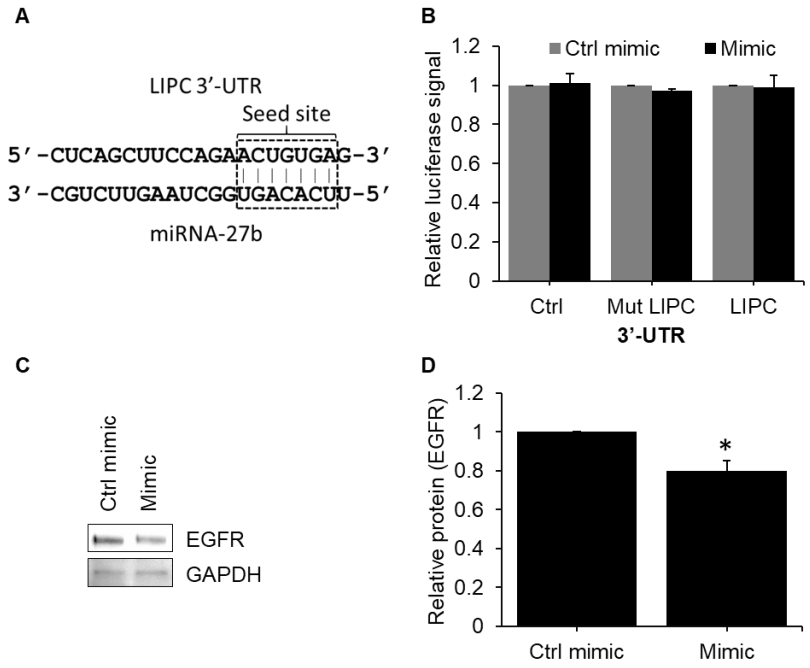

Figure 4.7: miR-27b does not target LIPC 3'-UTR. A) Seed site complementarity between LIPC 3'-UTR and miR-27b. B-D) Huh7.5 cells were transfected with a luciferase construct containing either the LIPC 3'-UTR, a mutated LIPC 3'-UTR, or negative control, then either miR-27b mimic or control mimic. Cells were lysed after 48h. B) Luciferase activity normalised to protein concentration. C) Western blotting analysis on LIPC 3'-UTR transfected lysates against known miR-27b target EGFR. D) Densitometric analysis on western blotting. Values shown are normalised to the control-transfected sample. Data represents mean values ± s.e.m. n=3 *$p \leq 0.05$ **$p \leq 0.01$

(PPARGC1A).[77] miR-27b was overexpressed and the expression of genes associated with the regulation of LIPC was quantified by qRT-PCR. Of this list, two proteins, JUN and HNF4α, were identified as targets of interest. (Fig 4.8d)

HNF4α is a transcription factor which has been shown to promote the transcription of LIPC.[77] In cells transfected with miR-27b mimic, HNF4α mRNA is decreased by 30%. Western blotting in mimic-transfected cells shows a significant decrease in protein expression at the molecular weight associated with the major active form of HNF4α, confirming that miR-27b decreases the expression of this transcription factor. (Fig 4.8a,c) Interestingly, blotting against HNF4α showed a second band at a lower molecular weight increasing in abundance with miR-27b treatment. (Fig 4.8a) Though efforts to identify this protein were not successful, it is possible for this band to represent an alternative splicing of the protein. This would not negate the functional effect of miR-27b on HNF4α, as these alternatively spliced forms possess less activity than the main form, and in, fact some reports indicate that they might hinder the DNA binding activity of the main form.[85] JUN is a transcription factor implicated in the regulation of cell proliferation and survival,[86] whose binding upstream of the LIPC coding sequence has been demonstrated to inhibit transcription.[83] Transfection with miR-27b mimic increases the expression of JUN by 60%. (Fig 4.8d) miR-27b modulation of LIPC expression might therefore proceeds from a simultaneous decrease of the positive regulators PPARα and HNF4α, and an increase in the negative regulator JUN.

The activity labelling by FP-biotin in cells transfected with miR-27b mimic or inhibitor was repeated in cells infected with the $JFH1_T$ strain of HCV. Though miR-27b modulation of LIPC activity and abundance was broadly reproduced in the presence of HCV, there were a few notable changes in the magnitude of the observed changes. The decreases observed in mimic-transfected samples was inferior to that seen in experiments with HCV-naïve cells, while the inhibitor was able to increase the expression

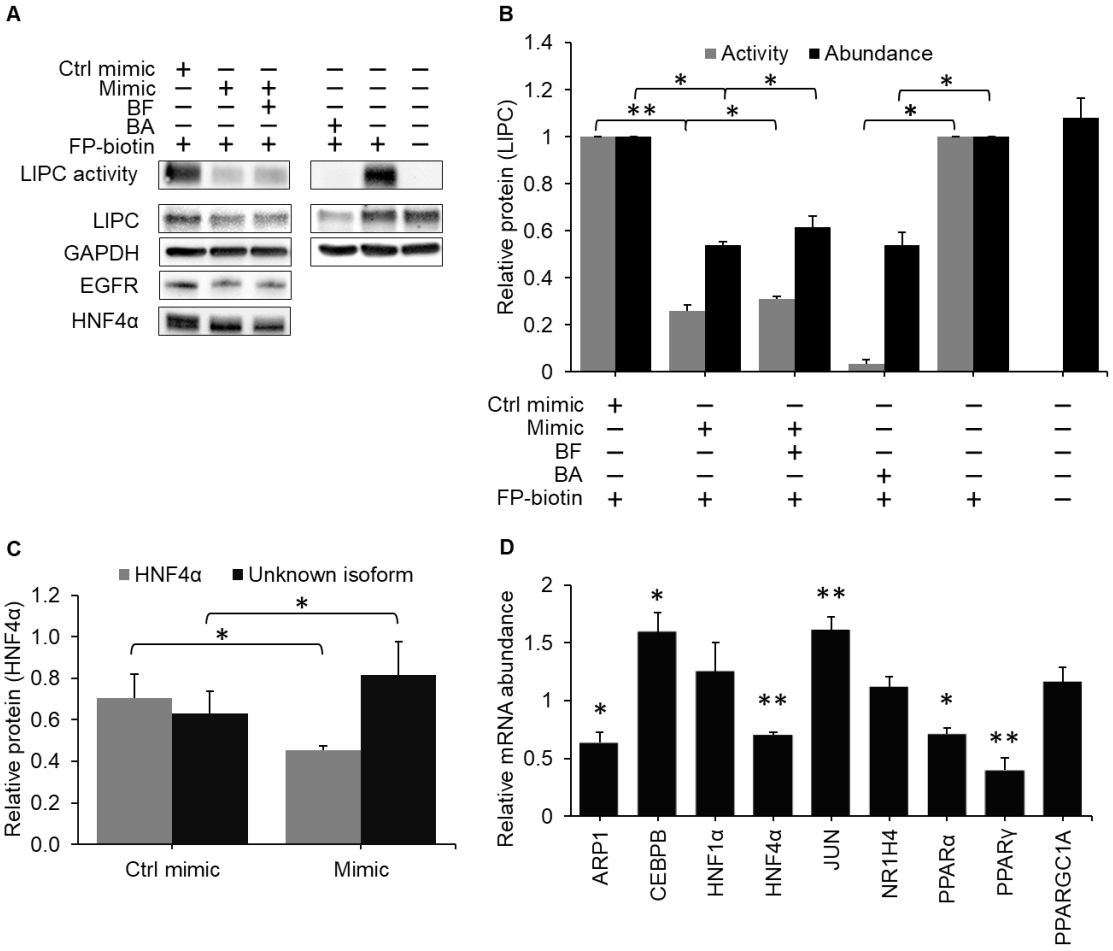

Figure 4.8: miR-27b modulation of LIPC expression is controlled by multiple transcription factors. Huh7.5 cells were A) transfected with miR-27b and treated with bezafibrate or treated with benzamide. Cells were lysed and labelled with FP-biotin, the labelled proteome was isolated by streptavidin enrichment and labelling was analysed by western blotting. B) Densitometric analysis of western blotting against LIPC, n=3 C) Densitometric analysis of western blotting against isoforms of HNF4α, n=3 D) qRT-PCR against LIPC transcription factors in Huh7.5 cells treated with miR-27b mimic or control, n=4. Values shown are normalised to the control sample. Data represents mean values ± s.e.m. *p ≤ 0.05 **p ≤ 0.01

and activity of LIPC to a much greater extent. (Fig 4.9a-d) These observations are consistent with reports that HCV increases the expression of miR-27b:[36] as miR-27b levels are already high, the addition of the mimic would less significant. Conversely, inhibition of miR-27b should lead to more dramatic effects when its endogenous expression is higher. Altogether, these results indicate that miR-27b regulation of LIPC function occurs during HCV infection.

Next, the link between the modulation of LIPC activity and HCV infection was examined by investigating both the effect of the virus on LIPC activity and the effect of LIPC activity on the virus. Protein lysates from Huh7.5 cells infected with the $JFH1_T$ cell culture strain of virus were labelled with FP-biotin and processed for mass spectrometry analysis. LIPC activity was decreased by nearly 50% in infected as compared to the naïve cells, (Fig 4.11a) and mRNA abundance was similarly decreased. (Fig 4.11b) This corroborates previous findings *in vivo,* in which a significant decrease in LIPC mRNA was observed in liver tissue of patients suffering from HCV as compared to healthy controls.[87] To investigate the dependence of HCV infection on LIPC activity, LIPC was knocked down by siRNA and intracellular RNA was measured by qRT-PCR. The production of infectious virions was also assessed by measuring the infectivity potential of the supernatants of the infected cells, as illustrated in Fig 4.10. A non-significant increase of 40% was observed in the amount of intracellular RNA. In contrast, the levels of infectious virions produced was significantly increased by 100% with LIPC KD.

A comparison of these two measurements shows a significantly higher increase in virion production than intracellular RNA. (Fig 4.11C) This indicates that while decreases in LIPC activity may play a role in promoting HCV replication, it is more important to the assembly and secretion of new virions.

4.5.2 Platelet Activating Factor 1B3 (PAFAH1B3)

ABPP-MS showed that miR-27b significantly upregulated the activity of PAFAH1B3, an upstream

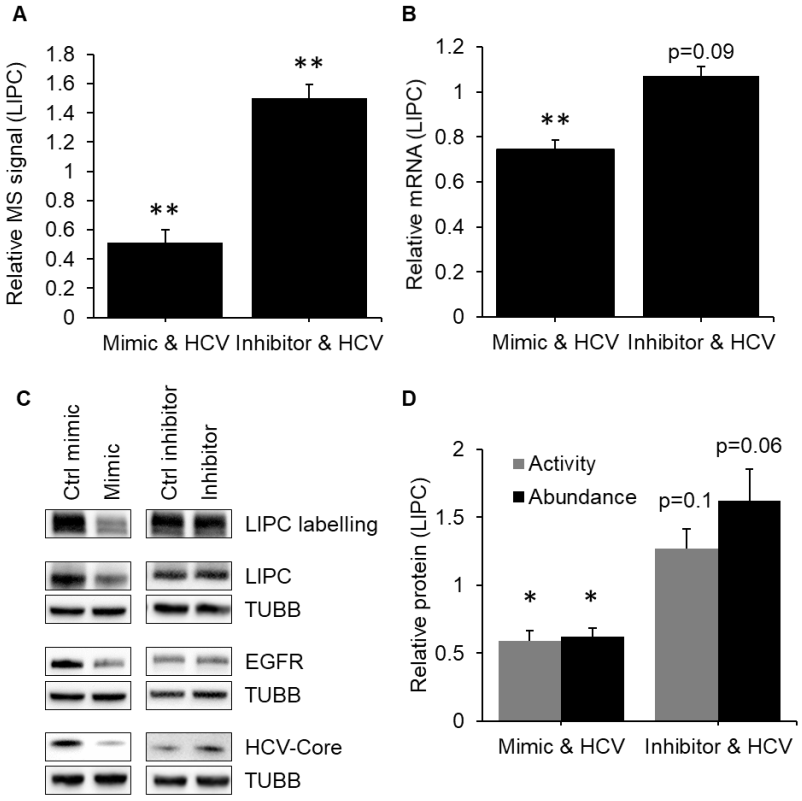

Figure 4.9: miR-27b modulates LIPC expression and activity in the context of HCV infection. Huh7.5 cells were infected with the JFH1$_T$ strain of HCV and subsequently transfected with miR-27b mimic, inhibitor, or the respective negative control and lysed after 72h. Results represent signal from mimic or inhibitor-transfected samples normalised to their respective controls. A) LC-MS/MS quantification of FP-biotin labelled of LIPC, n=3. B) qRT-PCR quantification of LIPC mRNA, n=4. C) Western blotting analysis of LIPC labelling by FP-biotin compared to the total abundance of LIPC and known direct target EGFR. D) Densitometric analysis of western blotting against LIPC, n=3. Values shown are normalised to the control-transfected sample. Data represents mean values ± s.e.m. *$p \leq 0.05$, **$p \leq 0.01$

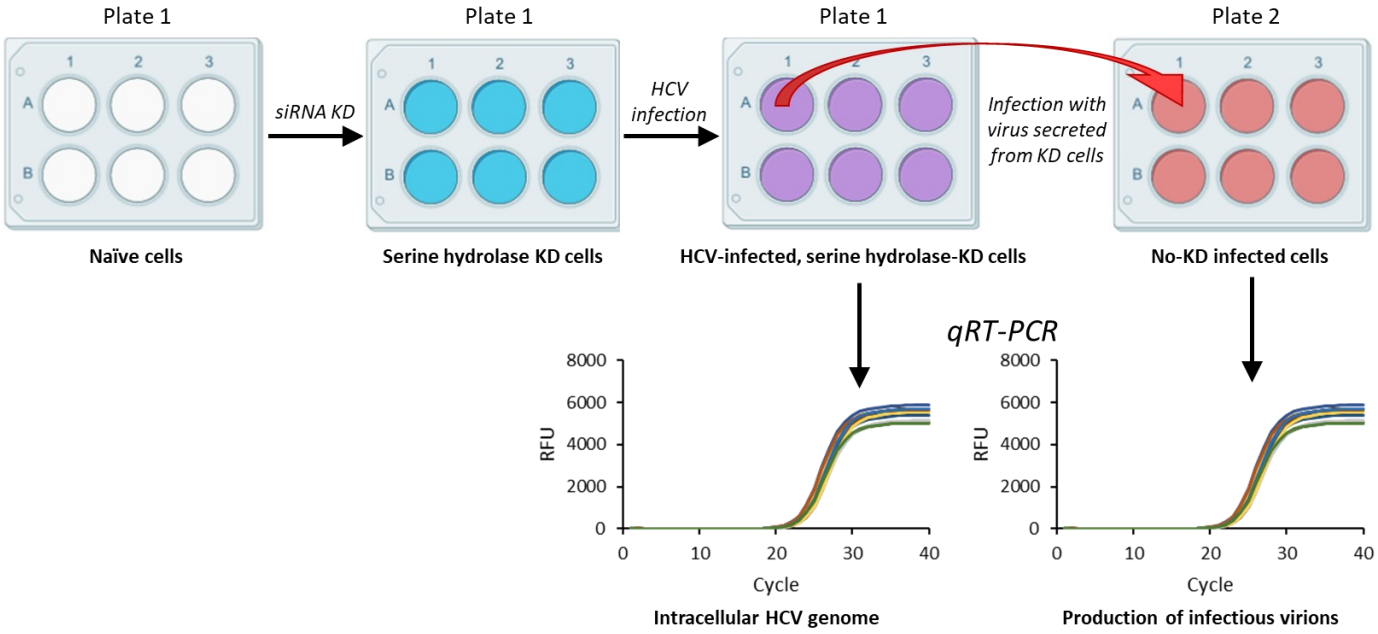

Figure 4.10: Workflow diagram of infectivity assays investigating importance of specific serine hydrolases to viral propagation. Huh7.5 cells are transfected with an siRNA against LIPC, PAFAH1B3, or ACOT1/2. Knock-down cells are then infected with the $JFH1_T$ strain of HCV. Supernatant from knock-down cells are used to infect new Huh7.5 cells. RNA is harvested from the knock-down cells to assess intracellular RNA levels and from the new Huh7.5 cells to measure the infectivity of the virions produced.

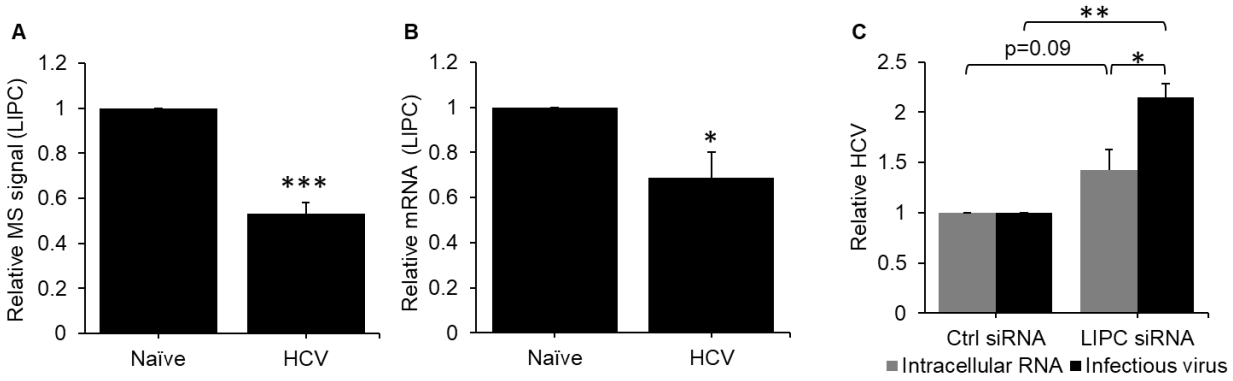

Figure 4.11: HCV-mediated decrease in LIPC activity promotes virion production. A-B) Huh7.5 cells were infected with the JFH1$_T$ strain of HCV and lysed after 72h. A) LC-MS/MS relative quantification of FP-biotin labelled LIPC, n=3. B) qRT-PCR quantification of LIPC mRNA, n=4. C) Huh7.5 cells were transfected with siRNA against ACOT1/2 and infected with the JFH1$_T$ strain of HCV. Intracellular RNA was harvested and quantified by qRT-PCR,and growth media from these cells was used to infect cells without siRNA knock-down. Intracellular RNA was harvested and quantified by qRT-PCR. Values shown are normalised to the control-transfected sample. Data represents mean values ± s.e.m. *$p \leq 0.05$, **$p \leq 0.01$, ***$p \leq 0.001$

regulator of multiple classes of lipids.[88] (Fig 4.12a) Western blotting of the FP-labelled and enriched proteome also showed a significant increase in labelling, and therefore activity. (Fig 4.12c,d) Blotting of unenriched whole protein samples revealed that miR-27b did not change the abundance of PAFAH1B3. PAFAH1B3 mRNA expression was also unchanged by over-expression of miR-27b. (Fig 4.12b) PAFAH1B3 activity is therefore upregulated post-translationally by miR-27b.

PAFAH1B3 is a subunit of the PAFAH1B complex, composed of two catalytic subunits, either PAFAH1B2 or PAFAH1B3, and the regulatory subunit PAFAH1B1, also known as LIS1.[89] While monomeric PAFAH1B3 is still capable of enzymatic activity, inclusion in a complex, as well as the composition of the complex, affects activity towards various substrates.[89–91] To determine whether the miR-27b-induced increase in PAFAH1B3 activity is mediated by modulation of the composition of the complex, the mRNA expression of PAFAH1B2 and PAFAH1B1 was measured by qPCR. While PAFAH1B2 expression remained unchanged, PAFAH1B1 expression was significantly increased. (Fig 4.13a) Western blotting confirmed that PAFAH1B1 expression is significantly increased by miRNA-27b. (Fig 4.13b, c) This suggests that PAFAH1B3 activity could be upregulated by an increase in interaction with the regulatory PAFAH1B1 subunit. A 50% knock-down of PAFAH1B1 expression by siRNA did not result in any change in PAFAH1B3 activity; (Fig 4.13d-f) however, it may be that the baseline level of interaction was already low, and that therefore decreasing expression of PAFAH1B3 does not change the oligomerization status of a sufficient amount of PAFAH1B3 to generate an observable change in activity.

Recent literature has suggested that PAFAH1B3 is palmitoylated, and that the presence of this post-translational modification is associated with the presence of downstream effects of PAFAH1B3 function.[92] To assess whether palmitoylation is important for PAFAH1B3 activity, cells were treated with the general palmitoylation inhibitor 2-bromopalmitate (2-BP) and lysates labelled by FP-biotin. (Fig

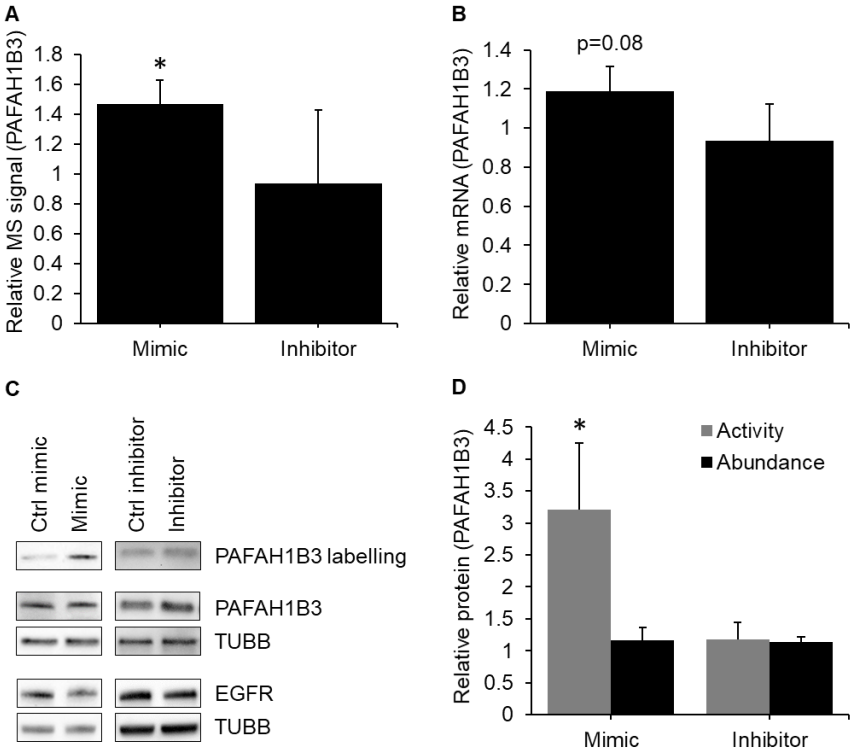

Figure 4.12: miR-27b increases the activity of PAFAH1B3 post-translationally. Huh7.5 cells were transfected with miR-27b mimic, inhibitor, or the respective negative control and lysed after 72h. Results represent signal from mimic or inhibitor-transfected samples normalised to their respective controls A) LC-MS/MS relative quantification of FP-biotin labelled PAFAH1B3, n=3 B) qRT-PCR quantification of PAFAH1B3 mRNA, n=4 C) Western blotting analysis of PAFAH1B3 labelling by FP-biotin compared to the total abundance of PAFAH1B3 and known direct target EGFR. D) Densitometric analysis of western blotting against PAFAH1B3, n=3. Values shown are normalised to the control-transfected sample. Data represents mean values ± s.e.m. *$p \leq 0.05$, **$p \leq 0.01$

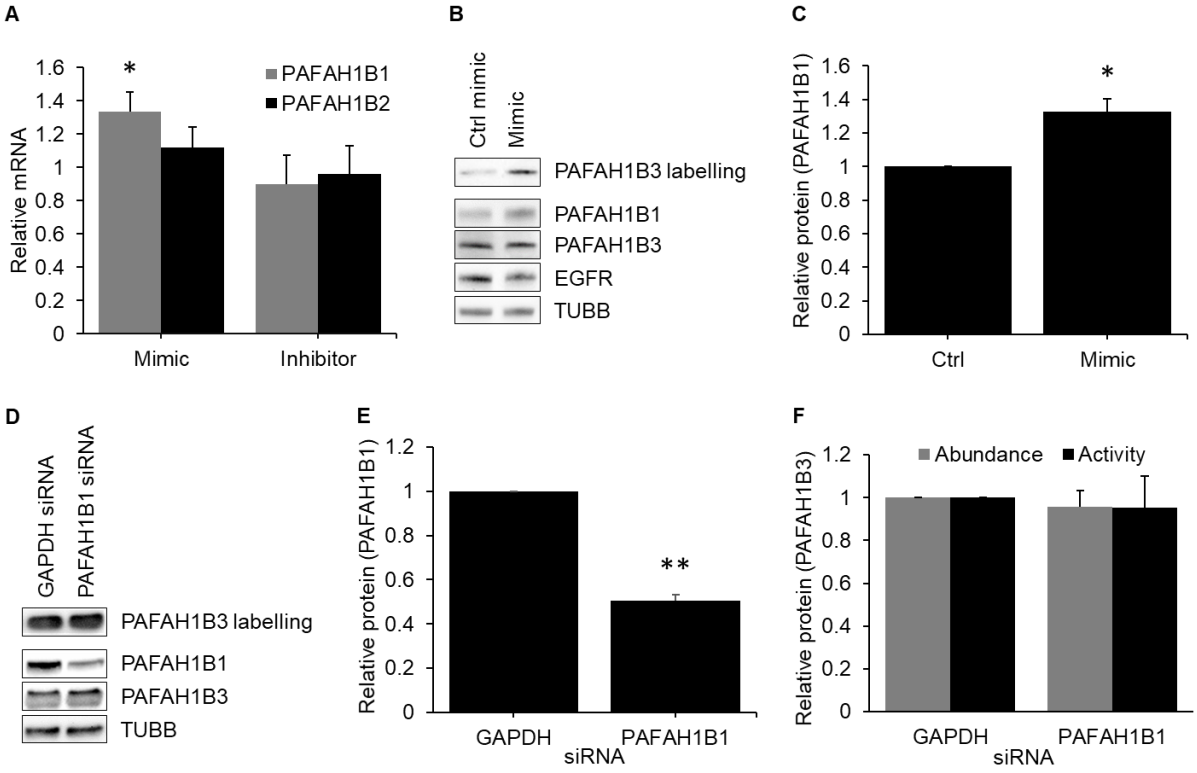

Figure 4.13: Expression of regulatory subunit PAFAH1B1 is increased by miR-27b. A-C) Huh7.5 cells were transfected with miR-27b mimic, inhibitor, or negative control and lysed after 72h. A) qRT-PCR quantification of mRNA encoding PAFAH1B subunits B1 and B2, n=4 B) Western blotting analysis of PAFAH1B3 labelling by FP-biotin compared to the total abundance of PAFAH1B1 and PAFAH1B3. C) Densitometric analysis of western blotting against PAFAH1B1, n=3. D-F) Huh7.5 cells were transfected with siRNA against PAFAH1B1 or GAPDH and lysed after 48h. D) Western blotting analysis of PAFAH1B3 labelling by FP-biotin compared to the total abundance of PAFAH1B1 and PAFAH1B3 E) Densitometric analysis of PAFAH1B1 protein expression following knockdown, n=3. F) Densitometric analysis of western blotting against PAFAH1B3, n=3. Values shown are normalised to the control-transfected sample. Data represents mean values ± s.e.m. *$p \leq 0.05$, **$p \leq 0.01$

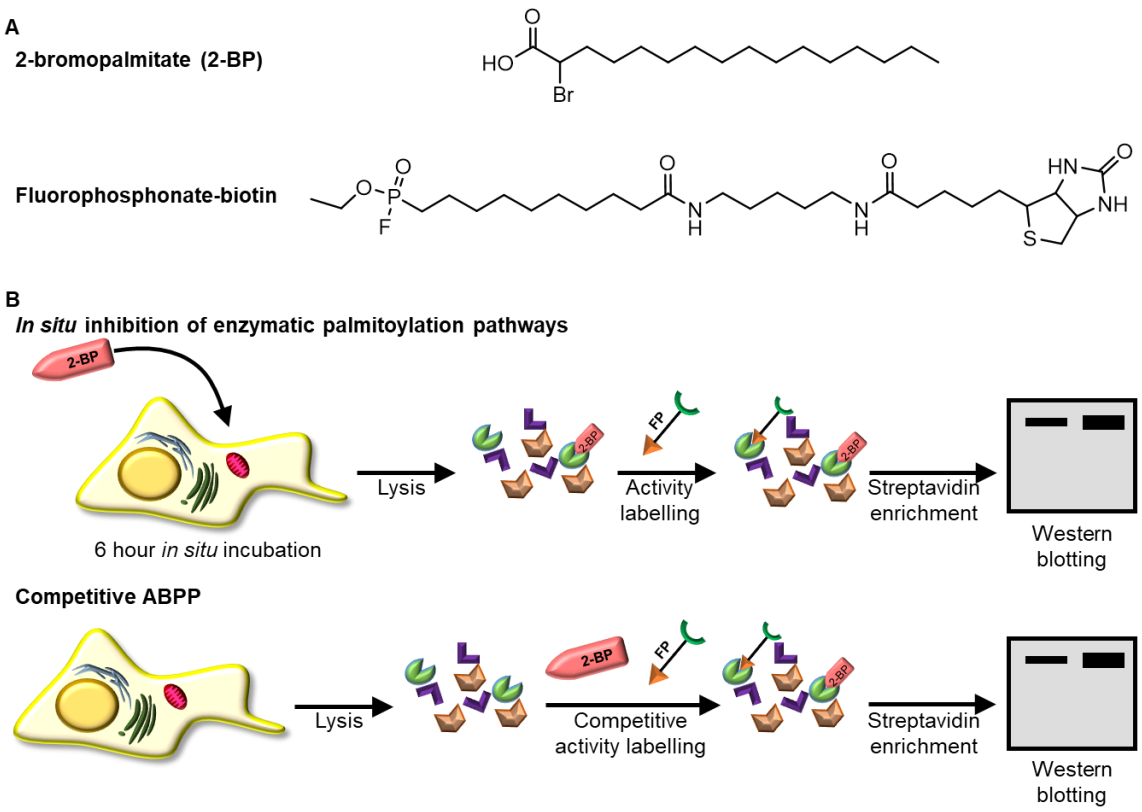

Figure 4.14: 2-bromopalmitate used to inhibit enzymatic palmitoylation pathways. A) Chemical structures of FP-biotin and 2BP B) Schematic representation of activity-based labelling work-flow used.

4.14) Western blotting on the enriched fraction revealed that inhibition of palmitoylation significantly decreased the activity of PAFAH1B3. (Fig 4.15a,b) Though 2-BP is a promiscuous inhibitor, it has not previously been shown to inhibit PAFAH1B3 in target screens.[93] A competitive ABPP assay, wherein samples were incubated with FP-biotin in the presence of 2-BP, (Fig 4.14) demonstrated no decrease in PAFAH1B3 labelling, (Fig 4.15a,c) indicating that 2-BP is not able to directly inhibit the activity of PAFAH1B3. Overall, these results demonstrate that PAFAH1B3 activity is regulated post-translationally by the addition or removal of a palmitate group.

In order to characterise the role of this miR-27b regulation of PAFAH1B3 activity in the context of HCV infection, activity of PAFAH1B3 in cells infected with HCV and transfected with miR-27b mimic or inhibitor was measured by FP-biotin labelling followed by enrichment and western blotting. Neither miR-27b mimic nor miR27b inhibitor significantly altered PAFAH1B3 activity, though it was slightly increased by the mimic. (Fig 4.16c,d) HCV infection did not demonstrate a consistent regulation either up or down of PAFAH1B3 activity as assessed by mass spectrometry on FP-biotin enriched lysates. (Fig 4.17a) Upon knock-down of PAFAH1B3, the intracellular expression of the HCV genome was increased two-fold, while the production of new virions was increased 1.5-fold. (Fig 4.17c) This indicates that PAFAH1B3 activity could potentially play a role in the suppression of HCV replication.

4.5.3 ACOT1/ACOT2

Acyl-CoA thioesterases are a large family of proteins which remove the CoA moiety from acyl-CoA, producing free fatty acid. ACOT1 and ACOT2 possess a 98% sequence homology[94] and target long-chain acyl-CoA, performing similar catalytic reactions at different cellular locales.[95] ACOT1 is localised to the cytosol, where it regulates the pool of acyl-CoA and free fatty acids.[95] ACOT2 is localised on the mitochondria, and promotes β-oxidation, thereby reducing the abundance of intracellular fatty acid.[95–97] Mass spectrometry quantification of activity-labelled serine hydrolases reported differential changes in

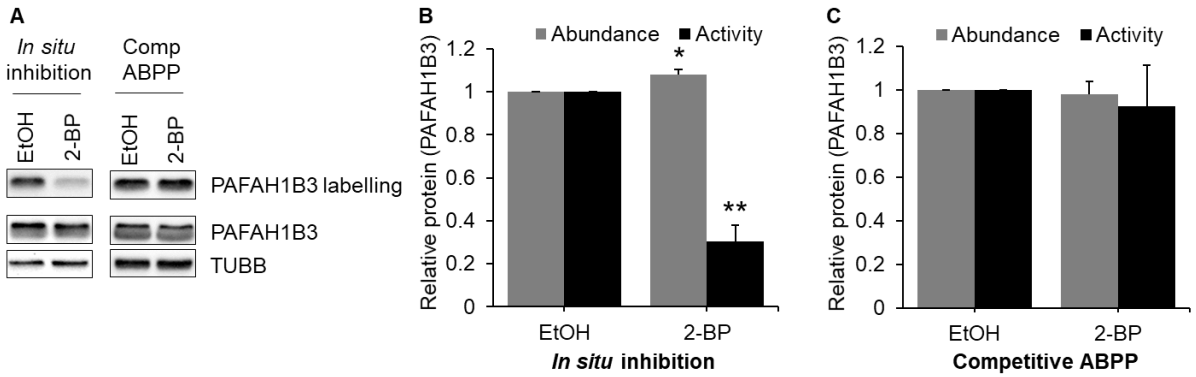

Figure 4.15: PAFAH1B3 activity is regulated by post-translational palmitoylation. Huh7.5 cells were either pre-treated with 2-BP for 6h, lysed, and labelled by FP-biotin, or lysed then pre-incubated with 2-BP for 10 minutes before FP-biotin labelling. A) Western blotting analysis of PAFAH1B3 labelling by FP-biotin compared to the total abundance of PAFAH1B3. B) Densitometric analysis of western blotting of 6h treatment. C) Densitometric analysis of western blotting of 10 min competitive ABPP. n=3.

activity for ACOT1 and ACOT2. However, while ACOT1 demonstrated a consistent decrease in activity, measurements of ACOT2 activity possessed high variability, even within technical replicates, wherein a samples from a single trial was repeatedly analysed by LC-MS/MS. (Fig 4.18a) This indicates the presence of a technical difficulty, as opposed to any high variability in the activity of the enzymes.

To circumvent this problem, the abundance of activity-labelled enzyme was measured by western blotting instead of mass spectrometry. Unfortunately, the high homology between ACOT1 and ACOT2 does not allow them to be differentiated using antibodies.[98] For this reason, western blotting was performed using an antibody raised against both proteins.

Transfection with miR-27b mimic significantly decreased the activity of ACOT1/2, while inhibition of miR-27b induced a small but significant increase in activity, indicating that inhibition of ACOT1/2 activity is a physiologically relevant phenomenon. (Fig 4.18c, d) qPCR performed on mRNA showed a decrease in abundance of ACOT1/2 in miR-27b mimic treated samples. (Fig 4.18b) Expression of both ACOT1 and ACOT2 has been demonstrated to be induced by PPARα,[99] whose abundance is decreased by miR-27b.[36] However, this change in mRNA abundance was much smaller than the change in activity, and did not result in a significant decrease in protein expression. Furthermore, no increase in abundance was observed with miR-27b inhibition. (Fig 4.18c, d) Altogether, this suggests that the primary method of miR-27b regulation of ACOT1/2 activity is post-translational. As ACOT2 is known to be palmitoylated,[100] the possibility that this PTM could regulate enzyme activity was investigated using 2-BP, as shown in figure 4.14. Interestingly, while *in situ* treatment did not show a consistent increase in activity, competitive ABPP in the presence of palmitoylation inhibitor resulted in large increases in activity labelling across three trials. (Fig 4.19) This suggests that the absence of palmitoylation on ACOT1/2 increases activity, but also that ACOT1/2 palmitoylation is regulated on a very short timescale, and that this modification can occur even in lysates.

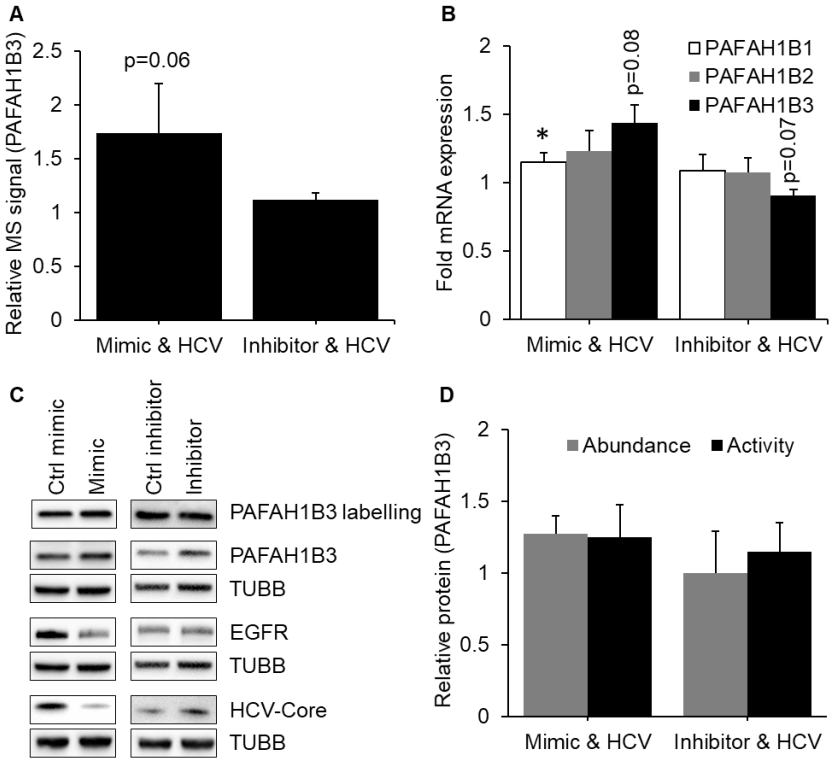

Figure 4.16: Effect of miR-27b on PAFAH1B3 in the context of HCV infection. Huh7.5 cells were infected with the $JFH1_T$ strain of HCV and subsequently transfected with miR-27b mimic, inhibitor, or the respective negative control and lysed after 72h. Results represent signal from mimic or inhibitor-transfected samples normalised to their respective controls. A) LC-MS/MS relative quantification of FP-biotin labelled PAFAH1B3, n=3. B) qRT-PCR quantification of mRNA encoding PAFAH1B subunits, n=4. C) Western blotting analysis of PAFAH1B3 labelling by FP-biotin compared to the total abundance of PAFAH1B3 and known direct target EGFR. D) Densitometric analysis of western blotting against PAFAH1B3, n=3. Values shown are normalised to the control-transfected sample. Data represents mean values ± s.e.m. *$p \leq 0.05$, **$p \leq 0.01$, ***$p \leq 0.001$

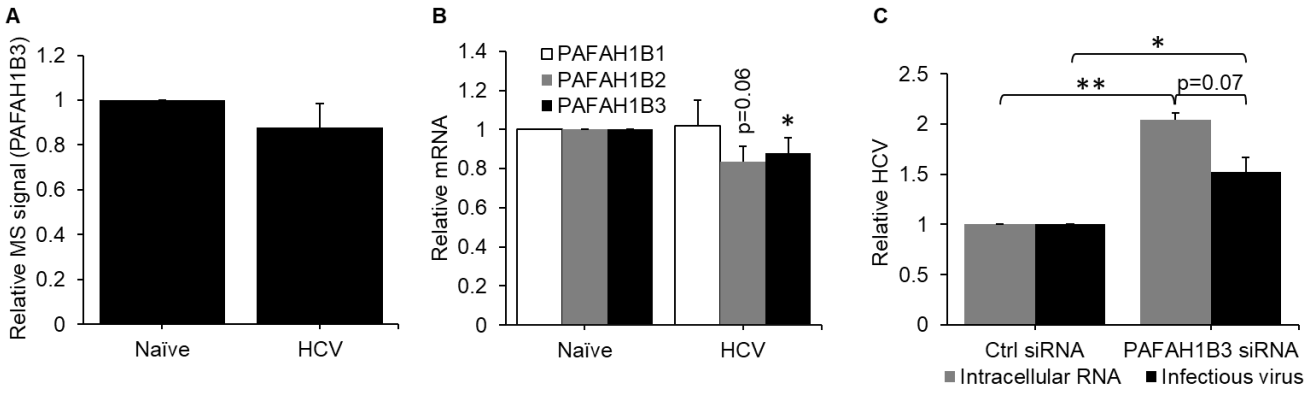

Figure 4.17: PAFAH1B3 is detrimental to virion production A-B) Huh7.5 cells were infected with the $JFH1_T$ strain of HCV and lysed after 72h. A) LC-MS/MS relative quantification of FP-biotin labelled PAFAH1B3, n=3. B) qRT-PCR quantification of mRNA encoding PAFAH1B subunits, n=4. C) Huh7.5 cells were transfected with siRNA against PAFAH1B3 and infected with the $JFH1_T$ strain of HCV. Intracellular RNA was harvested and quantified by qRT-PCR, and growth media from these cells was used to infect cells without siRNA knock-down. Intracellular RNA was harvested and quantified by qRT-PCR. Values shown are normalised to the control-transfected sample. Data represents mean values ± s.e.m. *$p \leq 0.05$, **$p \leq 0.01$, ***$p \leq 0.001$

Activity of ACOT1 has itself been identified as a regulator of S-palmitoylation: by reducing the intracellular concentration of palmitoyl-CoA, there is a decrease in the availability of the substrate used for S-palmitoylation.[101] As PAFAH1B3 activity is modulated by S-palmitoylation, as demonstrated above, the role of ACOT1/2 in regulating PAFAH1B3 activity was investigated. siRNA targeting both ACOT1 and ACOT2 reduced expression by 44% after 48h and by 60% after 72h, mimicking the inhibition induced by miR-27b transfection. (Fig 4.20a, c) Activity of PAFAH1B3 was unchanged at both 48h and 72h post knock-down, (Fig 4.20a, b) indicating that while modulation of S- palmitoylation may regulate PAFAH1B3 activity, this modulation was not regulated by ACOT1/2. Interestingly, the activity of ACOT1/2, decreased by 65% and 69% at 48h and 72h, respectively, was significantly more reduced than expression of ACOT1/2. (Fig 4.20a, c) This may indicate that ACOT1/2 activity could function as a positive-feedback loop, wherein ACOT1/2 reduces the availability of palmitoyl-CoA, which in turn decreases the palmitoylation of ACOT1/2, which increases ACOT1/2 activity.

The modulation of ACOT1/2 activity by miR-27b was less substantial in cells infected with HCV. (Fig 4.21a-d) This, however, may be due to the obfuscating influence of other regulatory mechanisms induced by HCV infection. A significant decrease in ACOT1/2 activity during HCV infection alone was observed by mass spectrometry. (Fig 4.22a) This may be caused by the HCV-induced increase in miR-27b,[36] which mediated post-translational inhibition of ACOT1/2 activity. However, inhibition of miR-27b in HCV-infected cells only induced a slight, insignificant increase in activity. (Fig 4.21c, d) The failure of miR-27b inhibition to reverse the HCV-induced decrease in ACOT1/2 activity suggests there are additional regulatory mechanisms also employed by the virus to modulate ACOT1/2 activity.

siRNA knock-down of ACOT1 and 2 followed by HCV infection resulted in increases in intracellular HCV RNA as well as infectious virion production. (Fig 4.22c) While this could indicate that the decrease in ACOT1/2 activity mediated by HCV in part via miR-27b acts to promote HCV infection, the observed

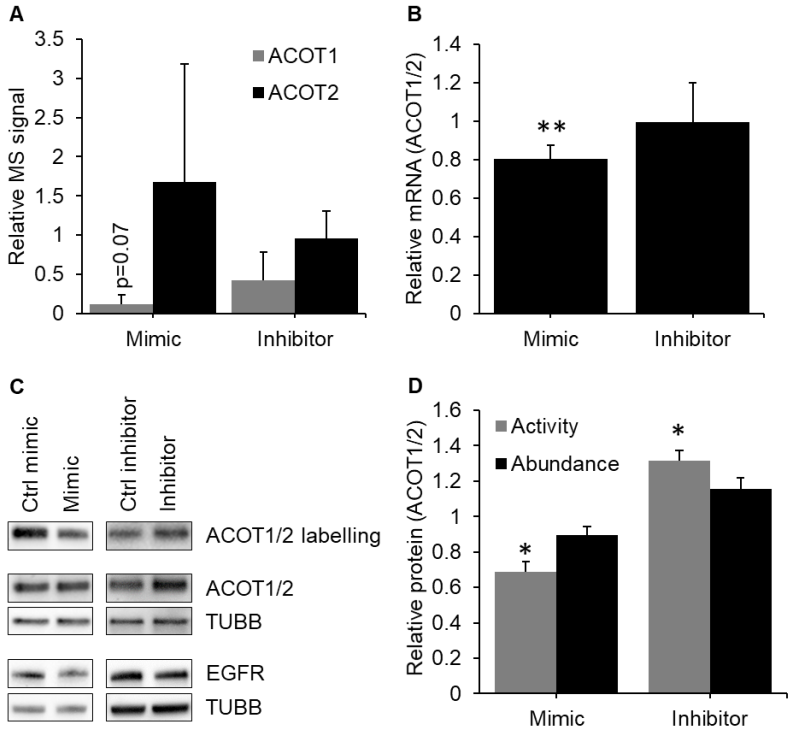

Figure 4.18: miR-27b decreases the activity of ACOT1/2. Huh7.5 cells were transfected with miR-27b mimic, inhibitor, or the respective negative control and lysed after 72h. Results represent signal from mimic or inhibitor-transfected samples normalised to their respective controls. A) LC-MS/MS relative quantification of FP-biotin labelled ACOT1 and ACOT2, n=3 B) qRT-PCR quantification of ACOT1/2 mRNA, n=4 C) Western blotting analysis of ACOT1/2 labelling by FP-biotin compared to the total abundance of ACOT1/2 and known direct target EGFR. D) Densitometric analysis of western blotting against ACOT1/2, n=3. Values shown are normalised to the control-transfected sample. Data represents mean values ± s.e.m. *$p \leq 0.05$, **$p \leq 0.01$

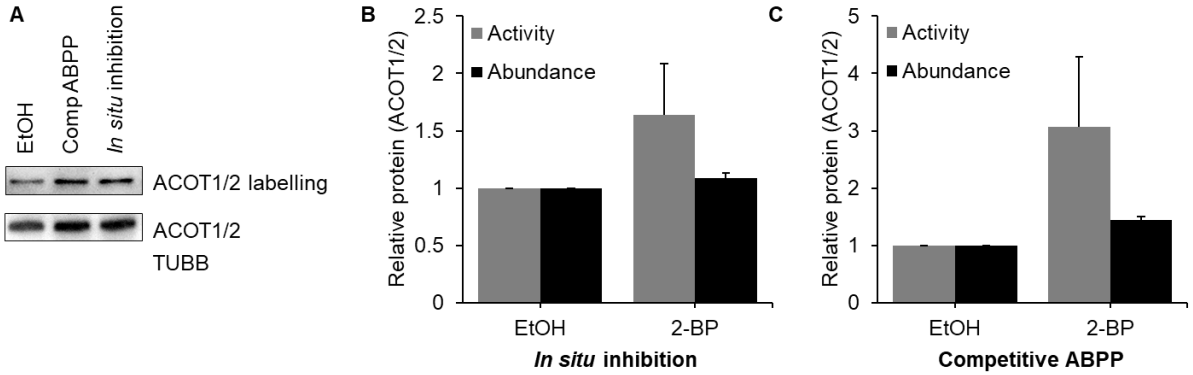

Figure 4.19: ACOT1/2 activity is regulated by post-translational palmitoylation. Huh7.5 cells were either pre-treated with 2-BP for 6h, lysed, and labelled by FP-biotin, or lysed then pre-incubated with 2-BP for 10 minutes before FP-biotin labelling. A) Western blotting analysis of ACOT1/2 labelling by FP-biotin compared to the total abundance of ACOT1/2. B) Densitometric analysis of western blotting of 6h treatment. C) Densitometric analysis of western blotting of 10 min competitive ABPP. n=3.

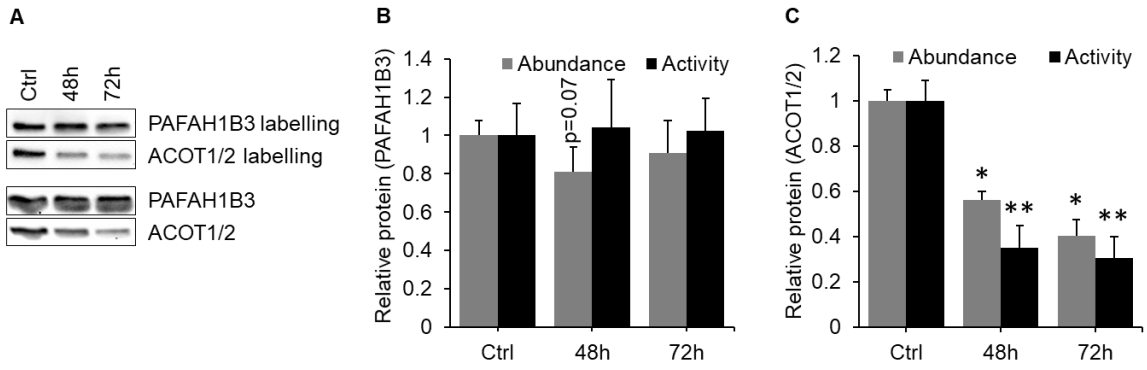

Figure 4.20: PAFAH1B3 activity is not regulated by ACOT1/2. Huh7.5 cells were transfected with siRNA against ACOT1/2, lysed after 48h, and labelled with FP-biotin. A) Western blotting against FP-biotin labelled PAFAH1B3. B) Densitometric analysis of PAFAH1B3 abundance and activity, n=3. C) Densitometric analysis of ACOT1/2 abundance and activity, n=3. Values shown are normalised to the control-transfected sample. *$p \leq 0.05$, **$p \leq 0.01$

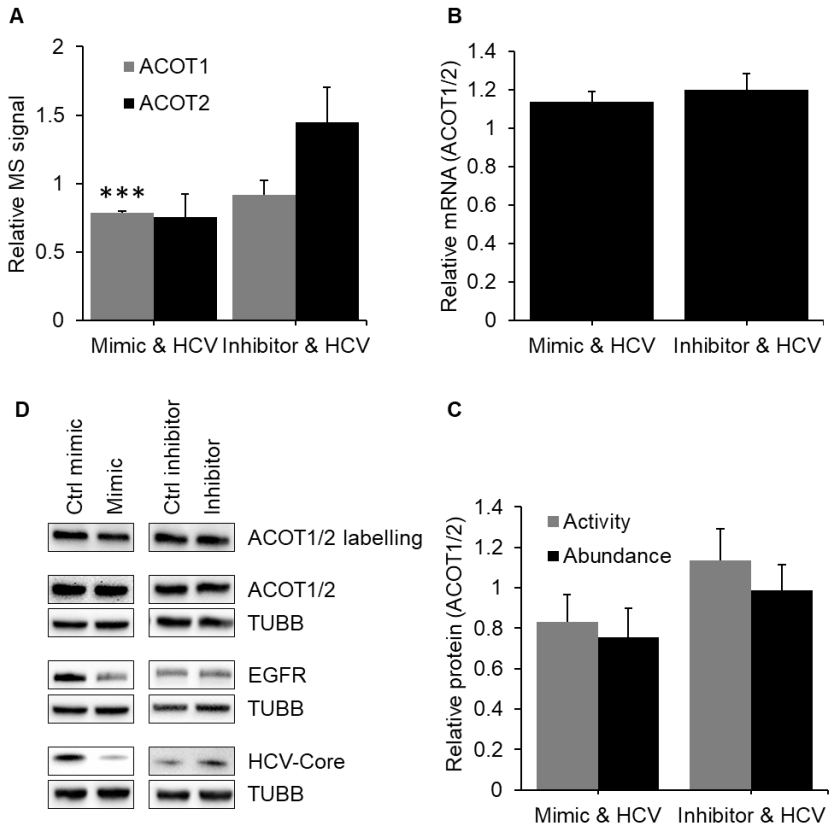

Figure 4.21: Effect of miR-27b on ACOT1/2 in the context of HCV infection. Huh7.5 cells were infected with the JFH1$_T$ strain of HCV and subsequently transfected with miR-27b mimic, inhibitor, or the respective negative control and lysed after 72h. Results represent signal from mimic or inhibitor-transfected samples normalised to their respective controls. A) LC-MS/MS relative quantification of FP-biotin labelled ACOT1 and ACOT2, n=3. B) qRT-PCR quantification of ACOT1/2 mRNA, n=4. C) Western blotting analysis of ACOT1/2 labelling by FP-biotin compared to the total abundance of ACOT1/2 and known direct target EGFR. D) Densitometric analysis of western blotting against ACOT1/2, n=3. Values shown are normalised to the control-transfected sample. Data represents mean values ± s.e.m. *$p \leq 0.05$, **$p \leq 0.01$, ***$p \leq 0.001$

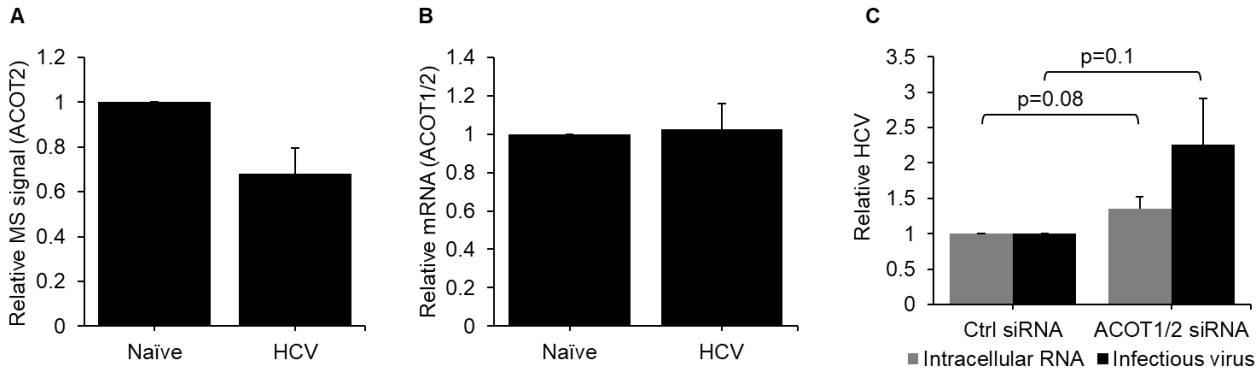

Figure 4.22: Possible HCV-mediated decrease in ACOT1/2 activity may increase HCV virion production. A-B) Huh7.5 cells were infected with the $JFH1_T$ strain of HCV and lysed after 72h. A) LC-MS/MS relative quantification of FP-biotin labelled ACOT1/2, n=3. B) qRT-PCR quantification of ACOT1/2 mRNA, n=4. C) Huh7.5 cells were transfected with siRNA against ACOT1/2 and infected with the $JFH1_T$ strain of HCV. Intracellular RNA was harvested and quantified by qRT-PCR,and growth media from these cells was used to infect cells without siRNA knock-down. Intracellular RNA was harvested and quantified by qRT-PCR. Values shown are normalised to the control-transfected sample. Data represents mean values ± s.e.m. *$p \leq 0.05$, **$p \leq 0.01$, ***$p \leq 0.001$

changes were not statistically significant.

4.5.4 Wnt pathway

One of the well-established targets of HCV-modulation of host cells is the Wnt signalling pathway.[102] Wnt proteins are growth stimulatory factors, responsible for shaping and maintaining tissue, the aberrant functionality of which plays a role in promoting cancer progression, both generally[103] and specifically in the case of HCV-induced hepatocellular carcinoma.[102,104] Previous work has demonstrated that miR-27b targets multiple components of the Wnt signalling pathway,[55,105–107] ultimately decreasing canonical Wnt signalling. PAFAH1B3 has also been shown to possess the ability to decrease Wnt signalling.[108] To investigate the role that miR-27b and PAFAH1B3 may play in modulating Wnt signalling in the context of viral infection of the liver, Huh7.5 cells were transfected with a luciferase reporter for Wnt activity[109] and miR-27b mimic, and treated with the specific PAFAH1B3 inhibitor P11.[110] Contrary to previous work, an increase in Wnt signalling was observed in miR-27b treated cells. (Fig 4.23a) P11 had no visible effect on Wnt signalling. As Huh7.5 cells produce very low levels of canonical Wnt proteins,[111] the experiment was repeated in the Wnt-producing HepG2 cells, with similar results. (Fig 4.23b) Treatment with 2-BP, which blocks the palmitoylation step necessary for Wnt secretion and subsequent signalling,[112] is used as a positive control of signalling inhibition. This confirms that in liver cell lines, miR-27b increases Wnt signalling, though it does not seem to rely on an increase in PAFAH1B3 activity to do so.

4.6 Discussion

The importance of miR-27b to the regulation of hepatic lipid metabolism, both in healthy tissue and in the context of disease, has been previously established;[36,38] however, the mechanisms by which this modulation of the cell's lipid profile is accomplished are not yet well understood. For example, previous work has shown that miR-27b, despite its ability to induce a lipid-rich intracellular environment

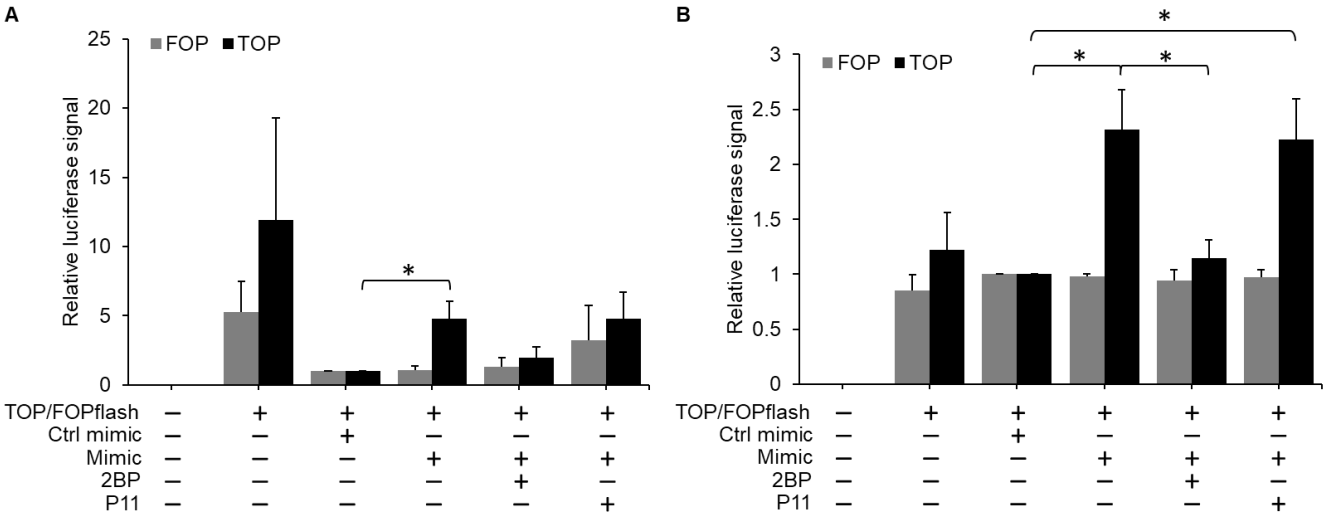

Figure 4.23: miR-27b increases Wnt signalling in a non-PAFAH1B3 dependent manner. A) Huh7.5 and B) HepG2 cells were transfected with the Wnt luciferase reporter system TOP/FOPflash and 100nM mir-27b mimic. After 24h cells were treated with 20µM 2-bromopalmitate and 5µM P11. Cells were lysed 48h after transfection and luciferase signal was measured and normalised by protein abundance. n=3, *p≤0.05

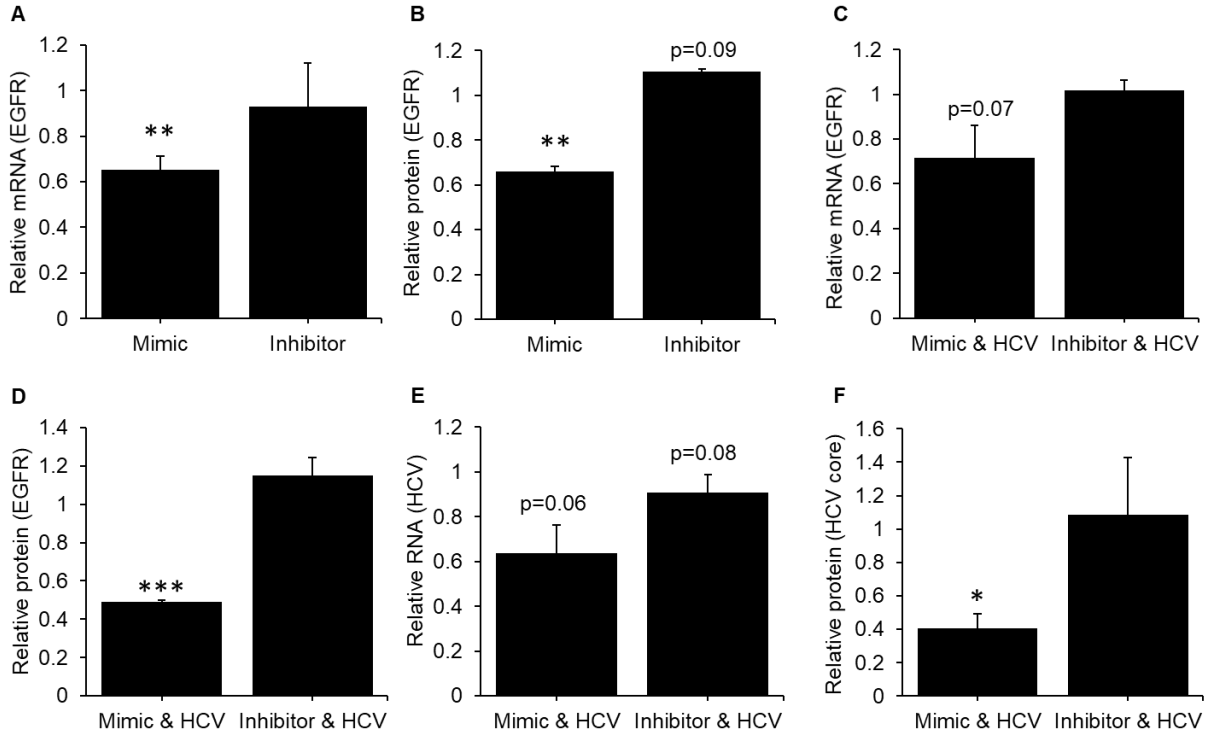

Figure 4.24: miR-27b decreases expression of established targets EGFR and HCV. A-B) Huh7.5 cells were transfected with miR-27b mimic, inhibitor, or negative control and lysed after 72h. A) qRT-PCR quantification of EGFR mRNA, n=4 B) Densitometric analysis of western blotting of EGFR expression, n=3. C-F) Huh7.5 cells were infected with the $JFH1_T$ strain of HCV and subsequently transfected with miR-27b mimic, inhibitor, or negative control and lysed after 72h. C) qRT-PCR quantification of EGFR mRNA, n=4. D) Densitometric analysis of western blotting of EGFR expression, n=3. E) qRT-PCR quantification of HCV RNA, n=4. F) Densitometric analysis of western blotting of HCV core protein expression, n=3. Values shown are normalised to the control-transfected sample. Data represents mean values ± s.e.m. *$p \leq 0.05$, **$p \leq 0.01$, ***$p \leq 0.001$

beneficial to the HCV infection,[20] decreases viral titre in infected cells.[36] This is confirmed in the present study, (Fig 4.24) and is likely due to other, unknown effects of miR-27b activity. While decreases in the miR-27b target EGFR is known to inhibit viral entry,[113] inhibition of viral entry alone is unlikely to fully explain the decrease in viral proteins and RNA observed, as a decrease in EGFR expression would only affect secondary infections from virions newly-produced by the initially-infected cells, and the infections performed were of short duration. It is therefore necessary for prior processes, from protein translation to RNA replication and virion assembly to be implicated in miR-27b's anti-viral activity.

A comprehensive understanding of these mechanisms could enable the development of techniques to counteract or enhance the effects of abnormal miRNA function which are implicated in the pathogenesis of multiple diseases. In this work, functional effectors of miR-27b regulation of lipid metabolism are identified, and the mechanisms by which their activities are controlled are explored.

Previous efforts to profile miR-27b-induced changes to the proteome have relied mainly on sequencing-based techniques such as Ago-HITS-CLIP,[28,114,115] which reports on only direct hydrogen-bonding interactions between miRNAs and mRNAs, and does not allow the detection of any potentially more significant changes occurring down-stream. Other studies have used microarrays to globally profile miR-27b's impact, direct or indirect, on the transcriptome.[116,117] However, this type of screen only reports on a pre-selected panel of genes and is furthermore incapable of reporting on any potential post-translational regulation of protein function. Use of an activity based-probe measures differential enzyme activity derived not only from direct miRNA targeting or altered gene expression, but also from changes to protein localisation, post-translational modifications, and protein-protein interactions, thereby providing a more complete and relevant picture of the functional role of the microRNA.

This is demonstrated by comparing results of Ago-HITS-CLIP screens to those of activity-based profiling. These screens of miRNA interactions in the liver identified only one metabolic serine hydrolase as a potential target of miR-27b, fatty acid synthase (FASN).[28,114,115] However, no change in either activity or abundance was detected, (Fig 4.25) illustrating that the presence of complementarity between miRNAs and mRNAs does not necessarily translate into a functional change. Conversely, activity-based profiling has been able to detect miR-27b-induced differential function in multiple lipid metabolic enzymes which had not been detected by complementarity-based screening.

Regulation of LIPC has not previously been associated with miR-27b. Though the new consensus sequence contained the miR-27b seed site within its 3'-UTR, the failure of miR-27b to target this sequence in the luciferase construct is not surprising. Base pairing outside the seed sequence plays an important role in stabilising the miRNA-mRNA interaction,[1] and the remainder of the sequence outside the seed site displayed very little complementarity.

Figure 4.26 describes the multiple modes of action used simultaneously by miR-27b to decrease LIPC expression, modulating the expression of three separate transcription factors: PPARα, JUN, and HNF4α. Interestingly, HNF4α has been shown to be pro-viral, and the inhibition of its activity decreased HCV replication.[118] The miR-27b-induced decrease in HNF4α expression discovered in this experiment therefore represents a novel potential mechanism by which miR-27b may reduce viral titres.

Fig 4.6d hints that LIPC activity may be simultaneously regulated by an additional, post-translational mechanism, as the large decrease in activity is only partially mirrored by the still statistically significant but smaller decrease in protein abundance. This discrepancy suggests the presence both pre- and post-translational regulation. Synthesis of active LIPC requires the activity of multiple chaperone proteins and folding factors,[119] as well as the addition of a glycosylation at Asn-56;[120] miR-27b induced

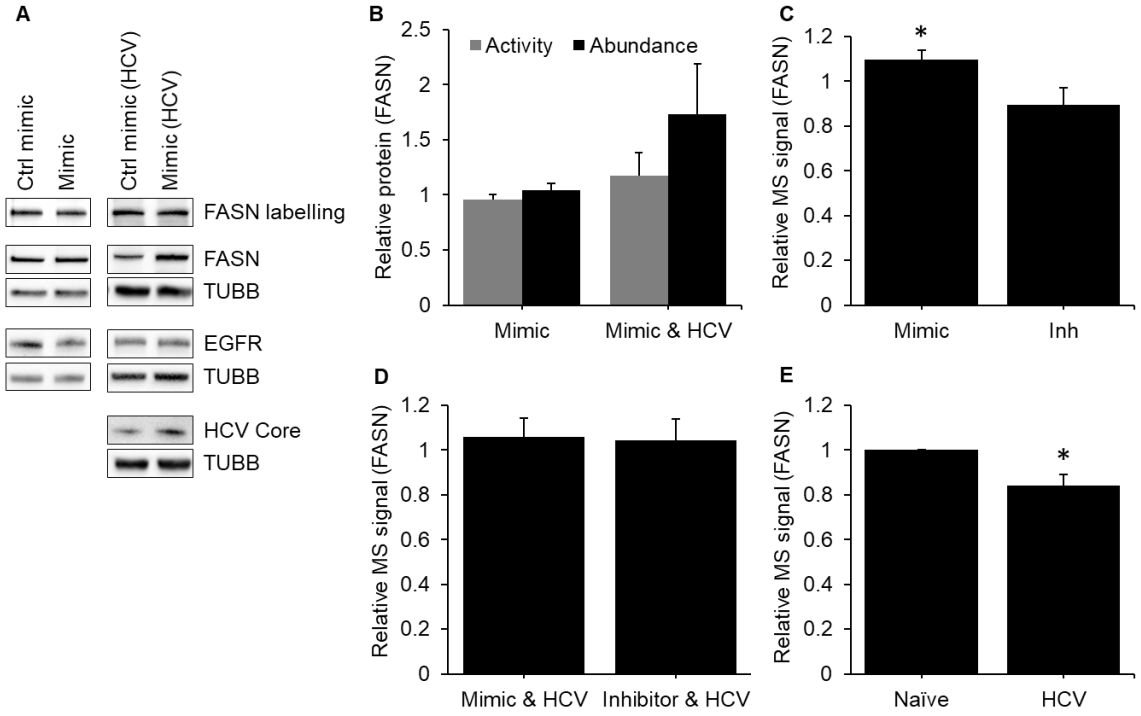

Figure 4.25: miR-27b does not alter expression of predicted target FASN. A-D) Naïve Huh7.5 cells or cells infected with the JFH1$_T$ strain of HCV were transfected with miR-27b mimic, inhibitor, or negative control and lysed after 72h. A) Western blotting analysis of FASN labelling by FP-biotin in miR-27b mimic-transfected samples compared to total abundance of FASN and known targets of miR-27b. B) Densitometric analysis of western blotting against FASN, n=3 C-D) LC-MS/MS relative quantification of FP-biotin labelled FASN, n=3. E) Huh7.5 cells were infected with the JFH1$_T$ strain of HCV and lysed after 72h. LC-MS/MS measured relative quantification of FP-biotin labelled FASN, n=3. Values shown are normalised to the control samples. Data represents mean values ± s.e.m. *p ≤ 0.05

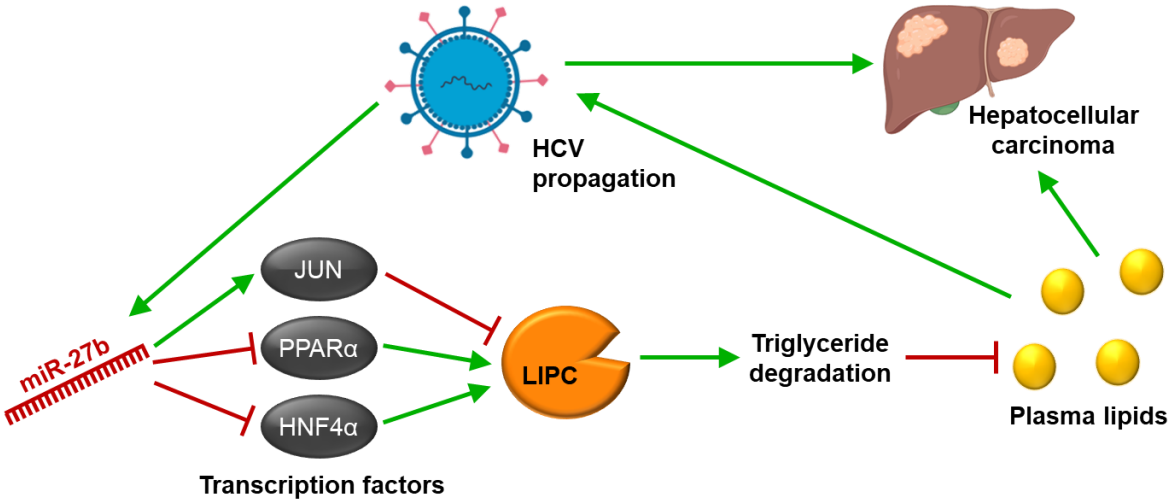

Figure 4.26: Scheme depicting role of mir-27b modulation of LIPC in HCV propagation and the development of HCC.

differential folding and glycosylation represent an opportunity for post-translational regulation of LIPC which could be an interesting basis for further investigation.

The observed decrease in LIPC activity would, in humans, cause a significant decrease in plasma triglycerides in high density lipoproteins (HDL), low-density lipoproteins (LDL), and very low density lipoproteins (VLDL).[66,75] A decrease in plasma triglycerides has been observed in mice treated with miR-27b mimics, which was attributed to a decrease in lipoprotein lipase (LPL) activity.[39] The results presented herein suggest that miR-27b simultaneous decreases LIPC as well as LPL, and that these changes could act in concert to increase circulating triglycerides.

The hepatitis C virion exists as a lipoviral particle, and uses the host cell's VLDL machinery in the formation and secretion of infectious particles.[19] As LIPC plays a significant role in regulating lipoparticles, this enzyme could be expected to likewise influence the lipoviral particle. Figure 4.11c replicates results from previous studies which have shown that infectivity of secreted virions is significantly increased when LIPC abundance is decreased,[121] though intracellular HCV is not affected,[121,122] which suggests that LIPC interferes with an important role in virion secretion. In this work, i*n vitro* HCV infection induced a significant decrease in LIPC activity and abundance, and previous work showed this decrease also occurs in human infection.[87] This decrease in LIPC abundance is more pronounced in HCV-HCC,[87] indicating that absence of LIPC activity could furthermore contribute to the development of liver cancer. The role of LIPC in cancer has not been extensively studied: it has been suggested to have a positive effect on the anti-cancer immune response[123] and has been associated with increased survival in some cancers,[124] though in others it has been associated with decreased survival.[125] Overall, this suggests that the down-regulation of LIPC activity during HCV infection via increased miR-27b performs an pro-viral function, and that this may create an oncogenic environment which contributes to the development of HCV-induced HCC. (Fig 4.24) This is in apparent contradiction to the previously

established anti-viral nature of miR-27b; however, as microRNAs typically modulate a large number of different targets, this pro-viral effect is most likely overshadowed by other anti-viral effects.

miR-27b also appears to induce an oncogenic environment via an upregulation of PAFAH1B3 activity. PAFAH enzymes typically hydrolyse platelet activating factors (PAFs).[126,127] PAFAH1B3 preferentially hydrolyses acetyl over longer-chain PAFs,[126] and is highly expressed compared to other PAFAHs in the model system used in this study[128] as well as in the adult liver.[129–131] As PAFAH1B3 abundance does not increase with activity with miR-27b treatment, catalytic activity must be regulated post-translationally. Modulation of the composition of the PAFAH1B complex represents one potential mechanism: differential activity of PAFAH1B3 has been observed based on the presence of the interacting proteins PAFAH1B1 and PAFAH1B2.[89,90,127] However, while the miR-27b-induced increase in the abundance of the regulatory factor PAFAH1B1 seems to suggest that an increase in complex formation may be the basis for the increase in activity, a 50% decrease in PAFAH1B1 expression did not affect PAFAH1B3 activity. It may be that the baseline level of interaction was already low, and that therefore decreasing expression of PAFAH1B1 does not change the oligomerization status of a sufficient quantity of PAFAH1B3 to generate an observable change in activity. Previous studies of purified recombinant proteins had suggested PAFAH1B1 either does not change PAFAH1B3 activity (when in complex with PAFAH1B2) or decreases it (in the absence of PAFAH1B2), though the changes appear to be primarily based in changes to PAFAH1B3 abundance and not activation state.[90] While it is therefore not possible at the present time to make a definitive conclusion about the role of PAFAH1B1 in the up-regulation of PAFAB1B3 activity by miR-27b, based on its ability to modulate PAFAH1B activity and its miR-27b-induced increase in expression, further investigation seems merited.

The activity of PAFAH1B3 can be said to be regulated by S-palmitoylation with somewhat more confidence. This post-translational modification was previously suggested to be important for

PAFAH1B3 function, though the presence of the modification itself on PAFAH1B3 had not been demonstrated.[92] The demonstrated dependence of PAFAH1B3 activity on a functional palmitoylation system confirms that this enzyme does indeed require the presence of an S-palmitoylation for catalytic activity. It furthermore suggests that modulation of palmitoylation by miR-27b may be responsible for the miR-27b-induced increase in PAFAH1B3 activity. It is not clear whether this is the result of changes to enzymes responsible for palmitoylation, or of an increase in substrate concentration due to miR-27b increase of intracellular lipids.

If PAFAH1B3 activity is increased by miR-27b, its activity should also be up-regulated by HCV, which induces miR-27b expression. In addition, a high-throughput screen of gene expression during HCV infection has indicated that PAFAH1B3 expression is increased by HCV infection.[132] This suggests that PAFAH1B3 activity could be increased during infection not only by a post-translational miR-27b mediated mechanism, but also by an independent upregulation of expression. As PAFAH1B3 expression has an inhibitory effect on HCV replication and, to a lesser, extent, the production of new virions, this could represent a mechanism by which miR-27b inhibits the life cycle of HCV, as shown in this work and in previous studies.[36]

The primary consequence of this heightened activity would likely be a decrease in the concentration of PAFs. PAFs act as messenger lipids,[133] activating inflammation[134] as well as PI3K, MAPK, and NFκB signalling. [135] They have been shown to play a role in viral pathogenesis of dengue and influenza viruses, increasing the virulence of the disease, though with no effect on overall viral titres.[136,137] By increasing PAFAH1B3 activity, the host may be attempting to decrease the detrimental effect of PAF signalling during viral infection. [137] Expression profiling of patients with HCV-associated HCC shows a further increase in expression of PAFAH1B3 compared to non-cancerous infectection,[138] while autoantibodies against PAFAH1B3, found in HCV-associated HCC patients, are thought to play a role in anti-viral and

anti-oncogenic host responses to infection.[139] Altogether, this supports the potential of PAFAH1B3 to contribute to the development of HCC from HCV.

PAFAH1B3 activity has previously been associated with the progression of multiple cancers[88,110,140] and evasion of apoptosis,[141] though the mechanism by which it promotes oncogenesis is unknown. In some cancers, the pro-oncogenic effect seems to occur at least partially through inhibition of PAF signalling,[142] through which it may promote tumour apoptosis by activating NFκB signalling.[133] However, the role of PAF in cancer is thought to be mainly pro- not anti-oncogenic,[133] though it may vary with the type of cancer studied. While it has also been suggested that PAFAHs could affect signalling by increasing levels of their product, lyso-PAF, which also has inflammatory properties,[133] others have speculated that PAFAH1B3 may have other substrates by which it alters cell signalling. PAFAH1B3 activity, either directly or indirectly, has been shown to broadly alter the cell's lipid profile[140] to increase the abundance of multiple anti-tumorigenic lipids.[88] However, these specific alterations to the lipid profile were not mirrored in the profile of miR-27b induced changes to the lipidome, indicating that this antitumor function of PAFAH1B3 activity does not occur in this context.

The most prominent miR-27b induced change to the lipid profile was the significant increase in triglycerides, which has previously been attributed to a decrease in fatty acid oxidation, among other factors.[36] Interestingly, while ACOT1 has been shown to decrease β-oxidation in liver,[143] ACOT2 has been shown to promote β-oxidation.[97] As ACOT2 is by far the higher expressed form within the cell model used,[144] this suggests that the miR-27b-induced decrease in ACOT2 activity plays a role in the inhibition of β-oxidation and the consequent increase in cellular triglycerides. ACOT2 preferentially targets long-chain substrates;[145] this may explain the tendency of longer length lipids to be more highly upregulated which was observed during miR-27b overexpression.

In this study, *in vitro* infection with HCV decreased ACOT1/2 activity, which is in agreement with previous research showing that HCV down-regulates ACOT1: the effect of HCV on ACOT2 has not previously been investigated.[146,147] The decreased β-oxidation which should result from a decrease in ACOT2 activity is characteristic of HCV infection[148] as well as HCV-induced HCC.[138] Decrease in ACOT2 has previously been associated with tumour incidence,[149] though no data exists on the role of ACOT2 in HCC specifically. Altogether, this suggests another pathway by which HCV-mediated increase of miR-27b might induce conditions conducive to the development of HCC.

The mechanisms by which miR-27b regulates ACOT2 activity are not clear. Transcription of ACOT2, like ACOT1, is thought to be regulated by PPARα and HNF4α;[150,151] as abundance of both these transcription factors decrease, this could explain the observed decrease in ACOT1/2 mRNA. However, in this case, ACOT1/2 protein abundance does not change in conjunction with mRNA, implying that a post-transcriptional mechanism of regulation may be responsible for the change in catalytic activity, something which has previously been suggested.[152] Given the lack of change in ACOT1/2 abundance, the decrease in activity must necessarily be due to some unknown method of post-translational regulation. Like PAFAH1B3, ACOT2 is palmitoylated,[100] and inhibition of palmitoylation seems to increase ACOT1/2 activity within a short-term time frame. This suggests that, contrary to the regulation of PAFAH1B3, palmitoylation of ACOT1/2 may possess an inhibitory function. miR-27b, then, appears to alter the activity of two enzymes possessing lipidation-based methods of regulation. It can therefore be hypothesized that miR-27b induces alterations to protein palmitoylation processes as part of a broader strategy to alter enzyme activity post-translationally. Though profiling changes to palmitoylation induced by miR-27b is beyond the scope of this study, characterisation of miRNA-induced changes to post-translational modifications could represent an interesting avenue of investigation into cross-talk between a cell's lipid metabolism and its enzymes' activity.

While this manuscript was in preparation, a study on adipocytes differentiation was published showing that, contrary the what is seen in hepatoma cells, miR-27b increases ACOT2 expression.[46] They furthermore showed that knock-down of ACOT2 decreased cellular triglycerides,[46] though it seems likely that this is not due to the inherent activity of ACOT2 but by inhibiting the differentiation into mature adipocytes. This seeming contradiction in the regulation of ACOT2 by miR-27b highlights the differences in miRNA function between cell types. While direct mRNA-miRNA interactions can differ between cell types due to alternative compartmentalisation, splicing, and protein interactions which alter the presence or availability of target sites,[1] functional targeting by miRNAs, which in addition relies on the presence of specific sets of cell signalling pathways, is bound to create an even greater disparity.

While miR-27b seems to play an onco-protective role in most cancers, [55–59] in the liver, it seems to act as an oncogene, increasing proliferation and decreasing survival[60–63] (though one paper to the contrary has been published),[59] indicating that miRNAs can play substantially different roles in different contexts. For instance, Wnt signalling, a key oncogenic driver,[112] is increased by miR-27b in both Huh7.5 and HepG2 models, whereas work in models derived from other systems, ranging from cancerous cell lines to *in vivo* cancer-free animal models, showed a marked decrease in Wnt signalling.[55,105–107] Wnt signalling plays a significant role in the pathogenesis of HCC,[153–155] and a link has been suggested between its tumorigenic potential and its ability to up-regulate the lipid content of cancerous cells.[156,157] It has previously been demonstrated that HCV induces Wnt via multiple mechanisms;[158] data presented in this paper suggests that modulation of miR-27b may be an additional novel method of Wnt dysregulation. Similarly, Wnt signalling may represent a potential mechanism of miR-27b induced modulation of lipid metabolism. While understanding of the relationship between miR-27b and Wnt signalling is still incomplete, the novel miR-27b targets identified in this study represent potential mediators. Though chemical inhibition of PAFAH1B3 did not affect Wnt signalling, as shown in Fig 23, knock-down of LIPC has been shown to modulate the expression of many genes involved in the Wnt

pathway,[159] and it has been hypothesised that it acts as a Wnt-antagonist analogue.[160] Though the ACOT1/2 enzymes have not been linked to Wnt signalling, their role in the regulation of palmitoylation pools[101] may allow them to affect the secretion of Wnt proteins, a process which relies on the presence of an S-palmitoylation post-translational modification which controls subsequent signalling.[112] Future work may therefore reveal novel links between miR-27b-regulated lipid metabolic genes and Wnt signalling.

The development of direct acting antivirals over the past decade has provided a cure for HCV infection with approximately 80-95% efficacy, depending on the genotype and stage of infection.[161] While these pharmaceuticals, by clearing the infection, prevent any more viral remodelling of host systems, and arrest the progression of fibrosis and cirrhosis, they are not able to reverse damage already done: the risk of HCC development remains high,[161,162] while some studies have even reported an increase in HCC incidence with certain antiviral treatments.[161,163] For this reason, surveying HCV-induced changes to the hepatic environment is essential to forestall the adverse sequalae of long-term infection. Current practice mostly involves assessment of fibrosis and cirrhosis upon viral clearance, which has limited predictive power, and regular imaging to detect tumour emergence.[164] Detection risk-related biomarkers, such as the activity of the enzyme discussed herein, upon virus clearance could allow a more sensitive assessment of the risk of developing HCC. As these LIPC, PAFAH1B3, and ACOT2 are known to play a role in the development of HCC, correction of their dysregulated activity could represent an attractive onco-protective strategy. More generally, this study, in identifying novel miR-27b mediated mechanisms of lipidome regulation, has provided new avenues of investigation which may be of interest in the study of the various pathogenicities with which this miRNA is associated.

Future work may further investigate the importance of alterations to the catalytic activity of these enzymes to the viral life cycle and to the development of HCC *in vivo*. This work was performed in

cancerous cell lines, whose metabolic functions closely resemble those of tumour cells.[165] The metabolism of Huh7.5 cells is therefore distinct from that of healthy hepatocytes, as the cell line has already undergone some of the metabolic reorientations typical of oncogenesis, resulting in a correlation coefficient of 0.6 between human liver and cell line gene expression.[166] In hepatocytes, this includes an increase in lipogenesis and a decrease in β-oxidation, necessary for the production of new cells which occurs during tumour growth.[167] It is of note, however, that the metabolisms of these cell lines recapitulate the early stages of HCC tumorigenesis, and therefore still possess many characteristics of hepatocytes which may be lost in more advanced stages.[165] Nevertheless, it would be worthwhile to investigate how miR-27b and the hepatitis C virus modulate the activity of these enzymes in healthy primary hepatic cells, as well as whether this miR-27b modulation of activity was required or detrimental to the establishment of infection.

Cell culture models allow an in-depth study of cell biology. However, crosstalk between different cell systems within an organism have the potential to significantly alter the host response to infection. For example, though LIPC is synthesised in hepatocytes, it is subsequently secreted and attaches to the surface of liver cells, including non-parenchymal cells, to which it binds at a considerably higher rate.[168] The repercussions of miR-27b's decrease of LIPC activity on overall lipid metabolism as well as HCV infection would therefore likely be exacerbated *in vivo*. For this reason, substantiating the role of miR-27b-regulation of these enzymes in the establishment of chronic infection and subsequent oncogenesis in a live model is of considerable value. In recent years, multiple strategies have been employed to develop various humanised mouse models to study HCV infection have been developed,[169,170] and could be used to investigate the role of miR-27b as well as LIPC, PAFAH1B3, and ACOT1/2 on infection, lipid metabolism, and oncogenesis.

In summary, this study has demonstrated that effectors of miRNA regulation of cellular systems are indirectly regulated via alteration of transcription or post-translational modifications. As this regulation of functional targets seem to be highly dependent on the cellular environment and cannot be predicted based on in silico complementarity-based methods, profiling miRNA-induced changes to enzyme activity is necessary to understand the role miRNAs in health and in diseases.

4.7 References

(1) O'Brien, J. J. Overview of MicroRNA Biogenesis, Mechanisms of Actions, and Circulation. *Frontiers in endocrinology.* Frontiers Research Foundation: [Lausanne] : 2018.

(2) Sun, W.; Julie Li, Y.-S.; Huang, H.-D.; Shyy, J. Y.-J.; Chien, S. MicroRNA: A Master Regulator of Cellular Processes for Bioengineering Systems. *Annu. Rev. Biomed. Eng.* **2010**, *12* (1), 1–27.

(3) Cai, Y.; Yu, X.; Hu, S.; Yu, J. A Brief Review on the Mechanisms of MiRNA Regulation. *Genomics. Proteomics Bioinformatics* **2009**, *7* (4), 147–154.

(4) Hayes, J.; Peruzzi, P. P.; Lawler, S. MicroRNAs in Cancer: Biomarkers, Functions and Therapy. *Trends Mol. Med.* **2014**, *20* (8), 460–469.

(5) Croce, C. M. Causes and Consequences of MicroRNA Dysregulation in Cancer. *Nat. Rev. Genet.* **2009**, *10* (10), 704–714.

(6) Hosseinahli, N.; Aghapour, M.; Duijf, P. H. G.; Baradaran, B. Treating Cancer with MicroRNA Replacement Therapy: A Literature Review. *J. Cell. Physiol.* **2018**, *233* (8), 5574–5588.

(7) O'Connell, R. M.; Rao, D. S.; Baltimore, D. MicroRNA Regulation of Inflammatory Responses. *Annu. Rev. Immunol.* **2012**, *30* (1), 295–312.

(8) Small, E. M.; Olson, E. N. Pervasive Roles of MicroRNAs in Cardiovascular Biology. *Nature* **2011**, *469* (7330), 336–342.

(9) Szabo, G.; Bala, S. MicroRNAs in Liver Disease. *Nat. Rev. Gastroenterol. Hepatol.* **2013**, *10* (9), 542–552.

(10) Liu, N.-K.; Xu, X.-M. MicroRNA in Central Nervous System Trauma and Degenerative Disorders. *Physiol. Genomics* **2011**, *43* (10), 571–580.

(11) Eulalio, A.; Schulte, L. N.; Voge, J. The Mammalian MicroRNA Response to Bacterial Infections. *RNA Biol.* **2012**, *9* (6), 742–750.

(12) Ding, S.-W.; Voinnet, O. Antiviral Immunity Directed by Small RNAs. *Cell* **2007**, *130* (3), 413–426.

(13) Cullen, B. R. Viruses and MicroRNAs: RISCy Interactions with Serious Consequences. *Genes Dev.* **2011**, *25* (18), 1881–1894.

(14) Powdrill, M. H.; Desrochers, G. F.; Singaravelu, R.; Pezacki, J. P. The Role of MicroRNAs in Metabolic Interactions between Viruses and Their Hosts. *Curr. Opin. Virol.* **2016**, *19*, 71–76.

(15) Trobaugh, D. W.; Klimstra, W. B. MicroRNA Regulation of RNA Virus Replication and Pathogenesis. *Trends Mol. Med.* **2017**, *23* (1), 80–93.

(16) Li, S.; Duan, X.; Li, Y.; Liu, B.; McGilvray, I.; Chen, L. MicroRNA-130a Inhibits HCV Replication by Restoring the Innate Immune Response. *J. Viral Hepat.* **2014**, *21* (2), 121–128.

(17) Slonchak, A.; Shannon, R. P.; Pali, G.; Khromykh, A. A. Human MicroRNA MiR-532-5p Exhibits Antiviral Activity against West Nile Virus via Suppression of Host Genes SESTD1 and TAB3 Required for Virus Replication. *J. Virol.* **2016**, *90* (5), 2388 LP – 2402.

(18) Zhu, X.; He, Z.; Hu, Y.; Wen, W.; Lin, C.; Yu, J.; Pan, J.; Li, R.; Deng, H.; Liao, S.; et al. MicroRNA-30e* Suppresses Dengue Virus Replication by Promoting NF-KB–Dependent IFN Production. *PLoS Negl. Trop. Dis.* **2014**, *8* (8), e3088.

(19) Neufeldt, C. J.; Cortese, M.; Acosta, E. G.; Bartenschlager, R. Rewiring Cellular Networks by Members of the Flaviviridae Family. *Nat. Rev. Microbiol.* **2018**, *16* (3), 125–142.

(20) Herker, E.; Ott, M. Unique Ties between Hepatitis C Virus Replication and Intracellular Lipids. *Trends Endocrinol. Metab.* **2011**, *22* (6), 241–248.

(21) Pekow, J. R.; Bhan, A. K.; Zheng, H.; Chung, R. T. Hepatic Steatosis Is Associated with Increased

Frequency of Hepatocellular Carcinoma in Patients with Hepatitis C-Related Cirrhosis. *Cancer* **2007**, *109* (12), 2490–2496.

(22) Bartosch, B. B. Hepatitis C Virus-Induced Hepatocarcinogenesis. *Journal of hepatology*. Elsevier: [London] : 2009, pp 810–820.

(23) Bassendine, M. F.; Sheridan, D. A.; Bridge, S. H.; Felmlee, D. J.; Neely, R. D. G. Lipids and HCV. *Semin. Immunopathol.* **2013**, *35* (1), 87–100.

(24) Singaravelu, R.; Russell, R. S.; Tyrrell, D. L.; Pezacki, J. P. Hepatitis C Virus and MicroRNAs: MiRed in a Host of Possibilities. *Curr. Opin. Virol.* **2014**, *7* (1), 1–10.

(25) Shrivastava, S.; Steele, R.; Ray, R.; Ray, R. B. MicroRNAs: Role in Hepatitis C Virus Pathogenesis. *Genes Dis.* **2015**, *2* (1), 35–45.

(26) Wong, C.-M.; Tsang, F. H.; Ng, I. O. L. Non-Coding RNAs in Hepatocellular Carcinoma: Molecular Functions and Pathological Implications. *Nat. Rev. Gastroenterol. Hepatol.* **2018**, *15* (3), 137–151.

(27) Li, Q.; Lowey, B.; Sodroski, C.; Krishnamurthy, S.; Alao, H.; Cha, H.; Chiu, S.; El-Diwany, R.; Ghany, M. G.; Liang, T. J. Cellular MicroRNA Networks Regulate Host Dependency of Hepatitis C Virus Infection. *Nat. Commun.* **2017**, *8* (1), 1789.

(28) Luna, J. M.; Scheel, T. K. H.; Danino, T.; Shaw, K. S.; Mele, A.; Fak, J. J.; Nishiuchi, E.; Takacs, C. N.; Catanese, M. T.; de Jong, Y. P.; et al. Hepatitis C Virus RNA Functionally Sequesters MiR-122. *Cell* **2015**, *160* (6), 1099–1110.

(29) Singaravelu, R.; O'Hara, S.; Jones, D. M.; Chen, R.; Taylor, N. G.; Srinivasan, P.; Quan, C.; Roy, D. G.; Steenbergen, R. H.; Kumar, A.; et al. MicroRNAs Regulate the Immunometabolic Response to Viral Infection in the Liver. *Nat. Chem. Biol.* **2015**, *11* (12), 988–993.

(30) Jopling, C. L.; Norman, K. L.; Sarnow, P. Positive and Negative Modulation of Viral and Cellular MRNAs by Liver-Specific MicroRNA MiR-122. *Cold Spring Harbor Symposia on Quantitative Biology*. 2006, pp 369–376.

(31) Lizio, M.; Harshbarger, J.; Shimoji, H.; Severin, J.; Kasukawa, T.; Sahin, S.; Abugessaisa, I.; Fukuda, S.; Hori, F.; Ishikawa-Kato, S.; et al. Gateways to the FANTOM5 Promoter Level Mammalian Expression Atlas. *Genome Biol.* **2015**, *16* (1), 22.

(32) Lizio, M.; Abugessaisa, I.; Noguchi, S.; Kondo, A.; Hasegawa, A.; Hon, C. C.; de Hoon, M.; Severin, J.; Oki, S.; Hayashizaki, Y.; et al. Update of the FANTOM Web Resource: Expansion to Provide Additional Transcriptome Atlases. *Nucleic Acids Res.* **2018**, *47* (D1), D752–D758.

(33) de Rie, D.; Abugessaisa, I.; Alam, T.; Arner, E.; Arner, P.; Ashoor, H.; Åström, G.; Babina, M.; Bertin, N.; Burroughs, A. M.; et al. An Integrated Expression Atlas of MiRNAs and Their Promoters in Human and Mouse. *Nat. Biotechnol.* **2017**, *35* (9), 872–878.

(34) Shaw, T. A.; Singaravelu, R.; Powdrill, M. H.; Nhan, J.; Ahmed, N.; Özcelik, D.; Pezacki, J. P. MicroRNA-124 Regulates Fatty Acid and Triglyceride Homeostasis. *iScience* **2018**, *10*, 149–157.

(35) Shirasaki, T.; Honda, M.; Shimakami, T.; Horii, R.; Yamashita, T.; Sakai, Y.; Sakai, A.; Okada, H.; Watanabe, R.; Murakami, S.; et al. MicroRNA-27a Regulates Lipid Metabolism and Inhibits Hepatitis C Virus Replication in Human Hepatoma Cells. *J. Virol.* **2013**, *87* (9), 5270–5286.

(36) Singaravelu, R.; Chen, R.; Lyn, R. K.; Jones, D. M.; O'Hara, S.; Rouleau, Y.; Cheng, J.; Srinivasan, P.; Nasheri, N.; Russell, R. S.; et al. Hepatitis C Virus Induced Up-Regulation of MicroRNA-27: A Novel Mechanism for Hepatic Steatosis. *Hepatology* **2014**, *59* (1), 98–108.

(37) Kida, K.; Nakajima, M.; Mohri, T.; Oda, Y.; Takagi, S.; Fukami, T.; Yokoi, T. PPARα Is Regulated by MiR-21 and MiR-27b in Human Liver. *Pharm. Res.* **2011**, *28* (10), 2467–2476.

(38) Vickers, K. C.; Shoucri, B. M.; Levin, M. G.; Wu, H.; Pearson, D. S.; Osei-Hwedieh, D.; Collins, F. S.; Remaley, A. T.; Sethupathy, P. MicroRNA-27b Is a Regulatory Hub in Lipid Metabolism and Is Altered in Dyslipidemia. *Hepatology* **2013**, *57* (2), 533–542.

(39) Xie, W.; Li, L.; Zhang, M.; Cheng, H.-P.; Gong, D.; Lv, Y.-C.; Yao, F.; He, P.-P.; Ouyang, X.-P.; Lan, G.; et al. MicroRNA-27 Prevents Atherosclerosis by Suppressing Lipoprotein Lipase-Induced Lipid Accumulation and Inflammatory Response in Apolipoprotein E Knockout Mice.

PLoS One **2016**, *11* (6).

(40) Castaño, C.; Kalko, S.; Novials, A.; Párrizas, M. Obesity-Associated Exosomal MiRNAs Modulate Glucose and Lipid Metabolism in Mice. *Proc. Natl. Acad. Sci. U. S. A.* **2018**, *115* (48), 12158–12163.

(41) Chen, S.-Z.; Xu, X.; Ning, L.-F.; Jiang, W.-Y.; Xing, C.; Tang, Q.-Q.; Huang, H.-Y. MiR-27 Impairs the Adipogenic Lineage Commitment via Targeting Lysyl Oxidase. *Obesity* **2015**, *23* (12), 2445–2453.

(42) Marques, A. P.; Rosmaninho-Salgado, J.; Estrada, M.; Cortez, V.; Nobre, R. J.; Cavadas, C. Hypoxia Mimetic Induces Lipid Accumulation through Mitochondrial Dysfunction and Stimulates Autophagy in Murine Preadipocyte Cell Line. *Biochim. Biophys. Acta - Gen. Subj.* **2017**, *1861* (3), 673–682.

(43) Hu, X.; Tang, J.; Hu, X.; Bao, P.; Pan, J.; Chen, Z.; Xian, J. MiR-27b Impairs Adipocyte Differentiation of Human Adipose Tissue-Derived Mesenchymal Stem Cells by Targeting LPL. *Cell. Physiol. Biochem.* **2018**, *47* (2), 545–555.

(44) Yu, J.; Lv, Y.; Di, W.; Liu, J.; Kong, X.; Sheng, Y.; Huang, M.; Lv, S.; Qi, H.; Gao, M.; et al. MiR-27b-3p Regulation in Browning of Human Visceral Adipose Related to Central Obesity. *Obesity* **2018**, *26* (2), 387–396.

(45) Zhang, M.; Li, F.; Sun, J.-W.; Li, D.-H.; Li, W.-T.; Jiang, R.-R.; Li, Z.-J.; Liu, X.-J.; Han, R.-L.; Li, G.-X.; et al. LncRNA IMFNCR Promotes Intramuscular Adipocyte Differentiation by Sponging MiR-128-3p and MiR-27b-3p. *Front. Genet.* **2019**, *10* (FEB).

(46) Murata, Y.; Yamashiro, T.; Kessoku, T.; Jahan, I.; Usuda, H.; Tanaka, T.; Okamoto, T.; Nakajima, A.; Wada, K. Up-Regulated MicroRNA-27b Promotes Adipocyte Differentiation via Induction of Acyl-CoA Thioesterase 2 Expression. *Biomed Res. Int.* **2019**, *2019*.

(47) Liu, W.; Ma, C.; Yang, B.; Yin, C.; Zhang, B.; Xiao, Y. LncRNA Gm15290 Sponges MiR-27b to Promote PPARγ-Induced Fat Deposition and Contribute to Body Weight Gain in Mice. *Biochem.*

Biophys. Res. Commun. **2017**, *493* (3), 1168–1175.

(48) Zhang, M.; Wu, J.-F.; Chen, W.-J.; Tang, S.-L.; Mo, Z.-C.; Tang, Y.-Y.; Li, Y.; Wang, J.-L.; Liu, X.-Y.; Peng, J.; et al. MicroRNA-27a/b Regulates Cellular Cholesterol Efflux, Influx and Esterification/Hydrolysis in THP-1 Macrophages. *Atherosclerosis* **2014**, *234* (1), 54–64.

(49) Goedeke, L.; Rotllan, N.; Ramírez, C. M.; Aranda, J. F.; Canfrán-Duque, A.; Araldi, E.; Fernández-Hernando, A.; Langhi, C.; de Cabo, R.; Baldán, Á.; et al. MiR-27b Inhibits LDLR and ABCA1 Expression but Does Not Influence Plasma and Hepatic Lipid Levels in Mice. *Atherosclerosis* **2015**, *243* (2), 499–509.

(50) Ouimet, M.; Hennessy, E. J.; Van Solingen, C.; Koelwyn, G. J.; Hussein, M. A.; Ramkhelawon, B.; Rayner, K. J.; Temel, R. E.; Perisic, L.; Hedin, U.; et al. MiRNA Targeting of Oxysterol-Binding Protein-like 6 Regulates Cholesterol Trafficking and Efflux. *Arterioscler. Thromb. Vasc. Biol.* **2016**, *36* (5), 942–951.

(51) O'Neill, L. A. J. L. A. J. A Guide to Immunometabolism for Immunologists. *Nature reviews.* Nature Pub Group: England : 2016, pp 553–565.

(52) González-Aldaco, K.; Torres-Reyes, L. A.; Ojeda-Granados, C.; José-Ábrego, A.; Fierro, N. A.; Román, S. Immunometabolic Effect of Cholesterol in Hepatitis C Infection: Implications in Clinical Management and Antiviral Therapy. *Ann. Hepatol.* **2018**, *17* (6), 908–919.

(53) Robertson, K. A.; Ghazal, P. Interferon Control of the Sterol Metabolic Network: Bidirectional Molecular Circuitry-Mediating Host Protection . *Frontiers in Immunology* . 2016, p 634.

(54) Chen, W.-J.; Yin, K.; Zhao, G.-J.; Fu, Y.-C.; Tang, C.-K. The Magic and Mystery of MicroRNA-27 in Atherosclerosis. *Atherosclerosis* **2012**, *222* (2), 314–323.

(55) Liu, B.; Chen, W.; Cao, G.; Dong, Z.; Xu, J.; Luo, T.; Zhang, S. MicroRNA-27b Inhibits Cell Proliferation in Oral Squamous Cell Carcinoma by Targeting FZD7 and Wnt Signaling Pathway. *Arch. Oral Biol.* **2017**, *83*, 92–96.

(56) Chen, X.; Cui, Y.; Xie, X.; Xing, Y.; Yuan, Z.; Wei, Y. Functional Role of MiR-27b in the

Development of Gastric Cancer. *Mol. Med. Rep.* **2018**, *17* (4), 5081–5087.

(57) Chen, D.; Si, W.; Shen, J.; Du, C.; Lou, W.; Bao, C.; Zheng, H.; Pan, J.; Zhong, G.; Xu, L.; et al. MiR-27b-3p Inhibits Proliferation and Potentially Reverses Multi-Chemoresistance by Targeting CBLB/GRB2 in Breast Cancer Cells. *Cell Death Dis.* **2018**, *9* (2).

(58) Luo, Y.; Yu, S.-Y.; Chen, J.-J.; Qin, J.; Qiu, Y.-E.; Zhong, M.; Chen, M. MiR-27b Directly Targets Rab3D to Inhibit the Malignant Phenotype in Colorectal Cancer. *Oncotarget* **2018**, *9* (3), 3830–3841.

(59) Liang, H.; Ai-Jun, J.; Ji-Zong, Z.; Jian-Bo, H.; Liang, Z.; Yong-Xiang, Y.; Chen, Y. Clinicopathological Significance of MiR-27b Targeting Golgi Protein 73 in Patients with Hepatocellular Carcinoma. *Anticancer. Drugs* **2019**, *30* (2), 186–194.

(60) Zhu, H.-T.; Liu, R.-B.; Liang, Y.-Y.; Hasan, A. M. E.; Wang, H.-Y.; Shao, Q.; Zhang, Z.-C.; Wang, J.; He, C.-Y.; Wang, F.; et al. Serum MicroRNA Profiles as Diagnostic Biomarkers for HBV-Positive Hepatocellular Carcinoma. *Liver Int.* **2017**, *37* (6), 888–896.

(61) Sun, X.-F.; Sun, J.-P.; Hou, H.-T.; Li, K.; Liu, X.; Ge, Q.-X. MicroRNA-27b Exerts an Oncogenic Function by Targeting Fbxw7 in Human Hepatocellular Carcinoma. *Tumor Biol.* **2016**, *37* (11), 15325–15332.

(62) He, S.; Zhang, J.; Lin, J.; Zhang, C.; Sun, S. Expression and Function of MicroRNA-27b in Hepatocellular Carcinoma. *Mol. Med. Rep.* **2016**, *13* (3), 2801–2808.

(63) Zhuo, L.; Liu, J.; Wang, B.; Gao, M.; Huang, A. Differential MiRNA Expression Profiles in Hepatocellular Carcinoma Cells and Drug-Resistant Sublines. *Oncol. Rep.* **2013**, *29* (2), 555–562.

(64) Barglow, K. T.; Cravatt, B. F. Activity-Based Protein Profiling for the Functional Annotation of Enzymes. *Nat. Methods* **2007**, *4* (10), 822–827.

(65) Cravatt, B. F.; Wright, A. T.; Kozarich, J. W. Activity-Based Protein Profiling: From Enzyme Chemistry to Proteomic Chemistry. *Annu. Rev. Biochem.* **2008**, *77* (1), 383–414.

(66) Long, J. Z.; Cravatt, B. F. The Metabolic Serine Hydrolases and Their Functions in Mammalian

Physiology and Disease. *Chem. Rev.* **2011**, *111* (10), 6022–6063.

(67) Liu, Y.; Patricelli, M. P.; Cravatt, B. F. Activity-Based Protein Profiling: The Serine Hydrolases. *Proc. Natl. Acad. Sci. U. S. A.* **1999**, *96* (26), 14694–14699.

(68) Hunerdosse, D.; Nomura, D. K. Activity-Based Proteomic and Metabolomic Approaches for Understanding Metabolism. *Curr. Opin. Biotechnol.* **2014**, *28*, 116–126.

(69) Strmiskova, M.; Desrochers, G. F.; Shaw, T. A.; Powdrill, M. H.; Lafreniere, M. A.; Pezacki, J. P. Chemical Methods for Probing Virus–Host Proteomic Interactions. *ACS Infect. Dis.* **2016**, *2* (11), 773–786.

(70) Desrochers, G. F.; Pezacki, J. P. ABPP and Host–Virus Interactions. *Current Topics in Microbiology and Immunology*. 2019, pp 131–154.

(71) Sharifzadeh, S.; Shirley, J. D.; Carlson, E. E. Activity-Based Protein Profiling Methods to Study Bacteria: The Power of Small-Molecule Electrophiles BT - Activity-Based Protein Profiling; Cravatt, B. F., Hsu, K.-L., Weerapana, E., Eds.; Springer International Publishing: Cham, 2019; pp 23–48.

(72) Dyer, B. W.; Ferrer, F. A.; Klinedinst, D. K.; Rodriguez, R. A Noncommercial Dual Luciferase Enzyme Assay System for Reporter Gene Analysis. *Anal. Biochem.* **2000**, *282* (1), 158–161.

(73) Kuusi, T.; Nikklä, E. A.; Virtanen, I.; Kinnunen, P. K. J. Localization of the Heparin-Releasable Lipase in Situ in the Rat Liver. *Biochem. J.* **1979**, *181* (1), 245–246.

(74) Connelly, P. W. The Role of Hepatic Lipase in Lipoprotein Metabolism. *Clin. Chim. Acta* **1999**, *286* (1), 243–255.

(75) Brunham, L. R.; Hayden, M. R. Human Genetics of HDL: Insight into Particle Metabolism and Function. *Prog. Lipid Res.* **2015**, *58*, 14–25.

(76) Rakhshandehroo, M.; Knoch, B.; Müller, M.; Kersten, S. Peroxisome Proliferator-Activated Receptor Alpha Target Genes. *PPAR Res.* **2010**, *2010*, 612089.

(77) Rufibach, L. E.; Duncan, S. A.; Battle, M.; Deeb, S. S. Transcriptional Regulation of the Human

Hepatic Lipase (LIPC) Gene Promoter. *J. Lipid Res.* **2006**, *47* (7), 1463–1477.

(78) Lee, G.; Elwood, F.; McNally, J.; Weiszmann, J.; Lindstrom, M.; Amaral, K.; Nakamura, M.; Miao, S.; Cao, P.; Learned, R. M.; et al. T0070907, a Selective Ligand for Peroxisome Proliferator-Activated Receptor γ, Functions as an Antagonist of Biochemical and Cellular Activities. *J. Biol. Chem.* **2002**, *277* (22), 19649–19657.

(79) Berger, J.; Moller, D. E. The Mechanisms of Action of PPARs. *Annu. Rev. Med.* **2002**, *53* (1), 409–435.

(80) Tenenbaum, A.; Motro, M.; Fisman, E. Z. Dual and Pan-Peroxisome Proliferator-Activated Receptors (PPAR) Co-Agonism: The Bezafibrate Lessons. *Cardiovasc. Diabetol.* **2005**, *4* (1), 14.

(81) Tenenbaum, A.; Fisman, E. Z. Balanced Pan-PPAR Activator Bezafibrate in Combination with Statin: Comprehensive Lipids Control and Diabetes Prevention? *Cardiovasc. Diabetol.* **2012**, *11* (1), 140.

(82) van Deursen, D.; Botma, G.-J.; Jansen, H.; Verhoeven, A. J. M. Down-Regulation of Hepatic Lipase Expression by Elevation of CAMP in Human Hepatoma but Not Adrenocortical Cells. *Mol. Cell. Endocrinol.* **2008**, *294* (1), 37–44.

(83) Oka, K.; Ishimura-Oka, K.; Chu, M.; Chan, L. Transcription of the Human Hepatic Lipase Gene Is Modulated by Multiple Negative Elements in HepG2 Cells. *Gene* **1996**, *180* (1), 69–80.

(84) Sirvent, A.; Verhoeven, A. J. M.; Jansen, H.; Kosykh, V.; Darteil, R. J.; Hum, D. W.; Fruchart, J.-C.; Staels, B. Farnesoid X Receptor Represses Hepatic Lipase Gene Expression. *J. Lipid Res.* **2004**, *45* (11), 2110–2115.

(85) Drewes, T.; Senkel, S.; Holewa, B.; Ryffel, G. U. Human Hepatocyte Nuclear Factor 4 Isoforms Are Encoded by Distinct and Differentially Expressed Genes. *Mol. Cell. Biol.* **1996**, *16* (3), 925 LP – 931.

(86) Mirzaei, H.; Khodadad, N.; Karami, C.; Pirmoradi, R.; Khanizadeh, S. The AP-1 Pathway; A Key Regulator of Cellular Transformation Modulated by Oncogenic Viruses. *Rev. Med. Virol.* **2020**,

30 (1), e2088.

(87) Wu, J.-M.; Skill, N. J.; Maluccio, M. A. Evidence of Aberrant Lipid Metabolism in Hepatitis C and Hepatocellular Carcinoma. *HPB* **2010**, *12* (9), 625–636.

(88) Mulvihill, M. M.; Benjamin, D. I.; Ji, X.; Le Scolan, E.; Louie, S. M.; Shieh, A.; Green, M.; Narasimhalu, T.; Morris, P. J.; Luo, K.; et al. Metabolic Profiling Reveals PAFAH1B3 as a Critical Driver of Breast Cancer Pathogenicity. *Chem. Biol.* **2014**, *21* (7), 831–840.

(89) Hattori, M.; Arai, H. Chapter Two - Intracellular PAF-Acetylhydrolase Type I. In *Platelet-Activating Factor Acetylhydrolases (PAF-AH)*; Inoue, K., Stafforini, D. M., Tamanoi, F. B. T.-T. E., Eds.; Academic Press, 2015; Vol. 38, pp 23–36.

(90) Manya, H.; Aoki, J.; Kato, H.; Ishii, J.; Hino, S.; Arai, H.; Inoue, K. Biochemical Characterization of Various Catalytic Complexes of the Brain Platelet-Activating Factor Acetylhydrolase. *J. Biol. Chem.* **1999**, *274* (45), 31827–31832.

(91) Hattori, M.; Adachi, H.; Tsujimoto, M.; Arai, H.; Inoue, K. Miller-Dieker Lissencephaly Gene Encodes a Subunit of Brain Platelet-Activating Factor. *Nature* **1994**, *370* (6486), 216–218.

(92) Wei, X.; Song, H.; Semenkovich, C. F. Insulin-Regulated Protein Palmitoylation Impacts Endothelial Cell Function. *Arterioscler. Thromb. Vasc. Biol.* **2014**, *34* (2), 346–354.

(93) Davda, D.; El Azzouny, M. A.; Tom, C. T. M. B.; Hernandez, J. L.; Majmudar, J. D.; Kennedy, R. T.; Martin, B. R. Profiling Targets of the Irreversible Palmitoylation Inhibitor 2-Bromopalmitate. *ACS Chem. Biol.* **2013**, *8* (9), 1912–1917.

(94) Brocker, C.; Carpenter, C.; Nebert, D. W.; Vasiliou, V. Evolutionary Divergence and Functions of the Human Acyl-CoA Thioesterase Gene (ACOT) Family. *Hum. Genomics* **2010**, *4* (6), 411.

(95) Tillander, V.; Alexson, S. E. H.; Cohen, D. E. Deactivating Fatty Acids: Acyl-CoA Thioesterase-Mediated Control of Lipid Metabolism. *Trends Endocrinol. Metab.* **2017**, *28* (7), 473–484.

(96) Svensson, L. T.; Engberg, T. S.; Aoyama, T.; Usuda, N.; Alexson, E. H. S.; Hashimoto, T. Molecular Cloning and Characterization of a Mitochondrial Peroxisome Proliferator-Induced

Acyl-CoA Thioesterase from Rat Liver. *Biochem. J.* **1998**, *329* (3), 601–608.

(97) Moffat, C.; Bhatia, L.; Nguyen, T.; Lynch, P.; Wang, M.; Wang, D.; Ilkayeva, O. R.; Han, X.; Hirschey, M. D.; Claypool, S. M.; et al. Acyl-CoA Thioesterase-2 Facilitates Mitochondrial Fatty Acid Oxidation in the Liver. *J. Lipid Res.* **2014**, *55* (12), 2458–2470.

(98) Kirkby, B.; Roman, N.; Kobe, B.; Kellie, S.; Forwood, J. K. Functional and Structural Properties of Mammalian Acyl-Coenzyme A Thioesterases. *Prog. Lipid Res.* **2010**, *49* (4), 366–377.

(99) Hunt, M. C.; Alexson, S. E. H. The Role Acyl-CoA Thioesterases Play in Mediating Intracellular Lipid Metabolism. *Prog. Lipid Res.* **2002**, *41* (2), 99–130.

(100) Peng, T.; Hang, H. C. Bifunctional Fatty Acid Chemical Reporter for Analyzing S-Palmitoylated Membrane Protein–Protein Interactions in Mammalian Cells. *J. Am. Chem. Soc.* **2015**, *137* (2), 556–559.

(101) Kathayat, R. S.; Cao, Y.; Elvira, P. D.; Sandoz, P. A.; Zaballa, M.-E.; Springer, M. Z.; Drake, L. E.; Macleod, K. F.; van der Goot, F. G.; Dickinson, B. C. Active and Dynamic Mitochondrial S-Depalmitoylation Revealed by Targeted Fluorescent Probes. *Nat. Commun.* **2018**, *9* (1), 334.

(102) Wang, W. W. Action and Function of Wnt/β-Catenin Signaling in the Progression from Chronic Hepatitis C to Hepatocellular Carcinoma. *Journal of gastroenterology.* Springer International: Tokyo : 2017, pp 419–431.

(103) Nusse, R.; Clevers, H. Wnt/β-Catenin Signaling, Disease, and Emerging Therapeutic Modalities. *Cell* **2017**, *169* (6), 985–999.

(104) Virzì, A.; Roca Suarez, A. A.; Baumert, T. F.; Lupberger, J. Rewiring Host Signaling: Hepatitis C Virus in Liver Pathogenesis. *Cold Spring Harb. Perspect. Med.* **2020**, *10* (1).

(105) Wu, D.; Talbot, C. C.; Liu, Q.; Jing, Z.-C.; Damico, R. L.; Tuder, R.; Barnes, K. C.; Hassoun, P. M.; Gao, L. Identifying MicroRNAs Targeting Wnt/β-Catenin Pathway in End-Stage Idiopathic Pulmonary Arterial Hypertension. *J. Mol. Med.* **2016**, *94* (8), 875–885.

(106) Geng, Y.; Lu, X.; Wu, X.; Xue, L.; Wang, X.; Xu, J. MicroRNA-27b Suppresses Helicobacter

Pylori-Induced Gastric Tumorigenesis through Negatively Regulating Frizzled7. *Oncol. Rep.* **2016**, *35* (4), 2441–2450.

(107) Lv, X.; Li, J.; Hu, Y.; Wang, S.; Yang, C.; Li, C.; Zhong, G. Overexpression of MiR-27b-3p Targeting Wnt3a Regulates the Signaling Pathway of Wnt/*β*-Catenin and Attenuates Atrial Fibrosis in Rats with Atrial Fibrillation. *Oxid. Med. Cell. Longev.* **2019**, *2019*, 5703764.

(108) Livnat, I.; Finkelshtein, D.; Ghosh, I.; Arai, H.; Reiner, O. PAF-AH Catalytic Subunits Modulate the Wnt Pathway in Developing GABAergic Neurons. *Front. Cell. Neurosci.* **2010**, *4*, 19.

(109) Veeman, M. T.; Slusarski, D. C.; Kaykas, A.; Louie, S. H.; Moon, R. T. Zebrafish Prickle, a Modulator of Noncanonical Wnt/Fz Signaling, Regulates Gastrulation Movements. *Curr. Biol.* **2003**, *13* (8), 680–685.

(110) Chang, J. W.; Zuhl, A. M.; Speers, A. E.; Niessen, S.; Brown, S. J.; Mulvihill, M. M.; Fan, Y. C.; Spicer, T. P.; Southern, M.; Scampavia, L.; et al. Selective Inhibitor of Platelet-Activating Factor Acetylhydrolases 1b2 and 1b3 That Impairs Cancer Cell Survival. *ACS Chem. Biol.* **2015**, *10* (4), 925–932.

(111) Carotenuto, P.; Fassan, M.; Pandolfo, R.; Lampis, A.; Vicentini, C.; Cascione, L.; Paulus-Hock, V.; Boulter, L.; Guest, R.; Quagliata, L.; et al. Wnt Signalling Modulates Transcribed-Ultraconserved Regions in Hepatobiliary Cancers. *Gut* **2017**, *66* (7), 1268 LP – 1277.

(112) Gao, X.; Hannoush, R. N. Visualizing Wnt Palmitoylation in Single Cells. In *Wnt Signaling: Methods and Protocols*; Barrett, Q., Lum, L., Eds.; Springer New York: New York, NY, 2016; pp 1–9.

(113) Lupberger, J.; Zeisel, M. B.; Xiao, F.; Thumann, C.; Fofana, I.; Zona, L.; Davis, C.; Mee, C. J.; Turek, M.; Gorke, S.; et al. EGFR and EphA2 Are Host Factors for Hepatitis C Virus Entry and Possible Targets for Antiviral Therapy. *Nat. Med.* **2011**, *17* (5), 589–595.

(114) Helwak, A.; Kudla, G.; Dudnakova, T.; Tollervey, D. Mapping the Human MiRNA Interactome by CLASH Reveals Frequent Noncanonical Binding. *Cell* **2013**, *153* (3), 654–665.

(115) Moore, M. J.; Scheel, T. K. H.; Luna, J. M.; Park, C. Y.; Fak, J. J.; Nishiuchi, E.; Rice, C. M.; Darnell, R. B. MiRNA–Target Chimeras Reveal MiRNA 3′-End Pairing as a Major Determinant of Argonaute Target Specificity. *Nat. Commun.* **2015**, *6* (1), 8864.

(116) Rogler, C. E.; LeVoci, L.; Ader, T.; Massimi, A.; Tchaikovskaya, T.; Norel, R.; Rogler, L. E. MicroRNA-23b Cluster MicroRNAs Regulate Transforming Growth Factor-Beta/Bone Morphogenetic Protein Signaling and Liver Stem Cell Differentiation by Targeting Smads. *Hepatology* **2009**, *50* (2), 575–584.

(117) Poon, V. Y.; Gu, M.; Ji, F.; VanDongen, A. M.; Fivaz, M. MiR-27b Shapes the Presynaptic Transcriptome and Influences Neurotransmission by Silencing the Polycomb Group Protein Bmi1. *BMC Genomics* **2016**, *17* (1), 777.

(118) Levy, G.; Habib, N.; Guzzardi, M. A.; Kitsberg, D.; Bomze, D.; Ezra, E.; Uygun, B. E.; Uygun, K.; Trippler, M.; Schlaak, J. F.; et al. Nuclear Receptors Control Pro-Viral and Antiviral Metabolic Responses to Hepatitis C Virus Infection. *Nat. Chem. Biol.* **2016**, *12* (12), 1037–1045.

(119) Doolittle, M. H.; Ben-Zeev, O.; Bassilian, S.; Whitelegge, J. P.; Péterfy, M.; Wong, H. Hepatic Lipase Maturation: A Partial Proteome of Interacting Factors. *J. Lipid Res.* **2009**, *50* (6), 1173–1184.

(120) Wolle, J.; Jansen, H.; Smith, L. C.; Chan, L. Functional Role of N-Linked Glycosylation in Human Hepatic Lipase: Asparagine-56 Is Important for Both Enzyme Activity and Secretion. *J. Lipid Res.* **1993**, *34* (12), 2169–2176.

(121) Shimizu, Y.; Hishiki, T.; Sugiyama, K.; Ogawa, K.; Funami, K.; Kato, A.; Ohsaki, Y.; Fujimoto, T.; Takaku, H.; Shimotohno, K. Lipoprotein Lipase and Hepatic Triglyceride Lipase Reduce the Infectivity of Hepatitis C Virus (HCV) through Their Catalytic Activities on HCV-Associated Lipoproteins. *Virology* **2010**, *407* (1), 152–159.

(122) Shinohara, Y.; Imajo, K.; Yoneda, M.; Tomeno, W.; Ogawa, Y.; Fujita, K.; Kirikoshi, H.; Takahashi, J.; Funakoshi, K.; Ikeda, M.; et al. Hepatic Triglyceride Lipase Plays an Essential Role

in Changing the Lipid Metabolism in Genotype 1b Hepatitis C Virus Replicon Cells and Hepatitis C Patients. *Hepatol. Res.* **2013**, *43* (11), 1190–1198.

(123) Stoll, G. G. Metabolic Enzymes Expressed by Cancer Cells Impact the Immune Infiltrate. *Oncoimmunology.* Taylor & Francis,: [Abingdon] : 2019.

(124) Curtis, C.; Shah, S. P.; Chin, S.-F.; Turashvili, G.; Rueda, O. M.; Dunning, M. J.; Speed, D.; Lynch, A. G.; Samarajiwa, S.; Yuan, Y.; et al. The Genomic and Transcriptomic Architecture of 2,000 Breast Tumours Reveals Novel Subgroups. *Nature* **2012**, *486* (7403), 346–352.

(125) Huang, J.-Y.; Zhang, W.-L.; Xing, Y.-N.; Hou, W.-B.; Yin, S.-C.; Wang, Z.-N.; Tan, Y.-E.; Xu, Y.-Y.; Zhu, Z.; Xu, H.-M. Increased Expression of LIPC Is Associated with Aggressive Phenotype of Borrmann Type 4 Gastric Cancer. *J. Gastrointest. Surg.* **2020**.

(126) Hattori, K.; Hattori, M.; Adachi, H.; Tsujimoto, M.; Arai, H.; Inoue, K. Purification and Characterization of Platelet-Activating Factor Acetylhydrolase II from Bovine Liver Cytosol. *J. Biol. Chem.* **1995**, *270* (38), 22308–22313.

(127) Kono, N.; Arai, H. Platelet-Activating Factor Acetylhydrolases: An Overview and Update. *Biochim. Biophys. Acta - Mol. Cell Biol. Lipids* **2019**, *1864* (6), 922–931.

(128) Barretina, J.; Caponigro, G.; Stransky, N.; Venkatesan, K.; Margolin, A. A.; Kim, S.; Wilson, C. J.; Lehár, J.; Kryukov, G. V; Sonkin, D.; et al. The Cancer Cell Line Encyclopedia Enables Predictive Modelling of Anticancer Drug Sensitivity. *Nature*. The Broad Institute of Harvard and MIT, Cambridge, Massachusetts 02142, USA. 2012, pp 603–607.

(129) Wang, D.; Eraslan, B.; Wieland, T.; Hallström, B.; Hopf, T.; Zolg, D. P.; Zecha, J.; Asplund, A.; Li, L.-H.; Meng, C.; et al. A Deep Proteome and Transcriptome Abundance Atlas of 29 Healthy Human Tissues. *Molecular systems biology*. Chair of Proteomics and Bioanalytics, Technische Universität München, Freising, Germany. 2019, p e8503.

(130) Pinto, S. M.; Manda, S. S.; Kim, M.-S.; Taylor, K.; Selvan, L. D. N.; Balakrishnan, L.; Subbannayya, T.; Yan, F.; Prasad, T. S. K.; Gowda, H.; et al. Functional Annotation of Proteome

Encoded by Human Chromosome 22. *J. Proteome Res.* **2014**, *13* (6), 2749–2760.

(131) Kim, M.-S.; Pinto, S. M.; Getnet, D.; Nirujogi, R. S.; Manda, S. S.; Chaerkady, R.; Madugundu, A. K.; Kelkar, D. S.; Isserlin, R.; Jain, S.; et al. A Draft Map of the Human Proteome. *Nature* **2014**, *509* (7502), 575–581.

(132) Diamond, D. L.; Syder, A. J.; Jacobs, J. M.; Sorensen, C. M.; Walters, K.-A.; Proll, S. C.; McDermott, J. E.; Gritsenko, M. A.; Zhang, Q.; Zhao, R.; et al. Temporal Proteome and Lipidome Profiles Reveal Hepatitis C Virus-Associated Reprogramming of Hepatocellular Metabolism and Bioenergetics. *PLoS Pathog.* **2010**, *6* (1), e1000719–e1000719.

(133) Lordan, R.; Tsoupras, A.; Zabetakis, I.; Demopoulos, C. A. Forty Years since the Structural Elucidation of Platelet-Activating Factor (PAF): Historical, Current, and Future Research Perspectives. *Molecules* **2019**, *24* (23).

(134) Prescott, S. M.; Zimmerman, G. A.; Stafforini, D. M.; McIntyre, T. M. Platelet-Activating Factor and Related Lipid Mediators. *Annu. Rev. Biochem.* **2000**, *69* (1), 419–445.

(135) Ishii, S. Platelet-Activating Factor (PAF) in Infectious Diseases. In *Bioactive Lipid Mediators: Current Reviews and Protocols*; 2015; pp 95–108.

(136) Souza, D. G.; Fagundes, C. T.; Sousa, L. P.; Amaral, F. A.; Souza, R. S.; Souza, A. L.; Kroon, E. G.; Sachs, D.; Cunha, F. Q.; Bukin, E.; et al. Essential Role of Platelet-Activating Factor Receptor in the Pathogenesis of Dengue Virus Infection. *Proc. Natl. Acad. Sci. U. S. A.* **2009**, *106* (33), 14138–14143.

(137) Garcia, C. C.; Russo, R. C.; Guabiraba, R.; Fagundes, C. T.; Polidoro, R. B.; Tavares, L. P.; Salgado, A. P. C.; Cassali, G. D.; Sousa, L. P.; Machado, A. V; et al. Platelet-Activating Factor Receptor Plays a Role in Lung Injury and Death Caused by Influenza A in Mice. *PLoS Pathog.* **2010**, *6* (11).

(138) Ueda, T.; Honda, M.; Horimoto, K.; Aburatani, S.; Saito, S.; Yamashita, T.; Sakai, Y.; Nakamura, M.; Takatori, H.; Sunagozaka, H.; et al. Gene Expression Profiling of Hepatitis B- and Hepatitis

C-Related Hepatocellular Carcinoma Using Graphical Gaussian Modeling. *Genomics* **2013**, *101* (4), 238–248.

(139) Ogishi, M.; Yotsuyanagi, H.; Moriya, K.; Koike, K. Delineation of Autoantibody Repertoire through Differential Proteogenomics in Hepatitis C Virus-Induced Cryoglobulinemia. *Sci. Rep.* **2016**, *6* (1), 29532.

(140) Kohnz, R. A.; Mulvihill, M. M.; Chang, J. W.; Hsu, K.-L.; Sorrentino, A.; Cravatt, B. F.; Bandyopadhyay, S.; Goga, A.; Nomura, D. K. Activity-Based Protein Profiling of Oncogene-Driven Changes in Metabolism Reveals Broad Dysregulation of PAFAH1B2 and 1B3 in Cancer. *ACS Chem. Biol.* **2015**, *10* (7), 1624–1630.

(141) Xu, J.; Zang, Y.; Cao, S.; Lei, D.; Pan, X. Aberrant Expression of PAFAH1B3 Associates with Poor Prognosis and Affects Proliferation and Aggressiveness in Hypopharyngeal Squamous Cell Carcinoma. *Onco. Targets. Ther.* **2019**, *12*, 2799–2808.

(142) Fiedler, E. R. C.; Bhutkar, A.; Lawler, E.; Besada, R.; Hemann, M. T. In Vivo RNAi Screening Identifies Pafah1b3 as a Target for Combination Therapy with TKIs in BCR-ABL11 BCP-ALL. *Blood Adv.* **2018**, *2* (11), 1229–1242.

(143) Franklin, M. P.; Sathyanarayan, A.; Mashek, D. G. Acyl-CoA Thioesterase 1 (ACOT1) Regulates PPARα to Couple Fatty Acid Flux With Oxidative Capacity During Fasting. *Diabetes : a journal of the American Diabetes Association.* American Diabetes Association: [Alexandria, Va.] : 2017, pp 2112–2123.

(144) Petryszak, R.; Keays, M.; Tang, Y. A.; Fonseca, N. A.; Barrera, E.; Burdett, T.; Füllgrabe, A.; Fuentes, A. M.-P.; Jupp, S.; Koskinen, S.; et al. Expression Atlas Update—an Integrated Database of Gene and Protein Expression in Humans, Animals and Plants. *Nucleic Acids Res.* **2015**, *44* (D1), D746–D752.

(145) Jones, J. M.; Gould, S. J. Identification of PTE2, a Human Peroxisomal Long-Chain Acyl-CoA Thioesterase. *Biochem. Biophys. Res. Commun.* **2000**, *275* (1), 233–240.

(146) Chang, M.-L.; Yeh, C.-T.; Chen, J.-C.; Huang, C.-C.; Lin, S.-M.; Sheen, I.-S.; Tai, D.-I.; Chu, C.-M.; Lin, W.-P.; Chang, M.-Y.; et al. Altered Expression Patterns of Lipid Metabolism Genes in an Animal Model of HCV Core-Related, Nonobese, Modest Hepatic Steatosis. *BMC Genomics* **2008**, *9* (1), 109.

(147) Chang, M.-L.; Yeh, C.-T.; Lin, D.-Y.; Ho, Y.-P.; Hsu, C.-M.; Bissell, D. M. Hepatic Inflammation Mediated by Hepatitis C Virus Core Protein Is Ameliorated by Blocking Complement Activation. *BMC Med. Genomics* **2009**, *2* (1), 51.

(148) Syed, G. H.; Amako, Y.; Siddiqui, A. Hepatitis C Virus Hijacks Host Lipid Metabolism. *Trends Endocrinol. Metab.* **2010**, *21* (1), 33–40.

(149) Snezhkina, A. V; Lukyanova, E. N.; Fedorova, M. S.; Kalinin, D. V; Melnikova, N. V; Stepanov, O. A.; Kiseleva, M. V; Kaprin, A. D.; Pudova, E. A.; Kudryavtseva, A. V. Novel Genes Associated with the Development of Carotid Paragangliomas. *Molecular biology.* MAIK Nauka Interperiodica in cooperation with Springer Sciences & Business Media BV: [Dordrecht, Netherlands] : 2019, pp 547–559.

(150) Dongol, B.; Shah, Y.; Kim, I.; Gonzalez, F. J.; Hunt, M. C. The Acyl-CoA Thioesterase I Is Regulated by PPARalpha and HNF4alpha via a Distal Response Element in the Promoter. *Journal of lipid research.* Rockefeller Institute Press: [Easton, PA] : 2007, pp 1781–1791.

(151) Fang, B.; Mane-Padros, D.; Bolotin, E.; Jiang, T.; Sladek, F. M. Identification of a Binding Motif Specific to HNF4 by Comparative Analysis of Multiple Nuclear Receptors. *Nucleic Acids Res.* **2012**, *40* (12), 5343–5356.

(152) Hatchwell, L.; Harney, D. J.; Cielesh, M.; Young, K.; Koay, Y. C.; O'Sullivan, J. F.; Larance, M. Multi-Omics Analysis of the Intermittent Fasting Response in Mice Identifies an Unexpected Role for HNF4α. *Cell Rep.* **2020**, *30* (10), 3566-3582.e4.

(153) El–Serag, H. B.; Rudolph, K. L. Hepatocellular Carcinoma: Epidemiology and Molecular Carcinogenesis. *Gastroenterology* **2007**, *132* (7), 2557–2576.

(154) Pez, F.; Lopez, A.; Kim, M.; Wands, J. R.; Caron de Fromentel, C.; Merle, P. Wnt Signaling and Hepatocarcinogenesis: Molecular Targets for the Development of Innovative Anticancer Drugs. *J. Hepatol.* **2013**, *59* (5), 1107–1117.

(155) Vilchez, V.; Turcios, L.; Marti, F.; Gedaly, R. Targeting Wnt/β-Catenin Pathway in Hepatocellular Carcinoma Treatment. *World J. Gastroenterol.* **2016**, *22* (2), 823–832.

(156) Yi, M.; Li, J.; Chen, S.; Cai, J.; Ban, Y.; Peng, Q.; Zhou, Y.; Zeng, Z.; Peng, S.; Li, X.; et al. Emerging Role of Lipid Metabolism Alterations in Cancer Stem Cells. *J. Exp. Clin. Cancer Res.* **2018**, *37* (1).

(157) Mancini, R.; Noto, A.; Pisanu, M. E.; De Vitis, C.; Maugeri-Saccà, M.; Ciliberto, G. Metabolic Features of Cancer Stem Cells: The Emerging Role of Lipid Metabolism. *Oncogene* **2018**, *37* (18), 2367–2378.

(158) Wang, W.; Smits, R.; Hao, H.; He, C. Wnt/β-Catenin Signaling in Liver Cancers. *Cancers (Basel).* **2019**, *11* (7).

(159) Liu, X.; Zuo, J.; Fang, Y.; Wen, J.; Deng, F.; Zhong, H.; Jiang, B.; Wang, J.; Nie, B. Downregulation of Hepatic Lipase Is Associated with Decreased CD133 Expression and Clone Formation in HepG2 Cells. *Int J Mol Med* **2018**, *42* (4), 2137–2144.

(160) Bartelt, A.; Beil, F. T.; Müller, B.; Koehne, T.; Yorgan, T. A.; Heine, M.; Yilmaz, T.; Rüther, W.; Heeren, J.; Schinke, T.; et al. Hepatic Lipase Is Expressed by Osteoblasts and Modulates Bone Remodeling in Obesity. *Bone* **2014**, *62*, 90–98.

(161) Spengler, U. Direct Antiviral Agents (DAAs) - A New Age in the Treatment of Hepatitis C Virus Infection. *Pharmacol. Ther.* **2018**, *183*, 118–126.

(162) Kanwal, F.; Kramer, J.; Asch, S. M.; Chayanupatkul, M.; Cao, Y.; El-Serag, H. B. Risk of Hepatocellular Cancer in HCV Patients Treated With Direct-Acting Antiviral Agents. *Gastroenterology* **2017**, *153* (4), 996-1005.e1.

(163) Roche, B. B. The Impact of Treatment of Hepatitis C with DAAs on the Occurrence of HCC. *Liver*

international : official journal of the International Association for the Study of the Liver. Blackwell Munksgaard: Oxford, UK : 2018, pp 139–145.

(164) Jacobson, I. M.; Lim, J. K.; Fried, M. W. American Gastroenterological Association Institute Clinical Practice Update—Expert Review: Care of Patients Who Have Achieved a Sustained Virologic Response After Antiviral Therapy for Chronic Hepatitis C Infection. *Gastroenterology* **2017**, *152* (6), 1578–1587.

(165) Nwosu, Z. C.; Battello, N.; Rothley, M.; Piorońska, W.; Sitek, B.; Ebert, M. P.; Hofmann, U.; Sleeman, J.; Wölfl, S.; Meyer, C.; et al. Liver Cancer Cell Lines Distinctly Mimic the Metabolic Gene Expression Pattern of the Corresponding Human Tumours. *J. Exp. Clin. Cancer Res.* **2018**, *37* (1), 211.

(166) Olsavsky, K. M.; Page, J. L.; Johnson, M. C.; Zarbl, H.; Strom, S. C.; Omiecinski, C. J. Gene Expression Profiling and Differentiation Assessment in Primary Human Hepatocyte Cultures, Established Hepatoma Cell Lines, and Human Liver Tissues. *Toxicol. Appl. Pharmacol.* **2007**, *222* (1), 42–56.

(167) Steenbergen, R.; Oti, M.; ter Horst, R.; Tat, W.; Neufeldt, C.; Belovodskiy, A.; Chua, T. T.; Cho, W. J.; Joyce, M.; Dutilh, B. E.; et al. Establishing Normal Metabolism and Differentiation in Hepatocellular Carcinoma Cells by Culturing in Adult Human Serum. *Sci. Rep.* **2018**, *8* (1), 11685.

(168) van Berkel, T. J. C. The Role of Non-Parenchymal Cells in Liver Metabolism. *Trends Biochem. Sci.* **1979**, *4* (9), 202–205.

(169) Yong, K. S. M.; Her, Z.; Chen, Q. Humanized Mouse Models for the Study of Hepatitis C and Host Interactions. *Cells* **2019**, *8* (6), 604.

(170) Burm, R.; Collignon, L.; Mesalam, A. A.; Meuleman, P. Animal Models to Study Hepatitis C Virus Infection. *Front. Immunol.* **2018**, *9*, 1032.

Chapter 5: General Discussion and Future Work

5.1 Summary

As obligate intracellular parasites, viruses rely on host cells for their completion of their life cycle. To this end, they hijack cell function to divert resources and metabolic energy to the production of new virions. Over the last several years, the emergence of novel viruses and their impact on global health has highlighted the importance of understanding how cellular structure and function is altered during infection, in order to cure the infection and counter its long-term sequelae. Identifying the enzymes whose altered activity is responsible for this cellular remodelling provides both novel biomarkers for disease progression and novel pharmaceutical targets. To this end, the development and application of activity-based probes, which allow for the functional state of target enzymes to be assessed, represent a valuable contribution to the investigative toolbox.

This thesis presents (1) a new kinase-targeting activity-based probe, (2) derivates of an activity-based probe which expand its functionality, and (3) the application of ABPP in characterizing the functional role of a miRNA. Each chapter furthermore demonstrates how these tools are used to further our understanding of viral infection, using the hepatitis C virus as a model.

5.1.1 Wortmannin-yne

Kinases play a fundamental role in propagating cell signals, and for this reason are of particular interest when studying the system reorganisation which results from viral infection. Wortmannin, a covalent kinase inhibitor, was modified to form wortmannin-yne, which contains an alkyne handle to which a reporter tag could be appended using copper-catalysed azide-alkyne cycloaddition, thereby enabling the detection of active kinases. Wortmannin-yne was used to identify enzymes whose activity was altered

by HCV replication. Functional analysis of differentially active enzymes identified, among others, the MAPK pathway as a target of HCV modulation whose enzymes could be profiled by wortmannin-yne.

5.1.2 PIKBPyne

Phosphatidylinositol phosphates and their kinases play a key role in cell organisation and signalling.[1] The activity of these kinases is regulated in part by protein-protein interactions which control post-translational modifications and subcellular localisation. It is therefore of interest to identify protein-protein interactions and quantify any changes to these interactions which occur during infection. Three novel probes were herein reported which contained linkers of variable lengths between a moiety targeting phoaphatidylinositol kinases and a benzophenone group capable of forming a covalent bond with adjacent proteins. The probe containing a long flexible linker was shown to be able to bind to PIK-interacting proteins in a PIK-dependent manner, confirming its ability to measure protein-protein interactions. This probe was then used to show that HCV alters the interactome of PI4KB during replication, suggesting a potential link between its interaction with the Golgi protein ACBD3, the increase in its activity[2] and the increase in PI4P in the double-membrane viral replication vesicles.[3]

5.1.3 miR-27b

microRNAs play a significant functional role in the regulation of cell systems. Their function can be hijacked by viruses via sponging or transcriptional control. miR-27b is a core regulator of lipid metabolism, and its activity is therefore implicated in the progression of hepatitis C infection, which relies on host cell lipids for each stage of its life cycle. Activity-based protein profiling, using the fluorophosphonate probe, was used to identify the functional targets of miR-27b. Three new functional, indirect targets were identified: LIPC, PAFAH1B3, and ACOT1/2. Activity of LIPC was decreased by a simultaneous up- or down-regulation of the transcription factors controlling its expression. Activity of PAFAH1B3 was increased in a post-translational manner, which was demonstrated to be linked to the

presence of post-translational palmitoylation. Activity of ACOT1/2 was similarly decreased in a post-translational manner. These changes in activity were considered in the context of hepatitis C and linked to the progression of hepatocellular carcinoma, a common result of long-term infection.

Overall, activity-based protein profiling has been used to characterise how the activity of enzymes is regulated in the context of hepatitis C infection, whether by hepatitis C directly of by an intermediate effector. Multiple activity-based probes were used to detected changes to the functional state of kinases and serine hydrolases, while expansion of the functionality of an activity-based probes allowed protein-protein interactions to be identified and quantified.

5.2 Perspective on future work

This work has focused on identifying functional changes to enzyme activity caused by the hepatitis C virus, or by a miRNA whose expression it induces. Many of these regulatory changes occurred in whole or in part post-translationally and resulted from alterations in cell signalling pathways. Future work might aim to characterise the mechanisms of activation or inhibition employed to regulate the activities of the enzymes identified in this thesis. Most post-translational regulatory mechanisms fall into one or more of three categories: post-translational modifications, protein-protein interactions, and changes to sub-cellular localisation.

5.2.1 Post-translational modifications

Multiple enzymes identified in these profiles are either known or predicted to possess sites of post-translational modification. As modulation of enzymatic activity often relies on post-translational addition or removal of biomolecules, it would be of interest to profile changes to the presence of these modifications within the proteome. Recently developed chemical biology tools allow proteins possessing these post-translational modifications to be identified and the abundance of the modification to be

quantified. This can be done either by labelling endogenous PTMs or by introducing analogues into cells which mimic the PTM but include a handle to which reporter tags can be appended. The identification of these changes would complement findings obtained by activity-based protein profiling, providing information on mechanisms by which the observed differential activity could be modulated under the conditions of interest. In this section, specific examples of techniques and the proteins of interest they might target will be presented.

Phosphorylation is one of the most common post-translational modifications, and the activities of many enzymes discussed in this work are known to be regulated by the addition or removal of a phosphate group, among other mechanisms. PI4KB,[4,5] MAPK,[6] and AKT2[6] are the most obvious examples of phosphorylation-dependent enzymes whose activities were both measurable by ABPP and relevant to viral infection. Profiling the phosphorylation of these and other proteins whose activity is altered under the conditions of interest would determine the extent to which this PTM is responsible for observed changes to activity. This could most easily be done by analysis of stable isotope-labelled whole proteome samples by mass spectrometry, which can identify and quantify phosphorylated peptides.[7] While this technique has the potential to annotate a large number of differentially-phosphorylated proteins, it risks overlooking lower-abundance proteins which may be of specific interest. For this reason, the inclusion of chemoproteomic techniques to enrich the fraction of the proteome carrying the modification of interest may be useful. A technique to replace the phosphate group on serine or threonine with a biotin tag, reported by Oda *et al*, allows phosphorylated proteins to be enriched, identified, and quantified by mass spectrometry.[8]

The presence of glycans has been detected or predicted on the wortmannin-yne targeted kinases AKT2,[9] PAK2,[10] PFKL,[11,12] PFKM,[11,12] and ATM,[13] and on the FP-targeted LIPC.[14] Though the presence of glycosylation can be detected by mass spectrometry,[15] chemoproteomics tools again offer the potential

for a more comprehensive annotation of this post-translational modification. New sugar-based chemoproteomic tools developed in recent years mimic the structure of sugars incorporated into proteoglycans but contain handles to which reporter tags could be appended. This allows for the detection and quantification of protein glycosylation.[16,17] Alternatively, endogenous glycosylation could be detected by oxidation of protein-linked sugars to aldehydes followed by coupling to immobilized hydrazide groups.[18] This technique possesses the advantage of not disrupting endogenous glycosylation by the addition of an unnaturally high concentration of a particular sugar.

The presence of lipid post-translational modifications was discussed in chapter 4; however, it focused specifically only on PAFAH1B3 and ACOT1/2. However, the presence of lipid post-translational modifications has also been detected or predicted on a large number of enzymes discussed in this work: the wortmannin-yne targeted kinases MAPK1,[19–21] MAP2K1,[21] AKT2,[22] CSNK2A1,[20] CSNK2A2,[21] DAK,[23–25] PIP4K2A,[26,27] CDK1,[21,28] CDK2,[19,21] CMPK1,[20] PAK2,[20,21] NME1,[20,21,29,30] GAK,[21] PCK2,[21] CAMK2D,[20] PFKL,[20] PFKM,[21] CAMK1,[31,32] PRKAR1A,[20,21] and TBRG4,[26] and the PI4KB-regulatory proteins ACBD3[33] and PRKD1.[21] Palmitoyl-mimic probes have been reported[34] and have been used to detect and quantify changes to palmitoylation.[20] The use of such techniques in the context of lipid-dysregulating viruses and miRNAs, however, risks failing to detect changes to palmitoylation which are caused by excessive or insufficient amounts of specific lipid species. Using endogenous labelling techniques such as acyl-biotin exchange, in which the palmitoyl groups on cysteine residues are replaced by biotin,[35] could allow for a more physiologically relevant measure of changes to palmitoylation.

5.2.2 Protein-protein interactions

Chapter 3 demonstrated an expansion of ABP functionality, using a PI kinase-based probe to profile proteins interacting with the active PI kinase. Mimicking this expansion with the wortmannin and fluorophosphonate based probes could consist of adding a photo-activatable crosslinker moiety attached

to the probe by a long linker. (Fig 5.1) Though there are several different types of photo-activatable crosslinkers, diazirine was chosen here, as it is capable of more efficient crosslinking, and its small size is less likely to cause problems crossing the cell membrane.[36] This would allow *in situ* labelling of live cells providing a more accurate picture of the interactions between proteins, as lysis procedures often disrupt protein complexes. The length of the linkers is undefined, any may rely on the specific goals of a project. However, linkers longer than those used in the probes characterised in Chapter 3 should almost certainly be used. The longer reach would allow the capture and detection of a larger proportion of a target's interactome, including proteins which may interact with a part of the enzyme distal to the active site. The choice of reporter used would also depend on the specific goals of the project. A bio-orthogonal handle, such as the terminal alkyne shown in Fig 5.1, would allow flexibility, as any reporter could be appended to the probe after labelling via click chemistry. However, the addition of another labelling step has the potential to increase the level of background signal, and although this can be controlled for, the presence of more background noise could obscure the detection of targets of interest. The use of a biotin reporter, or other affinity tag, already conjugated to the probe might therefore seem the more practical solution.

An interaction-map of active proteins would be useful for identifying potential activating proteins or for determining complexes and subcellular localities which contain the active form of the enzyme. Furthermore, as fluorophosphonate probes tend to be cell-permeable,[37,38] this technique may allow interactions to be captured in living cells, including weaker and more transient interactions. These types of interactions might be missed by traditional techniques such as co-immunoprecipitation, during which cells and cell lysates are subjected to conditions which may disrupt key protein-protein interactions. This type of experiment, however, only provides a partial look at protein-protein interactions and could not quantitatively measure changes to interactions which also altered activity, as enzyme activity acts as a prerequisite to co-factor labelling.

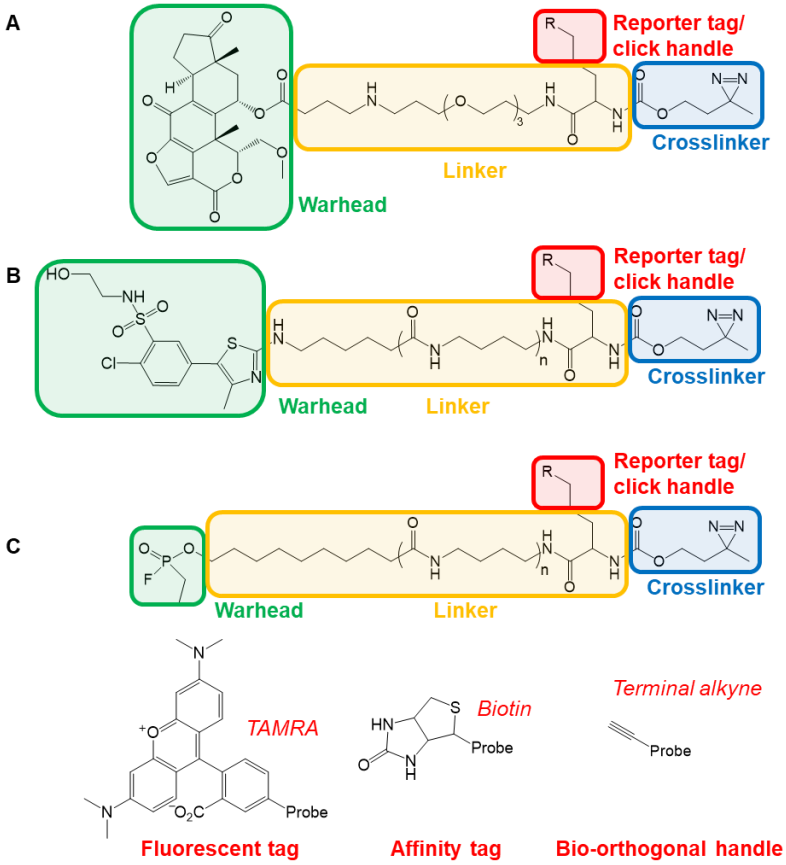

Figure 5.1 Proposed novel photoaffinity labelling probes to study the protein-protein interactions of different lipid metabolic enzymes. A) Wortmannin-based probe B) PIK93-based probe C) FP-based probe.

There are a number of methods by which protein-protein interactions can be identified and quantified. Proteins can be engineered to contain unnatural amino acids or sugars with a photo-activatable crosslinker, which upon irradiation with UV light forms a covalent bond with proteins directly in contact with the unnatural group.[39] Other strategies use recombinant proteins linked to an enzyme capable of generating reactive species conjugated to a biotin group. These reactive species then react with any nearby proteins, with the result that any protein near the recombinant protein of interest is labelled with biotin and can be detected by mass spectrometry or western blotting.[39] A third strategy uses chemical crosslinkers, such as formaldehyde, among many others, to create crosslinkages between proteins. A protein of interest along with its interacting proteins can then be purified by immunoprecipitation.[39] Recently, crosslinking agents with variable lengthed linkers, based on disuccinimidyl sulfoxide, have been described, which allows a more flexible capture of interacting proteins.[40] Using these strategies, changes to the interactomes of proteins of interest, such as PAFAH1B3, or PI4KB, could be quantitatively measured, providing a clearer picture of mechanisms of enzyme regulation and dysregulation.

The employment of these chemoproteomic post-translational modification and protein-protein interaction profiling methods in conjunction with activity-based protein profiling would generate a more complete annotation of the regulation of enzyme activity.

5.2.3 Expansion of work into other virus systems

Future work might also consist of applying these techniques to the study of different related viruses. As key modulators of regulatory processes, a not-insignificant proportion of kinases are likely to be dysregulated by viral infections. Lipids, meanwhile, act as both key building blocks and sources of metabolic energy which are exploited by many viruses.[41,42]

Viruses closely related to HCV, such as Dengue virus, West Nile virus, Yellow Fever virus, Japanese Encephalitus virus, and Zika virus[43] are likely to share some mechanisms of infection and pathogenesis – using the tools described herein to study how these viruses perturb pathway signalling kinases and lipid metabolic enzymes may provide useful information for the development of better pharmaceutical treatments. This is not limited to closely related viruses: viruses such as the novel SARS-CoV-2 and its precursor SARS-CoV also seems to both rely on lipid metabolism and induce a state of dyslipidemia.[42,44–46] As a lipid-regulatory miRNA, the modulation of miR-27b in the context of infection by these viruses may be of significant interest.

The study of phosphatidylinositols and their kinases may also be of particular interest. The formation of double-membrane vesicles from the endoplasmic reticulum is essential to the life cycle of numerous viruses, as they serve as sites for RNA replication. Like HCV, Dengue virus,[43] Zika virus,[43] and the SARS coronaviruses[47,48] all rely on the formation of double-membrane vesicles. The induction of the high curvature necessary for the formation of these double-membrane vesicles is theorized to require higher concentrations of phosphatidylinositols (PIs), particularly phosphatidylinositol-4-phosphate (PI4P).[49] PIs have been shown to promote membrane curvature, and PI4P's charged headgroup makes it a particularly strong promoter.[50] This makes PI4P and the kinases which form it, such as PI4KB, as well as the PIK probes described in chapter 3, valuable to the study of the above-mentioned viruses.

5.2.4 Expansion of work into other systems

The majority of studies using activity-based profiling are performed either *in vitro* on proteomes isolated from animal models or cultured cells, or *in situ* on live cell monocultures. While this has been able to provide information on targets of viral mediation of host cell systems, the physiological relevance of this information is not beyond doubt. Cell lysis and protein isolation procedures used in *in vitro* labelling have the potential to destroy enzyme-cofactor interactions which may result in loss of information about

the enzyme's true activity *in vivo*. Labelling cells *in situ* preserves the regulation of catalytic activity present in living cells; however, they do not always accurately represent the effects of infection on a live organism. As such, the development of probes which could be administered *in vivo* would provide the opportunity to characterise changes to enzyme activity in a more complex and physiologically relevant manner.

5.2.5 Therapeutic potential

The role of these host factors discussed within this work in promoting or preventing viral infection and virally-induced oncogenesis suggests that modulation of their activity may have therapeutic potential. Modulation or mimicry of protein-protein interactions, such as those detected by the photo-affinity probe PIKBPyne, may potentially be utilised to this end. Labelling by PIKBPyne, for example, showed that interactions between the Golgi protein ACBD3 and PI4KB were decreased by the hepatitis C virus, which suggests that PI4KB may be modulating the lipid profile elsewhere in the cell to promote viral replication. By promoting anchoring of PI4KB to the Golgi, or decreasing it's potential for catalytic activity generally, this virally-induced remodelling may be prevented. The activity of the other kinases and serine hydrolases discussed in this work also represent potential therapeutic targets either to suppress viral infection and its resulting alterations to cellular architecture, or to reverse these changes. The extent of the therapeutic potential of these host-targeting strategies in the context of HCV infection and the morbidities it causes must be subject to future investigations. Though current anti-viral strategies are direct acting,[51] the emergence of resistance mutants[51] opens the door to the possibility of new combinatorial therapies which target both viral and host factors. As dysregulation of lipid metabolism plays a significant role in oncogenesis,[52] targeting these factors is also an attractive strategy to prevent the development of HCV-induced HCV. Currently, there are few anti-cancer inhibitors of lipid metabolism beyond the cholesterol-targeting statins.[52–54] This study has provided potential novel targets for both small molecule inhibitor and gene-editing based strategies currently employed.

5.3 Concluding remarks

This work has described the use of activity-based probes to characterise the regulation and dysregulation of host cell systems. By focusing on detecting functional and not abundance-based modulation of cellular systems, the most significant changes to the normal operation of the cell can be identified. Though the majority of the work presented herein was performed while studying hepatitis C infection, many of the findings can be applied outside of this context. The novel wortmannin-yne and PIKBPyne probes, which report on kinase activity, may be useful both for the further elucidation of regulatory mechanisms and in the study of multiple pathogeneses which dysregulate the systems they control. miR-27b, meanwhile, is involved not only in lipid metabolism but also oxidative damage and oncogenesis, and as such, the identification of novel functional targets may further illuminate the role it plays in these processes.

5.4 References

(1) Balla, T. Phosphoinositides: Tiny Lipids With Giant Impact on Cell Regulation. *Physiol. Rev.* **2013**, *93* (3), 1019–1137.

(2) Sherratt, A. R.; Nasheri, N.; McKay, C. S.; O'Hara, S.; Hunt, A.; Ning, Z.; Figeys, D.; Goto, N. K.; Pezacki, J. P. A New Chemical Probe for Phosphatidylinositol Kinase Activity. *ChemBioChem* **2014**, *15* (9), 1253–1256.

(3) Zhang, L.; Hong, Z.; Lin, W.; Shao, R.-X.; Goto, K.; Hsu, V. W.; Chung, R. T. ARF1 and GBF1 Generate a PI4P-Enriched Environment Supportive of Hepatitis C Virus Replication. *PLoS One* **2012**, *7* (2), e32135.

(4) Hausser, A.; Storz, P.; Märtens, S.; Link, G.; Toker, A.; Pfizenmaier, K. Protein Kinase D Regulates Vesicular Transport by Phosphorylating and Activating Phosphatidylinositol-4 Kinase IIIβ at the Golgi Complex. *Nat. Cell Biol.* **2005**, *7* (9), 880–887.

(5) Hausser, A.; Link, G.; Hoene, M.; Russo, C.; Selchow, O.; Pfizenmaier, K. Phospho-Specific Binding of 14-3-3 Proteins to Phosphatidylinositol 4-Kinase III β Protects from

Dephosphorylation and Stabilizes Lipid Kinase Activity. *J. Cell Sci.* **2006**, *119* (17), 3613–3621.

(6) Wee, P.; Wang, Z. Epidermal Growth Factor Receptor Cell Proliferation Signaling Pathways. *Cancers (Basel).* **2017**, *9* (5).

(7) Espadas, G.; Borràs, E.; Chiva, C.; Sabidó, E. Evaluation of Different Peptide Fragmentation Types and Mass Analyzers in Data-Dependent Methods Using an Orbitrap Fusion Lumos Tribrid Mass Spectrometer. *Proteomics* **2017**, *17* (9).

(8) Oda, Y.; Nagasu, T.; Chait, B. T. Enrichment Analysis of Phosphorylated Proteins as a Tool for Probing the Phosphoproteome. *Nat. Biotechnol.* **2001**, *19* (4), 379–382.

(9) Wang, S.; Huang, X.; Sun, D.; Xin, X.; Pan, Q.; Peng, S.; Liang, Z.; Luo, C.; Yang, Y.; Jiang, H.; et al. Extensive Crosstalk between O-GlcNAcylation and Phosphorylation Regulates Akt Signaling. *PLoS One* **2012**, *7* (5), e37427.

(10) Deeb, S. J.; Cox, J.; Schmidt-Supprian, M.; Mann, M. N-Linked Glycosylation Enrichment for In-Depth Cell Surface Proteomics of Diffuse Large B-Cell Lymphoma Subtypes. *Mol. & Cell. Proteomics* **2014**, *13* (1), 240 LP – 251.

(11) Yi, W.; Clark, P. M.; Mason, D. E.; Keenan, M. C.; Hill, C.; Goddard, W. A.; Peters, E. C.; Driggers, E. M.; Hsieh-Wilson, L. C. Phosphofructokinase 1 Glycosylation Regulates Cell Growth and Metabolism. *Science (80-.).* **2012**, *337* (6097), 975 LP – 980.

(12) Sun, S.; Hu, Y.; Jia, L.; Eshghi, S. T.; Liu, Y.; Shah, P.; Zhang, H. Site-Specific Profiling of Serum Glycoproteins Using N-Linked Glycan and Glycosite Analysis Revealing Atypical N-Glycosylation Sites on Albumin and α-1B-Glycoprotein. *Anal. Chem.* **2018**, *90* (10), 6292–6299.

(13) Woo, C. M.; Lund, P. J.; Huang, A. C.; Davis, M. M.; Bertozzi, C. R.; Pitteri, S. J. Mapping and Quantification of Over 2000 O-Linked Glycopeptides in Activated Human T Cells with Isotope-Targeted Glycoproteomics (Isotag). *Mol. & Cell. Proteomics* **2018**, *17* (4), 764 LP – 775.

(14) Wolle, J.; Jansen, H.; Smith, L. C.; Chan, L. Functional Role of N-Linked Glycosylation in Human

Hepatic Lipase: Asparagine-56 Is Important for Both Enzyme Activity and Secretion. *J. Lipid Res.* **1993**, *34* (12), 2169–2176.

(15) Kuo, C.-W.; Khoo, K.-H. Strategic Applications of Negative-Mode LC-MS/MS Analyses to Expedite Confident Mass Spectrometry-Based Identification of Multiple Glycosylated Peptides. *Anal. Chem.* **2020**, *92* (11), 7612–7620.

(16) Zaro, B. W.; Yang, Y.-Y.; Hang, H. C.; Pratt, M. R. Chemical Reporters for Fluorescent Detection and Identification of O-GlcNAc-Modified Proteins Reveal Glycosylation of the Ubiquitin Ligase NEDD4-1. *Proc. Natl. Acad. Sci. U. S. A.* **2011**, *108* (20), 8146–8151.

(17) Gurcel, C.; Vercoutter-Edouart, A.-S.; Fonbonne, C.; Mortuaire, M.; Salvador, A.; Michalski, J.-C.; Lemoine, J. Identification of New O-GlcNAc Modified Proteins Using a Click-Chemistry-Based Tagging. *Anal. Bioanal. Chem.* **2008**, *390* (8), 2089–2097.

(18) Zhang, H.; Li, X.; Martin, D. B.; Aebersold, R. Identification and Quantification of N-Linked Glycoproteins Using Hydrazide Chemistry, Stable Isotope Labeling and Mass Spectrometry. *Nat. Biotechnol.* **2003**, *21* (6), 660.

(19) Peng, T.; Hang, H. C. Bifunctional Fatty Acid Chemical Reporter for Analyzing S-Palmitoylated Membrane Protein–Protein Interactions in Mammalian Cells. *J. Am. Chem. Soc.* **2015**, *137* (2), 556–559.

(20) Serwa, R. A.; Abaitua, F.; Krause, E.; Tate, E. W.; O'Hare, P. Systems Analysis of Protein Fatty Acylation in Herpes Simplex Virus-Infected Cells Using Chemical Proteomics. *Chem. Biol.* **2015**, *22* (8), 1008–1017.

(21) Won, S. J.; Martin, B. R. Temporal Profiling Establishes a Dynamic S-Palmitoylation Cycle. *ACS Chem. Biol.* **2018**, *13* (6), 1560–1568.

(22) Ren, W.; Jhala, U. S.; Du, K. Proteomic Analysis of Protein Palmitoylation in Adipocytes. *Adipocyte* **2013**, *2* (1), 17–27.

(23) Gould, N. S.; Evans, P.; Martínez-Acedo, P.; Marino, S. M.; Gladyshev, V. N.; Carroll, K. S.;

Ischiropoulos, H. Site-Specific Proteomic Mapping Identifies Selectively Modified Regulatory Cysteine Residues in Functionally Distinct Protein Networks. *Chem. Biol.* **2015**, *22* (7), 965–975.

(24) Shen, L.-F.; Chen, Y.-J.; Liu, K.-M.; Haddad, A. N. S.; Song, I.-W.; Roan, H.-Y.; Chen, L.-Y.; Yen, J. J. Y.; Chen, Y.-J.; Wu, J.-Y.; et al. Role of S-Palmitoylation by ZDHHC13 in Mitochondrial Function and Metabolism in Liver. *Sci. Rep.* **2017**, *7* (1), 2182.

(25) Collins, M. O.; Woodley, K. T.; Choudhary, J. S. Global, Site-Specific Analysis of Neuronal Protein S-Acylation. *Sci. Rep.* **2017**, *7* (1), 4683.

(26) Zhang, X.; Zhang, Y.; Fang, C.; Zhang, L.; Yang, P.; Wang, C.; Lu, H. Ultradeep Palmitoylomics Enabled by Dithiodipyridine-Functionalized Magnetic Nanoparticles. *Anal. Chem.* **2018**, *90* (10), 6161–6168.

(27) Kang, R.; Wan, J.; Arstikaitis, P.; Takahashi, H.; Huang, K.; Bailey, A. O.; Thompson, J. X.; Roth, A. F.; Drisdel, R. C.; Mastro, R.; et al. Neural Palmitoyl-Proteomics Reveals Dynamic Synaptic Palmitoylation. *Nature* **2008**, *456* (7224), 904–909.

(28) Wei, X.; Song, H.; Semenkovich, C. F. Insulin-Regulated Protein Palmitoylation Impacts Endothelial Cell Function. *Arterioscler. Thromb. Vasc. Biol.* **2014**, *34* (2), 346–354.

(29) Thinon, E.; Fernandez, J. P.; Molina, H.; Hang, H. C. Selective Enrichment and Direct Analysis of Protein S-Palmitoylation Sites. *J. Proteome Res.* **2018**, *17* (5), 1907–1922.

(30) Yang, W.; Di Vizio, D.; Kirchner, M.; Steen, H.; Freeman, M. R. Proteome Scale Characterization of Human <Em>S</Em>-Acylated Proteins in Lipid Raft-Enriched and Non-Raft Membranes. *Mol. & Cell. Proteomics* **2010**, *9* (1), 54 LP – 70.

(31) Zhang, M. M.; Wu, P.-Y. J.; Kelly, F. D.; Nurse, P.; Hang, H. C. Quantitative Control of Protein S-Palmitoylation Regulates Meiotic Entry in Fission Yeast. *PLOS Biol.* **2013**, *11* (7), e1001597.

(32) Hemsley, P. A.; Weimar, T.; Lilley, K. S.; Dupree, P.; Grierson, C. S. A Proteomic Approach Identifies Many Novel Palmitoylated Proteins in Arabidopsis. *New Phytol.* **2013**, *197* (3), 805–814.

(33) Hernandez, J. L.; Davda, D.; Majmudar, J. D.; Won, S. J.; Prakash, A.; Choi, A. I.; Martin, B. R. Correlated S-Palmitoylation Profiling of Snail-Induced Epithelial to Mesenchymal Transition. *Mol. Biosyst.* **2016**, *12* (6), 1799–1808.

(34) Martin, B. R.; Cravatt, B. F. Large-Scale Profiling of Protein Palmitoylation in Mammalian Cells. *Nat. Methods* **2009**, *6* (2), 135–138.

(35) Edmonds, M. J.; Geary, B.; Doherty, M. K.; Morgan, A. Analysis of the Brain Palmitoyl-Proteome Using Both Acyl-Biotin Exchange and Acyl-Resin-Assisted Capture Methods. *Sci. Rep.* **2017**, *7* (1), 3299.

(36) Murale, D. P.; Hong, S. C.; Haque, M. M.; Lee, J.-S. Photo-Affinity Labeling (PAL) in Chemical Proteomics: A Handy Tool to Investigate Protein-Protein Interactions (PPIs). *Proteome Sci.* **2016**, *15* (1), 14.

(37) Gillet, L. C. J.; Namoto, K.; Ruchti, A.; Hoving, S.; Boesch, D.; Inverardi, B.; Mueller, D.; Coulot, M.; Schindler, P.; Schweigler, P.; et al. In-Cell Selectivity Profiling of Serine Protease Inhibitors by Activity-Based Proteomics. *Mol. & Cell. Proteomics* **2008**, *7* (7), 1241 LP – 1253.

(38) Wang, C.; Abegg, D.; Dwyer, B. G.; Adibekian, A. Discovery and Evaluation of New Activity-Based Probes for Serine Hydrolases. *ChemBioChem* **2019**, *20* (17), 2212–2216.

(39) Mishra, P. K.; Yoo, C.-M.; Hong, E.; Rhee, H. W. Photo-Crosslinking: An Emerging Chemical Tool for Investigating Molecular Networks in Live Cells. *ChemBioChem* **2020**, *21* (7), 924–932.

(40) Yu, C.; Novitsky, E. J.; Cheng, N. W.; Rychnovsky, S. D.; Huang, L. Exploring Spacer Arm Structures for Designs of Asymmetric Sulfoxide-Containing MS-Cleavable Cross-Linkers. *Anal. Chem.* **2020**, *92* (8), 6026–6033.

(41) Heaton, N. S.; Randall, G. Multifaceted Roles for Lipids in Viral Infection. *Trends Microbiol.* **2011**, *19* (7), 368–375.

(42) Abu-Farha, M.; Thanaraj, T. A.; Qaddoumi, M. G.; Hashem, A.; Abubaker, J.; Al-Mulla, F. The Role of Lipid Metabolism in COVID-19 Virus Infection and as a Drug Target. *Int. J. Mol. Sci.*

2020, *21* (10).

(43) Neufeldt, C. J.; Cortese, M.; Acosta, E. G.; Bartenschlager, R. Rewiring Cellular Networks by Members of the Flaviviridae Family. *Nat. Rev. Microbiol.* **2018**, *16* (3), 125–142.

(44) Wei, X.; Zeng, W.; Su, J.; Wan, H.; Yu, X.; Cao, X.; Tan, W.; Wang, H. Hypolipidemia Is Associated with the Severity of COVID-19. *J. Clin. Lipidol.* **2020**.

(45) Vavougios, G. D. A Data-Driven Hypothesis on the Epigenetic Dysregulation of Host Metabolism by SARS Coronaviral Infection: Potential Implications for the SARS-CoV-2 Modus Operandi. *Med. Hypotheses* **2020**, *140*.

(46) Wu, Q.; Zhou, L.; Sun, X.; Yan, Z.; Hu, C.; Wu, J.; Xu, L.; Li, X.; Liu, H.; Yin, P.; et al. Altered Lipid Metabolism in Recovered SARS Patients Twelve Years after Infection. *Sci. Rep.* **2017**, *7* (1), 9110.

(47) Angelini, M. M.; Akhlaghpour, M.; Neuman, B. W.; Buchmeier, M. J. Severe Acute Respiratory Syndrome Coronavirus Nonstructural Proteins 3, 4, and 6 Induce Double-Membrane Vesicles. *MBio* **2013**, *4* (4), e00524-13.

(48) Snijder, E. J.; van der Meer, Y.; Zevenhoven-Dobbe, J.; Onderwater, J. J. M.; van der Meulen, J.; Koerten, H. K.; Mommaas, A. M. Ultrastructure and Origin of Membrane Vesicles Associated with the Severe Acute Respiratory Syndrome Coronavirus Replication Complex. *J. Virol.* **2006**, *80* (12), 5927 LP – 5940.

(49) Ishikawa-Sasaki, K.; Sasaki, J.; Taniguchi, K. A Complex Comprising Phosphatidylinositol 4-Kinase IIIβ, ACBD3, and Aichi Virus Proteins Enhances Phosphatidylinositol 4-Phosphate Synthesis and Is Critical for Formation of the Viral Replication Complex. *J. Virol.* **2014**, *88* (12), 6586 LP – 6598.

(50) Furse, S.; Brooks, N. J.; Seddon, A. M.; Woscholski, R.; Templer, R. H.; Tate, E. W.; Gaffney, P. R. J.; Ces, O. Lipid Membrane Curvature Induced by Distearoyl Phosphatidylinositol 4-Phosphate. *Soft Matter* **2012**, *8* (11), 3090–3093.

(51) Spengler, U. Direct Antiviral Agents (DAAs) - A New Age in the Treatment of Hepatitis C Virus Infection. *Pharmacol. Ther.* **2018**, *183*, 118–126.

(52) Snaebjornsson, M. T.; Janaki-Raman, S.; Schulze, A. Greasing the Wheels of the Cancer Machine: The Role of Lipid Metabolism in Cancer. *Cell Metab.* **2020**, *31* (1), 62–76.

(53) Cheng, C.; Geng, F.; Cheng, X.; Guo, D. Lipid Metabolism Reprogramming and Its Potential Targets in Cancer. *Cancer Commun.* **2018**, *38* (1), 27.

(54) Long, J.; Zhang, C.-J.; Zhu, N.; Du, K.; Yin, Y.-F.; Tan, X.; Liao, D.-F.; Qin, L. Lipid Metabolism and Carcinogenesis, Cancer Development. *Am. J. Cancer Res.* **2018**, *8* (5), 778–791.

6 Appendix

6.1 Synthesis of PIKBPyne probes

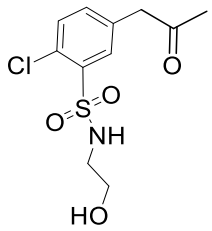

2-chloro-N-(2-hydroxyethyl)-5-(2-oxopropyl)benzenesulfonamide was synthesized as previously described.[37]

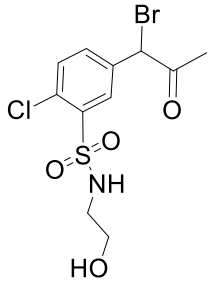

5-(1-bromo-2-oxopropyl)-2-chloro-N-(2 hydroxyethyl)benzenesulfonamide was synthesized as previously described.[37]

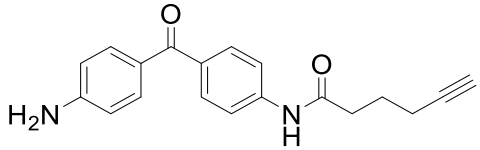

***N*-(4-(4-aminobenzoyl)phenyl)hex-5-ynamide.** Synthesized according to the procedure outlined by Cravatt[25], as previously described.[37]

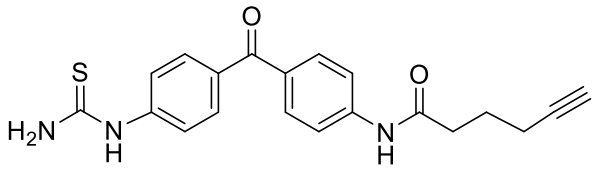

Hex-5-ynoic acid [4-(4-thioureido-benzoyl)-phenyl]-amide. Benzoyl chloride (13 µL, 8.5 M) was added dropwise to a solution of NaSCN (10 mg, 0.12 mmol) in acetone (1.5mL). The mixture was refluxed at 80°C for 15 minutes. *N*-(4-(4-aminobenzoyl)phenyl)hex-5-ynamide (31 mg, 0.1 mmol) in acetone (0.5 mL) was added. The mixture was refluxed for 2 h at 80°C. The solvent was evaporated and the product was dissolved in MeOH:H_2O (5:1, 2 mL) and stirred at room temperature for 2 h. The solvent was evaporated and the product isolated by column chromatography (CH_2Cl_2:MeOH, 95:5). The title compound was obtained as a pale yellow solid (22.5 mg, 62% yield). TLC R_f = 0.43 in 10% MeOH in CH_2Cl_2. ^{1}H NMR (400 MHz, $(CD_3)_2CO$-d_6) δ 9.54 (s, 1H), 9.49 (s, 1H), 7.87-7.79 (m, 2H), 7.82-7.72 (m, 6H), 7.24 (br s, 2H), 2.57 (t, J = 7.6 Hz, 2H), 2.39 (t, J = 2.8 Hz, 1H), 2.30 (td, J = 7.1, 2.7 Hz, 2H), 1.89 (p, J=7.2 Hz, 2H); ^{13}C NMR (100 MHz, Acetone-d_6) δ ppm 194.23 (C), 183.38(C) , 171.89(C), 171.81 (C), 144.17(C), 143.87(C), 134.61(C), 133.17(CH), 131.85(CH), 131.50(CH), 122.52(CH), 122.38 (CH), 119.13(CH), 119.04(CH), 84.29(CH), 70.45(CH), 36.29(C), 36.24(CH_2), 24.89(CH_2), 18.29 (CH_2).

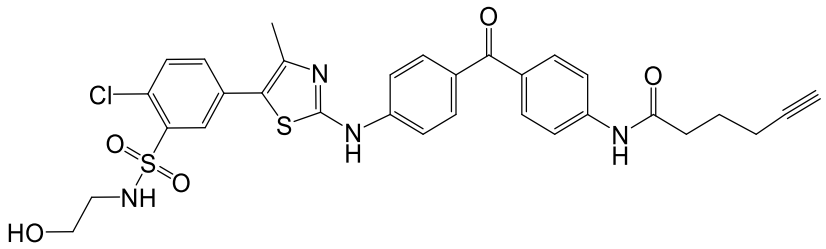

Hex-5-ynoic acid [4-(4-{5-[4-chloro-3-(2-hydroxy-ethylsulfamoyl)-phenyl]-4-methyl-thiazol-2-ylamino}-benzoyl)-phenyl]-amide. Hex-5-ynoic acid [4-(4-thioureido-benzoyl)-phenyl]-amide (10 mg, 0.0157 mmol) was dissolved in EtOH, heating to dissolve completely, and added to 5-(1-bromo-2-oxopropyl)-2-chloro-N-(2 hydroxyethyl)benzenesulfonamide (5.4 mg, 0.01457 mmol). The mixture was stirred and refluxed for 5.5 hours, until complete by TLC. The solvent was removed *in vacuo* and the product was isolated by column chromatography (2.5-10% MeOH in CH_2Cl_2). The title compound was obtained as a yellow solid (6.2 mg, 63% yield) TLC R_f = 0.55 in 10% MeOH in CH_2Cl_2. ^{1}H NMR (400 MHz, MeOD) δ ppm 8.09 (s,1H), 7.75 (m, 8H), 7.64 (s, 2H), 3.56 (t, J=Hz, 2H), 3.05 (t, J= 6.1Hz, 2H), 2.57 (t, J=7.5Hz, 2H), 2.42 (s, 3H), 2.28 (m, 3H), 1.91 (q, J=7.3Hz, 2H). ^{13}C NMR (100 MHz, MeOD) 196.50, 174.07, 162.61, 147.02 (CH), 146.44 (CH), 144.02 (CH), 139.62 (CH), 134.43 (CH), 134.37(CH), 133.37 (CH), 132.94 (CH), 132.14 (CH), 132.10 (CH), 131.74 (CH), 131.74, 131.51, 130.92, 123.44, 120.07, 117.51, 84.11, 70.33 (CH), 61.80 (CH_3), 46.17 (CH_2), 36.67 (CH_2), 25.51 (CH_2), 18.64 (CH_2), 16.64 (CH_2); HRMS (EI): Exact mass calcd for $C_{31}H_{29}ClN_4O_5S_2$ $[M]^+$ = 636.1268. Found: 637.2.

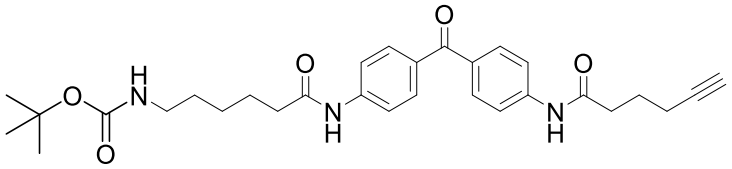

***tert*-Butyl (6-((4-(4-(hex-5-ynamido)benzoyl)phenyl)amino)-6-oxohexyl)carbamate.** To a solution of *N*-(4-(4-aminobenzoyl)phenyl)hex-5-ynamide (500 mg, 1.63 mmol) in DMF (8.15 mL, 0.200 M), 6-(Boc-amino)hexanoic acid (415 mg, 1.79 mmol), N-(3-diethylaminopropyl)-N'-ethyl carbodiimide hydrochloride (531 mg, 2.77 mmol), hydroxybenzotriazole (245 mg, 1.81 mmol), and triethylamine (0.682 mL, 4.89 mmol) were added. The reaction mixture was stirred under air for 18 h at 40 ºC. The reaction mixture was cooled to room temperature and concentrated *in vacuo*. The product was isolated by column chromatography (50-100% EtOAc in hexanes). The title compound was obtained as a yellow solid (205 mg, 29 % yield). TLC R_f = XX in 60 % EtOAc in hexanes. HRMS (EI): Exact mass calculated for $C_{30}H_{37}N_3O_5$ $[M]^+$ = 519.2733. Found: 542.2701.

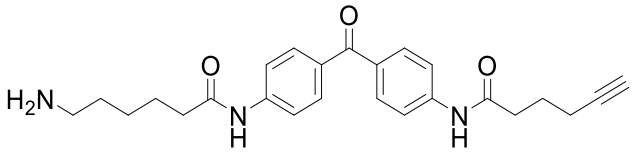

***N*-(4-(4-(6-aminohexanamido)benzoyl)phenyl)hex-5-ynamide.** *Tert*-Butyl (6-((4-(4-(hex-5-ynamido)benzoyl)phenyl)amino)-6-oxohexyl)carbamate (191 mg, 0.367 mmol) was dissolved in dichloromethane (5.48 mL, 0.067 M) and trifluoroacetic acid (0.283 mL, 3.67 mmol) was added. The reaction mixture was stirred at room temperature for 2.5 h, then concentrated *in vacuo*. The product was isolated by column chromatography (20% MeOH in CH_2Cl_2). The title compound was obtained as a yellow solid (264 mg, quantitative yield). TLC R_f = 0.33 in 20% MeOH in CH_2Cl_2. HRMS (EI): Exact mass calculated for $C_{25}H_{29}N_3O_3$ $[M]^+$ = 419.2209. Found: 420.2259.

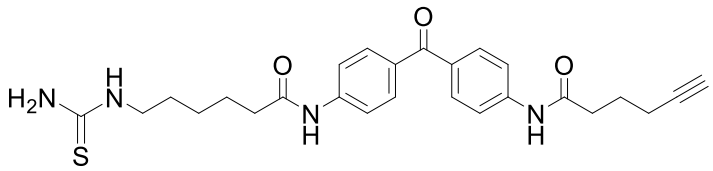

***N*-(4-(4-(6-thioureidohexanamido)benzoyl)phenyl)hex-5-ynamide.** To sodium thiocyanate (61.0 mg, 0.756 mmol) in acetone (15.8 mL, 0.040 M), benzoyl chloride (0.080 mL, 0.693 mmol) was added. The reaction mixture was heated at reflux for 15 minutes. The reaction solution was allowed to cool to room temperature. To this, a solution of *N*-(4-(4-(6-aminohexanamido)benzoyl)phenyl)hex-5-ynamide (265 mg, 0.630 mmol) in acetone (5 mL, 0.200 M) was added. The reaction mixture was heated at reflux for 2 h. The reaction mixture was cooled to room temperature and concentrated *in vacuo* to remove the solvent. The crude product was dissolved in a solution of MeOH:H_2O/4:1 (10.5 mL) and potassium carbonate (122 mg, 0.882 mmol) was added. The resulting mixture was allowed to stir at 30º C for 1 h, cooled to room temperature, then concentrated *in vacuo*. The product was isolated by column chromatography (2.5-20% MeOH in CH_2Cl_2). The title compound was obtained as a white solid (45.4 mg, 15 % yield). TLC R_f = 0.30 in 2.5% MeOH in CH_2Cl_2. HRMS (EI): Exact mass calculated for $C_{26}H_{30}N_4O_3S$ $[M]^+$ = 478.2039. Found: 479.2162.

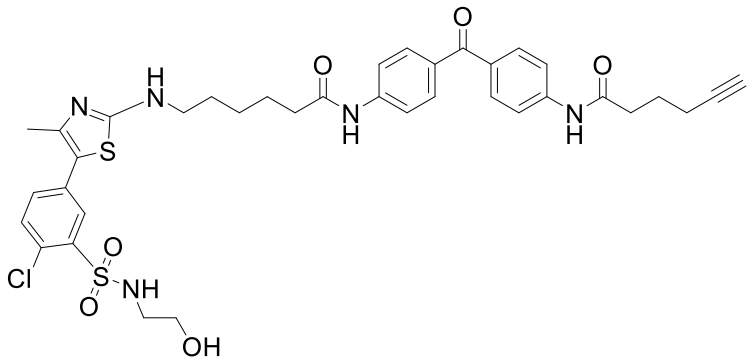

***N*-(4-(4-(6-((5-(4-chloro-3-(*N*-(2-hydroxyethyl)sulfamoyl)phenyl)-4-methylthiazol-2-yl)amino) hexanamido)benzoyl)phenyl)hex-5-ynamide.** To *N*-(4-(4-(6-thioureidohexanamido)benzoyl)phenyl) hex-5-ynamide (5.80 mg, 0.012 mmol) in ethanol (0.113 mL, 0.01M) was added 5-(1-bromo-2-oxopropyl)-2-chloro-N-(2 hydroxyethyl)benzenesulfonamide (4.20 mg, 0.011 mmol). The reaction mixture was stirred at reflux for 5.5 hours, until complete by TLC. The solvent was removed *in vacuo* and the product was isolated by column chromatography (3-5% MeOH in CH_2Cl_2). The title compound was obtained as a white solid (7.8 mg, 92% yield). TLC $R_f = 0.41$ in 5% MeOH in CH_2Cl_2. HRMS (EI): Exact mass calculated for $C_{37}H_{40}ClN_5O_6S_2$ $[M+Na]^+ = 772.2006$. Found: 772.2068.

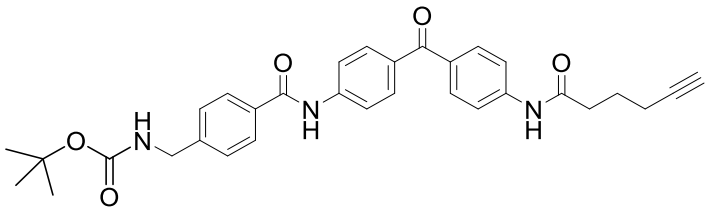

***tert*-Butyl 4-((4-(4-(hex-5-ynamido)benzoyl)phenyl)carbamoyl)benzylcarbamate.** To a solution of *N*-(4-(4-aminobenzoyl)phenyl)hex-5-ynamide (328 mg, 1.07 mmol) in DMF (5.35 mL, 0.200 M), 4-(Boc-aminomethyl) benzoic acid (403 mg, 1.60 mmol) and N,N-diisopropylethylamine (0.926 mL, 5.37 mmol) were added. *O*-7-azabenzotriazol-1-yl)-*N*,*N*,*N*′,*N*′-tetramethyluronium hexafluorophosphate (0.814 mg, 2.14 mmol) was added and the reaction mixture was stirred under air for 23 h at 100 ºC. The reaction mixture was cooled to room temperature and concentrated *in vacuo*. The product was purified by high performance liquid chromatography (40%-80% MeCN in water). The title compound was obtained as an off-white solid (109.1 mg, 19% yield). TLC R_f = 0.34 in 50% EtOAc in hexanes. LRMS: Exact mass calculated for $C_{32}H_{33}N_3O_5$ $[M]^+$ = 540.24. Found: 540.3

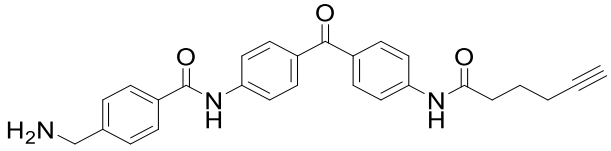

4-(aminomethyl)-*N*-(4-(4-(hex-5-ynamido)benzoyl)phenyl)benzamide. *Tert*-Butyl 4-((4-(4-(hex-5-ynamido)benzoyl)phenyl)carbamoyl)benzylcarbamate (50.0 mg, 0.090 mmol) was dissolved in dichloromethane (1.34 mL, 0.067 M) and trifluoroacetic acid (0.07 mL, 0.9 mmol) was added. The reaction mixture was stirred at room temperature for 3 h, then concentrated *in vacuo*. The product was isolated by column chromatography (100% CH_2Cl_2 -20% MeOH in CH_2Cl_2). The title compound was obtained as a white solid (28.7 mg, 73%). TLC R_f = 0.05 in 1% MeOH in CH_2Cl_2. HRMS (EI): Exact mass calculated for $C_{27}H_{25}N_3O_3$ $[M]^+$ = 439.1896.

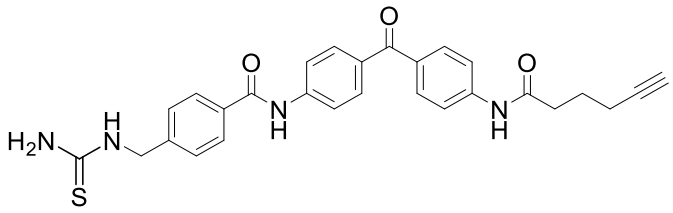

***N*-(4-(4-(hex-5-ynamido)benzoyl)phenyl)-4-(thioureidomethyl)benzamide.** To sodium thiocyanate (5.20 mg, 0.064 mmol) in acetone (1.33 mL, 0.040 M), benzoyl chloride (0.007 mL, 0.058 mmol) was added. The reaction mixture was heated at reflux for 15 minutes. The reaction solution was allowed to cool to room temperature. To this, a solution of 4-(aminomethyl)-*N*-(4-(4-(hex-5-ynamido)benzoyl)phenyl)benzamide (23.3 mg, 0.053 mmol) in acetone (1.00 mL, 0.040 M) was added. The reaction mixture was heated at reflux for 2 h. The reaction mixture was cooled to room temperature and concentrated *in vacuo* to remove the solvent. The crude product was dissolved in a solution of MeOH:H_20/4:1 (1.00 mL) and potassium carbonate (10.0 mg, 0.074 mmol) was added. The resulting mixture was allowed to stir at 30º C for 1 h, cooled to room temperature, then concentrated *in vacuo*. The product was isolated by flash column chromatography (20% EtOAc in hexanes-20% MeOH in EtOAC). The title compound was obtained as an off-white solid (7.40 mg, 28 % yield). TLC R_f = 0.16 in 50% EtOAc in hexanes.

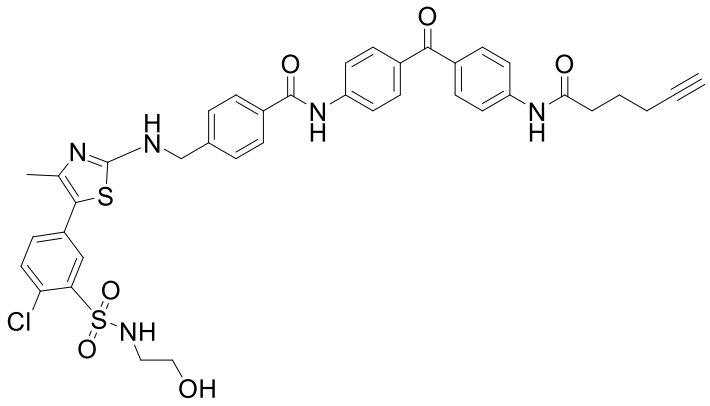

4-(((5-(4-chloro-3-(*N*-(2-hydroxyethyl)sulfamoyl)phenyl)-4-methylthiazol-2-yl)amino)methyl)-*N*-(4-(4-(hex-5-ynamido)benzoyl)phenyl)benzamide. To *N*-(4-(4-(hex-5-ynamido)benzoyl)phenyl)-4-(thioureidomethyl)benzamide (6.00 mg, 0.012 mmol) in ethanol (0.110 mL, 0.100 M) was added 5-(1-bromo-2-oxopropyl)-2-chloro-N-(2 hydroxyethyl)benzenesulfonamide (4.00 mg, 0.011 mmol). The reaction mixture was stirred at reflux for 4 hours. The solvent was removed *in vacuo* and the product was isolated by flash column chromatography (100% CH_2Cl_2-10% EtOH in CH_2Cl_2). The title compound was obtained as a light yellow solid (6.50 mg, 77% yield). TLC $R_f = 0.36$ in 100% CH_2Cl_2.

6.2 Primer sequences

Table 6.1: Primers used in qRT-PCR and mutagenesis

Gene	Forward sequence	Reverse sequence	T_A (°C)
qPCR primers			
18S	GCGATGCGGCGGCGTTATTC	CAATCTGTCAATCCTGTCCGTGTCC	65
ACOT1/2	CTGTCGTCATCAACGGCTCT	GGTCAGGTCCTTCCAAAGGG	61
ARP1	CTGCCTCAAGGCCATAGTCC	CTTTCCGAATCTCGTCGGCT	65
CEBPβ	CGACGAGTACAAGATCCGGC	TGCTTGAACAAGTTCCGCAG	63
EGFR	AGGCACGAGTAACAAGCTCAC	ATGAGGACATAACCAGCCACC	63
CPVL	CCCAGCTCAGATACAGCCAG	GGGAAGTCTCTGTCACGCAA	65
HCV	GTCTGCGGAACCGGTGAGTA	GCCCAAATGGCCGGGATA	60
HNF1A	CCAGGTCTTCACCTCAGACAC	CTGCTGGAGGACACTGTGG	65
HNF4A	ATGGACATGGCCGACTACAG	TGATGGGGACGTGTCATTGC	55
HNF4G	CAACGGTGTCAACTGTCTGTG	AAACGTGACTCTTACGAATGCT	63
JUN	ACATGCTCAGGGAACAGGTG	CTGCGTTAGCATGAGTTGGC	64
LIPC	ATCAAGTGCCCTTGGACAAAG	TGACAGCCCTGATTGGTTTCT	63.6
MGLL	AATGCAGACGGACAGTACCTC	GAGCAAGCTCTTCATAGCGG	63.6
NF1H4	GTGAGGGGTGTAAAGGCTTGTT	GCAGACCCTTTCAGCAAAGC	64
PAFAH1B1	GGATGGGAGTGAAGGACGGAA	GTAAGATTCATTCCACCGGAGC	65
PAFAH1B2	CAAACCCAGCAGCTATTCCG	GAACAGTACATCAGGCTCTTTGT	65
PAFAH1B3	ACATCCGGCCCAAGATTGTG	GGGCTGTCGCTCATTCACC	65
PPARA	CTATCATTTGCTGTGGAGATCG	AAGATATCGTCCGGGTGGTT	63.6
PPARG	AGCCTGCGAAAGCCTTTGGTG	GGCTTCACATTCAGCAAACCTGG	63.6
PPARGC1A	GCTTTCTGGGTGGACTCAAGT	GAGGGCAATCCGTCTTCATCC	
Mutagenesis primers			
LIPC-3'UTR	GCTTCCAGAACAGAAATAAATG	CATTTATTTCTGTTCTGGAAGC	55

6.3 Supplemental figures

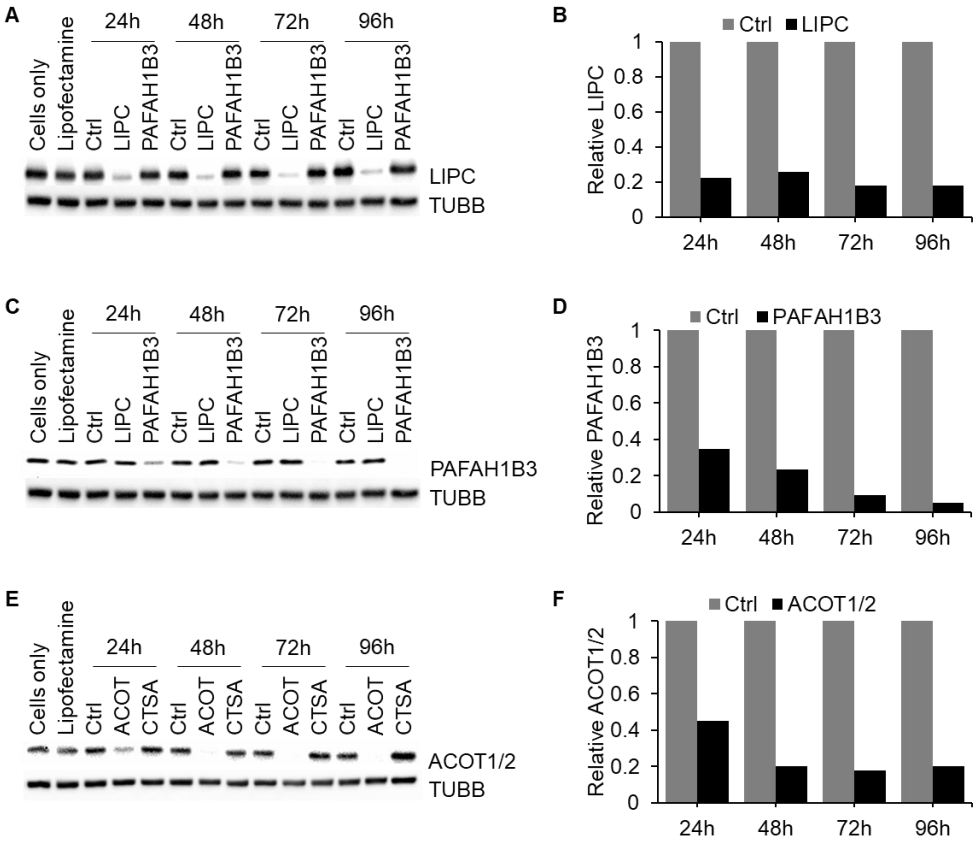

Figure 6.1: siRNAs efficiently knock down serine hydrolases between 48 and 96 hours after transfection. Huh7.5 cells were transfected with 10nM siRNAs and lysed after between 24 and 96 hours after transfection. Lysates were resolved on a 10% SDS-PAGE gel and western blotting performed against A,B) LIPC C,D) PAFAH1B3, and E,F) ACOT1/2. Densitometric analysis was performed to quantify the decrease in expression. Band intensity was normalised by the time-matched control siRNA-transfected sample. n=1